Targeting the glutamine metabolic pathway enhances sensitivity to BH3 mimetics in different malignancies

Thesis submitted in accordance with the requirements of the University of Liverpool for the degree of Doctor in Philosophy

By Aoula Al-Zebeeby

November 2019

DECLARATION

This thesis is the result of my own work. The material contained within this thesis has not been presented, nor is currently being presented, either wholly or in part for any other degree or qualification.

Aoula Al-Zebeeby

This research was carried out in the Department of Molecular and Clinical Cancer Medicine, University of Liverpool, UK.

Table of contents

List of Figures

Chapter 1

Chapter 3

Chapter 4

Chapter 5

Acknowledgements

My special thanks and gratitude go to my supervisor Dr. Shankar Varadarajan for his motivation, patience, immense knowledge and unlimited support. He filled every day of my lab work with enthusiasm and the challenge to learn and do something new. Besides Dr. Shankar, I would like to express my gratitude to Prof Gerald M Cohen for his help to build up my knowledge and his scientific support. I also greatly appreciate Varadarajan lab members Dr. Michael, Dr. Rachel, Mateus, Govinda and Georgia for all their scientific and emotional support.

Further enormous gratitude goes to the Republic of Iraq represented by the Ministry of Higher Education and Scientific Research and the University of Al-Qadisiyah, who gave the opportunity to complete PhD degree and funded my PhD scholarship as well as all the Iraqi cultural attaché team for their efforts and support.

My sincere thanks go to my mother, father, brothers (Mohammed and Saif) for their best wishes and emotional support. Finally, a special thank-you goes to my husband Ali for being always there to encourage me to continue and pass through all the challenges without fear. Thank you, Ali, for your unlimited love. A final thank-you to my kids Mohammed and Jannat for being in my life bringing all the joy and happiness.

List of Publications

1. **Al-Zebeeby A,** Vogler M, Milani M., Richards, C., Al-otaiby A, Greaves G, Dyer MJS, Cohen, GM, and Varadarajan S 'Targeting intermediary metabolism enhances the efficacy of BH3 mimetic therapy in haematological malignancies.' Haematologica, 2019 May;104(5):1016-1025. doi: 10.3324/haematol.2018.204701.

2. Henz K, **Al-Zebeeby,** A, Basoglu M, Fulda S, Cohen GM, Varadarajan, S and Vogler, M 'Selective BH3-mimetics targeting BCL-2, BCL-XL or MCL-1 induce severe mitochondrial perturbations' Biological Chemistry, June 2018 400(2):181-185. doi: 10.1515/hsz-2018-0233.

3. Milani M, Beckett AJ, **Al-Zebeeby A,** Luo X, Prior IA, Cohen, GM, and Varadarajan, S 'DRP-1 functions independently of mitochondrial fission to release cytochrome *c* in BH3 mimetic-mediated apoptosis.' Cell Death Discovery, July 2019 doi:10.1038/s41420-019-0199-x

4. Carter RJ, Milani M, Butterworth M, Harper N, Yedida G, Greaves G, **Al-Zebeeby A**, Jorgensen AL, Schache AG, Risk JM, Shaw RJ, Jones TM, Sacco JJ, Hurlstone A, Cohen GM and Varadarajan S 'High expression of MCL-1 and BCL-XL can be efficiently targeted in Head and Neck cancer' Manuscript accepted in Cell Death and Disease.

Abstract

The development of chemoresistance is a major obstacle facing several promising therapies in cancer. Resistance to anti-cancer agents occur *via* different mechanisms, including failure to undergo apoptosis. Apoptosis is a sophisticated cell death signalling pathway that is mainly regulated by the BCL-2 family of proteins, which can be anti- or pro-apoptotic. The anti-apoptotic members, such as BCL-2, BCL-X_L, MCL-1, BCL-w and BCL-2A1, are highly expressed in many cancers. These proteins antagonise apoptosis by binding and inhibiting pro-apoptotic members of the BCL-2 family. The balance among the different anti- and pro-apoptotic members dictates the fate of the cell towards survival or death. Small molecule inhibitors of the anti-apoptotic BCL-2 family members called BH3 mimetics have been developed in the last few years. BH3 mimetics that specifically inhibit BCL-2 (ABT-199), BCL-X_L (A-1331852) and MCL-1 (A-1210477 and S63845) demonstrate enormous potential to improve treatment in a wide variety of cancers. Of these, ABT-199 has been used successfully in several haematological cancers but resistance to ABT-199 is starting to emerge. Since all BH3 mimetics share a similar mechanism of action, it is likely that resistance will also emerge for other BH3 mimetics.

Therefore, the aims of this study were to (1) generate simple resistance models to the different BH3 mimetics, to mimic the rapid chemoresistance observed in the clinic, (2) identify novel combination therapies to overcome such chemoresistance, (3) characterise the underlying mechanisms by which the combination therapies could overcome chemoresistance and (4) extend these observations to other malignancies.

In the first results chapter, data presented discussed four different models of resistance to the different BH3 mimetics in three haematological cancer cell lines. In

all these models, resistance was attributed neither to consistent changes in expression levels of the anti-apoptotic proteins nor to interactions among different pro- and anti-apoptotic BCL-2 family members. However, resistance to a particular BH3 mimetic was overcome by exposing cells to BH3 mimetics targeting the other anti-apoptotic members, suggesting redundant functions of multiple BCL-2 family members in regulating apoptosis.

Since targeting multiple members of the BCL-2 family members together could be limited due to potential toxicity, other ways to tackle this issue were explored in the second results chapter. Targeting the uptake of glutamine as well as its downstream metabolic pathways, either by genetic knockdown or pharmacological inhibitors, overcame resistance to BH3 mimetic-mediated apoptosis. Interestingly, the enzyme that regulates glutamine metabolism, glutaminase (GLS) interacted exclusively with the critical pro-survival BCL-2 family member in all cell lines. For instance, GLS interacted with BCL-2 in MAVER-1 (BCL-2 dependent cell line), with BCL-X_L in K562 (BCL-X_L dependent cell line) and interacted with MCL-1 in H929 (MCL-1 dependent cell line), suggesting that GLS played a crucial role in apoptosis and potentially, chemoresistance.

The third results chapter is aimed at further exploring the downstream signalling pathway of glutamine metabolism for their roles in overcoming resistance to BH3 mimetics. Targeting the different downstream pathways namely: reductive carboxylation, lipogenesis and cholesterogenesis also overcame resistance to BH3 mimetics. Furthermore, the findings highlighted the possibility that repurposing widely used drugs, such as statins, to target intermediary metabolism could improve the efficacy of BH3 mimetic therapy in haematological malignancies.

In the final chapter, the validity of these findings in other malignancies was tested by extending these observations in cell lines derived from head and neck squamous cell carcinoma (HNSCC). Targeting GLS reduced the clonogenic potential of a panel of HNSCC cell lines, thus demonstrating a promising combination that could potentially improve therapy in HNSCC. Moreover, GLS expression assessed in tissue microarrays containing tumour cores from hundreds of HNSCC patients revealed that expression levels of GLS was high in the tumour core of oral cavity cancer patients and could be a prognostic marker in HNSCC.

Overall this study demonstrates that resistance to BH3 mimetics in haematological malignancies could be overcome by targeting distinct enzymes regulating intermediary metabolism. Moreover, this study demonstrates that targeting glutamine metabolism could be a promising therapeutic strategy in head and neck cancer.

Abbreviations

ACAT	Acetyl-Coenzyme A acetyltransferases
ACC	Acetyl-CoA Carboxylase
ACLY	ATP citrate lyase
ACO2	Aconitase
AF	Advancing front
α-KG	α-Ketoglutrat
ALL	Acute lymphoblastic leukaemia
AML	Acute myeloblastic leukaemia
ANOVA	Analysis of variance
AOA	Aminooxyacetate
APAF-1	Apoptotic protease activating factor-1
APS	Ammonium Persulphate
BAD	Bcl-2-associated death promoter
BAK	Bcl-2 homologous antagonist killer
BAX	Bcl-2-associated X protein
BCL-2	B-cell lymphoma 2
BCL-2A1	Bcl-2-related protein A1
BCL-W	Bcl-2-like protein 2
BCL-X_L	B-cell lymphoma-extra large
BCR-ABL	Translocation resulted in forming Philadelphia chromosome
BFL-1	Bcl-2-related protein A1
BH	Bcl-2 homology domain
BID	BH3 interacting-domain death agonist
BIK	Bcl-2-interacting killer
BIM	Bcl-2-like protein 11
BMF	Bcl-2-modifying factor
BSA	Bovine Serum Albumin
CaCl2	Calcium Chloride
CHAPS	3-Cholamidopropyl dimethylammonium 1-propane sulfonate
CLL	Chronic lymphoblastic leukaemia
CML	Chronic myeloblastic leukaemia
CxDx	Cycle x Day x x=number
Cyto	Cytosolic
DISC	Death-inducing signalling complex
DMEM	Dulbecco's Modified Eagle's Medium
DNA	Deoxyribonucleic acid
DRP-1	Dynamin-1-like protein
ECL	Electrochemiluminescence
EDTA	Ethylenediaminetetraacetic acid
EGCG	Green tea polyphenol epigallocatechin gallate
EGTA	Ethylene glycol-bis(β-aminoethylether)-N,N,N’,N’-tetraaciticacid

EGFR	Epidermal growth factor receptor
EM	Electron microscopy
EMEM	Eagle's minimal essential medium
FASN	Fatty acid synthesis
FBS	Foetal bovine serum
GAPDH	Glyceraldehyde 3-phosphate dehydrogenase
GFAT	Glutamine-fructose-6-phosphate transaminase
GLS	Glutaminase
GLUD	Glutamate dehydrogenase
GPNA	L-γ-Gamma-L-Glutamyl-p-Nitroanilide
H	Hour
HEPES	Hydroxyethyl-piperazine ethane-Sulfonic acid buffer
HMGR	3-Hydroxy-3-Methylglutaryl-CoA Reductase
HNSCC	Head and neck squamous cell carcinoma
Hpf	Hours post-fertilisation
HPV	Human papillomavirus
HRK	Harakiri
ICC	Immunocytochemistry
IDH	Isocitrate dehydrogenase
IHC	Immunohistochemistry
IMM	Inner mitochondrial membrane
IP	Immunoprecipitation
KCl	Potassium Chloride
MCL-1	Myeloid cell leukaemia 1
Mito	Mitochondrial
MOMP	Mitochondrial outer membrane permeabilization
NaCl	Sodium Chloride
NOXA	Phorbol-12-myristate-13-acetate-induced protein 1
OC	Oral cavity
OMM	Outer mitochondrial membrane
OPA-1	OPA1 mitochondrial dynamin like GTPase
PARP	Poly (ADP-ribose) polymerase
PB	Phosphate-Buffered
PBS	Phosphate-Buffered Saline
PBS-T	Phosphate-Buffered Saline-Tween
Pen-Strep	Penicillin-Streptomycin
PI	Propidium iodide
PS	Phosphatidylserine

PUMA	BCL2 binding component 3
Qpath	Quantitative Pathology Software
Ripa Buffer	Radioimmunoprecipitation assay
ROS	Reactive oxygen species
Rpm	Round per minute
RPMI	Roswell park memorial institute
SAS	Statistical Analysis System
SDS	Sodium Dodecyl Sulphate
SDS-PAGE	Sodium Dodecyl Sulphate Polyacrylamide gel
SEM	Standard error of the mean
SLC1A5(ASCT2)	Alanine, Serine, Cysteine Transporter 2
SPSS	Statistical Package for Social Sciences
TAAB	Epoxy hard Resin
TEMED	Tetramethylethylenediamine
TBS-T	Tris-buffered saline-tween
TCA	Tricarboxylic acid cycle
TMA	Tissue microarray
TMRE	Tetramethyl rhodamine ethyl ester
Tris-HCL	Hydroxy methyl aminomethane hydrochloride
WB	Western blots
Z-VAD.FMK	N-Benzyloxycarbonyl-Val-Ala-Asp(O-Me) fluoromethyl ketone

Chapter 1

General Introduction

1.1 Overview of apoptosis

Apoptosis or programmed cell death is a highly organised process of cellular suicide that occurs in both physiological and pathological conditions (Kerr et al. 1972). Apoptosis plays a vital role during development (Brill et al. 1999), immunity (Cohen et al. 1992) as well as in the conservation of cellular homeostasis in all multicellular organisms (Henson & Hume 2006). Terminologically, apoptosis comes from the ancient Greek word 'ἀπόπτωσις', which means separation and falling off, as characterised by the specific morphological and biochemical changes that occur in cells (Duque-Parra 2005). Scientists Kerr, Wyllie and Currie used the term 'apoptosis' for the first time to describe this distinct form of cell death (Kerr et al. 1972).

Numerous morphological changes, including nuclear pyknosis (DNA fragmentation and chromatin condensation), dense cytoplasm, tightly packed organelles, destruction of cytoskeleton, extensive plasma membrane blebbing and budding from the cell to form apoptotic bodies, have been observed in cells during apoptosis (Hacker 2000). Subsequently, these bodies are phagocytosed by macrophages and neighbouring cells, and eventually degraded within phagolysosomes (Kerr et al. 1972; Elmore 2007). Cells removed by apoptosis do not exhibit any inflammatory response due to the lack of release of the cellular constituents into surrounding tissue. Moreover, apoptotic bodies are phagocytosed rapidly before anti-inflammatory cytokines are produced (Savill & Fadok 2000; Kurosaka et al. 2003). Several biochemical changes, including protein cleavage and DNA fragmentation, have been observed during apoptosis (Hengartner 2000). The cleavage of proteins is brought about by enzymes called caspases, which are expressed in their inactive forms (pro-enzyme) in most cell types, and following activation, they initiate a protease

cascade. This cascade triggers cell death through proteolytic cleavage of various dynamic substrates, including nuclear lamins (Lazebnik et al. 1995), enzymes that are involved in DNA repair, such as poly-ADP-ribose polymerase (PARP) (Lazebnik et al. 1994) and cytoskeletal proteins (Mashima et al. 1995). Cleavage of PARP can also occur *via* the chromatin-bound Ca^{2+}/Mg^{2+}-dependent endonucleases during apoptosis (Bortner et al. 1995). These changes are accompanied by the expression of phosphatidylserine (which normally locates in the inner leaflet of the cell membrane) on the outer leaflet of the cell membrane in an apoptotic cell (Bratton et al. 1997). Externalisation of phosphatidylserine serves as cell surface markers of the apoptotic cells, for them to be recognised by macrophages, thus allowing quick phagocytosis. In addition to apoptosis, other types of cell death that are either programmed or non-programmed have been reported. These are summarised in Table 1.1 (Galluzzi et al. 2018).

Table 1.1 Different types of cell death

Type of cell death	Description	Morphological Changes
Necrosis	Form of cell death that occurs in the intracellular microenvironment due to increased cytosolic Ca^{+} and severe oxidative stress - leading to irreversible cell injury with necrotic phenotype.	-Cell and mitochondria swelling -Cell membrane rupture -Inflammatory response
Necroptosis	Form of cell death that occurs in the intracellular and extracellular microenvironment by the activation of death receptor. It shares similarities with apoptosis and necrosis.	-Cell and mitochondria swelling -Cell membrane rupture
Parthonatos	Form of cell death that occurs due to over activity of PARP	-Chromatin condensation -Nuclear fragmentation
Pyroptosis	Form of cell death that is associated with inflammation - related with innate immunity.	-Maintains mitochondrial integrity -Cell swelling -Cell membrane rupture
Ferroptosis	Form of cell death that occurs in an iron dependent manner due to accumulation of ROS and lipid peroxidation.	-Increased cell membrane density -Small sized mitochondria
Autophagy	Form of cell death that depends on autophagic machinery. Removes intracellular components by fusion with lysosomes	-Membrane blebbing -Autophagic vacuole formation -Accompanied by increased lysosomal activity

1.2 Apoptotic pathways

Apoptosis can be regulated through two main routes, namely intrinsic pathway (mitochondrial pathway) (Green & Reed 1998) or extrinsic pathway (activation death receptor pathway) (Ashkenazi & Dixit 1998). The main steps of these two pathways are summarised in (Fig 1.1). These two pathways regulate apoptosis in three distinct phases: initiation, integration and cell death execution. While the first two phases are highly variable between the extrinsic and intrinsic pathway, the execution phase involving caspase activation is similar between the two pathways (Elmore 2007). In essence, the extrinsic apoptotic pathway is induced at the level of cell surface by an external ligand, which interacts with a death receptor that subsequently forms an intracellular signalling complex. In contrast, the intrinsic apoptotic pathway perturbs mitochondrial integrity (Elmore, 2007).

Mitochondria are primary sites of energy production but also are critical determinants of the fate of cells (Wang & Youle 2009). Mitochondria consist of an outer mitochondrial membrane (OMM) and inner mitochondrial membrane (IMM), separated by an intermembrane space. The IMM comprises the cristae that forms the boundary to mitochondrial matrix (Nunnari and Suomalainen, 2012). During apoptosis, a variety of stress stimuli, such as ischemia, DNA damage, increased intracellular Ca^{2+} concentrations and oxidative stress, impacts mitochondrial integrity and function (Kim et al. 2003). The key protein that regulates apoptosis at this level is cytochrome *c* (Liu et al. 1996; Lomonosova & Chinnadurai 2008). Cytochrome *c* is the fourth member of the electron transport chain and transfers electrons from complexes III to V, along the IMM, during cellular respiration (Dodia 2014). Cytochrome *c* is localised in the intermembrane space and guarded within the cristae folds by a protein called OPA1 (optic atophy1). During apoptosis, OPA1 is

proteolysed, resulting in cristae re-modelling and cytochrome *c* release from the inner mitochondrial membrane folds (Varanita et al. 2015). While OPA1 proteolysis redistributes cytochrome *c* form the cristae folds to the intermembrane space, the release of cytochrome *c* from the mitochondria is achieved by proteins, such as BAX and BAK, that form pores in the mitochondrial membrane during apoptosis (Olichon et al. 2003; Griparic et al. 2007; Westphal et al. 2014). Upon release into the cytosol, cytochrome *c* binds to apoptotic activating factor1 (APAF1) and triggers oligomerisation of APAF1, which in turn binds pro-caspase-9 to form the apoptosome (Fig. 1.1). Caspase-9 is activated in the apoptosome, and subsequently activates other caspases, such as caspase-3 and caspase-7, thus initiating downstream apoptotic signalling (Li et al. 1997; Jiang & Wang 2000; Bratton et al. 2001).

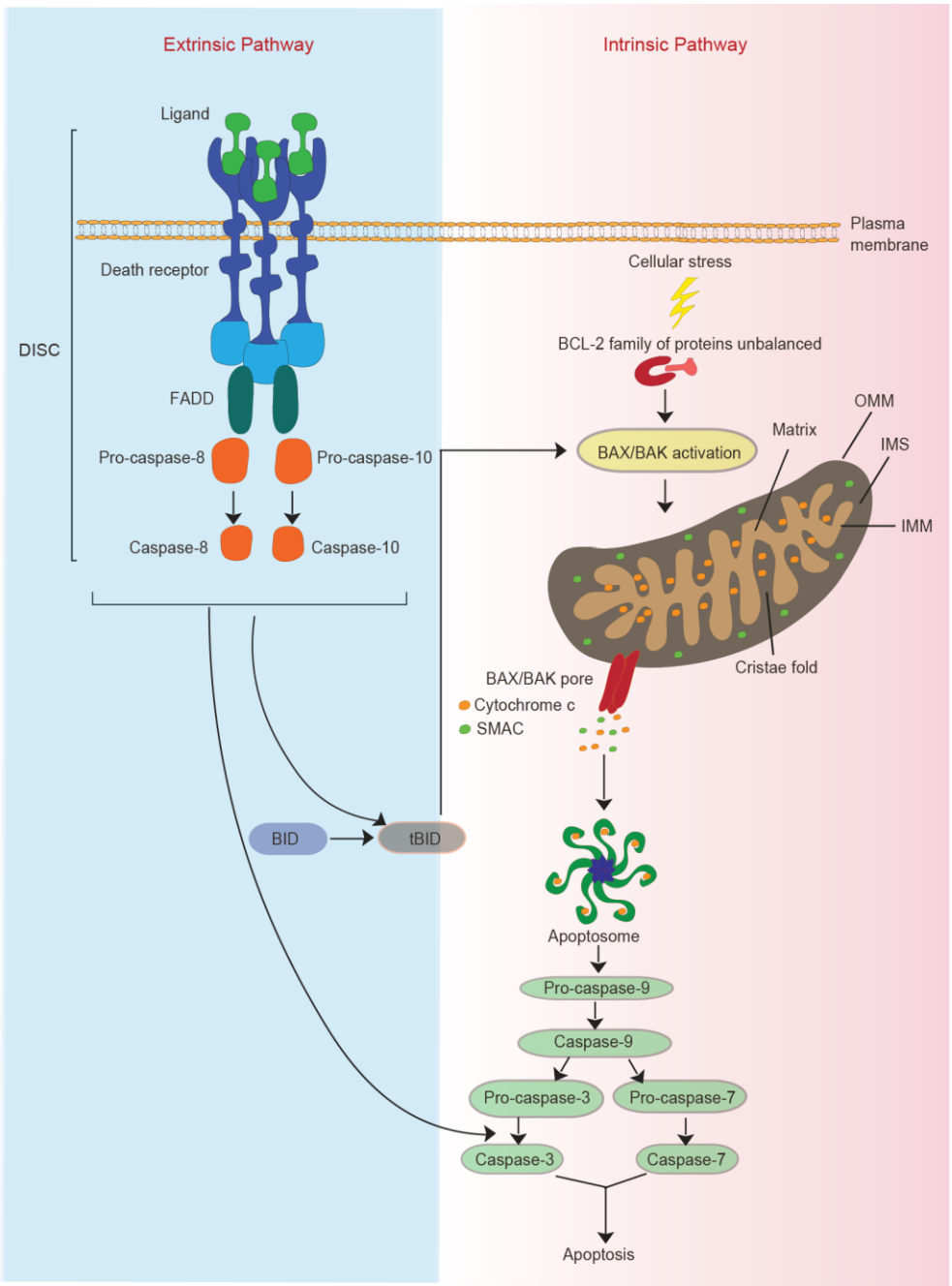

Fig 1.1. Two distinct apoptotic pathways converge on caspase cascade activation. The extrinsic apoptotic pathway initiates through extracellular stimuli that involve transmembrane receptor-mediated interactions with death ligands forming a death inducing signalling complex (DISC). DISC is composed of numerous proteins, such as FADD and caspases-8 and -10. Activation of these caspases truncates BID (tBID), which then translocates to the mitochondria to enable BAX/BAK oligomerisation and activation. In contrast, the intrinsic apoptotic pathway takes place through an intra-cellular stress that perturbs mitochondrial integrity, which is mediated by an imbalance in the BCL-2 family of proteins. Activation of BAX/BAK results in pore formation on mitochondrial membranes, through which cytochrome c is released to form apoptosome. These events result in the activation of other caspases, such as caspase-9, -3, and -7, to finally result in cell death.

Mitochondria are primary sites of energy production but also are critical determinants of the fate of cells (Wang & Youle 2009). Mitochondria consist of an outer mitochondrial membrane (OMM) and inner mitochondrial membrane (IMM), separated by an intermembrane space. The IMM comprises the cristae that forms the boundary to mitochondrial matrix (Nunnari and Suomalainen, 2012). During apoptosis, a variety of stress stimuli, such as ischemia, DNA damage, increased intracellular Ca^{2+} concentrations and oxidative stress, impacts mitochondrial integrity and function (Kim et al. 2003). The key protein that regulates apoptosis at this level is cytochrome *c* (Liu et al. 1996; Lomonosova & Chinnadurai 2008). Cytochrome *c* is the fourth member of the electron transport chain and transfers electrons from complexes III to V, along the IMM, during cellular respiration (Dodia 2014). Cytochrome *c* is localised in the intermembrane space and guarded within the cristae folds by a protein called OPA1 (optic atophy1). During apoptosis, OPA1 is proteolysed, resulting in cristae re-modelling and cytochrome *c* release from the inner mitochondrial membrane folds (Varanita et al. 2015). While OPA1 proteolysis redistributes cytochrome *c* form the cristae folds to the intermembrane space, the release of cytochrome *c* from the mitochondria is achieved by proteins, such as BAX and BAK, that form pores in the mitochondrial membrane during apoptosis (Olichon et al. 2003; Griparic et al. 2007; Westphal et al. 2014). Upon release into the cytosol, cytochrome *c* binds to apoptotic activating factor1 (APAF1) and triggers oligomerisation of APAF1, which in turn binds pro-caspase-9 to form the apoptosome (Fig. 1.1). Caspase-9 is activated in the apoptosome, and subsequently activates other caspases, such as caspase-3 and caspase-7, thus initiating downstream apoptotic signalling (Li et al. 1997; Jiang & Wang 2000; Bratton et al. 2001).

1.3 BCL-2 family of proteins

Two proteins that belong to the BCL-2 family - BAX and BAK - form pores in the mitochondrial membrane to release cytochrome *c*. Thus, these proteins can be categorised as pro-apoptotic. However, the BCL-2 family of proteins can be either pro- or anti-apoptotic, based on their functions. The anti-apoptotic members (BCL-2, BCL-X_L, BCL-w, MCL-1 and BCL2A1) drive cell survival, while the pro-apoptotic proteins are further divided into three subgroups: activators (BIM, PUMA and BID), sensitisers (NOXA, HRK, BMF, BAD and BIK) and effectors (BAX and BAK), all of which drive the apoptotic signalling events (Letai et al. 2002). The life-death balance of the cell depends on the relative expression levels and activities of these anti- and pro-apoptotic BCL-2 family members (Kale et al. 2018).

The anti- and pro-apoptotic BCL-2 family of proteins share strong similarities in the BCL-2 homology (BH) domains (Fig 1.2), which are composed of short (~20 amino acids), highly conserved, sequences (Sato et al. 1994) that control the interactions between different anti- and pro-apoptotic proteins. BH domains were first recognised in BCL-2 (Yin et al. 1994) and then, in BAK (Chittenden et al. 1995). Generally, it is suggested that the anti-apoptotic BCL-2 family members have four BH domains: BH1, BH2, BH3 and BH4, in addition to a transmembrane domain, permitting membrane insertion. MCL-1 is the only exception with no BH4 domain, but it has a PEST region that is not available in the other anti-apoptotic members (Fig 1.2). The pro-apoptotic effectors, BAX and BAK also contain BH1-4 domains, whereas the other pro-apoptotic members have only a BH3 domain and thus known as BH3-only proteins (Youle & Strasser 2008). The pro-apoptotic members through their α-helical BH3 domains bind to the hydrophobic groove of the anti-apoptotic members, and thus neutralize their activity (Petros et al. 2000; Qian et al. 2004).

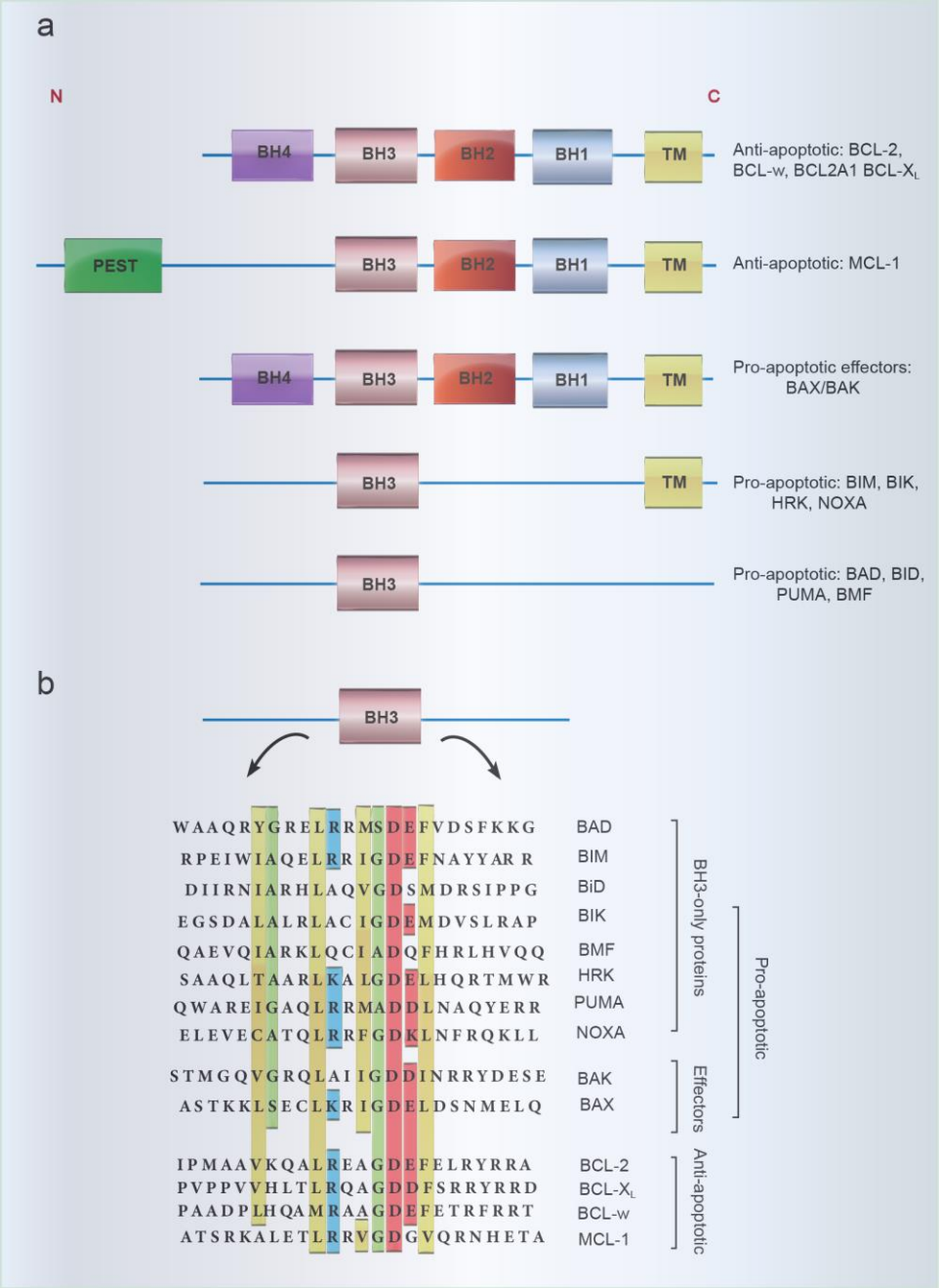

Fig 1.2. The BCL-2 family of proteins exhibit a high degree of homology in their structure. A schematic representation of the BH domains in all the BCL-2 family of proteins. Most of these members have transmembrane domain (TM) which used for membrane translocation. The anti-apoptotic, such as BCL-2, BCL-w, BCL-2A1 and BCL-X_L, and pro-apoptotic (effectors) BAX and BAK contain BH4. MCL-1 has an elongated N-terminal tail, known as PEST (consisting of proline, glutamic acid, serine and threonine) (Rogers et al. 1986; Kozopas et al. 1993; Germain & Duronio 2007). **(b)** Amino acid sequence alignment of BH3 domain showing the conserved regions (the hydrophobic residues) in yellow, positively charged residues in blue, negatively charged residues in red and neutral residues in green (Feng et al. 2007).

1.3.1 BCL-2

BCL-2 (B-cell lymphoma2), was the first anti-apoptotic member to be identified (Schenk et al. 2017) and recognised in t(14;18) chromosomal translocated follicular lymphoma (Tsujimoto et al. 1984). High expression levels of BCL-2 have been reported in different types of cancer, such as cancers of the bladder (Swellam et al. 2004), brain (Lamers et al. 2012), breast (Hellemans et al. 1995), lung (Jiang et al. 1995), colorectal (Zhao et al. 2005) and prostate (Karnak and Xu, 2010), as well as in non-Hodgkin's lymphoma (Hermine et al. 1996), chronic lymphocytic leukaemia (CLL) (Vogler et al. 2013) and acute myeloid leukaemia (AML) (Campos et al. 1993). Mainly, BCL-2 is localised in the mitochondrial outer membrane and the membranes of the endoplasmic reticulum with no evidence supporting BCL-2 re-localisation following the apoptotic stimuli (Kale et al. 2018). BCL-2 interacts with BAX but not BAK, and of all the BH3-only proteins, only BAD, BIM, PUMA, BID, HRK and BMF interact with BCL-2 (Fig. 1.3).

1.3.2 BCL-XL

The open reading frame of BCL-X_L (B-cell lymphoma extra-large) shares 44% similarity with respect to its amino acid sequence with BCL-2. It is high expressed in cancers of the prostate (Li et al. 2001; Castilla et al. 2006), head and neck (Zhang et al. 2014) and colorectal (Scherr et al. 2016), as well as in chronic myeloid leukaemia (CML) (Harb et al. 2013; Lucas et al. 2016). Normally, BCL-X_L is localised in the cytosol and some of it in. the outer mitochondrial membrane. During apoptosis, BCL-X_L gets translocated from cytosol to the outer mitochondrial membrane and endoplasmic reticulum (Kale et al. 2018). BCL-X_L interacts with both BAX and BAK, as well as with BAD, BIM, BID, PUMA, BMF and HRK (Fig. 1.3).

1.3.3 MCL-1

Myeloid cell leukemia-1 was firstly described as a gene that was involved in the early induction of the myeloblastic leukaemia cell line differentiation. It shares sequence homology to all anti-apoptotic BCL2 family of proteins (BH1-BH3) but it lacks the BH4 domain, which is compensated by PEST (consisting of proline, glutamic acid, serine and threonine) (Kirkin et al. 2004). Numerous studies have been shown MCL-1 has an anti-apoptotic function in triggering cell survival (Kozopas et al. 1993; Lømo et al. 1996; Zhou et al. 1998; Opferman et al. 2003). MCL-1 is highly expressed in variety of cancers, such as lung (Zhang et al. 2011; Yin et al. 2016), breast (Young et al. 2016; Merino et al. 2017; Caenepeel et al. 2018), ovaries (Zervantonakis et al. 2017), thyroid (Krajewski et al. 1995), head and neck (Palve et al. 2014), prostate (Reiner et al. 2015), pancreas (Wei et al. 2015), AML (Kaufmann et al. 1998) and multiple myeloma (Wuillème-Toumi et al. 2005). MCL-1 has three isoforms, with the long isoform proposed to localise to the outer mitochondrial membrane and involved in anti-apoptotic function (Yang et al. 1995; Kim et al. 2009). The short isoform is proposed to exhibit cytosolic localisation with potential pro-apoptotic functions (Palve et al. 2014; Palve & Teni 2012), whereas the shortest isoform proposed to localise to the mitochondrial matrix, facilitating mitochondrial respiration and energetics (Perciavalle et al. 2012). MCL-1 interacts with BAX and BAK and also with most other BH3-only members, except BAD, BMF, HRK and BIK (Fig. 1. 3).

1.3.4 Other anti-apoptotic members: BCL-w and BCL2A1

Besides the previously mentioned anti-apoptotic BCL-2 family of proteins, overexpression of other anti-apoptotic members, such as BCL2A1 (also known BFL-

1) and BCL-w have been reported in many types of cancers. Overexpression of BCL-w has been reported in melanoma (Placzek et al. 2010), colorectal cancers (Wilson et al. 2000), breast cancer (Shen et al. 2012) and B cell malignancies (Adams et al. 2017). Similarly, high expression of BCL2A1 is observed in breast cancers (Yoon et al. 2003), CLL and acute lymphocytic leukaemia (ALL) (Nagy et al. 2003; Olsson et al. 2007; Yecies et al. 2010). BCL-w and BCL2A1 exhibit mitochondrial localisation (Yan et al. 2000; Brien et al. 2009) and interact with BAX but not BAK. While BCL-w interacts with BAD, BIM, BID, PUMA and BMF, BCL-2A1 interacts with BIM, BID, BIK and NOXA (Fig. 1.3).

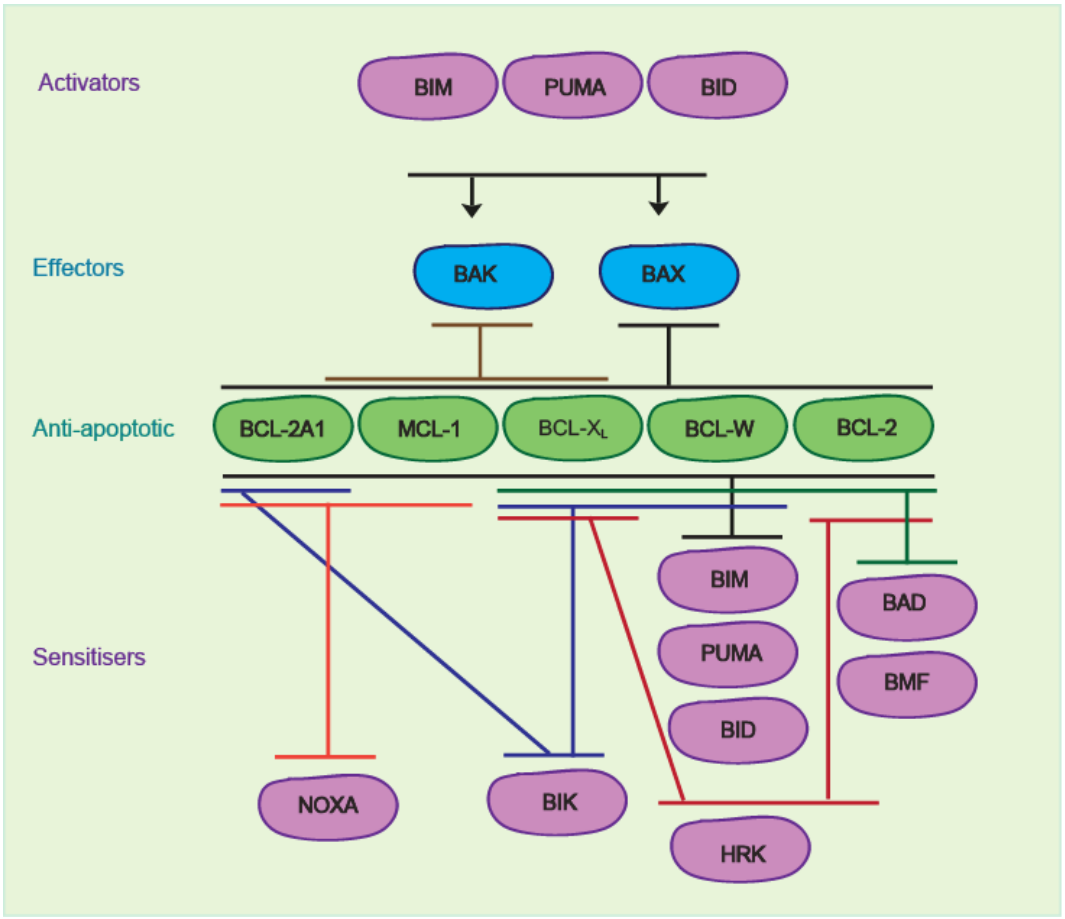

Fig 1.3. The major members of BCL-2 family of proteins and their interactions. Anti-apoptotic BCL-2 family of proteins (green) are suggested to interact with both sensitiser/activator and effector members (purple/blue) to facilitate regulation of apoptosis within a cell. The activator (BH3-only proteins) can interact with the major anti-apoptotic and pro-apoptotic (effector) members, while the sensitiser (BH3-only proteins) exhibit more specific interaction patterns for each anti-apoptotic member. For instance, BCL-X_L, BCL-w and BCL-2 can interact with and inhibit BAD. While, MCL-1 and BCL-2A1 have a unique interaction with NOXA. (Eskes et al. 2000; Letai et al. 2002; Kuwana et al. 2005; Opferman et al. 2003; Certo et al. 2006; Kim et al. 2006; Chen et al. 2005; Leo et al. 1999; Willis et al. 2005)

1.4 Targeting BCL-2 family of proteins for cancer therapy

Over three decades, researches have extensively studied the main regulators of apoptosis as possible targets for cancer therapy. As previously explained, BCL-2 family of proteins have a crucial role in the regulation of apoptosis, and the anti-apoptotic members are highly expressed in several cancers. Therefore, these proteins garnered attention as promising therapeutic targets in cancer. Attempts to target these proteins using antibodies (such as the single-chain anti-BCL-2 antibody (sFvs) used to modulate BCL-2 levels) (Piche et al. 1998), adenoviral systems (such as the overexpression of BAX *gene*) (Kagawa et al. 2000), miRNAs, such as miR24-2, miR-195 and miR-365-2 that result in BCL-2 inhibition, have resulted in generally promising outcomes (Singh & Saini 2011). Moreover, antisense inhibitors have been developed for targeting BCL-2 and moved to clinical trials, such as Oblimersen (also known BCL-2 antisense). This inhibitor has been reported to increase survival rate in refractory or relapsed CLL patients in combination with other anti-cancer agents (O'Brien et al. 2007). In contrast, targeting BCL-2 in small-cell cancer lung (SCLC) by using this approach in clinical trials did not improve patient outcome (Rudin et al. 2008). The most promising approach for targeting the BCL-2 family of proteins has been the use of small molecules (also called BH3 mimetics) that bound to the hydrophobic groove of anti-apoptotic members to block their function and drive cell death (Wang et al. 2000). Some of these BH3 mimetics are in preclinical/ clinical trials or approved for use in patients.

1.4.1 BH3 mimetics - Pan BCL-2 family inhibitors

Gossypol is the first BH3 mimetic that was developed to target multiple members of the BCL-2 family, such as BCL-2, BCL-X_L and MCL-1 (Liu et al. 2009).

In clinical trials for the treatment of CLL (in combination with rituximab) and prostate cancer (in combination with docetaxel), gossypol exhibited gastrointestinal toxicity in patients (Liu et al. 2009; Kang & Reynolds 2009). Derivatives of gossypol, such as apogossypol, apopgossypolone (ApoG2) and TW37 have been developed subsequently (Azmi et al. 2011; Quinn et al. 2011; Arnold et al. 2008; Wei et al. 2011). Similarly, obatoclax (also known GX15-070) was developed to bind all five anti-apoptotic BCL-2 family members (Nguyen et al. 2007). However, later studies showed that obatoclax can induce cell death even in BAX/BAK deficient cells, suggesting that this is non-specific and could potentially have toxic side-effects (Vogler, et al. 2009). In spite of this, obatoclax has been tested in clinical trials for different types of cancer, and was later discontinued due to the neurological toxicity in patients (Goard & Schimmer 2013; Billard 2013). It must be noted that both gossypol family and obatoclax have shown caspase-independent cell death, and thus are non-specific (Vogler, et al. 2009).

This necessitated the development of a more specific BH3 mimetic that selectively targeted multiple members of the BCL-2 family. More effort was spent on discovering such promising BH3 mimetics. An NMR-based screen, for an inhibitor that could disrupt the protein-protein interactions between the pro- and anti-apoptotic BCL2 family members, resulted in several hits, which were then subjected to extensive structural modifications to mimic the structure of the BH3-only protein, BAD, thus resulting in the development of the BAD-mimetic, ABT-737 (Oltersdorf et al. 2005). This inhibitor bound and inhibited BCL-2, BCL-X_L and BCL-w (just like BAD), but not MCL-1 or BCL-2A1 (Oltersdorf et al. 2005). Moreover, ABT-737 induced apoptosis at low nanomolar concentrations (~10 nM) to trigger cytochrome *c* release from the mitochondria of several solid and haematological cancer cell lines. Moreover,

ABT-737 exhibited low nanomolar activity in CLL and follicular lymphoma cells derived from patients, as well as reduced the tumour volume and improved the survival rate in the xenograft models of small cell lung cancer (Oltersdorf et al. 2005).

ABT-263 is structurally similar to ABT-737 and exhibits similar levels of potency, affinity and inhibition of BCL-2, BCL-X_L and BCL-w, while being orally bioavailable. This indicated that ABT-263 could have a great therapeutic anti-tumour activity in clinic (Tse et al. 2008). Due to the promising outcomes, ABT-263 was moved to clinical trials (Phase I and II) in both solid (small cell lung cancer) and lymphoid cancer. However, the usage of ABT-263 in the clinic was limited by on-target thrombocytopenia (as BCL-X_L is essential for survival of the platelets) observed in several patients (Mason et al. 2007).

1.4.2 BCL-2-specific inhibitors

ABT-199 (Venetoclax), a specific inhibitor of BCL-2 was developed for treatment in CLL, as CLL cells depend on BCL-2 for survival (Del Gaizo Moore et al. 2007; Souers et al. 2013). ABT-199 also induced rapid apoptosis in other BCL-2-dependent cell lines, such as non-Hodgkin's lymphoma cell lines, as well as in several xenograft models, in which ABT-199 reduced tumour size and increased survival, all without any indication of thrombocytopenia (Souers et al. 2013). Moreover, administration of ABT-199 in refractory CLL patients resulted in the rapid reduction of cancer burden within 24 h of administration, while sparing platelets (Vogler et al. 2013; Souers et al. 2013). Due to its remarkable success, ABT-199 is the first BH3 mimetic to have been approved by FDA (Food and Drug Administration/US) recently,

for the treatment of refractory CLL with the 17p deletion (Core & Reed 2016; Roberts et al. 2016).

Other BCL-2 specific inhibitors have also been developed in the last few years. S55746 (also called BCL201) was developed as a specific inhibitor of BCL-2 with no significant interaction with BCL2A1or MCL-1 and does not bind BCL-X_L (Casara et al. 2018). It can induce apoptosis through BAX/BAK and caspase cascades activation in mantle cell lymphoma and CLL patients. Moreover, it has a distinct mode of binding with the hydrophobic groove of BCL-2, and is distinct from the binding of ABT-199 to BCL-2 (Casara et al. 2018). This is particularly promising to tackle chemoresistance that could develop in patients to ABT-199 therapy, as a result of mutations in BCL-2 (Casara et al. 2018). This inhibitor is currently being tested in clinical trials (Clinicaltrials.gov; identifiers NCT02920697 and NCT02603445) (Casara et al. 2018).

Disarib is a selective BCL-2 inhibitor that binds BH1 domain of BCL-2 but not other pro-survival members and induces apoptosis in leukemic cell lines and primary patient samples (Lyer et al. 2016). Therefore, the mechanism of action of this inhibitor is unique, when compared to the well-known BH3 targeting domain. It has been reported that Disarib induces apoptosis through the perturbation of BCL-2 and BAK interaction (Vartak et al. 2017).

1.4.3 BCL-X_L specific inhibitors

Several specific inhibitors of BCL-XL have been developed in the last few years. WEHI-539 was the first inhibitor that was identified through a screen of ~100,000 compounds. WEHI-539 induced apoptosis in cells lacking MCL-1 but not

BAK, indicating that this inhibitor induced apoptosis in the absence of MCL-1 (Lessene et al. 2013). Despite being considered as an important leap in the development of BH3 mimetics, WEHI-539 has been banned from being used in the clinic (Lessene et al. 2013; Koehler et al. 2014; Tao et al. 2014). Furthermore, this inhibitor induced thrombocytopenia, by enhanced apoptosis of platelets (Lessene et al. 2013). Efforts to identify other BCL-X_L inhibitors have resulted in the development of A-1155463 (Tao et al. 2014) and A-1331852 (Leverson, et al. 2015). These compounds triggered apoptosis in a BCL-X_L-specific manner at low nanomolar concentrations. The comparison between A-1331852 and A-1155463 indicated that A-1331852 was more potent, more selective and orally available than A-1155463 (Leverson, et al. 2015).

1.4.4 MCL-1 specific inhibitors

Several inhibitors have been developed targeting MCL-1 in the recent past, starting with A-1210477 (Leverson, et al. 2015). This inhibitor was considered as a *bona fide* inhibitor of MCL-1, as it induced apoptosis in MCL-1-dependent cell lines (Leverson, et al. 2015). Although *in vitro* binding affinity of A-1210477 to MCL-1 was low, concentrations required to induce apoptosis *in vivo* were excessively high (micromolar), thus restricting its use in the clinic (Leverson, et al. 2015). Recently developed inhibitors, such as AMG-176 (developed by Amgen) exhibit picomolar binding affinity *in vitro*, while also inducing rapid apoptosis in a variety of cancer cell lines and tumour xenograft models (Caenepeel et al. 2018). Another novel MCL-1 inhibitor, AZD5991 (developed by Astra-Zeneca) exhibits a potent anti-cancer activity and shows regression of tumour in several models of AML and multiple myeloma (Tron et al. 2018). This compound has been used as a single agent or in combination

with venetoclax or bortezomib. Based on these promising observations, AZD5991 has entered phase I clinical trial to treat patients with haematological cancer (Tron et al. 2018). Similarly, S63845 (developed by Servier) induces rapid apoptosis in several cell lines (Kotschy et al. 2016) and synergises with other chemotherapeutic drugs in different cancers including AML (Moujalled et al. 2019), T-cell acute leukaemia (Li et al. 2019) and breast cancer (Merino, et al. 2017).

1.5 Challenges facing BH3 mimetic therapy

The development of BH3 mimetics as anti-cancer agents that target the interaction between anti-apoptotic members and the BH3-only proteins possesses a major influence on cancer therapy (Deng et al. 2007; Lessene et al. 2008; Billard 2012; Davids & Letai 2012). Significant progress has been made in this field and efforts to take these drugs to the clinic are currently being explored. As previously mentioned, ABT-199 has already been approved for use in patients (Roberts et al. 2016) and other BH3 mimetics are being currently trialled in the clinic for several malignancies. At this point, the major challenge that faces BH3 mimetic therapy is chemoresistance. It has been reported that resistance to ABT-199 in haematological cancer can occur *via* different mechanisms, including upregulation of other anti-apoptotic members (BCL-XL or MCL-1) (Tahir et al. 2017; Lin et al. 2016), downregulation of BCL-2 and/or BIM (Bodo et al. 2016) or acquired target-site mutations (Fresquet et al. 2014). Therefore, it becomes important to screen the patients to identify the primary cause of resistance as well as to administer patients with a more appropriate drug to tackle resistance.

Several approaches to predict responsiveness of tumours to different chemotherapeutic agents have been developed. The most studied approach is BH3 profiling, which is a peptide-based technique that measures mitochondrial depolarisation to predict the responsiveness of cancer cells to specific chemotherapeutic agents (Ni Chonghaile et al. 2011). This has been used to screen patients suffering from multiple myeloma ((Touzeau et al. 2016) and T-cell acute lymphoblastic leukaemia (Jain et al. 2016; Ni Chonghaile et al. 2014).

Mito-priming (or mitochondrial profiling) is an improved version of BH3 profiling, and it is designed to assess the basal levels of anti-apoptotic proteins and/or BH3 only proteins. Mito-priming is considered to be a promising technique to classify the dependency of cancer cells to a particular BCL-2 family member, so that patients can be treated with an appropriate and selective chemotherapeutic agent to improve therapy (Ishizwa et al. 2015). For instance, BH3 profiling revealed that AML is a BCL-2-dependent malignancy, thus suggesting ABT-199 to be the most appropriate therapy for AML (Ishizwa et al. 2015). However, subsequent mito-priming of resistant AML cell lines revealed that AML cells could very well depend on BCL-X_L and MCL-1 for survival (Ishizwa et al. 2015).

Targeting BCL-2, BCL-X_L and MCL-1 using BH3 mimetics, either singly or together, induces rapid apoptosis of different cancer cell lines (Leverson, et al. 2015). While haematological malignancies depend on a single BCL-2 family member, solid tumours express multiple members of these proteins, and hence the requirement to target several members together is unavoidable. This could be a problem because many of these proteins share redundancy in their functions and more importantly, have other vital functions, that are required to maintain normal cellular homeostasis. In particular, targeting BCL-2 could result in neutropenia (neutrophils depends on BCL-

2 for survival) (Stilgenbauer et al. 2016; Roberts et al. 2016), whereas targeting BCL-X_L has been shown to cause thrombocytopenia (Roberts et al. 2012; Gandhi et al. 2011; Rudin et al. 2012). Similarly, targeting MCL-1 could exhibit cardiotoxicity (due to the alteration of mitochondrial function) (Wang et al. 2013; Thomas et al. 2013). Therefore, this will have to be taken into consideration while targeting multiple members of the BCL-2 family. However, a careful dose escalation study with these drugs could help us achieve a therapeutic window, at which a combination strategy involving BH3 mimetics could be extremely promising.

1.6 Drug resistance in cancer

Resistance to chemotherapy is the major obstacle for any successful therapy in cancer. Chemoresistance occurs through different mechanisms including drug efflux, drug target alteration, drug inactivation, cell death inhibition, epigenetic effect, DNA damage repair and inherent cell heterogeneity (Housman et al. 2014). Chemoresistance can be innate or acquired. Innate resistance is a type of chemoresistance found in individual cancer cells (Rytelewski 2015). A population of cancer cells could be inherently resistant to any therapy due to the high degree of intratumor diversity (Kessler et al. 2014; Bhang et al. 2015). For instance, hundreds of pre-existing resistant clones to erlotinib (EGFR inhibitor) have been recognised in a lung cancer cell line, HCC827 (Bhang et al. 2015). This suggests that any tumour cell population may include several resistant subclones leading to treatment failure. In contrast, the acquired resistance or evolutionary resistance develops during/after treatment (Bhang et al. 2015). Acquired resistance to anti-cancer drugs limits the success of cancer treatment and may occur even following a robust response to initial

therapy (Housman et al. 2014). Therefore, it is important to understand the mechanism of resistance and identify strategies to overcome resistance once it emerged.

1.7 Amino acid deprivation as a measure to overcome chemoresistance

Amino acids control critical metabolic functions in cancer cells. One of these functions is to support the precursors for protein biosynthesis and control ROS levels inside the cell. Amino acids are classified into essential (valine, phenylalanine, tryptophan, threonine, histidine, leucine, isoleucine, lysine, and methionine) and conditionally essential (glutamine, arginine, glycine, cysteine, proline, and tyrosine). In addition to the previous two, a third group called non-essential amino acids (aspartate, asparagine, glutamate, alanine, and serine) exists and these can be synthesised *de novo* through different reactions (Tabe et al. 2019). Normal cells rely less on amino acid metabolism when compared to cancer cells. Cancer cells rewire cellular metabolism to meet the continuous demands of quick proliferation and growth (Tabe et al. 2019). Amino acids deprivation strategy is used to modulate the activity of different metabolic enzymes and enhance the sensitivity of cells to different chemotherapeutic agents (Lam & Chan 2017).

The immediate response to amino acid deprivation in cells is to increase the expression of amino acid transporters, which in turn would increase amino acid up take (Chen et al. 2014). If this is hampered, the cells may then activate autophagy to facilitate recycling of different proteins to resynthesise non-essential amino acids (Ondera & Ohsumi 2005). However, if the extent of stress is overwhelming, the cell will not be able to achieve homeostasis and as a result, execute the autophagic cell death or apoptosis (Ondera & Ohsumi 2005).

Enormous efforts have been placed on this strategy as a promising therapeutic intervention in cancer. For instance, glutamine deprivation studies has resulted in the development of CB-839, which is a specific glutaminase inhibitor and is currently used in multiple clinical trials to treat different types of cancer (Altman et al. 2016). Another example is that of asparagine depletion by L-asparaginase, which is used as a therapeutic approach to treat acute lymphoblastic leukaemia in clinic (Panosyan et al. 2004). Similarly, strategies have been conceived to modulate levels of other amino acids, including serine and arginine, as these play important roles in cellular proliferation and nucleotide synthesis (Feun et al. 2008; Gravel et al. 2014; Mattaini et al. 2016).

1.8 Aims of this study

Major efforts over the last decade have resulted in the extremely promising group of small molecule inhibitors called BH3 mimetics in cancer therapy. As previously mentioned, the major challenge that needs to overcome in relation to BH3 mimetic therapy is chemoresistance. Tackling this problem becomes necessary, as the resistance is now starting to emerge in haematological cancers. Therefore, this study is aimed at exploring the mechanism of resistance to BH3 mimetic-mediated apoptosis and identifying ways to overcome resistance. In order to accomplish that, the following questions have been addressed in this thesis:

1. Do cell lines derived from haematological malignancies acquire rapid resistance to BH3 mimetics? Can they be overcome by co-administration of multiple BH3 mimetics?

2. Since cancer cells depend on glutamine as an energy source, could targeting glutamine metabolic pathways enhance sensitivity to BH3 mimetics, and overcome chemoresistance?

3. Could strategies modulating glutamine metabolism to overcome resistance in haematological cancers be extended to solid tumours?

Chapter 2

Materials and Methods

2.1 Cell lines

Table 1. Cell lines used in the study, and other information pertaining to the procurement and culture of these cells. All the media were supplemented with 10% foetal bovine serum (FBS) (Life Technologies Inc. Warrington, UK).

Medium	Cell lines and origin	Source
Roswell Park Memorial Institute (RPMI) 1640 Cat. No. 61870044 Life Technologies Inc.	MAVER-1 (mantle cell lymphoma)	Dr. J. Slupsky (University of Liverpool, UK)
	K562 (chronic myeloid leukaemia; CML)	Prof. R. Clark (University of Liverpool, UK)
	H929 (multiple myeloma)	ATCC (Middlesex, UK)
	Peripheral blood samples from CLL patients	Prof. J.S. Dyer (University of Leicester Haematological Tissue Bank, UK)
Dulbecco's modified Eagle Medium (DMEM) Cat. No. 31966047 Life Technologies Inc.	Mouse fibroblast L	MRC -Toxicology Unit, Leicester, UK
	UM-SCC-1 (HNSCC/Oral cavity)	Prof. T. Carey (University of Michigan, USA)
	UM-SCC-11B (HNSCC/Larynx)	
	UM-SCC-17A (HNSCC/Larynx)	
	UM-SCC-74A (HNSCC/Oropharynx)	
	UM-SCC-81B (HNSCC/Oropharynx)	
McCoy's 5A Cat. No. 1978477 Life Technologies Inc.	A253 (HNSCC/Oral cavity)	ATCC
Eagle's Minimum Essential Medium (EMEM) Cat. No. RNBG8005 Sigma-Aldrich (Gillingham, UK)	FaDu (HNSCC/Hypopharynx)	ATCC
	Detroit562 (HNSCC/Hypopharynx)	

2.2 Patients-derived primary cells

According to ethics committee approval (06_Q2501_122) from Leicester Haematological Tissue Bank and the patient consent, the peripheral blood samples were obtained from CLL patients, registered in a Phase 1/2 a Study of ABT-263 (Navitoclax) with relapsed or resistant CLL (NCT00481091). In this trial, patients were administered increasing doses of ABT-263 for a specific number of days, which is categorised as the lead-in period. Following this, patients were dosed with ABT-263 over 5 cycles of treatments, in which each cycle was continued for 7 days of treatment followed by 21 days drug free. The blood samples were collected 4 h after dosing of ABT-263 during the day 1 of lead-in-period (L1D1), cycle 1 day1 (C1D1), cycle2 day1 (C2D1), cycle3 day1 (C3D1), cycle4 day1 (C4D1) or cycle5 day1 (C5D1). CLL cells isolated from these samples were then assessed for potential resistance to ABT-263.

Since CLL cells are not viable for more than 16-24 hours in culture, it was critical to adopt a co-culture system involving mouse fibroblast L cells to extend the lifespan of CLL cells *in vitro*. For this, the mouse fibroblast L cells were exposed to 75 Gy irradiation and seeded in 12-well plates (3×10^5 cells/well). After 24 h, the media was aspirated and washed with warm PBS (ThermoFisher Scientific, MA, USA). Then, 1.5×10^6 CLL cells were added per well to the irradiated mouse fibroblast L cells and removed after 24 h, by gentle resuspension with RPMI, for treatments with relevant drugs.

2.3 Cell culture

Cells were cultured in their appropriate media as listed in Table 1. The growth conditions were set at 37 °C and 5 % CO2. For haematological cell lines, cells were passaged, and media replaced every 48 h. For adherent cell lines, the media was removed, the cells washed once with warm PBS, incubated with 0.05 % trypsin-EDTA (ThermoFisher Scientific) at 37 °C for 5 minutes, followed by the addition of fresh media and passaged in a new dish according to the doubling time of each cell line. For 3D spheroid culture, two HNSCC cell lines (UM-SCC-17A and FaDu) were seeded at the density of 500 cells /100 μL in a well of a 96-well polystyrene round bottom microplates (Cell carrier spheroid ULA, PerkinElmer, UK), incubated at 37 ^{o}C with 5% CO_2 for 72 hours (3 days), then exposed to the relevant drugs for a period of 12 days. Images were captured on days 0, 3, 6, 9 and 12, using Floid (EVOS Floid Cell Imaging station, Life Technology, UK) and changes in spheroid volumes measured using a plug-in for imageJ (public software, National Institutes of Health, Maryland, USA). Subsequently, the spheroid volume was calculated by the mathematical equation: Volume = (4/3) x π(diameter/2)^3 (unit: μm^3).

2.4 Cell authentication

By using the DNeasy kit (Qiagen/ Cambridge, UK), the genomic DNA was isolated from all cell lines that are used in this study. The short tandem repeat (STR) profiling to detect the authenticity of the cell lines were performed at the Cell Line Authentication Facility/ University of Liverpool by using GenePrint® 10 (Promega, Madison, WI, USA).

Table 2. Percentage of authenticity (match) of cell lines with established database.

Cell line	% Match with established databases
MAVER-1	94%
K562	83% (potential contamination with another blast crisis CML cell line)
H929	100%
Mouse fibroblast L	100%
UM-SCC-1	100%
A253	Newly purchased/ Not-tested
UM-SCC-11B	100%
UM-SCC-17A	100%
UM-SCC-74A	100%
UM-SCC-81B	100%
FaDu	Newly purchased/ Not-tested
Detroit562	Newly purchased/ Not-tested

2.5 Generation of resistance models

Four resistance models to BH3 mimetic-mediated apoptosis were established in three different haematological cell lines: MAVER-1, K562 and H929. In the **first**

resistance model, parental cells (depicted as A) of MAVER-1, K562 and H929 were exposed to their appropriate BH3 mimetics, ABT-199 (10 nM), A-1331852 (10 nM) or A-1210477 (5 μM), respectively for 24 h. The cells were washed once with warm PBS and then resuspended in fresh media and incubated for 2 weeks (2 W) without drug (recovery period). This resulted in the generation of cells, labelled B. The resulting cells were exposed to their appropriate BH3 mimetics for further 24 h, and the process repeated to result in C. The most resistance cells E were obtained by repeating the explained procedure further two times. This model of resistance was also used to develop resistance to Ibrutinib in MAVER-1.

In the **second resistance model**, parental cells (depicted as A) of MAVER-1, K562 and H929 were exposed once to their appropriate BH3 mimetics, ABT-199 (10 nM), A-1331852 (10 nM) or A-1210477 (5 μM), respectively for 24 h, centrifuged and resuspended with fresh media. The cells were incubated for 2 weeks without the addition of any extra drug, resulting in cells labelled, A1. Every 2 weeks (2W), the resistance was checked, cells collected, and labelling changed to A2, A3 and A4 respectively.

In the **third resistance model**, parental cells (depicted as A) of MAVER-1, K562 and H929 were exposed to their appropriate BH3 mimetic (1 nM) for 5 days (5 d) resulting in the cells considered as A-a, then centrifuged and washed with warm PBS. These cells were further exposed to their appropriate BH3 mimetic (2 nM) for a further 5 days (5 d) resulting in cells considered as A-b. This procedure was repeated twice more, with concentrations (4 and 8 nM), resulting in cells depicted as A-d.

In the **fourth resistance model**, the parental cells of MAVER-1, K562 or H929 were exposed to BH3 mimetic (1 nM) for 2 days (2 d) followed by 3 days (3 d) without drug, resulting in the cells considered as A-i. These cells were further exposed

to their appropriate BH3 mimetic (2 nM) for a further 2 days resulting in cells depicted as A-ii. This procedure was repeated twice more, with concentrations (4 and 8 nM), resulting in cells considered as A-iv.

2.6 Reagents and inhibitors

Table 3. The inhibitors used in this study, along with their target, concentration, time of exposure and source.

Inhibitor	Target	Concentration	Source
ABT-199	BCL-2	10 nM	Selleck (TX, USA)
A-1331852	BCL-X_L	10 - 100 nM	Abbvie (IL, USA)
A-1210477	MCL-1	5 -10 μM	Abbvie
ABT-263	BCL-2, BCL-X_L and BCL-W	50 nM	Abbvie
S63845	MCL-1	100 nM	Selleck
Ibrutinib	BTK	10 μM	Selleck
GPNA	SLC1A5	5 mM	Insight Biotechnology (Middlesex, UK)
CB-839	GLS	10 μM	Selleck
Azaserine	GFAT	25 μM	Cambridge Bioscience (Cambridge, UK)
EGCG	GLUD1	50 μM	Selleck
AOA	Aminotransferase	500 mM	Sigma-Aldrich
SB 204990	ACLY	1 μM	Tocris (Abingdon, UK)
GSK2194069	FASN	100 nM	Tocris
Simvastatin	HMGR	250 nM	Selleck
Atorvastatin	HMGR	10 μM	Tocris
Pitavastatin	HMGR	1 μM	Selleck
MG-132	Proteasome	10 μM	Active Biochem (Hong Kong, USA)
Z-VAD.FMK	Caspases	25 μM	Selleck

2.7 Antibodies

Table 4. Antibodies used in the study along with relevant information. BD stands for BD BioSciences (California, USA), CST stands for cell signalling, SC stands for Santa Cruz Biotechnology (CA, USA), abcam stands for Abcam (Cambridge, UK)

and Millipore stands for Calbiochem/Merck (Darmstadt, Germany). ICC stands for immunocytochemistry, WB stands for western blots, IHC immunohistochemistry and IP Immunoprecipitation.

Antibody	Use	Epitope	CatLog No.	Source
Apoptosis				
Cytochrome *c*	ICC	Around AA 62	556432	BD
Caspase-9	WB	Around D315	9502	CST
Caspase-3	WB	Full length	9662	CST
PARP-1 (F-2)	WB	AA 764-1014	sc-8007	SC
BCL-2 Family				
BCL-2 (D55G8)	WB	Around G47	4223	CST
BL-X_L	WB	Around D61	2762	CST
MCL-1	WB	AA 89-139	SC-819	SC
BCL-W(31H4)	WB	Full length	2724	CST
BFL-1/A1	WB	Full length	4647	CST
BAX(2D2)	WB	AA 3-16	SC-20067	SC
BAK (G23)	WB	Internal	SC-832	SC
BIM(C3435)	WB, IP	Around P25	2933	CST
BAD	WB	Around S112	9292	CST
PUMA	WB, IP	C-terminus	4976	CST
NOXA	WB	Full length	OP180	Calbiochem
BID	WB	Cleaved site	2002	CST
Metabolism				
SLC1A5	WB	AA 217-266	ab58690	Abcam
GLS	WB, IHC	AA 50-150	ab156876	Abcam
GFAT	WB	AA 600-700	ab125069	Abcam
GLUD1	WB	AA 64-366	ab153973	Abcam
IDH2(D8E3B)	WB	Around V195	56439	CST
IDH3A	WB	AA 37-86	ab58641	Abcam
ACO2(D6D9)	WB	Around G540	6571	CST
ACLY	WB	Around V34	13390	CST
FASN	WB	C-terminus	ab22759	Abcam
HMGR	WB	AA 400-500	ab174830	Abcam
Miscellaneous				
GAPDH (FL-335)	WB	Full length	sc-25778	SC

2.8 siRNA knockdowns

Table 5. siRNAs (Qiagen Ltd, Manchester, UK) used in the study.

SiRNA	Catalog No.	Targeted sequence
SLC1A5	SI00079730	5'-CACGCTGCCGCTGATGATGAA-3'
GLS #1	SI03155019	5'-ATGGTGGTTTCTGCCCAATTA-3'
GLS #2	SI04185678	5'-AAGGAGATTCTGACAACGGGA-3'
GFAT	SI03246355	5'-CTGCCTGATTTGATTAAGGAA-3'
GLUD	SI02654743	5'-CGGGTGCATCTGAGAAAGACA-3'
IDH2	SI02654820	5'-TAAGACCGACTTCGACAAGAA-3'
IDH3	SI00300524	5'-AACGTCACTGCCATTCAAGGA-3'
ACO2	SI03019037	5'-CGGGAAGACATTGCCAATCTA-3'
ACLY	SI02663332	5'-CCGAGTGAAGTCGATAAACAA-3'
FASN	SI00059752	5'-CAGGCTTCAGCTCAACGGGAA-3'
HMGR	SI00017136	5'-CCGAGCCTAATGAAAGGGAAA-3'
Control siRNA	1027310	5'-AACTGGGGGAGGATTGTGGCC-3'

Cells were counted, plated based on their doubling time and then transfected with 10 nM of siRNA prepared in Opti-Mem Reduced Serum media in presence of Interferin (PolyplusTransfection Inc, NY) and incubated for 72 h.

2.9 Glutamine uptake

Glutamine uptake experiments were carried out using a slightly modified of glutamine uptake protocol (Carr et al. 2010). Briefly, 2 x 10^6 cells were spun-down, washed once with PBS, resuspended in glutamine-free medium and incubated at 37 °C for 2 hours. Following, the cells were spun-down and resuspended in uptake medium (consist from 50 µl of glutamine-free medium in presence of 1 µCi (45 nmol) of L-2,3,4-[^{3}H]-glutamine), then added on the top layer of 0.7 µl microfuge tube, containing 25 µl of 20% perchloric acid and 8% sucrose in the bottom layer and 200

μl of 1-bromododecanein as the intermediate layer and incubated at room temperature for 10 minutes to allow the cells to take up the radiolabelled glutamine. Then, cells were spun-down in a microcentrifuge at 14000 rpm for 1 minute, to allow cells to pass through the intermediate and the bottom layers. The reaction was then stopped by removing the layers and keeping the pelleted cells. Following this, the cells were lysed using 25 μl of 10% Triton X-100, added to scintillation cocktail and counted by Tri-Carb scintillation counter (Graphic Measures International, MN, USA).

2.10 Glutamine deprivation and supplementation studies

For glutamine deprivation experiments, cells were washed gently with warm PBS and re-suspended in SILAC RPMI 1640 Flex media (Life Technologies Inc.), supplemented with FBS. This media lacked glucose and glutamine and hence, also supplemented with 2 mg/mL glucose to obtain glutamine-free media. For cells cultured in DMEM, glutamine-free DMEM (Life Technologies Inc.), supplemented with FBS and 5 mg/mL glucose was used. The different metabolic supplementations (as listed in Table 6) were added to the glutamine-deprived cells and experiments performed.

Table 6. The metabolic supplements used in this study, along with their concentrations, time of exposure and source.

Supplementation	Concentration	Time	Source
L-glutamine	2 mM	16 h	Life Technologies Inc.
Dimethyl α-Ketoglutarate	4 mM	16 h	Sigma-Aldrich
Oxaloacetic acid	4 mM	16 h	Sigma-Aldrich
Citrate	4 mM	16 h	Sigma-Aldrich
Pyruvate	4 mM	16 h	Life Technologies Inc.
Sodium Palmitate - BSA*	50 uM	24h	Sigma-Aldrich

* In order to prepare 100 mM stock of sodium palmitate-BSA, the powder was dissolved in autoclaved distilled water at 70 °C. Then, the resulting stock was mixed with an appropriate amount of warm fatty acid-free- BSA (10%) under sterile conditions to get the final concentration 10 mM.

2.11 Apoptosis measurements - Flow cytometry (Annexin-PI and TMRE)

To measure the extent of apoptosis, cells were collected and resuspended with 200 µl of 1X Annexin-V buffer (containing 10 mM HEPES, 140 mM NaCl, 2.5 mM CaCl2, pH 7.4) and Annexin-V (1:20,000), made in-house and 5 µl of PI (propidium iodide). The extent of cells undergoing apoptosis was quantified through the Attune NxT flow cytometer (ThermoFisher) using the blue laser for Annexin-V and red laser for PI. The voltage settings and cells scatter were determined according to the cells type used. 10,000 events were recorded per sample and for each experiment three independent biological replicates analysed. For mitochondrial depolarisation, cells were resuspended in 500 µl of medium containing TMRE (Tetramethylrhodamine, ethyl ester; 200 nM/ mL) and passed through the flow cytometer using the blue laser to quantify the extent of mitochondrial depolarisation.

2.12 Clonogenic assays

Cells were seeded in 12 well plates at different densities according to the cell type. After 24 h, the cells were exposed to the relevant inhibitors. Colonies formed over a 7-day period were fixed at room temperature using acetic acid/ methanol (1:7 ratio) for 5 minutes and stained using crystal violet (20ml Methanol, 80ml water, 0.5g crystal violet) for 1 hour. The plates were then gently rinsed with tape water and dried.

Colonies were counted by using Gelcount tumour colony counter (Oxford Optronix, Abingdon, UK). The capacity to form colonies was calculate with these two equations:

Plating Efficiency= Colony counted / Cells plated

% Survival Fraction= Colony counted / (Cells plated x Plating Efficiency) x100.

2.13 Transmission Electron microscopy

For Transmission electron microscopy, 20 x 10^6 cells were collected and washed twice with PBS. The cells were then fixed using (2.5%) glutaraldehyde in phosphate buffer (PB; 0.1 M) pH 7.4 in a Bio-wave (PELCO Bio-wave, Ted Pella Inc, USA) for 3 minutes (Protocol 1: 1 minute On, 1 minute Off and 1 minute On/ 20 Hg chamber), washed 3 times in PB and pelleted. Following this, cell pellets were resuspended with 100-200 µl Agarose (1%), kept on ice for 30 minutes and sliced to very thin blocks (around 0.5 mm^3 blocks). For reduced osmium staining, Osmium tetra oxide (2%) in DdH_2O (Double distilled water) and Potassium Ferrocyanide (1.5%) in DdH_2O (mixed at the time of adding) were added to the blocks, then processed in Bio-wave for 1 minute (Protocol 2: 20 seconds On-20s off, 20s On / 20 Hg chamber) and washed 3 times (5 minutes for each was with DdH_2O). The blocks were then incubated with Thiocarbohydrate (1%), prepared in DdH_2O, on the rotator for 5 minutes and washed with DdH_2O 3 times (5 minutes each). Following this, the blocks were incubated again with Osmium tetra oxide (2%) at Bio-wave for 1 minute using Protocol 2 (mentioned above) and washed 3 times (5 minutes each). The blocks were then stained with Uranyl acetate (1%) at Bio-wave for 1 minute using Protocol 2 and washed 2 times (3 minutes each). For dehydration step, the blocks were immersed in increasing concentrations of acetone (30, 50, 70 and 90 %) for 3 minutes each, and

then then twice with 100% acetone for 5 minutes (each immersion carried out on ice). For the final step of infiltration, equal volume of TAAB (hard resin; 100%) and acetone (100%) were mixed, added to the blocks in the Bio-wave and subjected to the infiltration protocol for 3 minutes. Following this, the infiltration step was repeated for further 3 minutes. Then, fresh resin was added in the rubber coffin mould, the blocks placed on the end in each side of the chambers, baked at 65 ^{o}C for 24 h.

Following this, the blocks were sharpened to be used in the microtome (Leica). Then by using specially-made glass blades on the microtome, each block was cut to make a proper square, with the dimensions of 350 microns on each side. The blocks were then sectioned using diamond knife (Agar Scientific, Essex, UK) to obtain finer sections and finally placed on pre-processed grids. Subsequently, the grids were stained with Uranyl acetate (4%) at the room temperature and dark for 1 minute, washed 20 times with DdH_2O, and then scanned using electron microscopy (TECNAI 200 Kv transmission electron microscope).

2.14 SDS-PAGE immunoblotting

SDS-PAGE (Sodium dodecyl sulfate polyacrylamide gel electrophoresis) was carried out using in-house made gels. Each gel consisted a stacking gel (made up of Tris-HCL 0.5 M, 0.4% SDS, pH 6.8) and a resolving gel (made up of 1.5 M Tris-HCL, 0.4% SDS, pH 8.8), which are polymerised using Protogel acrylamide (30%) (National Diagnostics, GA, USA), 10% APS (ammonium persulphate) and TEMED (Tetramethylethylenediamine).

The cells under study were harvested and pelleted at 2000 rpm for 5 minutes. Then, the protein lysates were prepared by incubating the pellets with RIPA buffer

(radioimmunoprecipitation assay) (10 mM Tris-HCl (pH 8.0), 1 mM EDTA, 0.5 mM EGTA, 1% Triton X-100, 0.1% sodium deoxycholate, 0.1% SDS, 140 mM NaCl) containing protease inhibitor tablet (Roche, Basel, Switzerland) and MG-132 (20 μM), on ice for 15 minutes and then sonicated using a Bandelin SONOPULS ultrasonic homogeniser (Bandelin, Berlin, Germany). The resulting cell lysate was centrifuged once (2000 rpm) for 3 minutes. Following this, protein concentration was estimated by preparing 1X of BioRad Protein Assay Dye Reagent (BioRad, CA, USA). 1 ul of each cell lysate was added to 1 mL of the BioRad reagent and the absorbance (OD600, optical density at 600 nm) measured by using spectrophotometer (Eppendrof, Hamburg, Germany). The protein concentration for each sample was compared to a standard known concentration of BSA. Then, protein lysate (10-50 μg) was mixed with 4x NuPAGE LDS Sample buffer (Life Technologies), heated for 5 minutes at 70°C (ThermoFisher Scientific) and centrifuged at 2000 rpm for 3 minutes.

Samples were then loaded in SDS-PAGE gel, and the electrophoresis carried out using the electrode buffer (25 mM Tris-HCL, 192 mM glycine, 10% SDS) at 130 V (Voltage) for 90 minutes. Following this, the separated proteins were transferred to Amersham™ Protran™ 0.45 μM nitrocellulose blotting membranes (GE Healthcare, Germany) with supporting sandwich, using the transfer buffer (25 mM Tris-HCL, 192 mM glycine, 20% methanol) at 100 V (Voltage) for 60 minutes. Subsequently, membranes were blocked in semi-skimmed milk (5%) prepared in 1X TBS-T (10X stock contains: Tris-buffered saline with 0.1% Tween, 20 mM Tris-HCL, 150 mM NaCl, 0.1% Tween-20) for 1 hour, rinsed with TBS-T and incubated with primary antibodies (1:1000 diluted in TBS-T) at 4°C overnight. Then, membranes were rinsed 3 times with TBS-T and incubated with secondary antibody (anti-mouse or anti rabbit IGg HRP-linked 1:2000 diluted in TBS-T) (Cell signalling technology) at room

temperature for 1 hour. Following, the membranes rinsed 3 times for 15 minutes (for each time 5 minutes) in TBS-T. The developing step was carried out using ECL reagents (GE Healthcare, Germany) and imaging the protein band using ChemiDoc imagin system (BioRad).

2.15 Immunoprecipitation

Immunoprecipitation study was performed using protein G or A Dynabeads (25µl) (Thermo Fisher scientific) rinsed 3 times with 1 mL of PBS-T (PBS-Tween 0.05%). On the rotator, the beads were incubated with 2-5 µg at 4°C for 4 h. Then, the beads were washed 2 times with 0.2 M triethanolamine (Sigma-Aldrich). Subsequently, the conjugation step of antibody-beads was cross-linked using 5.4 mg/ml dimethylpimelidate (Sigma-Aldrich) at room temperature with mixing for 30 minutes. The reaction of cross-linking was then mixed at room temperature with 50 mM Tris-HCL pH 7.5 for 15 minutes for neutralisation. Following this, the cross-linking reaction was washed 3 times with PBS-T and resuspended with (500 µg) cell lysate. In order to prepare cell lysate for immunoprecipitation, cell pellets were resuspended in 1% CHAPS lysis buffer (150 mM KCl, 50 mM HEPES (pH 7.4) 1 % CHAPS in addition to 20 µM MG-132 and a protease inhibitor tablet). The mixture was incubated on ice for 30 minutes and centrifuged at max-speed (14000 rpm) for 10 minutes. The cell lysate was then incubated with the beads-antibody complex overnight at 4°C. Then, the flow through was collected and kept. The beads were rinsed 3 times with TBS-T then incubated with 2x loading dye and heated at 55 °C for 10 minutes on the shaker to elute the protein. Subsequently, the input samples were prepared from the same lysates that employed for immunoprecipitation. Following

this, according to the protocol of immunoblotting was described previously, the eluted products (immunoprecipitation products) and the input samples loaded onto the gels.

2.16 Immunocytochemistry

Suspension (0.1×10^6) cells were collected and resuspended with PBS. 50 µl of the mix was placed on the polysine™ adhesion slide (Menzel-Glaser, UK) and left for 5 minutes for the cells to attach to the slides. Cells were then fixed with paraformaldehyde (4%) for 5 minutes and permeabilised with Triton X-100 (0.5%) diluted in PBS for 10 minutes, after removing the fixative by Pasteur pipette. Subsequently, the cells were incubated with primary antibody (anti-cytochrome *c*) diluted 1:500 in 3% BSA at room temperature for 1 hour and removed then incubated with an Alexa-Fluor fluorescently-conjugated secondary antibody (Life Technologies) diluted 1:2000 in 3 % BSA for 1 hour and removed. Following this, the cells were washed gently with distilled water, then sealed with coverslips using Polymount (Polysciences, PA, USA). The cytochrome *c* release was counted for each group using light microscope- 1000X objective lens with oil immersion. The equation used to analyse the data is: % Cytochrome *c* release = (Cyto/Cyto+Mito)x100.

2.17 Immunohistochemistry

This work was done in collaboration with Dr. Rachel J. Carter (Dr Varadarajan's lab at the University of Liverpool). The explants were surgically removed (as a primary treatment) from SCCHN (Oral cavity tumor) patients with notified consent under REC10/H1002/53, incubated overnight with DMEM, containing 10% FBS (Life Technologies Inc), 1% pen-strep (ThermoFisher) and 1% amphotericin B (Sigma-Aldrich) at 37 °C, and then exposed to increasing concentrations of CB-839 for 72 h. Following this, the explants were fixed in 4%

paraformaldehyde for 24 h at 4 °C. The samples were processed for the dehydration step using Histocore PEARL Tissue processor (Leica). Samples were paraffin-embedded and by using a microtome, the embedded tissues were cut into 5 µm thick sections, mounted on slides and then, the slides were baked overnight at 37 °C. The staining steps were performed using Bond RXm autostainer (Leica). Briefly, all the slides were deparaffinised, incubated with primary antibody (cleaved PARP) and non-specific linker HRP to amplify the signal, which was then detected using DAB+ chromogen. The sectioned were stained using haematoxylin, dehydrated and cleared. Then, all the slides were mounted using EcoMount (Biocare Medical). The images were captured at 20x magnification by Nikon Eclipse E800 microscope and MetaMorph 6.3r7 software or through using scanning at 40x magnification by an Aperio slide scanner (Leica). Similar steps were used to prepare TMA slides.

2.18 TMA analysis

This analysis was done in collaboration with Dr. Rachel Carter. The TMA (tissue micro array) slides were obtained from Liverpool Tissue Biobank, and the sections stained with the appropriate antibodies and mounted by Dr. Rachel J. Carter. Following this, the TMA slides were scanned, and the images uploaded to Qpath (Quantitative Pathology software, Queen's University, Belfast) (Bankhead et al. 2017). Then, TMAs were analysed for the intensity of staining of GLS in the tumour and normal tissues to get the H-scores. Thus, obtained H-scores, were then used in combination with the survival information of the patients to create Kaplan-Meier estimators.

2.19 Zebrafish studies

These studies were also done in collaboration with Dr. Rachel Carter. Zebrafish studies were completed under the approval of the University of

Liverpool/Animal Welfare and Ethical Review Body, using the strain known as Nacre *ubiq*:secAnnexinV-mVenus embryos (Morsch et al. 2015), obtained from the University of Manchester/Biological Services Facility. These embryos were incubated at 28 °C in egg water (consisting 60 µg/ml tropic marin salt in distilled water) for 48 hpf (hours post-fertilisation). Then, the fish were transferred to a humidified light-cycling incubator (14 h on and then 10 h off) at 34 °C. Following this, at 72 hpf, fish in 5 mL of egg water were exposed to increasing concentrations of CB-839 (0, 0.5, 5 and 10 µM). Fish were imaged and mortality rate was assessed up to 120 hpf (for each treatment, the number of alive versus dead fish were quantified). Finally, fish were euthanised by 120 hpf using 250 µg/ml MS-222 (Ethyl 3-aminobenzoate methanesulfonate from Sigma-Aldrich) in egg water.

2.20 Statistical analysis

One-way ANOVA multiple comparisons and Fishers LSD test were carried out to compare different time point groups exposed to BH3 mimetics in cell validation studies, comparing sensitive and resistant cells in overcoming resistance studies. One-way repeated measures ANOVA with Fishers LSD test were performed for CLL patient samples. Two-way ANOVA multiple comparisons and Fishers LSD test were carried out for colony formation assay studies and 3D-spheroid studies. Log rank/match SPSS and SAS were performed for survival probability and the number of the patients at risk in TMA analysis studies. The statistics were analysed using GraphPad Prism 6 software (La Jolla,CA). The asterisks depicted in the plots throughout this thesis represent *p* values: * for $p \leq 0.05$, ** for $p \leq 0.01$ and *** for p ≤ 0.001.

Chapter 3

Haematological cancer cell lines develop rapid resistance to BH3 mimetic-mediated apoptosis

3.1 Introduction

Numerous studies in cancer biology have suggested that changes in several cell signalling pathways are responsible for carcinogenesis, thus making the critical players in these pathways the most vital targets for the development of new therapies (Vogelstein & Kinzler 2004; Hanahan & weinberg 2000). One of these pathways is the intrinsic apoptotic pathway, which is regulated at the level of mitochondria by the BCL-2 family of proteins. The anti-apoptotic members of this family primarily antagonise apoptosis by binding and inhibiting the pro-apoptotic BH3-only proteins (Wilson et al. 2010), thus inhibiting mitochondrial outer membrane permeabilization (MOMP), cytochrome *c* release and apoptosis. It has been found that the anti-apoptotic BCL-2 family proteins are highly expressed in different types of cancers, and thus are candidates for promising chemotherapeutic targets (Youle & Strasser 2008). This has resulted in the discovery of several BH3 mimetics, which target the BCL-2 family of proteins to result in apoptosis.

ABT-737, the first *bona fide* BH3 mimetic to be characterised (Oltersdorf et al. 2005) and its orally bio-available analogue, ABT-263 (Navitoclax) target BCL-2, BCL-W and BCL-X_L (Tse et al. 2008). This was soon followed by the discovery of ABT-199 (Venetoclax), which was established as a specific BCL-2 inhibitor (Souers et al. 2013) and has recently been approved by the FDA to treat chemorefractory CLL patients with a 17p depletion (Roberts et al. 2016). In addition, ABT-199 is used in many other clinical trials in both solid tumours and other BCL-2-dependent haematological malignancies (Ashkenazi et al. 2017). Moreover, selective inhibitors of BCL-X_L (A-1331852) and MCL-1 (A-1210477; AMG 176; AZD5991; S63845) have recently been identified (Leverson, Phillips, et al. 2015; Leverson, Zhang, et al. 2015; Caenepeel et al. 2017; Tron et al. 2018; Kotschy et al. 2016). While A-1331852

is a very potent BCL-X_L-specific inhibitor, which triggers extensive apoptosis in CML (Lucas et al. 2016), A-1210477 is a specific MCL-1 inhibitor that induces apoptosis in H929 cells (Milani et al. 2016). Similarly, AMG176, AZD5991 and S63845 also demonstrate significant potency and specificity in targeting MCL-1 in different malignancies (Caenepeel et al. 2017; Tron et al. 2018; Kotschy et al. 2016).

The major obstacle facing cancer chemotherapy is drug resistance, which significantly limits the clinical response of an otherwise promising drug. Acquired resistance is commonly associated with long term treatment and is one of the important ways by which cancer cells escape from the host defence mechanisms (Borst et al. 2000). Cancer cells that are resistant to a particular drug can display cross-resistance to numerous other drugs, with different chemical structures and modes of actions. Emergence of multidrug resistance results in more aggressive disease and significantly reduces survival rates. This could be due to the upregulation of drug transporters (Borst et al. 2000), antiapoptotic proteins (Huang et al., 1997) and by many other mechanisms. Recently, microRNAs were also shown to be involved in chemoresistance (Kovalchuk et al. 2008).

In this chapter, selective BH3 mimetics, namely ABT-199, A-1331852 and A-1210477 will be tested for their ability to induce distinct hallmarks of apoptosis in three haematological cell lines, MAVER-1 (derived from mantle cell lymphoma), K562 (derived from CML) and H929 (derived from multiple myeloma). The cell lines are chosen based on their previously-reported dependence on distinct BCL-2 family of proteins for survival. Upon validation of the extent of apoptosis induced by specific BH3 mimetics in the relevant cell lines, different resistance models to the specific BH3 mimetics will be established to identify the underlying mechanism(s) of chemoresistance.

3.2 Results

3.2.1 BH3 mimetics induce rapid apoptosis in haematological cancer cell lines

The anti-apoptotic BCL2 proteins prevent apoptosis and protect mitochondrial integrity by inhibiting MOMP and the downstream caspase activity. In order to investigate this, three haematological cancer cell lines, MAVER-1 (BCL-2 dependent), K562 (BCL-X_L dependent) and H929 (MCL-1 dependent) were exposed to their specific BH3 mimetics namely ABT-199, A-1331852 and A-1210477 respectively. Exposure of ABT-199 in MAVER-1 cells resulted in a rapid time-dependent increase in phosphatidylserine (PS) externalisation, mitochondrial depolarisation and cytochrome *c* release (Fig 3.2.1 a). Similarly, exposure of A-1331852 in K562 cells resulted in a rapid time dependent apoptosis (Fig 3.2.2 a). However, the extent of mitochondrial depolarisation was marked by a sharp decrease following an initial increase at the 0.5 h time point, showing a reversibility in mitochondrial depolarisation in the A-1331852 treated cells (Fig 3.2.2 a). This was unique to K562 and A-1331852, as this reversibility was not observed in ABT-199-treated MAVER-1 cells or A-1210477-treated H929 cells (Fig 3.2.1 a, 3.2.2 a and 3.2.3 a). A-1210477 induced a rapid time-dependent increase in PS externalisation and cytochrome *c* release, as well as modest mitochondrial depolarisation in H929 cells (Fig 3.2.3 a).

Next, changes in mitochondrial morphology were assessed following the exposure to specific BH3 mimetics in the relevant haematological cancer cell lines. The results indicated that massive mitochondrial morphological changes, characterised by mitochondrial matrix swelling, severe alteration of cristae structure and mitochondrial outer membrane rupture, were observed following exposure to BH3 mimetics (Figs 3.2.1 b, 3.2.2 b and 3.2.3 b).

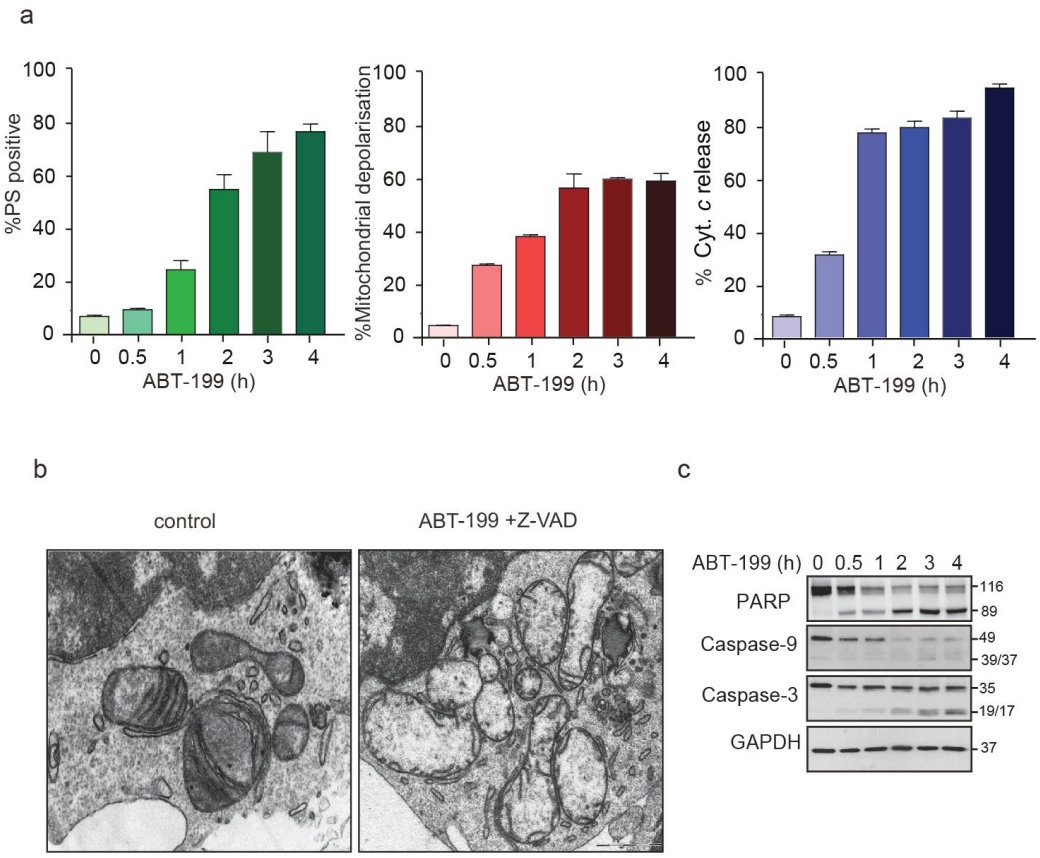

Fig 3.2.1. ABT-199 induces rapid apoptosis in a BCL-2 dependent haematological cell line. (a) MAVER-1 cell line (derived from Mantle cell lymphoma) was exposed to ABT-199 (10 nM) for the indicated time points and apoptosis was assessed by phosphatidylserine (PS) externalisation. Mitochondrial depolarisation (a loss of mitochondrial membrane potential; Ψ_m) was detected by tetramethyl rhodamine, ethyl ester (TMRE) staining and cytochrome *c* release was detected by immunocytochemistry. (b) Changes in mitochondrial morphology were detected by electron microscopy. Scale bar =0.2 μm (c) Immunoblots showed cleavage of the caspase substrate, poly ADP-ribose polymerase (PARP), as well as processing of caspase-9 and the caspase-3. Error bars = Mean ± SEM (n=3).

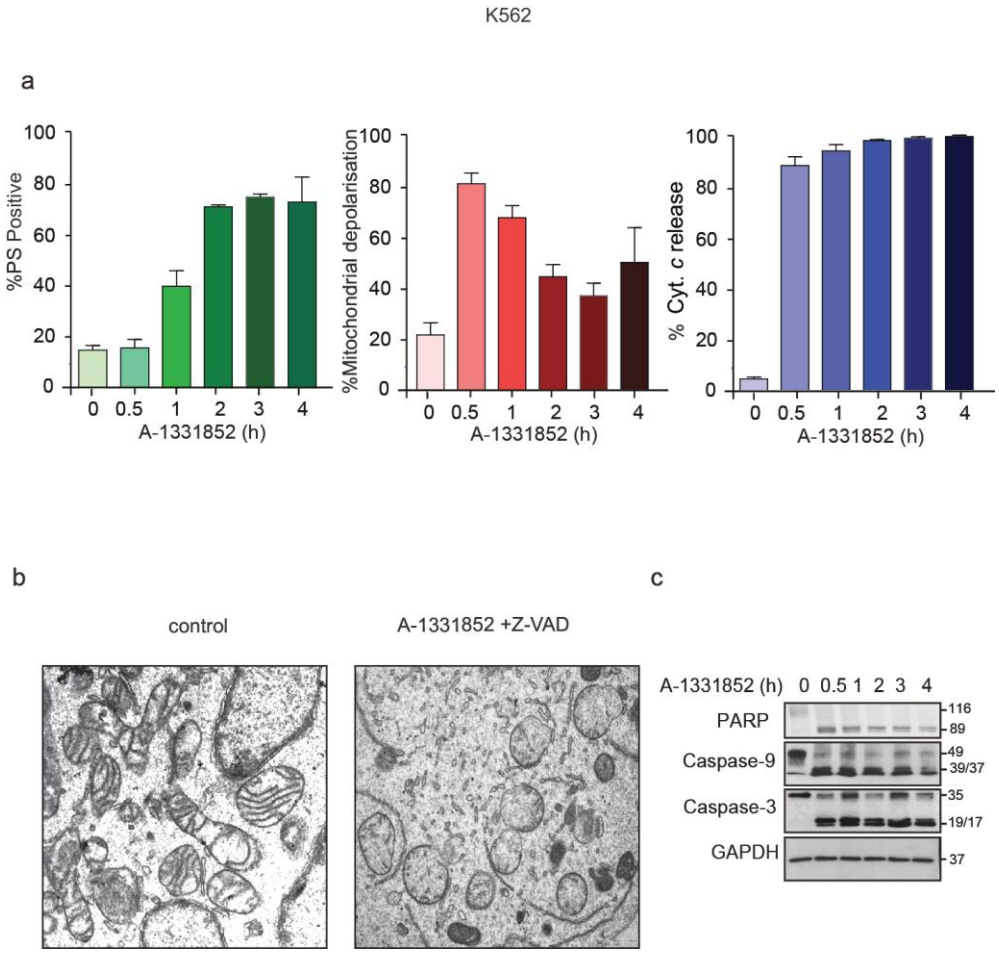

Fig 3.2.2. A-1331852 induces rapid apoptosis in a BCL-X_L dependent haematological cell line. (a) K562 cell line (derived from chronic myeloid leukaemia) was exposed to A-1331852 (10 nM) for the indicated time points and apoptosis was assessed by phosphatidylserine (PS) externalisation. Mitochondrial depolarisation was detected by tetramethylrhodamine, ethyl ester (TMRE) staining and cytochrome *c* release was detected by immunocytochemistry. (b) Changes in mitochondrial morphology were detected by electron microscopy. Scale bar =1 μm (c) Immunoblots showed cleavage of the caspase substrate, poly ADP-ribose polymerase (PARP), as well as processing of caspase-9 and the caspase-3. Error bars = Mean ± SEM (n=3).

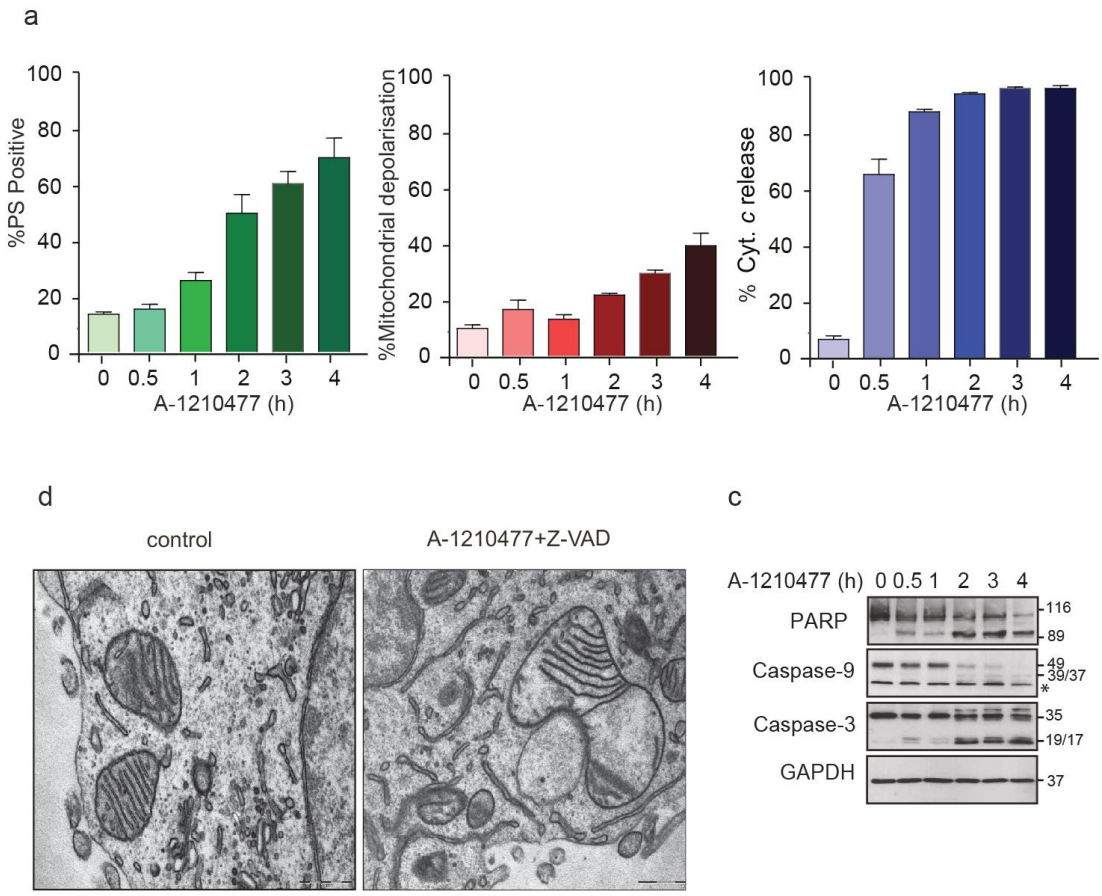

Fig 3.2.3. A-1210477 induces rapid apoptosis in a MCL-1 dependent haematological cell line. (a) H929 (derived from multiple myeloma) was exposed to A-1210477 (10 μM) for the indicated time points and apoptosis was assessed by phosphatidylserine (PS) externalisation. Mitochondrial depolarisation was detected by tetramethylrhodamine, ethyl ester (TMRE) staining and cytochrome *c* release was detected by immunocytochemistry. (b) Changes in mitochondrial morphology were detected by electron microscopy. Scale bar = 0.5 μm (c) Immunoblots showed cleavage of the caspase substrate, poly ADP-ribose polymerase (PARP), as well as processing of caspase-9 and the caspase-3. Error bars = Mean ± SEM (n=3). *= non-specific band.

Moreover, the cleavage of caspase substrate, PARP (poly ADP-ribose polymerase) and processing of caspase-3 and caspase-9 were also detected by immunoblotting (Figs 3.2.1 c, 3.2.2 c and 3.2.3 c). Taken together, these results suggested that specific BH3 mimetics induce rapid apoptosis in relevant haematological cancer cell lines that was accompanied by massive mitochondrial perturbations.

3.2.2 Haematological cancer cell lines develop rapid resistance to BH3 mimetics

In order to characterize the potential mechanism(s) of resistance and identify ways to overcome resistance, resistance models of the three validated cell lines to the relevant BH3 mimetics were generated, using four different strategies. In the first resistance model, the cells (A) were exposed to BH3 mimetics for 24 h followed by two weeks (2 W) of recovery period without drug. This process was repeated four more times to reach resistance in cells, labelled (E) (Fig3.2.4 a). Then, the level of resistance to BH3 mimetic-mediated apoptosis was checked by exposing the cells to the relevant BH3 mimetics. A significant decrease in the sensitivity of all three relevant cell lines was revealed in cells labelled (E), compared to the initial cell lines labelled (A) (Fig 3.2.5 a).

Since resistance was acquired within 8 weeks of repeated exposure to BH3 mimetics, another strategy was performed in which the cells (A) were exposed to the drugs just once, followed by 8 weeks of recovery. Cells were collected every 2 weeks (cells were labelled as A1, A2, A3 and A4) and the extent of resistance to BH3 mimetic-mediated apoptosis was monitored. Surprisingly, single exposure to specific BH3 mimetics also resulted in similar levels of resistance, as witnessed in the first model (Figs 3.2.4 b and 3.2.5 b).

To make these resistance models more clinically relevant, a third strategy was developed in which the parental cells (A) were exposed to increasing concentrations of the specific BH3 mimetic, every 5 days (5 d) resulting in cells labelled as A-a, A-b, A-c and A-d (Fig 3.2.4 c). Next, sensitive (A) and resistant (A-d) cells were exposed to their specific BH3 mimetics and assessed for resistance, as detailed above. A significant decrease in the sensitivity of the cells (A-d) was observed, similar to the first two resistance models (Fig 3.2.5 c). While this model of resistance is more clinically relevant, the cells in this model were constantly exposed to the BH3 mimetics throughout the 8-week period. This is not clinically relevant, as patients in BH3 mimetics therapy often receive a 'drug holiday' period, during which they are rested to recover before they receive the next dose of BH3 mimetics.

To mimic this scenario, a fourth resistance model was generated in which, cells were exposed to the relevant BH3 mimetics (similar to the third resistance model) but instead of a continuous exposure to the drugs for five days (5 d), the treatment period was divided into two days (2 d) of drug treatment, followed by three days (3 d) without drug (drug free), resulting in cells labelled as A-i, A-ii, A-iii and A-iv (Fig 3.2.4 d). Next, the sensitive (A) and resistant (A-iv) exposed to BH3 mimetics to check the level of resistance to BH3 mimetics (Fig 3.2.5.d). Surprisingly, all four resistance models showed similar sort of resistance to BH3 mimetic-mediated apoptosis.

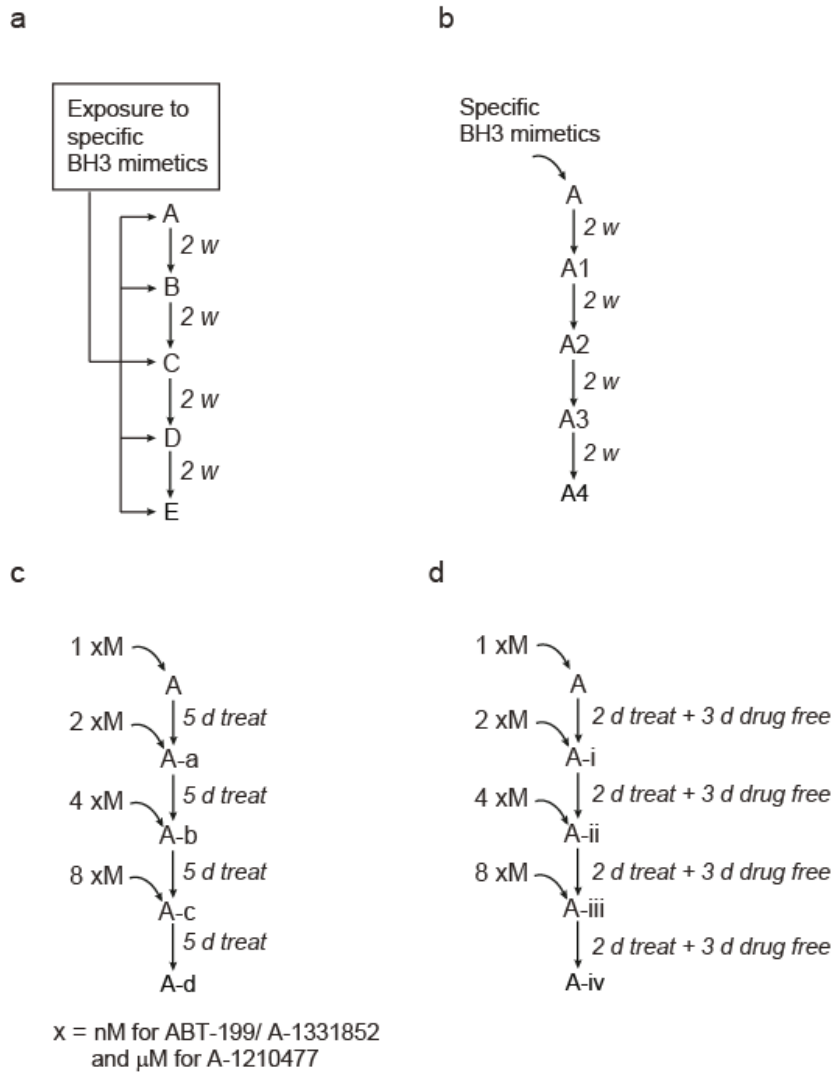

Fig 3.2.4. Schemes for establishing resistance to specific BH3 mimetics in relevant cell lines. (a-d) Schemes for developing the different resistance models, as detailed in the methods and results sections.

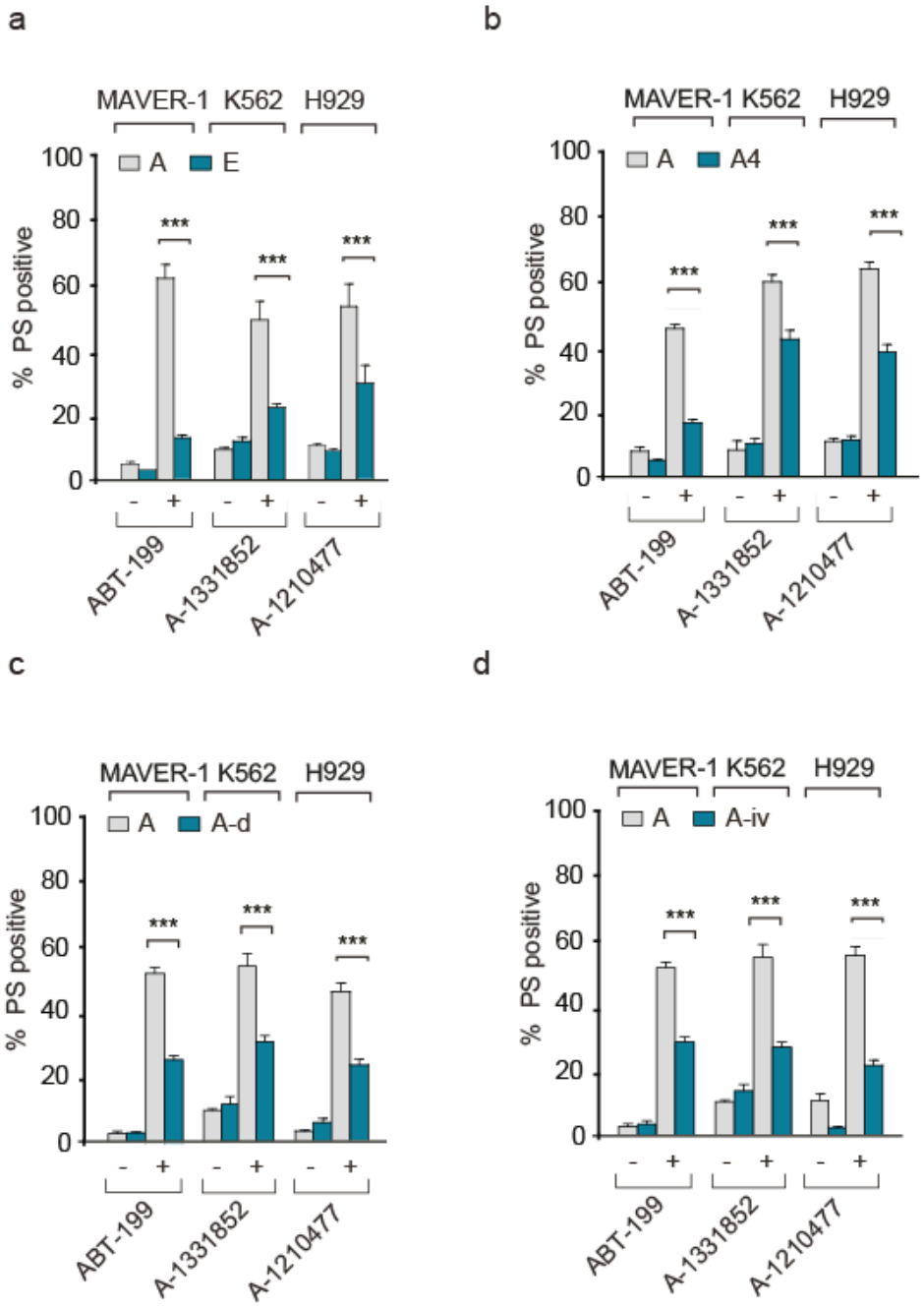

Fig 3.2.5. Cell lines derived from distinct haematological malignancies acquire rapid resistance to BH3 mimetics. (a-d) The sensitive (naive) and resistant cells lines of MAVER-1, K562 and H929, as explained in previous figure, were exposed for 4 h to ABT-199 (10 nM), A-1331852 (10 nM) and A-1210477 (5 μM) respectively, and apoptosis assessed by PS externalisation. ***P ⩽0.001, Error bars = Mean ± SEM (n=3).

3.2.3 Resistance to BH3 mimetics did not alter the expression level of BCL-2 family of proteins

Since the resistance to BH3 mimetics is often attributed to elevated expression levels of BCL-2 family members, comparison of the sensitive (A), moderately resistant (C) and resistant (E) cells from the different cell lines was performed. The results demonstrated that resistance to BH3 mimetic-mediated apoptosis did not accompany a consistent alteration of the expression levels of BCL-2 family of proteins. For instance, in the BCL-2 dependent, MAVER-1 cell line, no change in the expression levels of BCL-2 was observed in the sensitive and resistant cells. The traces of BCL-X_L and MCL-1 in MAVER-1 also did not seem to be changed in the resistant cells (Fig. 3.2.6). Similarly, in K562 cells, the expression levels of the major survival protein, BCL-X_L did not change between the sensitive and resistant cells. These cells do not express BCL-2 and the modest expression of MCL-1 in these cells also did not change between the sensitive and resistant cells (Fig. 3.2.6). In H929, the only anti-apoptotic family member that was highly expressed is MCL-1, and the levels appear to slightly decrease in the resistant cells compared to the sensitive cells (Fig. 3.2.6). In contrast, BCL-w was expressed in the resistant MAVER-1 cells, whereas the its expression seemed to decrease in the resistant K562 cells, thus complicating a consistent interpretation regarding BCL-w in chemoresistance. These results suggested that the resistance in these cells could not be attributed to the expression levels of other members of the BCL-2 family. It is possible that resistance could be due to the downregulation of pro-apoptotic BCL-2 family members. The expression of BAX and BAK increased in resistant K562 cells but did not change in other two cell lines (MAVER-1 and H929), suggesting that their expression levels could not be attributed to chemoresistance. In marked contrast, the expression levels of BID did not exhibit any change in MAVER-1 (comparing sensitive and resistant cells), increased

in resistant K562 cells and decreased in H929 resistant cells. Similarly, the expression levels of BIM and BAD did not show any change in MAVER-1, increased in resistant K562 cells and decreased in H929 resistant cells. The expression level of PUMA did not change in MAVER-1 and K562 while in resistant H929 cells showed modest decrease. NOXA could not be detected in all three cell lines. These results suggested that there were no consistent changes in the pro- and anti-apoptotic members of the BCL-2 family that could be attributed to resistance (Fig 3.2.6). However, possible alterations in specific post-translational modifications were not studied.

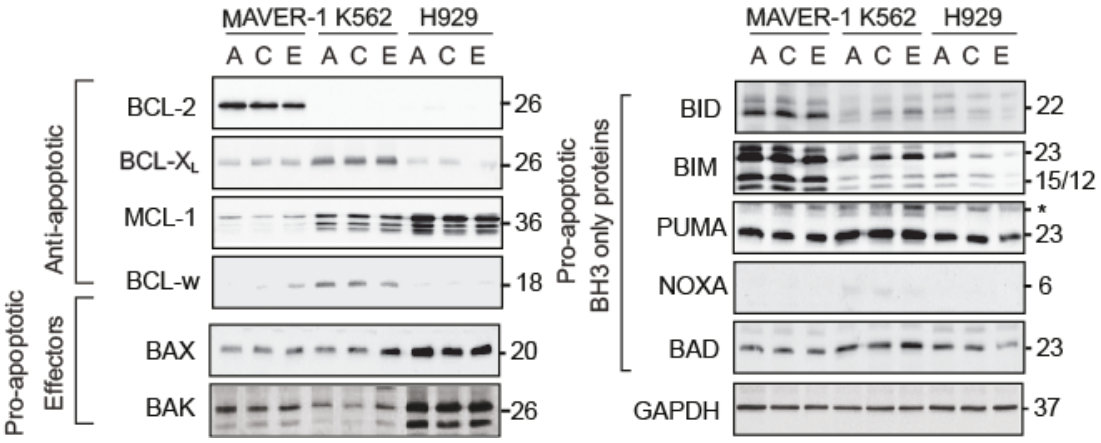

Fig 3.2.6. The expression levels of BCL2 family of proteins does not change significantly between the sensitive and resistant cells. Immunoblots of BCL-2 family of proteins in MAVER-1, K562 and H929 cells depicted as A, C and E. A is the sensitive parent line, whereas C and E are relatively more resistant to the BH3 mimetics compared to A. * depicts a non-specific band

3.2.4 Resistance to BH3 mimetics did not alter the protein-protein interactions between the pro- and anti-apoptotic BCL-2 family of proteins

Although the expression levels of the BCL-2 family members do not appear to greatly change between sensitive and resistant cells, it is possible that chemoresistance to BH3 mimetics could be attributed to changes in the protein-protein interactions between the BH3-only proteins (pro-apoptotic members) and their counterparts (anti-apoptotic members). For this, immunoprecipitation experiments were carried out in sensitive (A) and resistant (E) cells. Since PUMA and BIM were almost highly expressed in all cell lines (Fig. 3.2.6) and have been shown to promiscuously interact with all the pro-survival members of the BCL-2 family (Fig1.1.3), immunoprecipitation was carried out using PUMA and BIM antibodies. In all cell lines, there was no difference between the sensitive (A) and resistant (E) cells in terms of their ability to bind the different pro-survival proteins (Fig 3.2.7). In MAVER-1 cells, immunoprecipitation of BIM exhibited a strong interaction with BCL-2, BCL-X_L and the shortest isoform of MCL-1 in both sensitive and resistant cells (Fig 3.2.7 a). Immunoprecipitation of PUMA in MAVER-1 was not as efficient as BIM, however it showed no change between sensitive and resistant cells, in terms of the interaction between with the anti-apoptotic members (BCL-2 and BCL-X_L but not MCL-1) (Fig 3.2.7 a). In K562 cells, BIM interacted equally (comparing sensitive and resistant cells) with BCL-X_L and MCL-1L (long isoform of MCL-1) but not BCL-2 (as these cells did not express BCL-2). PUMA also exhibited a similar pattern of interaction (Fig 3.2.7 b). These results were largely reproducible in H929 cells, with the only exception of BIM not interacting with BCL-X_L (Fig 3.2.7 c). Taken together, these results suggested that resistance to BH3 mimetic-mediated apoptosis did not significantly alter protein-protein interaction.

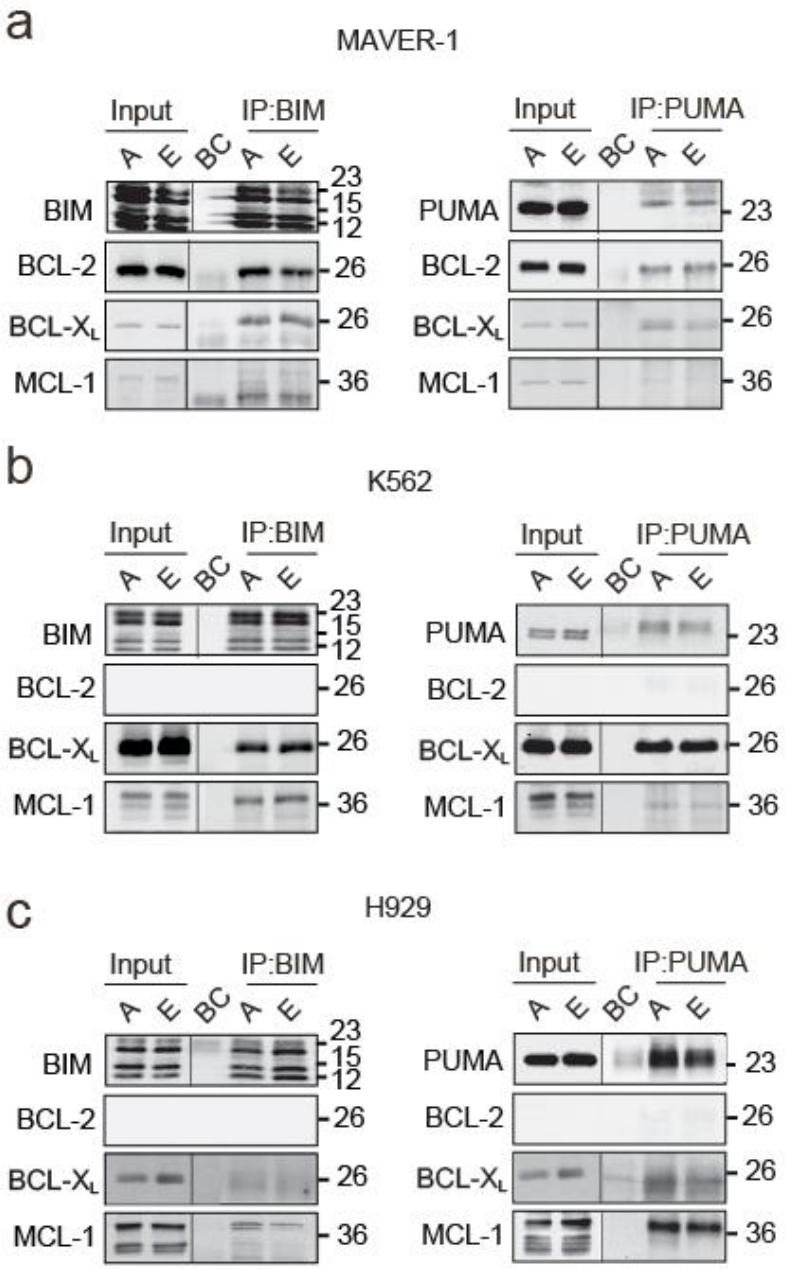

Fig 3.2.7. The interactions among different anti-apoptotic and pro-apoptotic BCL2 family of proteins are mostly identical between the sensitive and resistant cells. (a-c) Immunoprecipitates of BIM and PUMA in haematological cell lines MAVER-1, K562 and H929 (A and E) cells were probed for interactions with their anti-apoptotic counterparts. BC represents the beads control.

3.2.4 Resistance to BH3 mimetics in different cell lines cannot solely be attributed to other anti-apoptotic BCL-2 family members.

Numerous reports have demonstrated that multiple members of BCL-2 family of proteins can compensate for the lack of a specific member in a particular malignancy, thus conferring resistance to a given therapy. For instance, CLL cells that are no longer sensitive to ABT-199 are often associated with enhanced expression levels of BCL-X_L, MCL-1 or even BCL2-A1 (Vogler et al. 2011; Tahir et al. 2017). Therefore, the previous results suggesting no obvious differences in the expression levels of BCL-2 family of proteins or their protein-protein interactions was rather surprising.

To assess whether inhibition of multiple members of the anti-apoptotic BCL-2 family members would restore the sensitivity of the resistant cells, sensitive and resistant cells of the relevant cell lines were exposed to the different BH3 mimetics alone or in combination. Resistance to ABT-199 in MAVER-1 cells could not be overcome by A-1331852 or A-1210477 alone (Fig 3.2.8 a). This suggested that targeting anti-apoptotic members individually or together, without targeting the specific survival member in MAVER-1 (BCL-2) was not enough to induce apoptosis and bypass resistance. Similarly, resistance to A-1331852 in K562 or A-1210477 in H929 could not be overcome by the other BH3 mimetics, when used as single agents (Fig 3.2.8 b and c). This suggested that BCL-X_L (in K562) and MCL-1 (in H929) are still the major players in antagonising cell death.

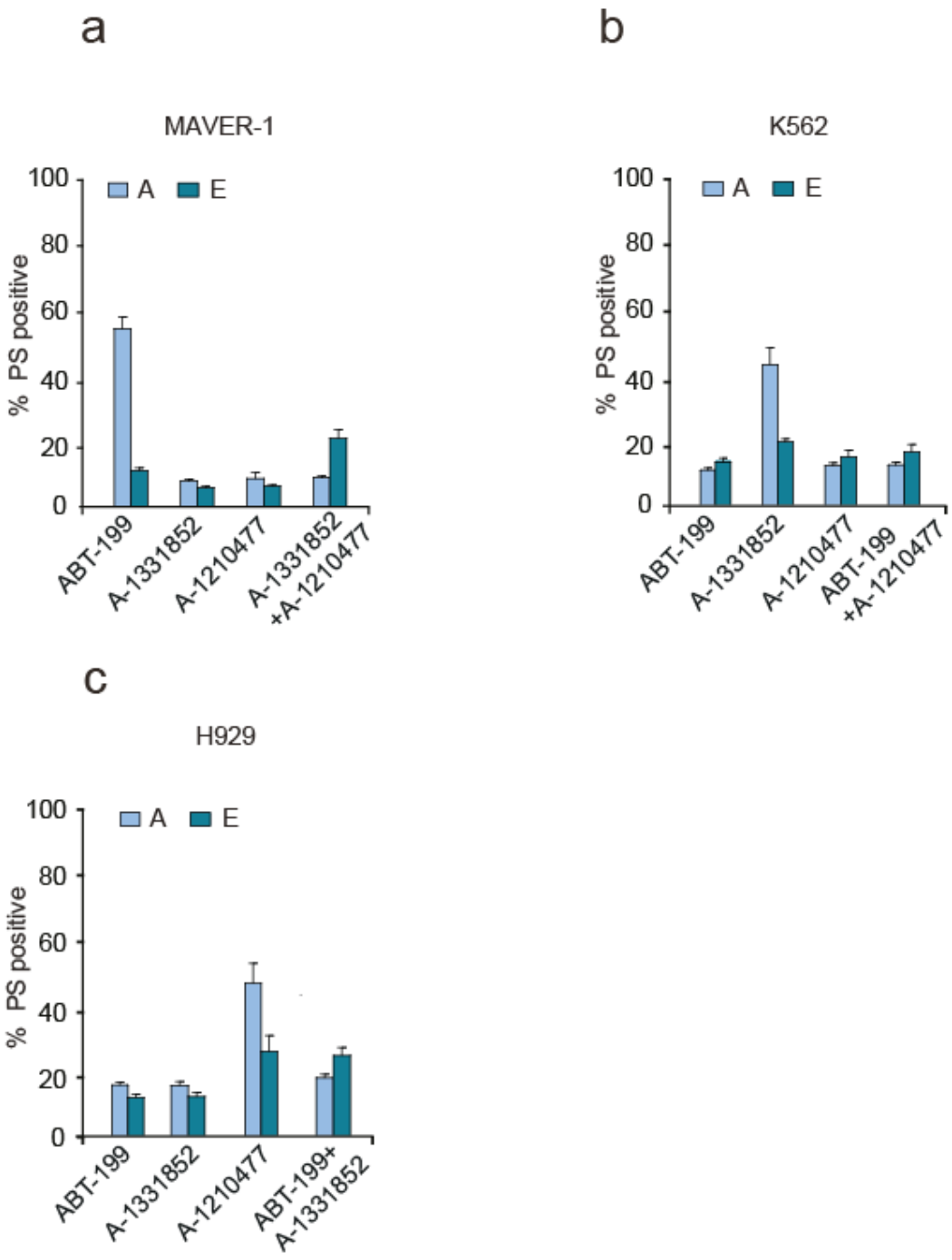

Fig 3.2.8. BH3 mimetics alone do not overcome resistance to BH3 mimetic-mediated apoptosis in haematological cell lines. (a-c) Sensitive (A) and resistant (E) cells of MAVER-1, K562 or H929 were exposed for 4 h to ABT-199 (10 nM), A-1331852 (10 nM) or A-1210477 (5 μM) alone. Then, apoptosis was assessed by PS externalisation. (n=3).

3.2.5 Simultaneous inhibition of multiple anti-apoptotic BCL-2 members overcomes resistance to BH3 mimetics in different cell lines

Although inhibition of BCL-2 family members using BH3 mimetics as single agents was ineffective in reversing chemoresistance, a combination of ABT-199 with either A-1331852 or A-1210477 resulted in enhanced cell death even in the resistant MAVER-1 cells (Fig 3.2.9 a). This suggested that BCL-2 played the primary role in driving cell survival in resistant MAVER-1 cells, with further contribution from the other two members. More surprisingly, a combination of all three BH3 mimetics killed almost all of the resistant cells, but not the sensitive cells (Fig 3.2.9 a). Similarly, inhibition of BCL-X_L and MCL-1, in addition to BCL-2, overcame resistance to ABT-199 in other three resistance models (Fig 3.2.9 b-d). This suggested that all resistance models of MAVER-1 depended on all three anti-apoptotic members (BCL-2, BCL-X_L and MCL-1).

In K562 and H929 cells, a combination of A-1331852 and A-1210477 but not ABT-199 enhanced the sensitivity of the resistant cells (3.2.10 a and 3.2.11 a). However, combination of all three increased the sensitivity of the resistant cells, suggesting that BCL-2 still has a role in antagonising cell death in the presence of the other two members, namely BCL-X_L and MCL-1. In agreement with the earlier observations, similar results were obtained in the other three resistance models (3.2.10 b-d and 3.2.11 b-d). Taken together, these results suggested that the resistant cells changed their dependency on a specific BCL-2 family member, under stress stimuli that specifically targeted one or the other member of the BCL-2 family.

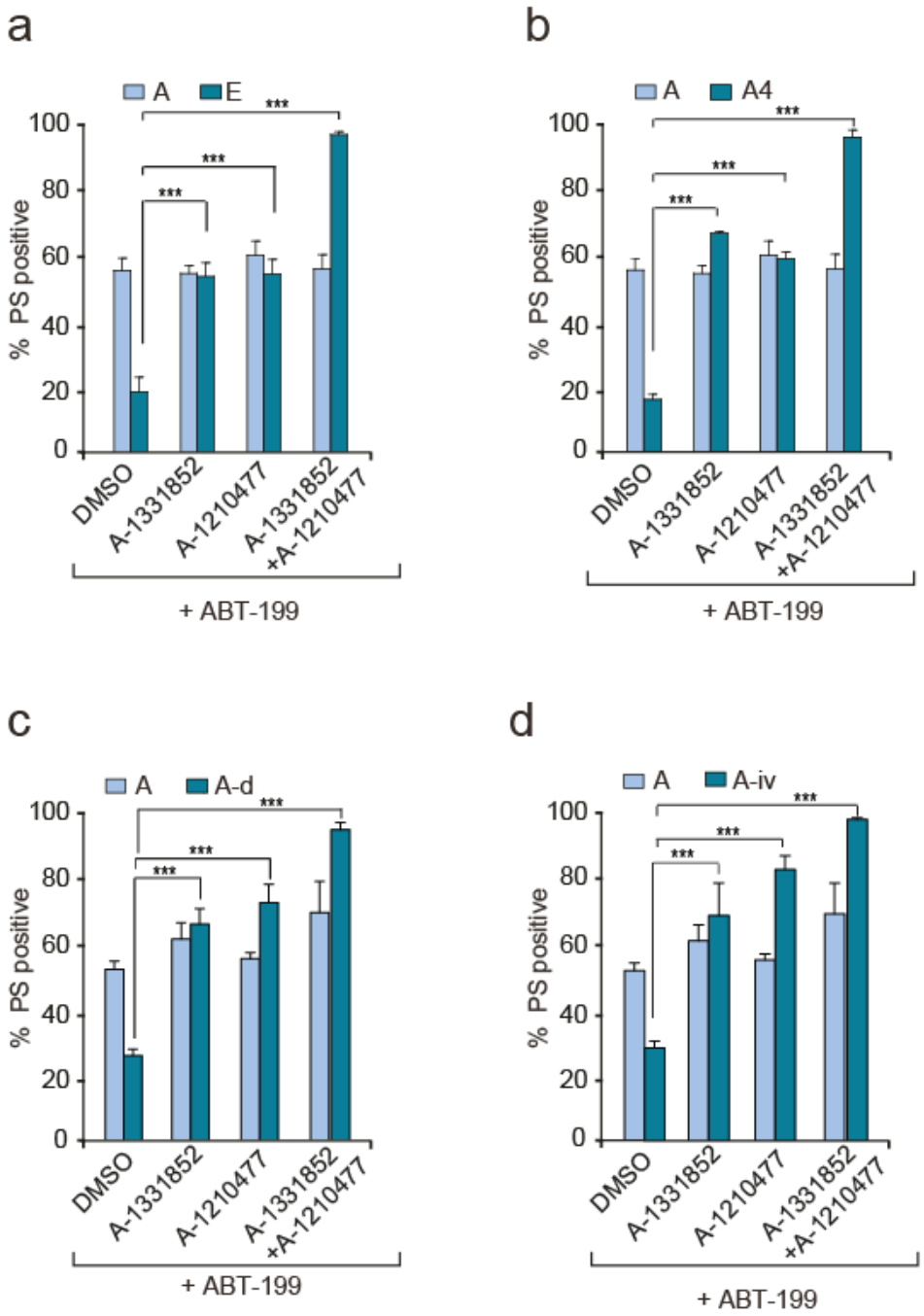

Fig 3.2.9. Simultaneous inhibition of multiple BCL-2 family members overcomes resistance to BH3 mimetics in MAVER-1 cells. (a-c) Sensitive and resistant cells of MAVER-1 from the different resistance models were exposed for 4 h to ABT-199 (10 nM) alone or in combination with A-1331852 (10 nM) and/or A-1210477 (5 μM). Then, apoptosis was assessed by PS externalisation. ***P ⩽0.001, **P⩽0.01; Error bars = Mean ± SEM (n=3).

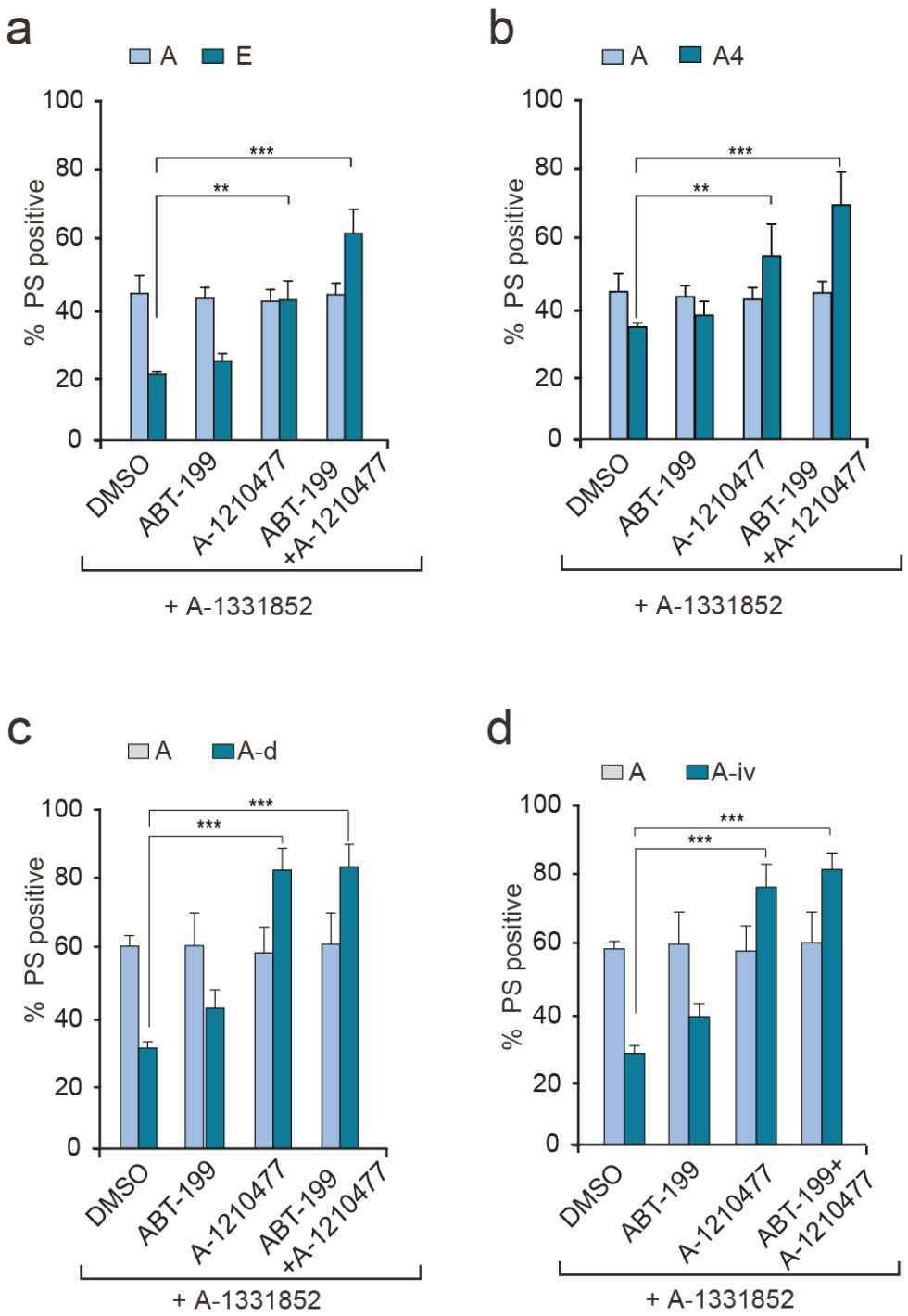

Fig 3.2.10. Simultaneous inhibition of multiple BCL-2 family members overcomes resistance to BH3 mimetics in the K562 cell line. (a-c) Sensitive and resistant K562 cells from the different resistance models, were exposed for 4 h to A-1331852 (10 nM) alone or in combination with ABT-199 (10 nM) and/or A-1210477 (5 μM). Then apoptosis was assessed by PS externalisation. ***P ⩽0.001, **P⩽0.01; Error bars = Mean ± SEM (n=3)

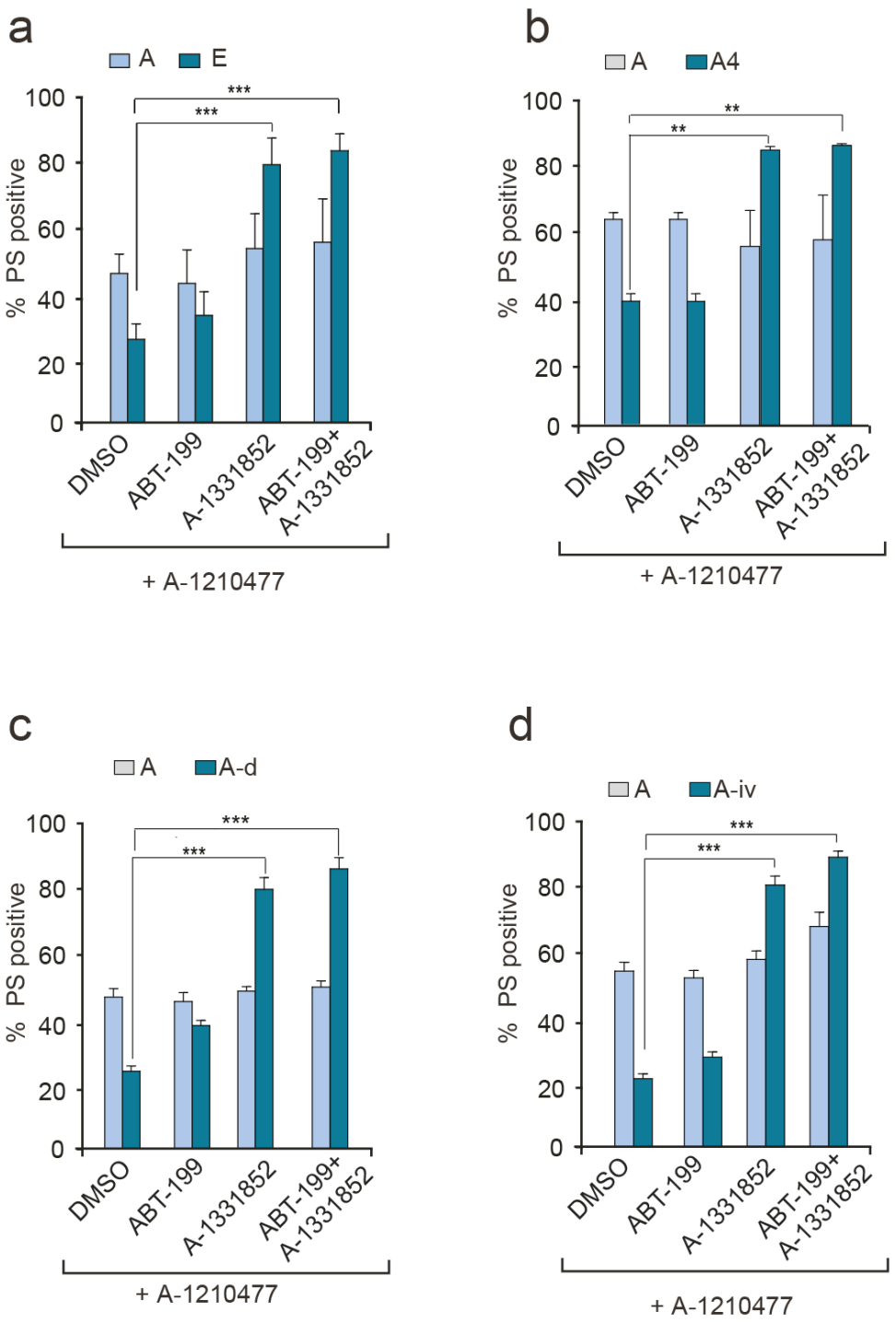

Fig 3.2.11. Simultaneous inhibition of multiple BCL-2 family members overcomes resistance to BH3 mimetics in the H929 cell line. (a-c) Sensitive and resistant H929 cells, from the different resistance models, were exposed for 4 h to A-1210477 (5 µM) alone or in combination with ABT-199 (10 nM) and/or A1331852 (10 nM). Then, apoptosis was assessed by PS externalisation. ***P ⩽0.001, **P⩽0.01; Error bars = Mean ± SEM (n=3)

3.3 Discussion

BCL-2 family members are the key regulators of apoptosis and hence are promising targets in cancer therapy. Inhibitors of the BCL-2 family of proteins (BH3 mimetics) have been revolutionary in rapidly and potently activating the intrinsic apoptotic pathway in a wide variety of cancers (Delbridge et al. 2016). Even with the accumulation of vast amounts of supportive *in vitro* data, the usage of BH3 mimetics in treating cancer is still at its infancy, with ABT-199 (venetoclax), a BCL-2 specific inhibitor, being the only drug of this class to be recently approved for treatment of refractory CLL (Roberts et al. 2016). The recent development of specific BH3 mimetics that target other members of the BCL-2 family, such as BCL-X_L and MCL-1 will be enormously useful in treating patients suffering from different cancers. While BH3 mimetic therapy is generally quite promising, challenges facing this therapy include chemoresistance. Therefore, the possible mechanisms of resistance to BH3 mimetics and ways to bypass such resistance need to be recognized, as it emerges. Variety of mechanisms, such as drug efflux due to elevation of P-gp (P-glycoprotein) in addition to other drug efflux transporters, mediate acquired resistance to different chemotherapeutic agents (Bao et al. 2011; Yoshimori et al. 2015). Moreover, mutation in the drug target site, such as modifications in the BH3 domain of BCL-2 family members could prevent BH3 mimetics from binding and inhibiting their targets. For instance, the identification of a novel G101V mutation in BCL-2 in CLL has been shown to prevent the binding of ABT-199 (Blombery et al. 2019). Other mutations that affect the mitochondrial translocation of BAX have also been identified (Fresquet et al. 2014). In addition, other post-translational changes that alter the expression levels of the BCL-2 family members could also contribute to resistance (Konopleva et al. 2006; van Delft et al. 2006; Szakács et al. 2006).

Earlier studies have generated resistance models to BH3 mimetics by continued exposure (several months) of their chosen cell lines to different BH3 mimetics (Fresquet et al. 2014), or by co-culturing cells in a feeder layer to mimic the cancer microenvironment, which developed resistance within few hours (Vogler, Butterworth, et al. 2009). This resulted in a remarkable upregulation of other anti-apoptotic BCL-2 family members and/or acquisition of mutations in the BCL-2 family members (Vogler, Butterworth, et al. 2009; Tahir et al. 2017). In order to assess how soon resistance develops, in the present study the chosen cell lines were exposed to the relevant BH3 mimetics for a short period of time. Surprisingly, in all the models, resistance to BH3 mimetics developed rapidly (within 8 weeks) but was modest, unlike what was reported in the previous studies, when cells were exposed to BH3 mimetics for several months. Moreover, the modest extent of resistance that was observed potentially reflected the magnitude of resistance commonly observed in the clinic (Al-Zebeeby et al. 2018).

Alterations in the balance between pro-survival and the pro-apoptotic BCL-2 family members is commonly attributed to cancer maintenance, progression and chemoresistance to BH3 mimetics (Souers et al. 2013; Tse et al. 2008; Leverson JD. 2015). However, observations from the current study suggested that resistance to BH3 mimetics did not increase the expression levels of most anti-apoptotic BCL-2 family members (Fig 3.2.6). Similarly, the expression levels of most pro-apoptotic BCL-2 family members did not exhibit significant differences during the generation of chemoresistance (Fig 3.2.6). Furthermore, no changes in the protein-protein interactions among BH3 only proteins (BIM and PUMA) and their anti-apoptotic counterparts were observed (Fig 3.2.7). In agreement with previous findings (Tahir et al. 2017), resistance to ABT-199 was overcome when it was used in combination with

A-1331852 or A-1210477 (Fig 3.2.9). In addition, resistance to A-1331852 was overcome by using it in combination with A-1210477 (Fig 3.2.10) and similarly, resistance to A-1210477 was overcome by using it in combination with A-1331852 (Fig 3.2.11). These results strongly suggested that BCL-X_L and MCL-1 play crucial roles in resistance to BH3 mimetic-mediated apoptosis. Possibly, the modest resistance that was observed in the current models was insufficient to induce a noticeable change in the expression levels of BCL-2 family members. Potential post-translational modifications of these proteins, which could have contributed to resistance, cannot be excluded.

Although targeting multiple anti-apoptotic BCL-2 family of proteins simultaneously overcame resistance to BH3 mimetic-mediated apoptosis, this combination could have toxic side-effects, as these proteins maintain vital functions inside the cells. This is true especially when the treatment requires simultaneous targeting of multiple members of anti-apoptotic BCL-2 family of proteins. The exception to this comes in the form of acute myeloid leukaemia wherein clinical trials are currently exploring the possibility of targeting both BCL-2 and MCL-1 in these patients (Moujalled et al. 2019; Prukova et al. 2019; Grundy et al. 2018). Nevertheless, to overcome potential toxicities associated with this approach, identification of alternative strategies to tackle chemoresistance to BH3 mimetic-mediated apoptosis is required. Targeting cell metabolism may be one of these strategies, as glutamine deprivation has recently been shown to enhance ABT-199-mediated apoptosis by overcoming MCL-1-mediated resistance in multiple myeloma (Bajpai, et al. 2016). This will be discussed in the next chapter.

Chapter 4

Targeting glutaminolysis overcomes resistance to BH3 mimetic-mediated apoptosis

4.1 Introduction

Targeting metabolic pathways is currently considered a promising strategy to enhance the efficacy of chemotherapeutic agents (Graham et al. 2012; Wise & Thompson 2010; Yuneva et al. 2007; Son et al. 2013; Still & Yuneva 2017). In relation to BH3 mimetics, recent findings revealed that targeting glutamine metabolism enhances ABT-199 (Venetoclax) mediated-apoptosis in MCL-1 dependent multiple myeloma (Bajpai et al. 2016). This is a particularly promising approach and could be employed to enhance the sensitivity of cells to BH3 mimetic-mediated apoptosis.

Glutamine is an important amino acid and can be categorised as either conditionally essential or nonessential, based on the cell type (Noguchi et al. 1997). Mammalian cells can synthesize glutamine by glutamine synthetase (GLUL), however GLUL is not highly expressed in most rapidly proliferating cells, such as cancer cells (Dang 2010). In such cases, glutamine becomes conditionally essential and cell rely on glutamine uptake from outside the cell (Lacey & Wilmore 1990). Membrane-anchored amino acid transporters, such as SLC1A5 (ASCT2) facilitate such glutamine uptake (Gao et al. 2009). Pharmacological inhibition of SLC1A5 using L-γ-glutamyl-p-nitroanilide (GPNA) has been shown to reduce cell proliferation (Hassanein et al. 2013). Glutamine upon entering the cell gets converted to glutamate in a process called glutaminolysis, which is catalysed by the enzyme, GLS (glutaminase). Mammalian glutaminase are encoded through two paralogous genes, *GLS* and *GLS2* (Porter et al. 2002; Pérez-Gómez et al. 2003), giving rise to two isozymes, GLS and GLS2 (Liver-type glutaminase) (Mates et al. 2013). GLS exists has two isoforms, KGA (kidney isoform) and the GAC (splice variant isoform glutaminase c) (Fig 4.1.1) (Mates et al. 2013; Elgadi et al. 1999).

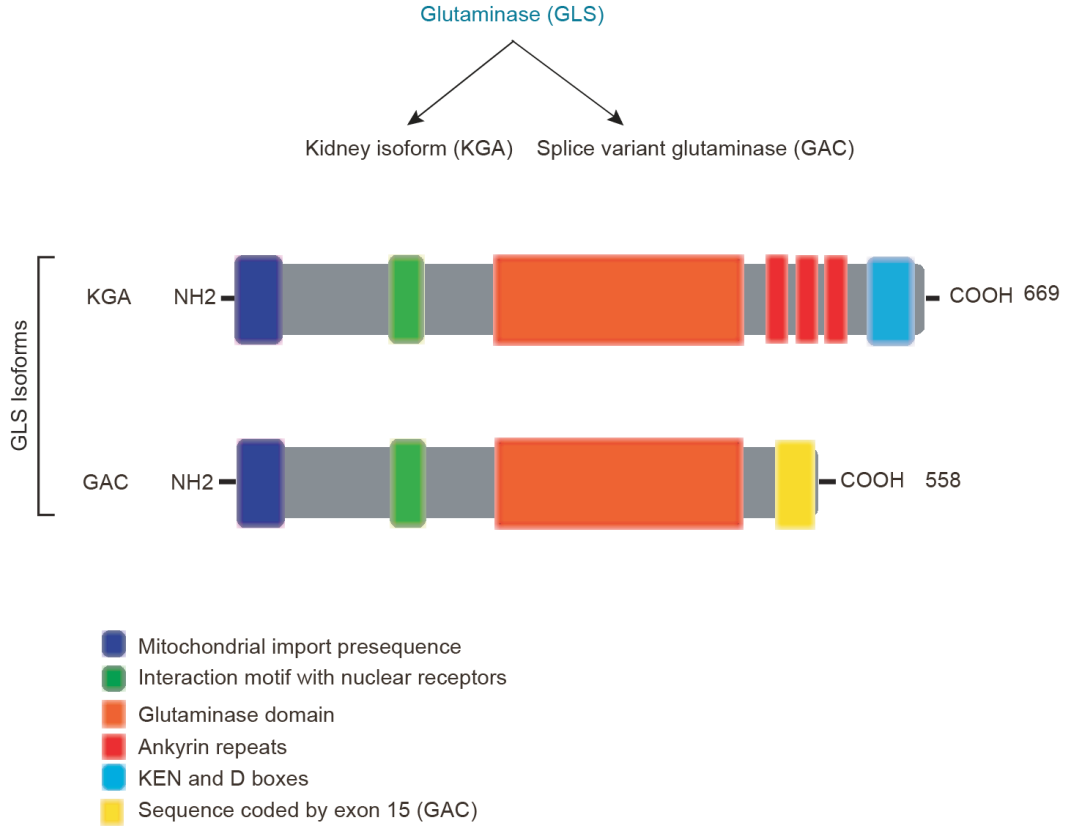

Fig 4.1.1. Glutaminase isoforms. GLS is an enzyme that catalyses the conversion of glutamine to glutamate. Schematic representation of two glutaminase isoforms, kidney isoform (KGA 669 residues) and splice variance of KGA, also called glutaminase c (GAC 558 residues) with the different motifs and domains. Mitochondrial import pre-sequences (which enables mitochondrial import) (blue), interaction motif with nuclear receptors (green), glutaminase domain (contains the GLS active site) (orange), Ankyrin repeats (which controls protein-protein interaction) (red), KEN and D boxes (that are targeted by proteasome for GLS degradation) (light blue) and sequence coded by exon 15 (GAC) (yellow) (Thangavelu et al. 2012; Marquez et al. 2016)

Drugs, such as DON (6-diazo-5-oxy-L-norleucine) (Crosby & Miller 2016), dibenzophenanthridine-968 (Kalra & Brosnan 1973), BPTES (Le et al. 2012), CB-839 (Gross et al. 2014) and UPGL00004 (Huang et al. 2018) have been generated to target GLS. Of the different GLS inhibitors, CB-839 is a selective inhibitor of glutaminase and exhibits antiproliferative activity in different types of cancers. It is currently in clinical trials for treatment of breast cancer and haematological cancer (Calithera Biosciences NLM Identifier: NCT02071927; Calithera Biosciences NML Identifier: NCT02071888). In addition to glutaminolysis mediated by GLS, glutamine can also be converted to glutamate through hexosamine pathway, which is catalysed by GFAT (glutamine: fructose-6-phosphate-amidotransferase) (Marshall et al. 1991). GFAT is effectively inhibited by the glutamine analogue, Azaserine (Tarnowski & Stock 1957; Moore & Lepage 1957; Foley & Eagle 1958; Viswanathan et al. 2008). Thus derived glutamate is converted to α-KG (α-Ketoglutarate) either by a dehydrogenase reaction, catalysed by GLUD (glutamate dehydrogenase) (Jin et al. 2015) or a series of aminotransferase reactions (Hensley et al. 2013). EGCG (epigallocatechin gallate) inhibits the enzymatic activity of GLUD (Li et al. 2011), whereas AOA (aminooxyacetic acid) inhibits aminotransferases (Hensley et al. 2013) (Fig 4.1.2).

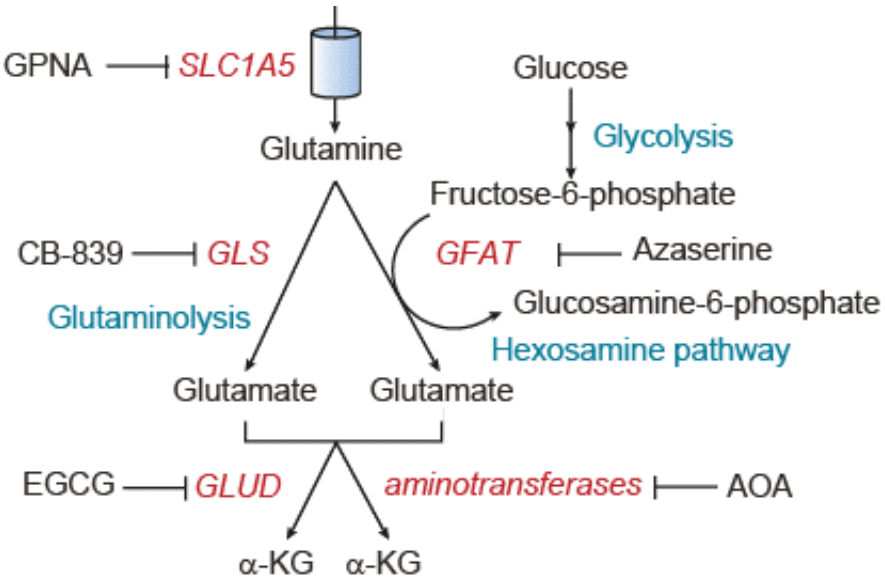

Fig 4.1.2. Glutamine metabolism pathway. Scheme representing the different enzymes in the glutamine metabolic pathway: glutamine, transported into cells *via* SLC1A5 (inhibited by GPNA), is converted to glutamate either *via* GLS-mediated glutaminolysis (inhibited by CB-839) or by the GFAT-mediated hexosamine pathway (inhibited by azaserine). Glutamate can then generate α–ketoglutarate (α–KG) either *via* GLUD1-mediated dehydrogenation (inhibited by ECGC) or by a series of aminotransferase reactions (inhibited by AOA).

4.2 Results

4.2.1 Glutamine deprivation enhances BH3 mimetic-mediated apoptosis in haematological cell lines

To explore the potential of targeting glutamine metabolism in overcoming resistance to BH3 mimetics, sensitive and resistant cells derived from the three haematological cell lines were deprived of glutamine for 16 h. Glutamine deprivation at this time point did not exhibit any toxic effect on its own in the cells. However, glutamine deprivation enhanced BH3 mimetic mediated-apoptosis in both sensitive and resistant cells significantly (Fig 4.2.1), in addition to overcoming resistance in all other resistance models significantly (Fig 4.2.2 a-c). To confirm the above results, sensitive (A) and resistant (E) K562 cells that were deprived of glutamine for 16 h were then supplemented with glutamine. As expected, glutamine supplementation restored resistance to BH3 mimetic-mediated apoptosis in the tested cells (Fig 4.2.3).

Next, to assess whether the uptake of glutamine was higher in the resistant cells than sensitive cells, sensitive (A) and resistant (E) cells were deprived of glutamine, followed by supplementation with radiolabelled glutamine. The glutamine uptake measurements revealed that the uptake of radiolabelled glutamine was higher in the resistant cells than the sensitive cells in all three relevant cell lines (Fig 4.2.4 a). Higher uptake could be attributed to enhanced expression levels of glutamine transporter, SLC1A5. However, no change in the expression level of SLC1A5 was detected between the sensitive and resistant cells (4.2.4 b). In agreement with the glutamine deprivation studies, down regulation of SLC1A5 significantly overcame resistance to A-1331852-mediated apoptosis in K562 cells (4.2.4 b). Taken together, these results strongly suggested that targeting glutamine uptake could potentially be a promising way to bypass chemoresistance to BH3 mimetic-mediated apoptosis.

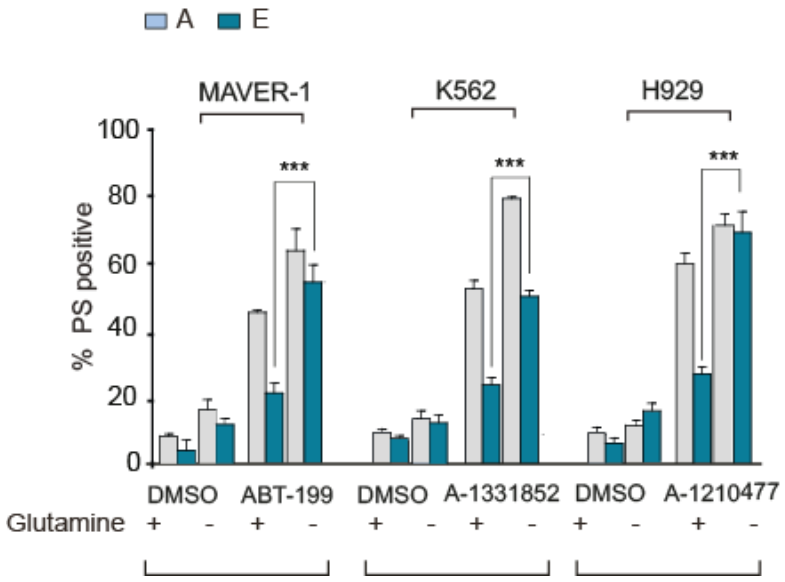

Fig 4.2.1. Glutamine deprivation enhances BH3 mimetic-mediated apoptosis. Sensitive (A) and resistant (E) MAVER-1, K562 and H929 cells from the first resistance model were deprived of glutamine for 16 h followed by 4 h exposure to specific BH3 mimetics ABT-199 (10 nM), A-1331852 (10 nM) or A-1210477 (5 μM), respectively. Then, apoptosis was assessed by PS externalisation. ***P ⩽0.001, Error bars = Mean ± SEM (n=3).

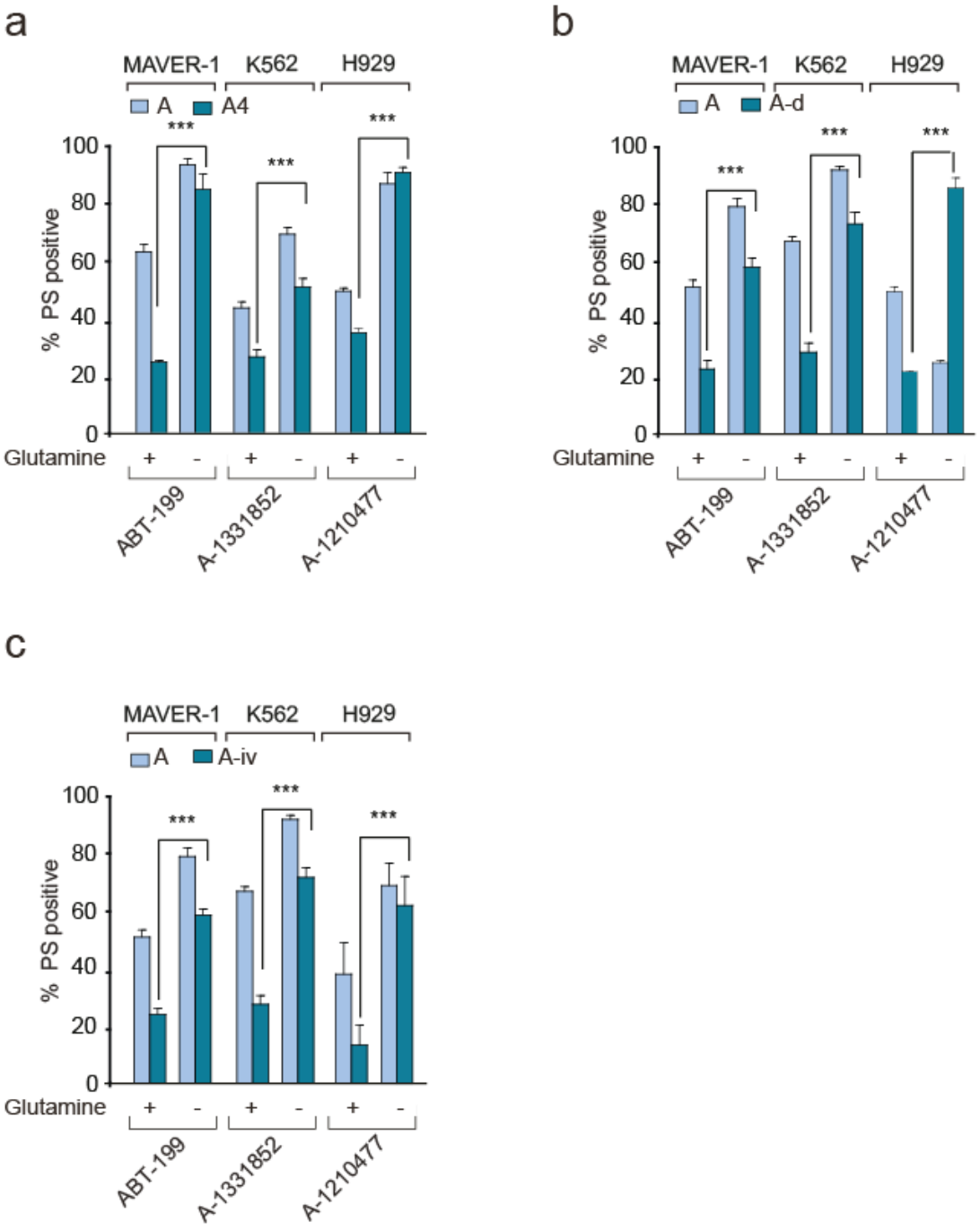

Fig 4.2.2. Glutamine deprivation enhances BH3 mimetic-mediated apoptosis in other resistance models. (a-c) Sensitive and resistant MAVER-1, K562 and H929 cells from resistant models (2-4) were deprived of glutamine for 16 h followed by 4 h exposure to specific BH3 mimetics ABT-199 (10 nM), A-1331852 (10 nM) or A-1210477 (5 μM), respectively. Then, apoptosis was assessed by PS externalisation. ***P ⩽0.001, Error bars = Mean ± SEM (n=3).

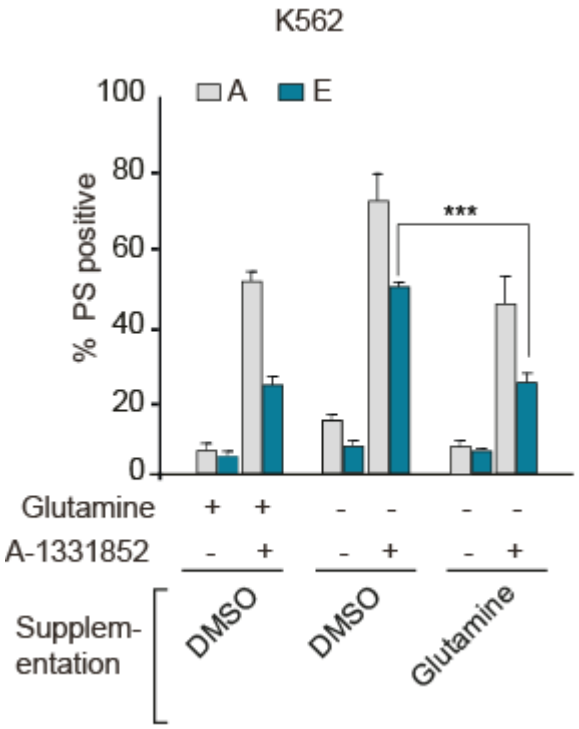

Fig 4.2.3. Glutamine supplementation restores resistance to BH3 mimetic-mediated apoptosis. Sensitive (A) and resistant (E) K562 cells were incubated with RPMI medium or glutamine free medium in presence or absence of glutamine (2 mM) for 16 h, followed by 4 h of exposure to A-1331852 (10 nM). Then, apoptosis was assessed by PS externalisation. ***P ⩽0.001; Error bars = Mean ± SEM (n=3).

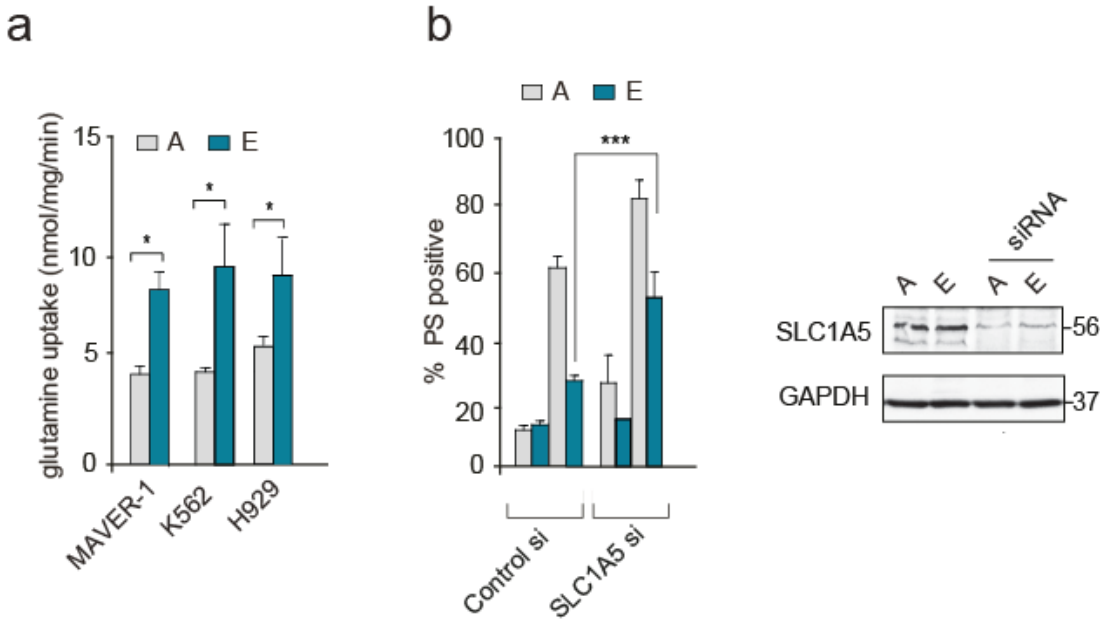

Fig 4.2.4. Glutamine uptake is greater in the resistant compared to the sensitive cells. (a) Sensitive (A) and resistant (E) MAVER-1, K562 and H929 cells were incubated with glutamine free media for 2 h followed by the addition of uptake medium containing L-[2,3,4-3H]-glutamine (1 μCi) for 10 min. Then, the cells were lysed and analysed in the liquid scintillation analyser. (b) Sensitive (A) and resistant (E) K562 cells were transfected with SLC1A5 siRNA for 72 h, followed by 4 h exposure to A-1331852 (10 nM). Then, apoptosis was assessed by PS externalisation. The western blots were carried out to confirm the knockdown efficiency of the different siRNAs. *P ⩽0.05, Error bars = Mean ± SEM (n=3).

4.2.2 Modulation of glutamine metabolism overcomes resistance to BH3 mimetics

Since glutamine deprivation overcame resistance to BH3 mimetic-mediated apoptosis, and glutamine underwent glutaminolysis and other metabolic changes to yield α-KG (Fig.4.2.5 a), sensitive and resistant K562 cells were deprived of glutamine and supplemented with α-KG. α-KG supplementation restored resistance to BH3 mimetic-mediated apoptosis (Fig 4.2.5 b), suggesting that glutamine uptake and glutamine metabolism to yield α-KG could be linked to chemoresistance in these cells. Further support for this was gained by experiments involving the downregulation of different steps of glutaminolysis pathway.

Pharmacological inhibition of the different players involved in the glutamine metabolic pathway were first performed. GPNA (to inhibit SLC1A5), CB-839 (to inhibit GLS), Azaserine (to inhibit GFAT), EGCG (to inhibit GLUD) and AOA (to inhibit aminotransferase) were used (Fig 4.2.6 a). The final concentrations of these inhibitors were chosen based on both published literature and a careful concentration-response carried out in these cells (data not shown). The results revealed that pharmacological inhibition of the different steps of the glutamine metabolic pathway significantly overcame resistance except GLUD inhibition by EGCG (Fig 4.2.6 b). This could be because of a lack of involvement of GLUD in this reaction or due to a lack of the specificity of the EGCG inhibitor. To test this, genetic knockdowns of selected targets, namely GLS, GFAT and GLUD were performed in both sensitive and resistant cells (Fig 4.2.7). While genetic knockdowns of GLS resulted in maximal reversal of resistance to BH3 mimetic-mediated apoptosis in sensitive and resistant K562 cells, knocking down other enzymes in the glutamine metabolic pathway exhibited more modest effects (Fig 4.2.7).

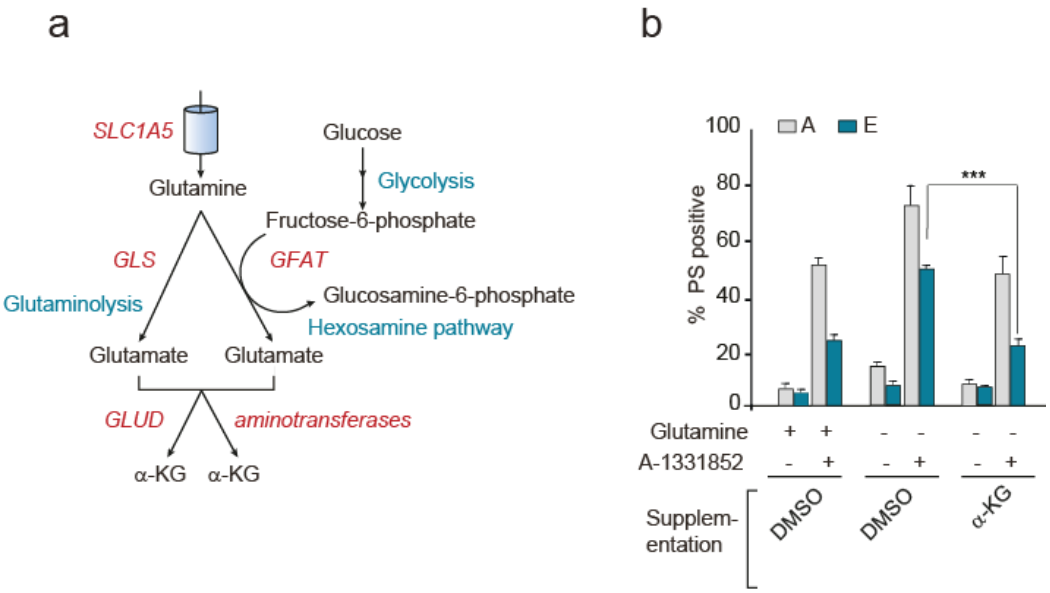

Fig 4.2.5. α-KG supplementation reverses the effect of glutamine deprivation and restores resistance to BH3 mimetic-mediated apoptosis. (a) Scheme representing the glutaminolysis pathway. (b) Sensitive (A) and resistant (E) K562 cells were incubated with RPMI medium or glutamine free medium in the presence or absence of □-ketoglutarate (α-KG) (4 mM) for 16 h, followed by 4 h exposure to A-1331852 (10 nM). Then, apoptosis was assessed by PS externalisation. ***P ⩽0.001; Error bars = Mean ± SEM (n=3).

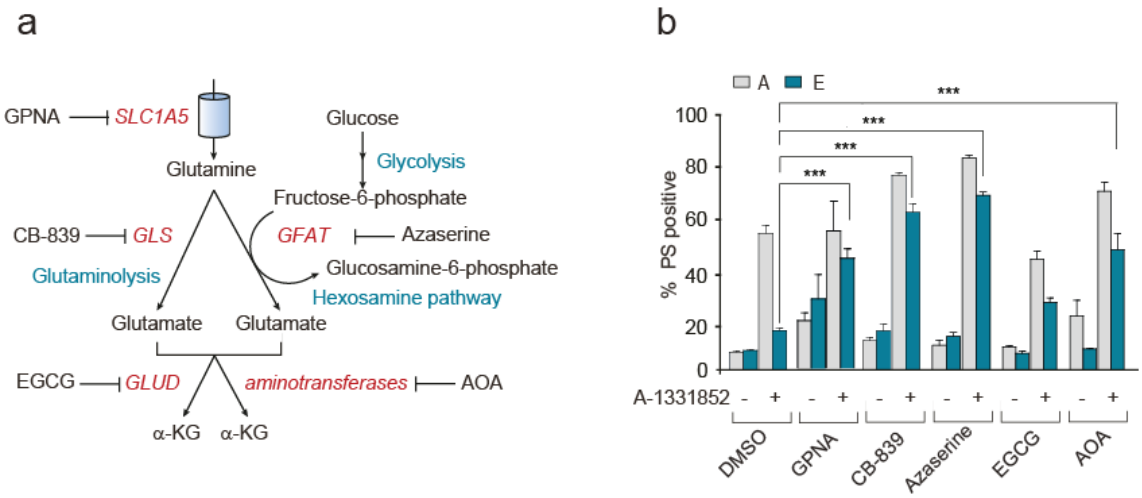

Fig 4.2.6. Pharmacological inhibition of the glutaminolysis pathway overcomes resistance to BH3 mimetic-mediated apoptosis. (a) Scheme representing the enzymes of the glutaminolysis pathway with their inhibitors. (b) Sensitive (A) and resistant (E) K562 cells were exposed to GPNA (5 mM) for 48 h, CB-839 (10 μM) for 72 h, Azaserine (25 mM) for 16 h, EGCG (50 μM) and AOA (500 μM) for 24 h, followed by 4 h exposure to A-1331852 (10 nM). Then, apoptosis was assessed by PS externalisation. ***P ⩽0.001. Error bars = Mean ± SEM (n=3).

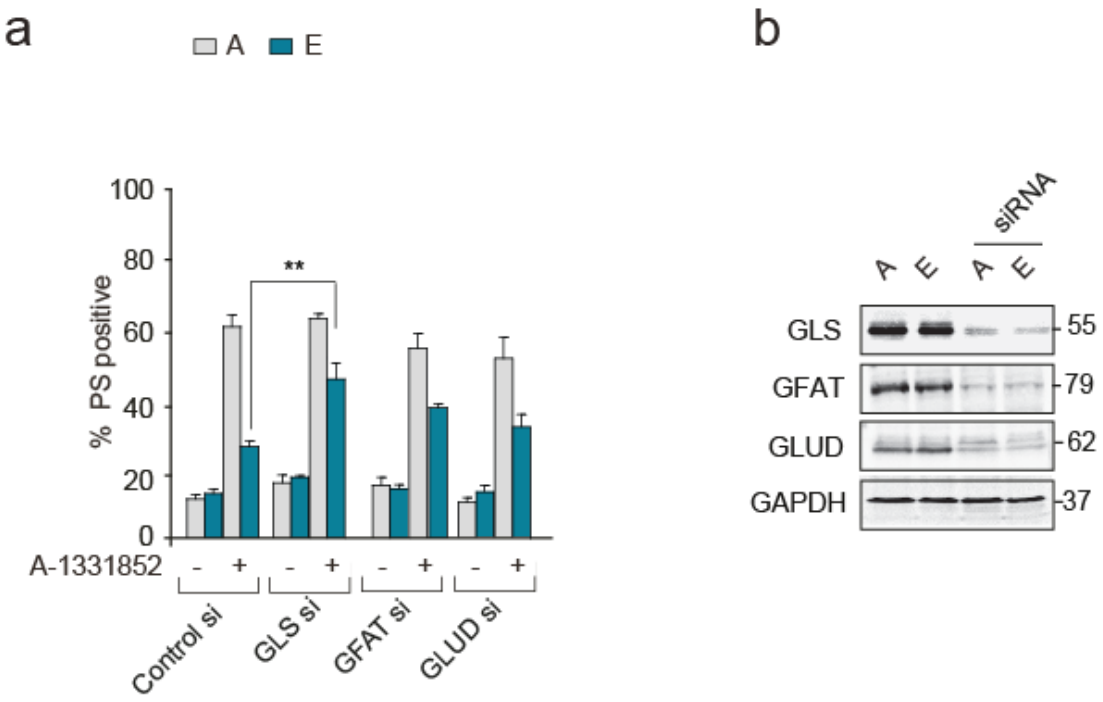

Fig 4.2.7. Genetic knockdown of the enzymes involved in the glutaminolysis pathway overcomes resistance to BH3 mimetic-mediated apoptosis. (a) Sensitive (A) and resistant (E) K562 cells were transfected with GLS, GFAT and GLUD siRNAs for 72 h, followed by 4 h exposure to A-1331852 (10 nM). Then, apoptosis was assessed by PS externalisation. (b) Western blots confirmed the knockdown efficiency of the different siRNAs. ***P ⩽0.001, **P⩽0.01; Error bars = Mean ± SEM (n=3).

4.2.3 Identification of novel interactions between GLS and anti-apoptotic BCL-2 family members

Pharmacological and genetic targeting of GLS restored sensitivity to BH3 mimetic-mediated apoptosis. Since GLS has been identified to localise to the mitochondria (Huang et al. 2018; Cassago et al. 2012; Olalla et al. 2002), the next set of experiments were performed to assess whether GLS could interact with anti-apoptotic BCL-2 family of proteins at the level of mitochondria, and thus play important roles in apoptosis. Immunoprecipitation of GLS were performed in sensitive (A) and resistant (E) in all three relevant cells lines. Strikingly, GLS (both isoforms) interacted exclusively with the specific survival member of anti-apoptotic BCL-2 family in the relevant cell lines. For example, in MAVER-1 (BCL-2 dependent cell line), GLS interacted with BCL-2. In K562 (BCL-X_L dependent cell line), GLS interacted with BCL-X_L. In H929 (MCL-1 dependent cell line) GLS interacted with the long isoform in the sensitive cells, whereas in the resistant cells, GLS interacted with the long (anti-apoptotic) and short (pro-apoptotic) isoforms (Fig 4.2.8 a). These results also were confirmed in the reverse immunoprecipitation studies, using antibodies against BCL-2, BCL-X_L and MCL-1, all of which interacted with GLS in the different cell lines, as observed above. Briefly, in MAVER-1 BCL-2 interacted with both GLS isoforms, while BCL-X_L and MCL-1 interacted with the splice variant isoform glutaminase c (GAC) in K562 and H929, respectively (Fig 4.2.8 b). Taken together, these results strongly demonstrated that GLS could be playing a novel role in controlling the fate of cancer cells.

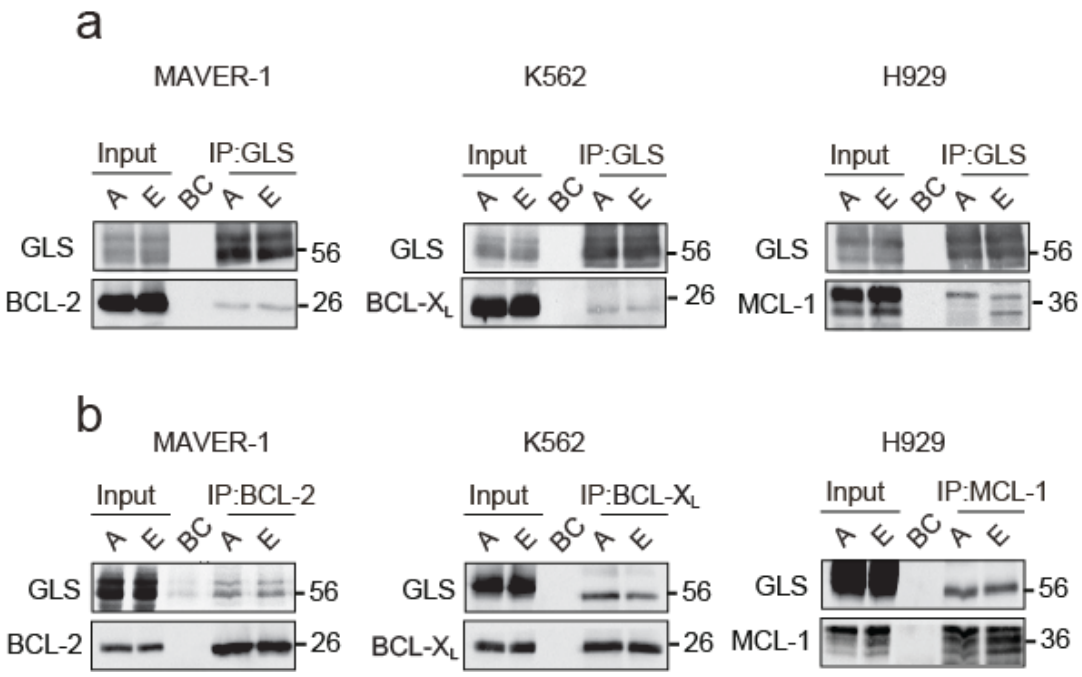

Fig 4.2.8. Identification of novel interaction between GLS and anti-apoptotic members. (a) Immunoprecipitation of GLS in haematological cell lines MAVER-1, K562 and H929 (A and E) cells revealed for interactions with anti-apoptotic BCL-2 family members.(b) Immunoprecipitation of specific survival members of BCL-2 family of protein in haematological cell lines MAVER-1, K562 and H929 (A and E) cells revealed for interactions with GLS. BC represents the beads control.

4.2.4 Glutamine deprivation enhanced ibrutinib-mediated apoptosis in MAVER-1

Since targeting glytaminolysis pathway overcame resistance to BH3 mimetic mediated-apoptosis, experiments were performed to assess whether this would be reproducible in overcoming resistance to another chemotherapeutic agents. Therefore, resistance to ibrutinib was generated in MAVER-1 cells (according to the procedure detailed in the first resistance model) and validated (Fig 4.2.9 a). Interestingly, glutamine deprivation overcame resistance to ibrutinib-mediated apoptosis in these cells (Fig 4.2.9 b). Taken together, these results suggest that targeting glutamine could be a promising way to overcome resistance to several chemotherapeutic agents.

4.2.5 Targeting GLS enhanced sensitivity and overcame resistance to ABT-263 (navitoclax) in primary CLL patient samples

To extend the potential of targeting GLS to primary patient samples, CLL cells from a navitoclax trial (as detailed in the methods) were used. These cells were isolated from patients during the L1D1 (lead-in period) as well as after five cycles C5D1 of navitoclax therapy (as explained in materials and methods). To assess whether targeting GLS could overcome resistance to ABT-263-mediated apoptosis in CLL samples, CLL cells were exposed to CB-839 for 24 h followed by exposure to ABT-263 for 4 h then the apoptosis assessed. Similar to the results observed in the cell lines, CB-839 in combination with ABT-263 overcame resistance to ABT-263 mediated-apoptosis in CLL primary patient samples (Fig 4.2.10). Taken together, these results strongly suggested that targeting GLS is a promising approach to tackle chemoresistance to BH3 mimetic-mediated apoptosis in CLL patients.

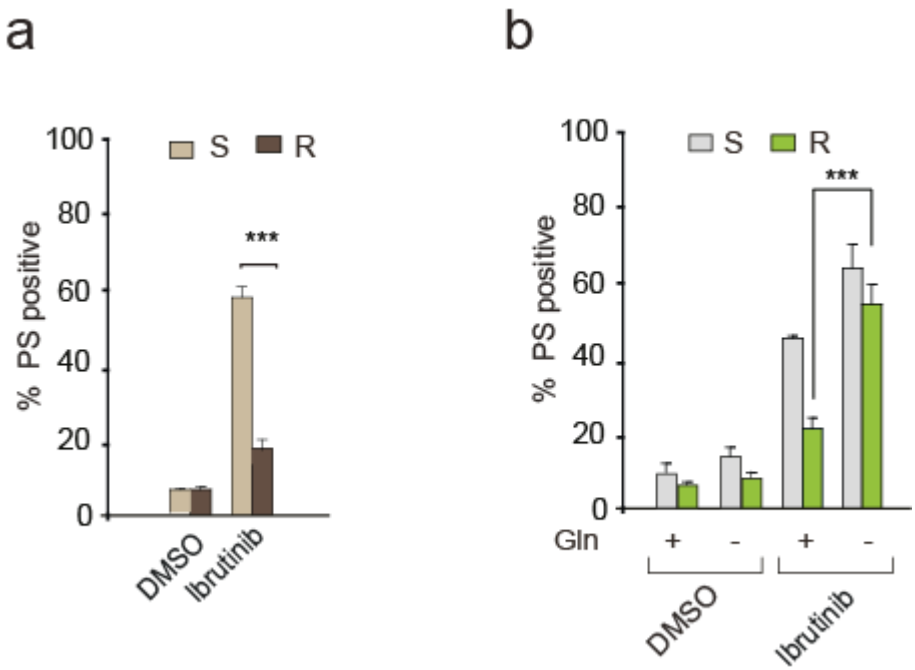

Fig 4.2.9. Glutamine deprivation enhances Ibrutinib-mediated apoptosis in MAVER-1 cells. (a)Sensitive and resistant MAVER-1 cells were exposed to Ibrutinib (10 μM) for 72 h. Then, apoptosis was assessed by PS externalisation. (b) Sensitive and resistant MAVER-1 cells were deprived of glutamine for 16 h followed by 72 h exposure to Ibrutinib (10 μM). Then apoptosis assessed as in (a). ***P ⩽0.001, Error bars = Mean ± SEM (n=3).

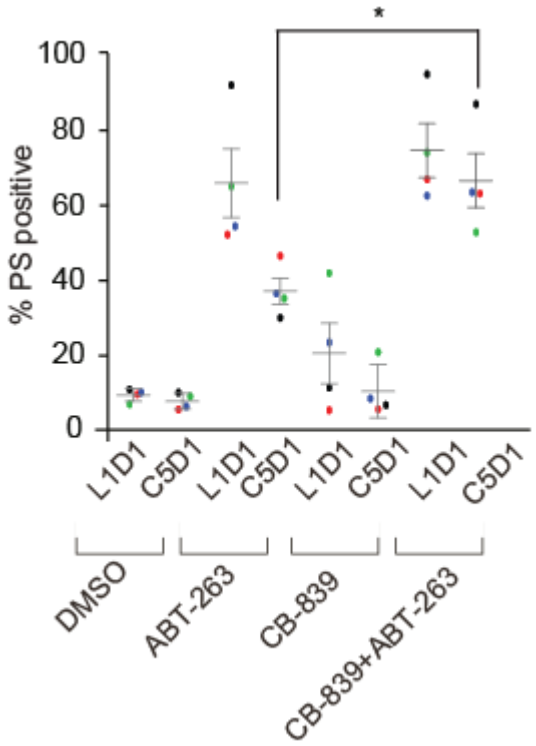

Fig 4.2.10. Pharmacological inhibition of Glutaminase overcomes navitoclax-mediated resistance in primary chronic lymphocytic leukaemia cells. Primary cells were isolated from five CLL patients during the initial lead-in-period (L1D1) or day 1 of cycle 5 (C5D1) of navitoclax therapy. The isolated cells were cultured *ex vivo* on feeder layer (mouse fibroblast L) cells for 24 h. This was followed by a 24 h exposure to CB-839 (50 nM). The cells were then removed from the feeder layer and exposed to ABT-263 (50 nM) for 4 h and apoptosis assessed by PS externalisation. *P $\leqslant$0.05. Error bars = Mean ± SEM (n=5). Each colour represents the data from an individual patient.

4.3 Discussion

Increasing proliferation rate in cancer cells corelates with increasing metabolic rate, as cancer cells require much higher levels of nutrients compared to normal cells (Lacey & Wilmore 1990). This variation between normal and cancer cells in consuming the basic nutrients and their altered metabolism as a result, have been exploited as a promising target for cancer therapy. In this context, the metabolism of glutamine and glucose has been more studied, as these are highly consumed by the cancer cells (Garber 2006; Bode et al. 2002).

It has been reported that glutamine deprivation can bypass resistance and enhance ABT-199-mediated apoptosis in multiple myeloma (Bajpai et al. 2016). In agreement, the results presented here suggest that targeting glutaminolysis pathway could be a promising strategy to overcome resistance to BH3 mimetic-mediated apoptosis. Moreover, glutamine deprivation enhances sensitivity to BH3 mimetic-mediated apoptosis in both sensitive and resistant cells (Fig 4.2.1 and Fig 4.2.2), suggesting that glutamine deprivation most likely acts indirectly to reverse or tackle the mechanism of resistance to BH3 mimetic mediated-apoptosis. Nevertheless, the fact that glutamine deprivation could overcome resistance to BH3 mimetic-mediated apoptosis in the other three resistance models as well as in the ibrutinib-resistant MAVER-1 cells (Fig 4.2.9) suggests that deprivation of glutamine primed all cells to undergo apoptosis and provides the cytotoxic cue to circumvent resistance.

Previous models of resistance to BH3 mimetics have always attributed it to either enhanced levels of other anti-apoptotic proteins, thus compensating for the loss of the primary anti-apoptotic member or a change in protein-protein interactions between the BH3-only proteins and their anti-apoptotic counterparts (Konopleva et al. 2006; van Delft et al. 2006; Szakács et al. 2006; Vogler, Hamali, et al. 2011; Tahir et al. 2017).

Furthermore, glutamine deprivation has been shown to alter these changes, as in the case of MCL-1 dependent multiple myeloma, in which glutamine deprivation enhances ABT-199 mediated-apoptosis through upregulation of BCL-2 binding BIM (Bajpai, et al. 2016). The results presented in this thesis did not indicate any significant change in the expression levels or protein-protein interactions that can relate to resistance and/or glutamine deprivation. However, the results also raise an interesting possibility that glutamine may be required for maintaining resistance. This is evident from the higher uptake of glutamine in the resistant cells compared to the sensitive cells (Fig 4.2.4). SLC1A5, a sodium coupled (Na^+-coupled) transporter for glutamine is upregulated by Myc (Gao et al. 2009) and downregulated by Rb (retinoblastoma protein) (Reynolds et al. 2014). The enhanced glutamine uptake dependence is clearly not due changes in SLC1A5 expression levels (Fig 4.2.4), thus suggesting that it possibly increased due to an increase in the activity of SLC1A5 or through another unrecognised mechanism of glutamine uptake and dependence must exist to explain why glutamine deprivation increases the sensitisation of cells and overcomes resistance to BH3 mimetic-mediated apoptosis.

The results also indicate that GLS interacts just with the primary survival proteins (BCL-2, BCL-X_L or MCl-1) in the relevant cell lines (Fig 4.2.8), thus highlighting a potential role for GLS in the regulation of cell survival and death. Thus, it is possible that many of BCL-2 family of proteins could also function as modulators of metabolism, and in fact, their role in apoptosis could well be secondary to their ability to regulate intermediary metabolism. Therefore, the availability/ unavailability of substrates could regulate the so-called anti and pro-apoptotic BCL-2 family of proteins to alter their expression levels and activity to dictate the fate of a cell, during stress conditions.

Targeting glutamine metabolism is clinically made possible by the administration of drugs, such as L-asparaginase to treat ALL (acute lymphoblastic leukemia) (Panosyan et al. 2004), as well as CB-839 to treat leukaemia, multiple myeloma and non- Hodgkin's lymphoma (Altman et al. 2016). In the context of BH3 mimetics, CB-839 has been used in combination with ABT-199 to enhance apoptosis of AML cells (Jacque et al. 2015). In agreement, results presented in this chapter confirm that CB-839 can be co-administered with BH3 mimetics, such as ABT-263 to overcome resistance in primary CLL samples (Fig 4.2.10).

The ability of glutamine to regulate the programmed cell death and/or resistance to BH3 mimetic-mediated apoptosis could also due to the involvement of other downstream glutamine metabolic pathways, which will be explored in the next results chapter.

Chapter 5

Downregulation of reductive carboxylation, lipogenesis and cholesterogensis enhances sensitivity to BH3 mimetics

5.1 Introduction

Metabolic reprogramming is one of the major hallmarks of cancer and associated with cancer progression (Pavlova & Thompson 2016; DeNicola & Cantley 2015; Hanahan & Weinberg 2011). Many studies have reported an increase in glycolysis, which provides ATP to support the rapid proliferation of cancer cells (Pavlova & Thompson 2016; DeNicola & Cantley 2015). As a result, glucose consumption in cancer cells is very high. Most of the carbon derived from enhanced glucose uptake is used to generate lactate, instead of the conventional metabolic steps involving tricarboxylic acid cycle (TCA) cycle, which generates reducing equivalents for the oxidative phosphorylation and electron transport chain (ETC) (Reitzer et al. 1979), as well as induces different signalling pathways that are necessary to support synthesis of substrates, such as fatty acids (Mayers & Vander Heiden 2015). To compensate for a lack of these pathways, cancer cells exhibit enhanced dependence on the amino acid glutamine, which supports lipid synthesis *via* the reductive carboxylation of the TCA cycle intermediate, citrate (DeBerardinis et al. 2007; Sellers et al. 2015; Mullen et al. 2012) (Figs 5.1.1 and 5.1.2).

Reductive carboxylation is the process by which α-ketoglutarate (α-KG), that is derived from glutamine and glutamate in the glutaminolysis pathway, is converted to isocitrate. This enzymatic reaction is catalysed by isocitrate dehydrogenases 1 and 2 (IDH1 and IDH2) and involves the consumption of NADPH (Nicotinamide adenine dinucleotide phosphate) (Ward et al. 2010; Altman et al. 2016). Thus obtained isocitrate is then converted to citrate in a reaction catalysed by aconitase (Mullen et al. 2014) (Fig 5.1.1). It has been reported that cancer cells depend on glutamine-dependent reductive carboxylation to support fatty acid synthesis, thus enhancing cell proliferation and growth, even during mitochondrial dysfunction.

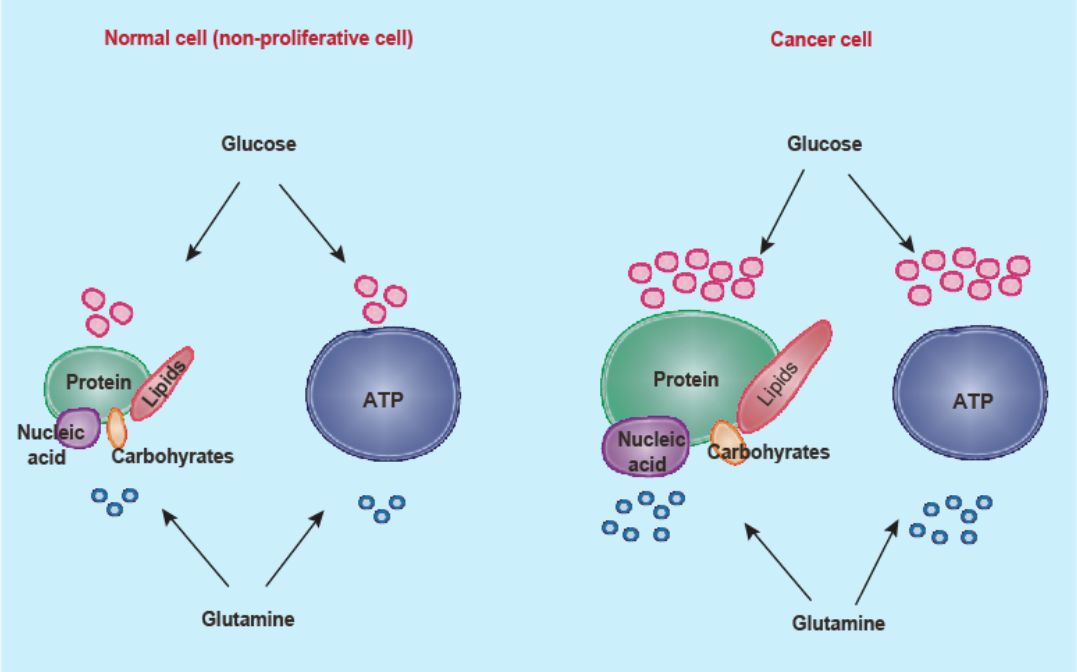

Fig 5.1.1. Comparison between normal cell and cancer cell metabolism. Scheme representing glucose and glutamine uptake in a normal cell and cancer cell.

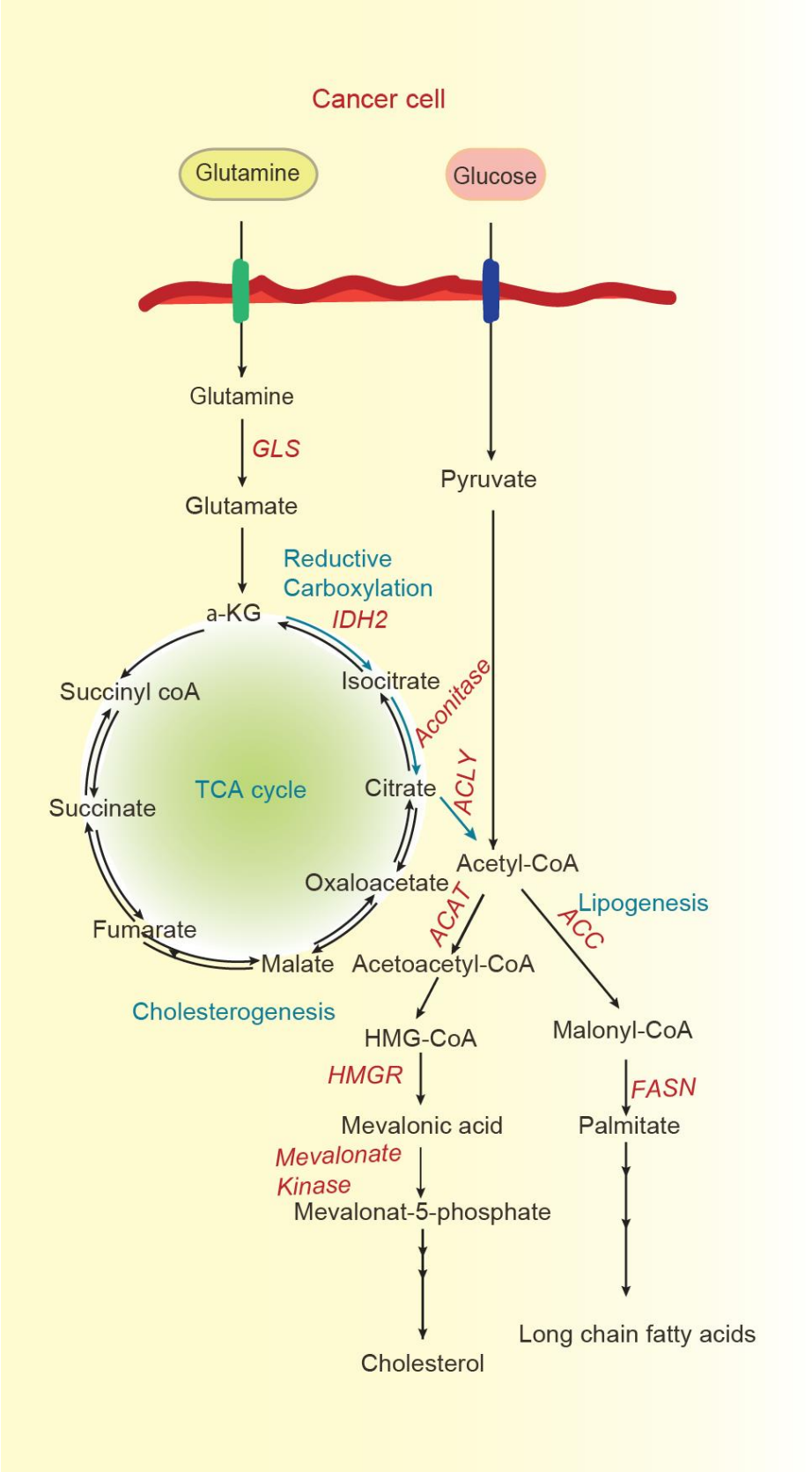

Fig 5.1.2. Metabolism in cancer cells. Scheme representing different steps of glucose and glutamine metabolism in cancer cell.

Citrate derived as a result of reductive carboxylation of α-KG is then cleaved to Acetyl-CoA and oxaloacetate *via* ATP-citrate-lyase (ACLY), which feeds into two distinct pathways of lipid synthesis (Mullen et al. 2012). The first pathway is called lipogenesis and it facilitates fatty acid synthesis by the serial of reactions: Acetyl-CoA is acted upon ACC (Acetyl-CoA carboxylase) for conversion to malonyl-CoA, which in turn is converted to palmitate by the key multifunctional enzyme, fatty acid synthase (FASN). Palmitate then undergoes a series of reactions to generate long chain fatty acids (Mair et al. 2008; Vrablik & Watts 2012; Rohrig & Schilze 2016) (Figs 5.1.2 and 5.1.3a).

The second pathway of lipid synthesis is called cholesterogenesis or the mevalonate pathway, which involves the conversion of acetyl-CoA to acetoacetyl-CoA through ACAT (acetyl-Coenzyme A acetyl transferases) then in turn converted to HMG-CoA. HMG-CoA is then catalysed to mevalonic acid by the key enzyme of this pathway, HMGR (3-hydroxy-3-methylglutaryl coenzyme A reductase) (Goldstein & Brown 1990). The second critical enzyme in this pathway, mevalonate kinase is responsible for the conversion of mevalonic acid to mevalonate-5-phosphate (Hinson et al. 1997). Then, mevalonate-5-phosphate is converted by a series of reactions till reach to farnesyl-pyrophosphate, which in turn is converted to squalene *via* squalene synthase. Later, squalene is converted to lanosterol and then finally to cholesterol after a series of reactions (Tricarico et al. 2015) (Figs 5.1.2 and 5.1.3b).

This chapter is aimed at investigating whether targeting the downstream events of glutamine metabolism (such as reductive carboxylation, lipogenesis and cholesterogenesis) could also overcome resistance to BH3 mimetic-mediated apoptosis.

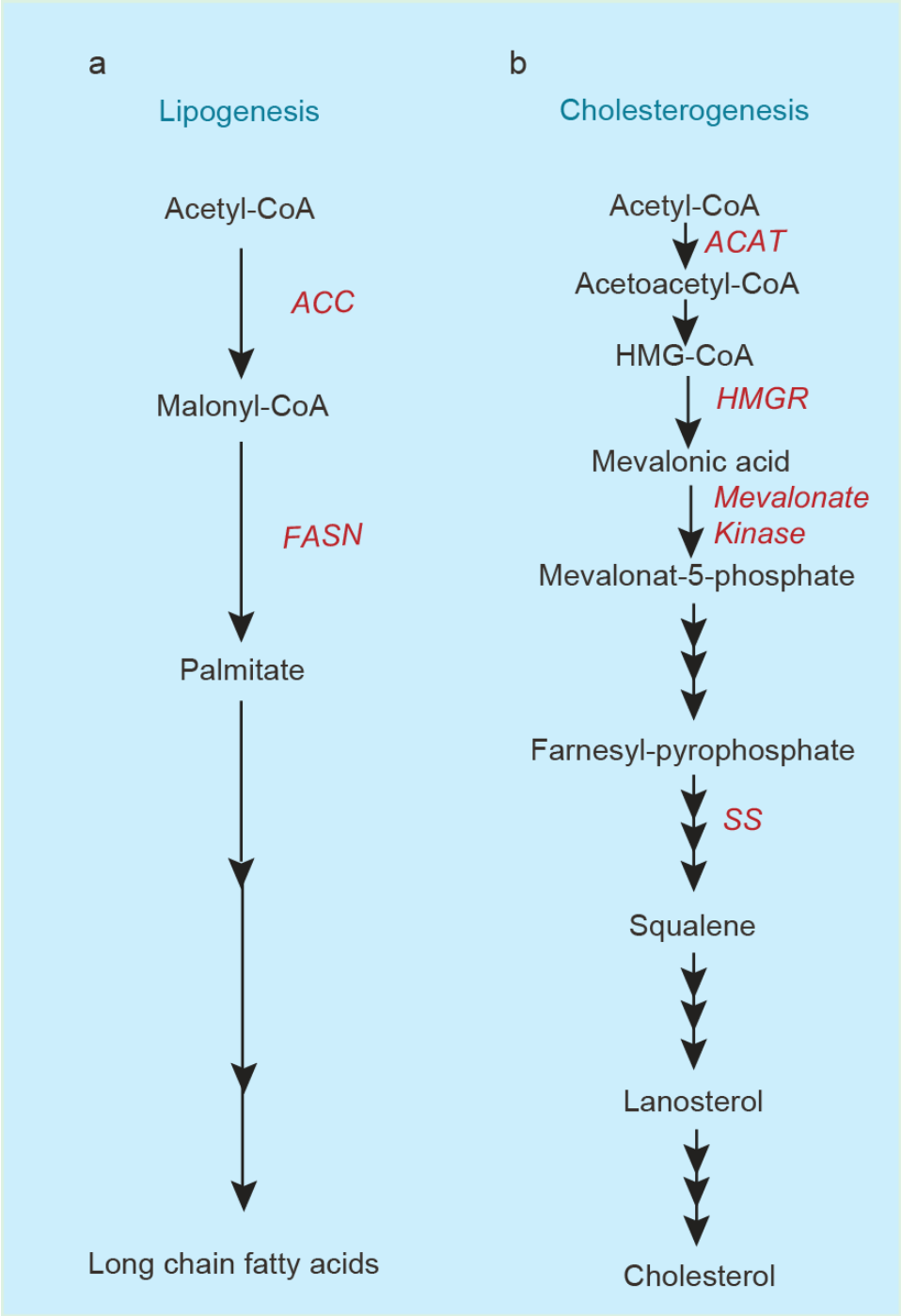

Fig 5.1.3. Scheme representing (a) lipogenesis and (b) cholesterogenesis pathways.

5.2 Results

5.2.1 Targeting reductive carboxylation overcomes resistance to BH3 mimetics-mediated apoptosis

In order to assess whether targeting signalling pathways downstream of glutamine metabolism could overcome resistance to BH3 mimetic-mediated apoptosis, sensitive and resistance K562 cells were deprived of glutamine and supplemented with a few metabolic intermediates of TCA cycle (Fig 5.2.1 a). The intermediates chosen for this study were oxaloacetate (which is downstream of α-KG in the TCA cycle), citrate (which is immediately downstream of oxaloacetate) and pyruvate (which can undergo irreversible carboxylation to generate oxaloacetate (Gailiusis et al. 1964). The other intermediates of TCA cycle were not used in this study because it was challenging to obtain cell-permeable variants of the other intermediates.

As observed previously, glutamine deprivation enhanced sensitivity of both the sensitive and resistant K562 cells to A-1331852-mediated apoptosis (Fig 5.2.1 b). Supplementation with oxaloacetate did not alter the effects of glutamine deprivation on A-1331852-mediated apoptosis in K562 cells (Fig 5.2.1 b), whereas supplementation with glutamine or α-KG has previously been shown to restore resistance to A-1331852-mediated apoptosis in the glutamine-deprived cells (Fig. 4.2.5). This suggested that the intermediates downstream of α-KG but upstream of oxaloacetate in the TCA cycle could hold the key to overcoming resistance to BH3 mimetics. However, we were not able to perform experiments with cell-permeable succinate, fumarate or malate to address this possibility. Interestingly, supplementation with citrate effectively restored the resistance of K562 cells to A-1331852-mediated apoptosis (Fig 5.2.1 b).

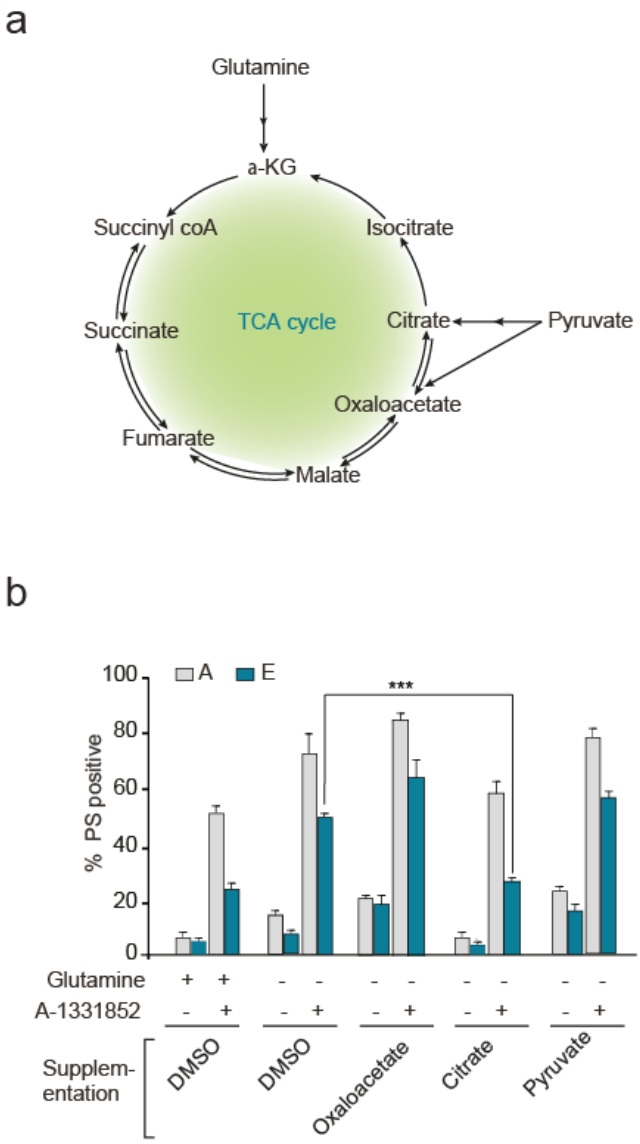

Fig 5.2.1. Citrate supplementation reverses the effect of glutamine deprivation and restores the resistance to BH3 mimetic-mediated apoptosis. (a) Scheme representing the TCA cycle (tricarboxylic acid cycle). (b) Sensitive (A) and resistant (E) K562 cells were incubated with either RPMI medium or with glutamine free medium in the presence or absence of oxaloacetate, citrate or pyruvate (4 mM) for 16 h. The cells were then exposed to A-1331852 (10 nM) for 4 h and apoptosis assessed by PS externalisation. ***P ⩽0.001 Error bars = Mean ± SEM (n=3).

These findings suggested that the conversion of α-KG to oxaloacetate *via* the TCA cycle may not be essential for conferring chemoresistance to BH3 mimetics (Fig 5.2.1 a). However, the very next step of TCA cycle (generation of citrate) proved to be critical for chemoresistance. Moreover, metabolic supplementation of pyruvate (the product of glycolysis), which could also generate Acetyl-CoA, which in turn can produce citrate to feed into TCA cycle (Wise et al. 2011; Metallo et al. 2012), failed to alter A-1331852-mediated apoptosis in these cells, suggesting that the conversion of pyruvate to Acetyl-CoA/ oxaloacetate was not essential for the maintenance of resistance to BH3 mimetic-mediated apoptosis (Fig 5.2.1 b). Taken together, these findings suggested the involvement of an alternative metabolic pathway that generated citrate from α-KG, without the involvement of oxaloacetate.

As discussed before, reductive carboxylation regulates the conversion of α-KG to isocitrate catalysed *via* IDH2 (mitochondrial isocitrate dehydrogenase 2), and subsequently the conversion of isocitrate to citrate *via* aconitase (Fig 5.2.2 a). In order to investigate whether this pathway is involved in chemoresistance/ chemosensitivity to BH3 mimetics, sensitive and resistant K562 cells were transfected with siRNAs against IDH2 and aconitase. A negative control of IDH3 siRNA was also included in this experiment, as IDH3 catalyses the reverse reaction of isocitrate to α-KG, and hence will be an appropriate negative control. Silencing the expression of IDH2 or aconitase but not IDH3 re-sensitised the resistant cells to A-1331852-mediated apoptosis (Fig 5.2.2 b and c). This finding suggested that the availability of citrate is critical for the maintenance of chemoresistance, as depletion of citrate (either via glutamine deprivation, GLS inhibition, IDH2 or aconitase downregulation) re-sensitised cells to BH3 mimetic-mediated apoptosis.

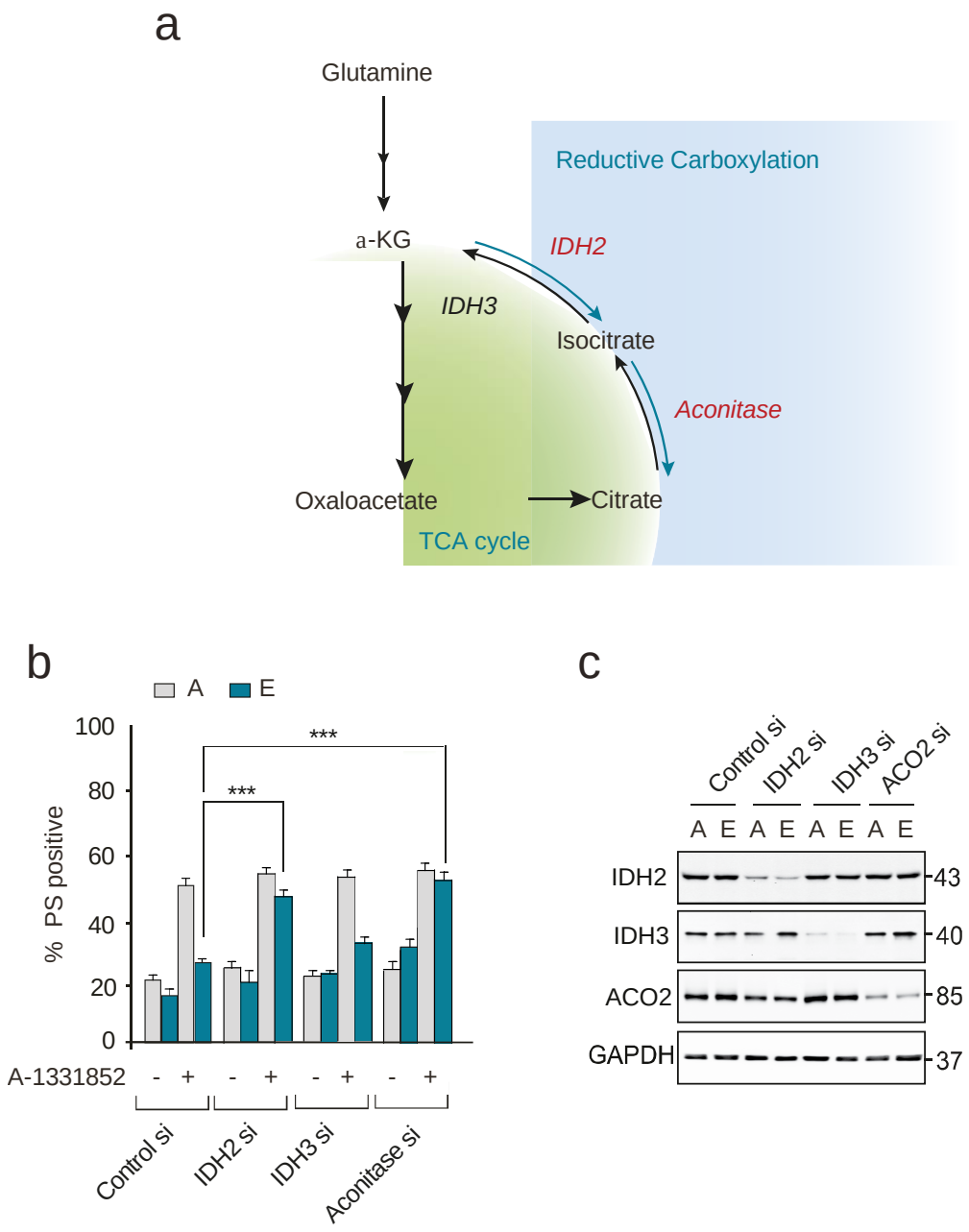

Fig 5.2.2. Targeting reductive carboxylation overcomes resistance to BH3 mimetic-mediated apoptosis. (a) Scheme representing reductive carboxylation. (b) Sensitive (A) and resistant (E) K562 cells were transfected with IDH2, IDH3 and ACO2 siRNAs for 72 h, followed by a 4 h exposure to A-1331852 (10 nM). Apoptosis was then assessed by PS externalisation. (c) Western blots confirmed the knockdown efficiency of the different siRNAs. ***P ⩽0.001; Error bars = Mean ± SEM (n=3

To investigate this further, sensitive and resistant K562 cells were transfected with siRNA against IDH2 and supplemented with metabolic intermediates that acted upstream (glutamine and α-KG) or downstream (citrate) of IDH2. Metabolic supplementation of glutamine and α-KG had no effect on IDH2 downregulation, in terms of its ability to re-sensitise cells to BH3 mimetic-mediated apoptosis. However, metabolic supplementation of citrate demonstrated a remarkable decrease in BH3 mimetic-mediated apoptosis, thus restoring resistance to A-1331852-mediated apoptosis, thus confirming that citrate played a critical role in chemoresistance to BH3 mimetics (Fig 5.2.3).

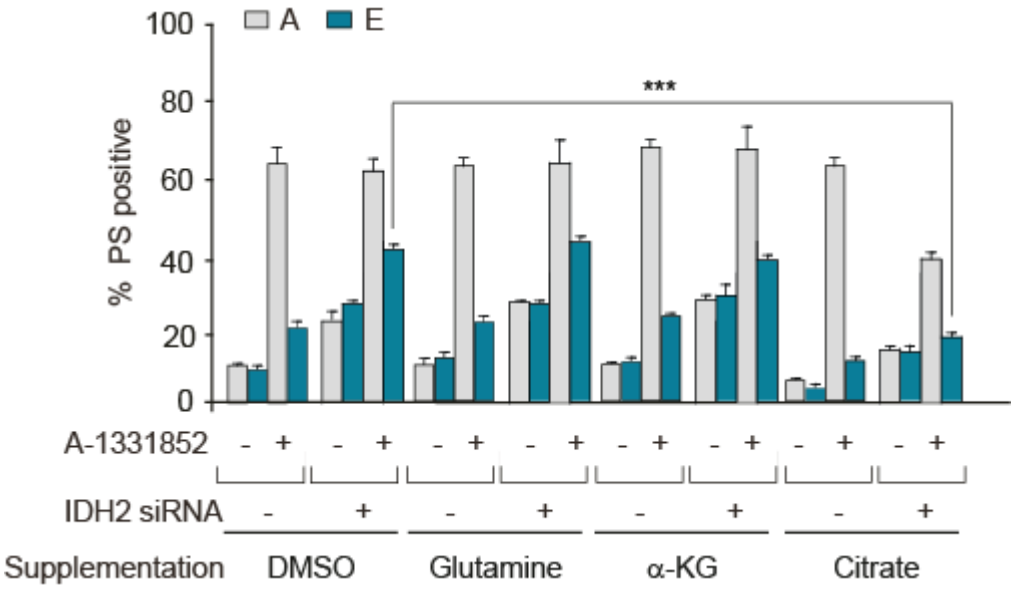

Fig 5.2.3. Citrate supplementation reverses the effect of IDH2 downregulation and restores the resistance to BH3 mimetic-mediated apoptosis. Sensitive (A) and resistant (E) K562 cells were transfected with IDH2 siRNAs for 72 h, followed by 16 h supplementation with glutamine (2 mM), α-KG (4mM) or citrate (4 mM). The cells were then exposed exposure to A-1331852 (10 nM) for 4 h and apoptosis assessed by PS externalisation. ***P ⩽0.001; Error bars = Mean ± SEM (n=3).

5.2.2 Targeting lipogenesis overcomes resistance to BH3 mimetic- mediated apoptosis

To investigate the metabolic steps downstream of citrate synthesis, enzyme ACLY, which converts citrate to Acetyl-CoA (Fig 5.2.4 a), was downregulated using genetic knockdowns (siRNA) or pharmacological inhibition (using SB204990). Downregulation of ACLY, in both approaches detailed above, overcame resistance to A-1331852-mediated apoptosis in K562 cells (Figs 5.2.4 b and c), as well as ABT-199-mediated apoptosis in MAVER-1 and A-1210477-mediated apoptosis in H929 (Fig 5.2.4 c). Upon confirmation of a role for ACLY in chemoresistance/ sensitivity to BH3 mimetic-mediated apoptosis, the next set of experiments involved targeting downstream metabolic pathways. Since acetyl-CoA has been shown to generate palmitate through a series of reactions, catalysed by FASN (Guan et al. 2017; Mashima et al. 2009) (Figure 5.2.5 a), experiments were performed to assess whether modulation of lipogenesis pathway by downregulation of FASN could overcome resistance to BH3 mimetic-mediated apoptosis. To do this, sensitive and resistant K562 cells were transfected with FASN siRNA or exposed to a pharmacological inhibitor of FASN (GSK194069). Downregulation of FASN using both these strategies resulted in the restoration of sensitivity to A-1331852-mediated apoptosis in the chemoresistant K562 cells (Figs 5.2.5 and 5.2.6). Exposure to GSK2194069 also restored sensitivity in chemoresistant MAVER-1 and H929 cells to their respective BH3 mimetics (Fig. 5.2.6 b), thus suggesting the conserved nature of this metabolic pathways in several cell lines. Finally, metabolic supplementation of palmitate (product of FASN) abolished the effects of GSK2194069 and restored the original chemoresistance phenotype (Fig 5.2.6 c), thus obviating a requirement for FASN. Taken together, these results strongly suggested that lipogenesis was important to

maintain resistance to BH3 mimetic-mediated apoptosis and targeting lipogenesis could bypass such resistance.

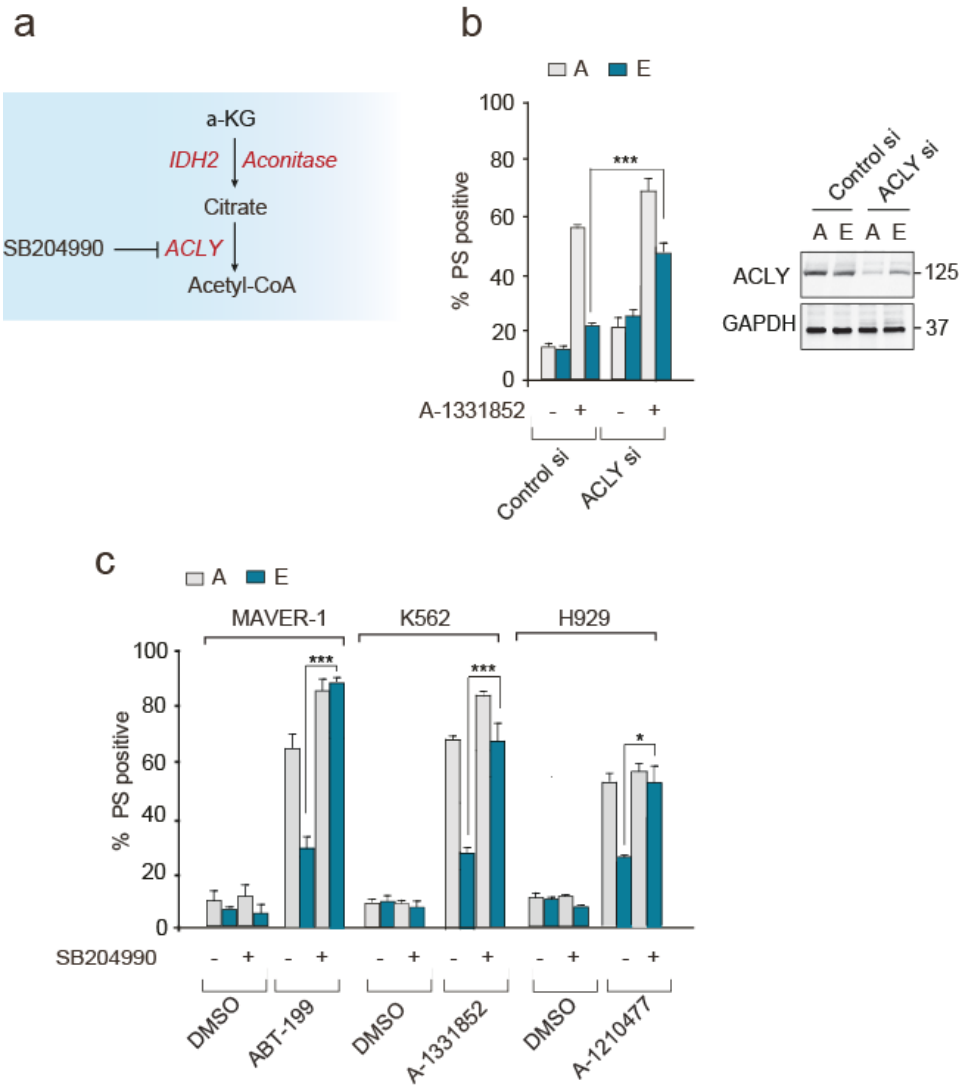

Fig 5.2.4. Genetic knockdown or pharmacological inhibition of ACLY enhances sensitivity to BH3 mimetic-mediated apoptosis. (a) Scheme representing the metabolisim of a-kg to Acetyl-CoA. (b) Sensitive (A) and resistant (E) K562 cells were transfected with ACLY siRNA for 72 h, followed by 4 h exposure to A-1331852 (10 nM). Then, apoptosis was assessed by PS externalisation. Western blots confirmed the knockdown efficiency of the different siRNAs. (c) Sensitive (A) and resistant (E) MAVER-1, K562 and H929 cells were exposed to SB-204990 (1 μM) for 72 h followed by 4 h exposure to specific BH3 mimetics namely ABT-199 (10 nM), A-1331852 (10 nM) or A-1210477 (5 μM), respectively. Apoptosis was assessed by PS externalisation. ***P ⩽0.001, *P ⩽0.05; Error bars = Mean ± SEM (n=3).

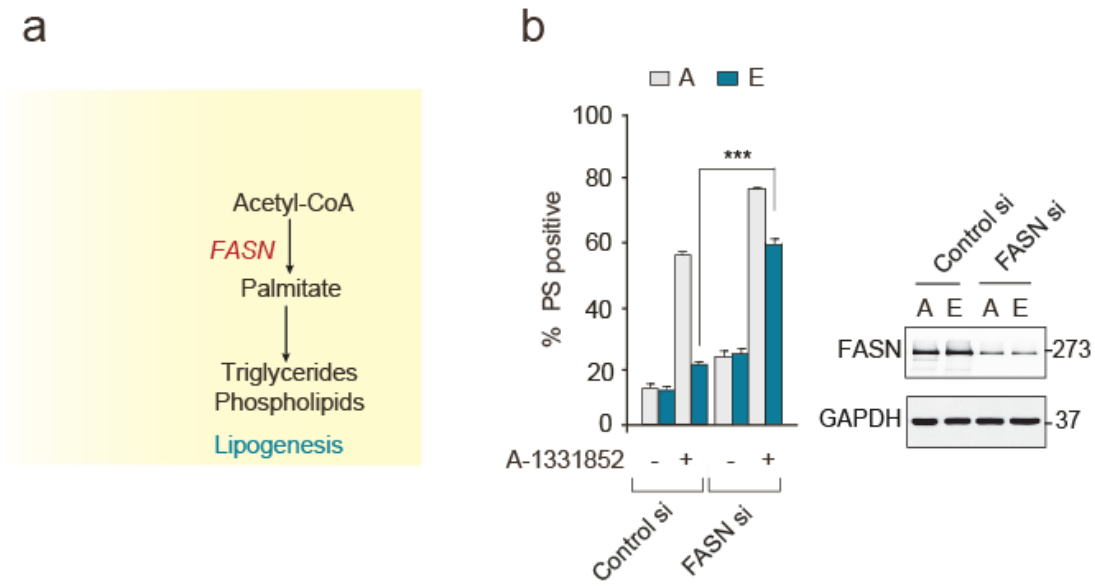

Fig 5.2.5. Genetic knockdown of FASN enhances sensitivity to BH3 mimetic-mediated apoptosis. (a) Scheme representing the lipogenesis pathway (b) Sensitive (A) and resistant (E) K562 cells were transfected with FASN siRNAs for 72 h, followed by 4 h exposure to A-1331852 (10 nM). Then, apoptosis was assessed by PS externalisation. Western blots confirmed the knockdown efficiency of the different siRNAs. ***P ⩽0.001; Error bars = Mean ± SEM (n=3).

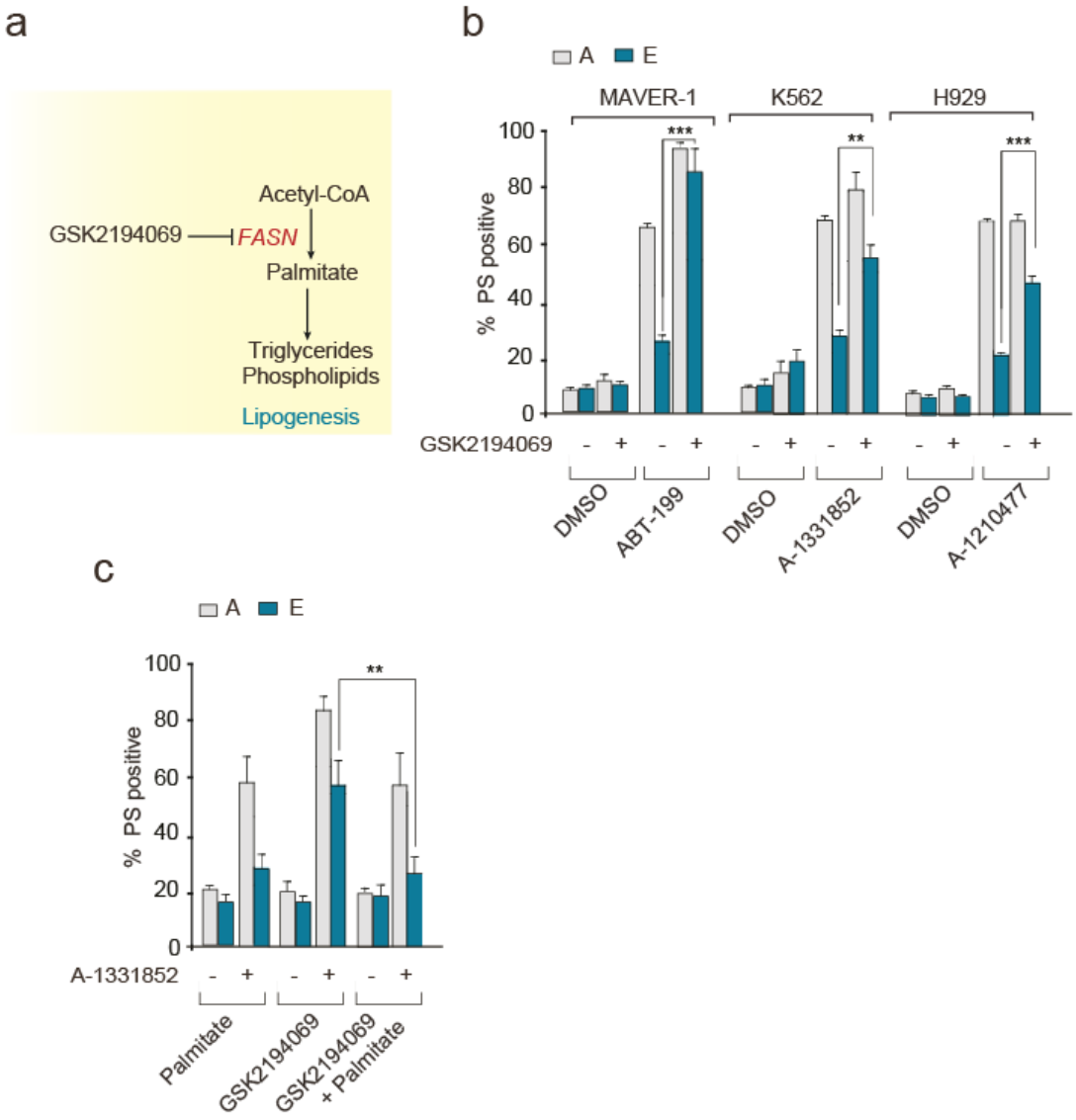

Fig 5.2.6. Pharmacological inhibition of FASN enhances sensitivity to BH3 mimetic- mediated apoptosis. (a) Scheme representing the lipogenesis pathway with the FASN inhibitor GSK2194069. (b) Sensitive (A) and resistant (E) MAVER-1, K562 and H929 cells were exposed to GSK2194069 (100 nM) for 48 h followed by 4 h exposure to specific BH3 mimetics namely ABT-199 (10 nM), A-1331852 (10 nM) or A-1210477 (5 μM), respectively. Then, apoptosis was assessed by PS externalisation. (c) Sensitive (A) and resistant (E) K562 cells were exposed to GSK2194069 (100 nM) for 24 h, supplemented with palmitate (50 □M) for a further 24 h. The cells were exposed to A-1331852 (10 nM) for 4 h and apoptosis assessed as in (b). ***P ⩽0.001, **P ⩽0.01; Error bars = Mean ± SEM.

5.2.3 Targeting cholestrogenesis also overcomes resistance to BH3 mimetics-mediated apoptosis

Since Acetyl-CoA could also feed into the cholesterol biosynthetic pathway (Fig 5.2.7 a), experiments were performed to downregulate this pathway by genetically silencing HMGR expression or by pharmacological inhibition of the enzyme using three mostly-used statins, namely simvastatin, pitavastatin or Atorvastatin. These studies were carried out to assess whether targeting the key enzyme of the cholesterogenesis pathway (HMGR) could enhance the sensitivity to BH3 mimetic-mediated apoptosis and overcome resistance. The results indicated that this was indeed true and that genetic knockdown of HMGR or exposure to the different statins reversed the resistance and enhanced the sensitivity to BH3 mimetic-mediated apoptosis in all the relevant cell lines (Figs 5.2.7 b, c and 5.2.8). Taken together, these results suggested that targeting cholesterogenesis could overcome chemoresistance to BH3 mimetic-mediated apoptosis.

5.2.4 Targeting HMG-CoA reductase enhances sensitivity and overcomes resistance to ABT-263 (navitoclax) in primary CLL patient samples

To further extend these observations to primary patient samples, CLL cells isolated from patients during the L1D1 (lead-in period) and after five cycles C5D1 of navitoclax therapy (as explained in the previous chapter as well as materials and methods) were exposed to simvastatin for 24 h followed by exposure to ABT-263 for 4 h then the apoptosis assessed. Similar to the results observed in cell lines, simvastatin in combination with ABT-263 overcame resistance to ABT-263-mediated apoptosis in CLL primary patient samples (Fig 5.2.9).

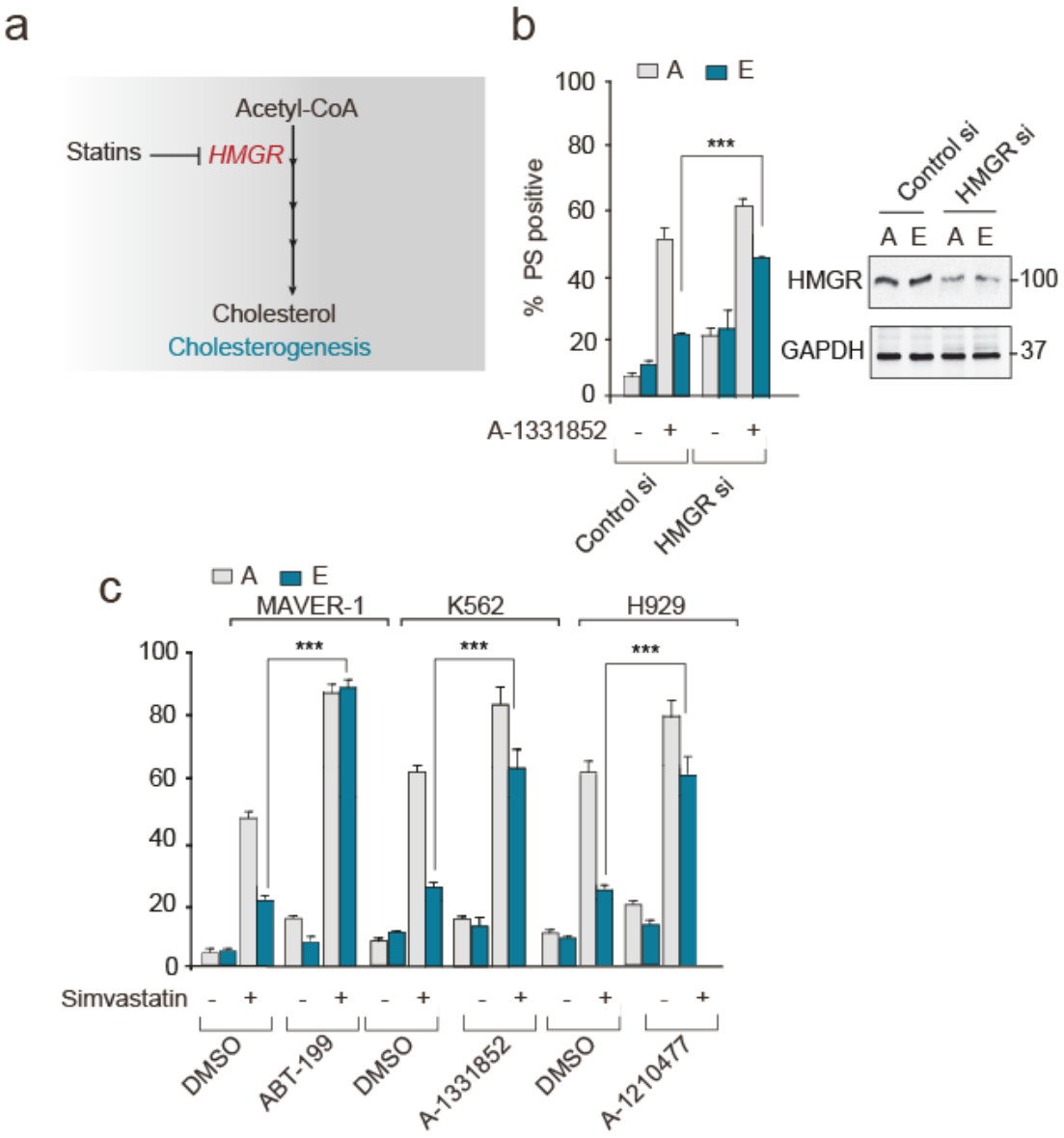

Fig 5.2.7. Genetic knockdown or pharmacological inhibition of HMGR enhances sensitivity to BH3 mimetic-mediated apoptosis. (a) Scheme representing cholestrogenesis as the other arm of the fatty acid synthesis pathway. (b) Sensitive (A) and resistant (E) K562 cells were transfected with HMGR siRNA for 72 h, followed by 4 h exposure to A-1331852 (10 nM). Apoptosis was then assessed by PS externalisation. Western blots confirmed the knockdown efficiency of the HMGR siRNA. (c) Sensitive (A) and resistant (E) MAVER-1, K562 and H929 cells were exposed to Simvastatin (250 nM) for 72 h followed by 4 h exposure to ABT-199 (10 nM), A-1331852 (10 nM) and A-1210477 (5 μM), respectively. Apoptosis was assessed as in (b). ***P ⩽0.001; Error bars = Mean ± SEM (n=3).

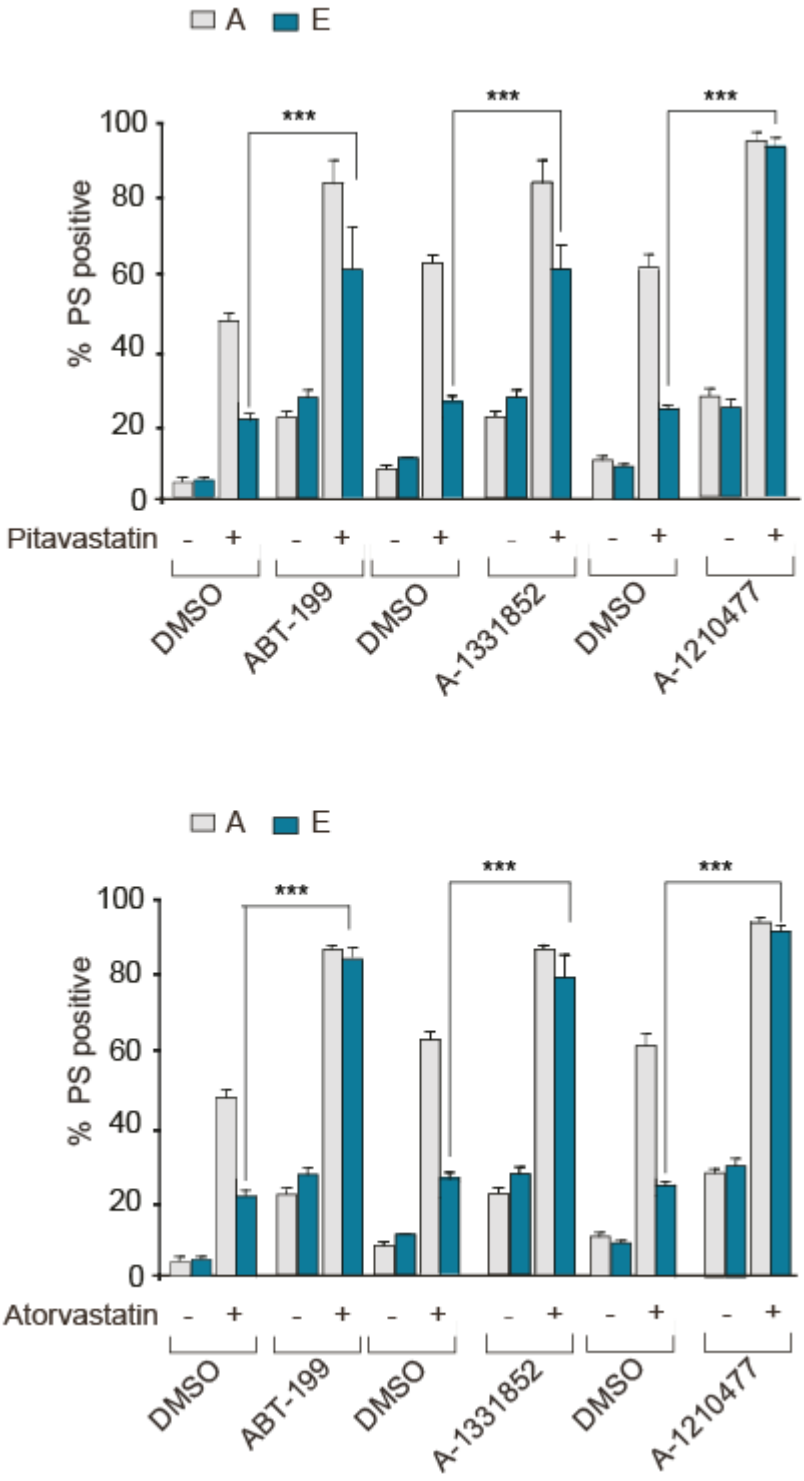

Fig 5.2.8. Other statins also enhance sensitivity to BH3 mimetics-mediated apoptosis. Sensitive (A) and resistant (E) MAVER-1, K562 and H929 cells were exposed to Pitavastatin (1 μM) or Atorvastatin (10 μM) for 72 h followed by 4 h exposure to ABT-199 (10 nM), A-1331852 (10 nM) or A-1210477 (5 μM), respectively. Apoptosis was then assessed by PS externalisation. ***P ⩽0.001; Error bars = Mean ± SEM (n=3).

.

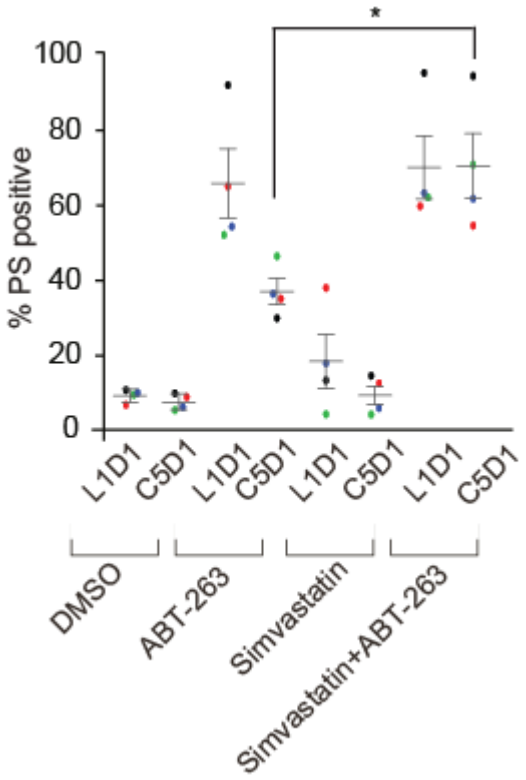

Fig 5.2.9. Pharmacological inhibition of HMG-CoA reductase overcomes navitoclax-mediated resistance in primary chronic lymphocytic leukaemia cells. Primary cells were isolated from five CLL patients during the initial lead-in-period (L1D1) or day 1 of cycle 5 (C5D1) of navitoclax therapy. The isolated cells were cultured *ex vivo* on feeder layer (mouse fibroblast L) cells for 24 h. This was followed by a 24 h exposure to Simvastatin (10 nM). The cells were then removed from the feeder layer and exposed to ABT-263 (50 nM) for 4 h and apoptosis assessed by PS externalisation. *P ⩽0.05. Error bars = Mean ± SEM (n=5). Each colour represents the data from an individual patient.

5.3 Discussion

Results from the previous chapters of this thesis implicated a role for glutamine uptake and metabolism in chemoresistance to BH3 mimetics. Targeting multiple steps of this metabolic pathway has been proven to show enhanced sensitivity to apoptosis in the different chemoresistance models, thus offering several promising strategies to circumvent chemoresistance in cancer (Figure 5.3.1).

Citrate is an essential component for fatty acid synthesis, and this is derived either from glutamine *via* reductive carboxylation or from acetyl-coA and pyruvate, as a result of glycolysis and oxidative decarboxylation (Wise et al. 2011; Metallo et al. 2012). The current study convincingly demonstrates that resistance to BH3 mimetic-mediated apoptosis is associated with glutamine-derived citrate not glycolysis-driven citrate, as supplementation with pyruvate or oxaloacetate had no effect on chemoresistance/ chemosensitivity to BH3 mimetics, in marked contrast to the effects of glutamine or α-KG (Fig 5.2.1). Moreover, downregulation of IDH2 but not IDH3 could bypass resistance to BH3 mimetic-mediated apoptosis (Fig 5.2.2), as well as downregulation of IDH2 then supplementation with citrate (Fig 5.2.3), suggesting a crucial role of citrate in chemoresistance.

It has been proposed that FASN overexpression is involved with drug resistance in cancer, and inhibiting FASN, using orlistat has been shown to sensitise cancer cells to anticancer therapy (Liu et al. 2008). GSK2194069 was identified as a highly potent inhibitor of human FASN reaction, inhibiting growth of cancer cells (Hardwicke et al. 2014). These suggestions strongly correlated with the current results as targeting FASN genetically and pharmacologically overcome resistance to BH3 mimetic-mediated apoptosis (Figs 5.2.5 and 5.2.6 a and b) as it strongly supported by supplementation study of palmitate (Fig 5.2.6 c).

The current study also demonstrates that using different statins, namely simvastatin, atorvastatin or pitavastatin, BH3 mimetic-mediated apoptosis can be enhanced and resistance overcome in the three haematological cancer cell lines (Figs 5.2.7 c and 5.2.8). Furthermore, statins also overcame resistance to ABT-263-mediated apoptosis in resistant CLL samples (Fig 5.2.9). These results strongly support the importance of cholesterogenesis pathway in cancer (Mullen et al. 2016). More importantly, the current study provides a promising strategy of repurposing drugs, such as statins that are most commonly used in patients, to treat cancer and overcome chemoresistance.

Collectively, the current findings strongly demonstrate that targeting different steps of intermediary metabolism could enhance BH3 mimetic mediated-apoptosis and overcome resistance in several haematological cancers. Therefore, the next results chapter will focus on extending these findings to improve therapy in solid tumours, and in particular, head and neck squamous cell carcinoma (HNSCC).

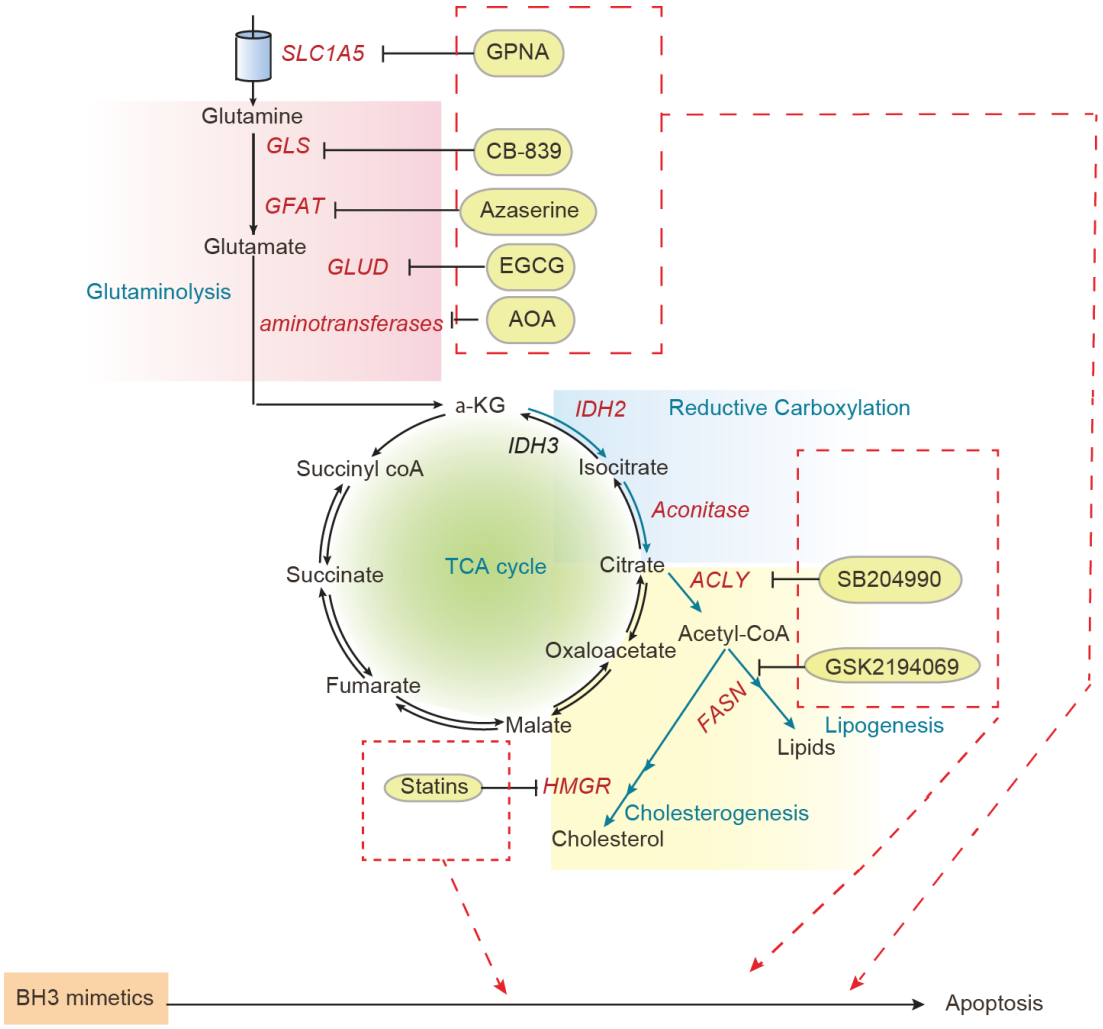

Fig 5.3.1. Targeting different steps of the glutamine metabolic pathway enhances sensitivity to BH3 mimetic-mediated apoptosis. Scheme representing the different enzymes in the glutamine metabolic pathway: glutamine, transported into cells *via* SLC1A5 (inhibited by GPNA), is converted to glutamate either *via* GLS-mediated glutaminolysis (inhibited by CB-839) or by the GFAT-mediated hexosamine pathway (inhibited by azaserine). Glutamate can then generate α–ketoglutarate (α–KG) either *via* GLUD1-mediated dehydrogenation (inhibited by ECGC) or by a series of aminotransferase reactions (inhibited by AOA). α-ketoglutarate (α–KG) feeds into the TCA cycle to generate citrate through reductive carboxylation. Citrate is then catalysed by ACLY (inhibited by SB204990) to produce acetyl-CoA, which ultimately results in lipogenesis by FASN (inhibited by GSK2194069) and cholesterogenesis by HMGR (inhibited by statins). Inhibiting these enzymes pharmacologically or genetically in combination with BH3 mimetics overcomes resistance in haematological cell lines.

Chapter 6

Exploring the potential of targeting glutaminase in head and neck squamous cell carcinoma

6.1 Introduction

Glutamine is converted to glutamate through a hydrolysis reaction by the key enzyme GLS. GLS plays an essential role in the proliferation of neoplastic cells *via* the glutaminolysis pathway. It has been shown that GLS is highly expressed in a wide variety of cancers, including AML, oesophagus, breast and head and neck (Saha et al. 2019; Jacque et al. 2015).This high expression was linked with poor prognosis. Targeting GLS using a specific inhibitor, such as CB-839, exhibited reduction in tumour cell proliferation (Gross et al. 2014).

Head and neck squamous cell carcinoma (HNSCC) is the sixth most common cancer worldwide, with around 600,000 new cases recorded annually and a mortality rate of ~40-50% (Ferlay et al. 2015). HNSCC is a major public health issue because of late diagnosis and the poor treatment outcomes (Yang et al. 2019). The tumors derive from the epithelial cells of the mucosal layer, which line the upper passages of the digestive system and upper airways (oral cavity, larynx, oropharynx and hypopharynx). The main causes of HNSCC are smoking and excessive use of alcohol. Currently, infection with human papillomaviruses (HPVs) causes a large proportion of these tumours (Castellsagué et al. 2016). It is now well recognised that HNSCC can be divided into HPV-negative and HPV-positive (Lawrence & et al 2015; Seiwert et al. 2015). Interestingly, the incidence of both HPV-negative and HPV-positive HNSCC is higher among men than women (Chaturvedi et al. 2008). The higher amount of tobacco smoking and excessive use of alcohol among men are assumed to be associated with the higher incidence of HPV-negative HNSCC in men. It is not clear why the incidence of HPV-positive HNSCC is significantly higher among men than women (Nielson et al. 2007; Giuliano et al. 2011).

Different treatment strategies, including surgery, radiation and chemotherapy, are used to tackle HNSCC. These strategies are used in various combinations, depending on the stage of the tumour (Marur & Forastiere 2008). The type of surgery used is determined by the tumour size and site. In addition to classical surgery, transoral robotic surgery has recently been introduced (Kofler et al. 2014; Cohen et al. 2011). For locally advanced HNSCC, radiation therapy is used a co-treatment with surgery or simultaneously with chemotherapy. The radiation dose varies, between 60-70 Gy, depending on the treatment plan (Marur & Forastiere 2008; Marur & Forastiere 2016). However, long term radiation, with doses >55 Gy, have been shown to be toxic (Langendijk et al. 2008). Chemotherapy, as a part of primary curative multi-modality plan, has been used as a co-treatment with radiotherapy (Marur & Forastiere 2008; Marur & Forastiere 2016). Cisplatin, a chemotherapeutic agent, is utilized in combination with radiation for HNSCC treatment (Vermorken et al. 2008). The meta-analysis of different HNSCC clinical trials, between the years 1965-2000, has indicated that the combination of cisplatin and radiation is considered to be the best combination (Pignon et al. 2000; Blanchard et al. 2011). However, use of cisplatin is associated with significant toxicity, including nephrotoxicity, neurotoxicity and ototoxicity, as well as inducing tumour resistance (Peddi et al. 2015; Galluzzi et al. 2012). Moreover, other drugs/antibodies have been identified as alternatives for cisplatin to be used in combination with radiation. Of these, cetuximab and panitumumab (EGFR monoclonal antibodies) are approved for HNSCC (Bonner et al. 2006; FDA 2006; Bonner et al. 2010; Kian Ang et al. 2014; Giralt et al. 2015). An initial randomized phase III trial indicated that cetuximab in combination with radiation improved overall survival (Bonner et al. 2006). Addition of cisplatin to this combination resulted in high toxicity (Kian Ang et al. 2014). Similarly, high toxicity

was observed when panitumumab was combined with cisplatin and radiation together with a poor overall survival outcome compared with the combination of cisplatin and radiation alone (Giralt et al. 2015).

The therapeutic outcomes of treating HNSCC are often limited by acquired resistance to both chemotherapy and radiation therapy, as well as their combined toxicity. In order to circumvent the resistance, I have targeted intermediary metabolism, as explained in previous chapters, to overcome resistance to BH3 mimetic-mediated apoptosis. Therefore, in this chapter I will investigate whether using a similar strategy of targeting glutaminolysis could offer benefits in HNSCC.

6.2 Results

6.2.1 Glutamine is a critical nutrient for growth in head and neck squamous carcinoma cell lines

GLS was highly expressed in eight cell lines derived from four regions of the head and neck, namely oral cavity, larynx, oropharynx and hypopharynx (Fig 6.2.1).

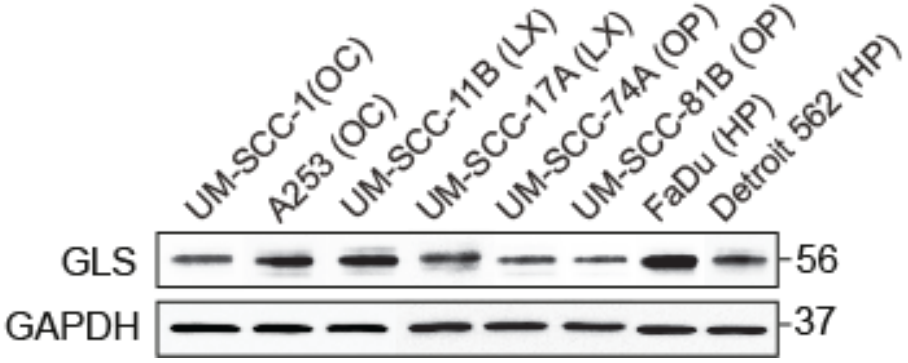

Fig 6.2.1. GLS is highly expressed in HNSCC cell lines. Immunoblots of GLS in eight cell lines derived from four regions of the head and neck, namely oral cavity (OC-UM-SCC-1 and A253), larynx (LX-UM-SCC-11B and UM-SCC-17A), oropharynx (OP-UM-SCC-74A and UM-SCC-81B) and hypopharynx (HP-FaDu and Detroit 562).

To assess whether glutamine was essential for growth, the cell lines were deprived of glutamine and the clonogenicity assessed. Glutamine deprivation completely inhibited cell growth (Fig 6.2.2), demonstrating that glutamine was critical for clonogenic formation and survival in HNSCC cell lines.

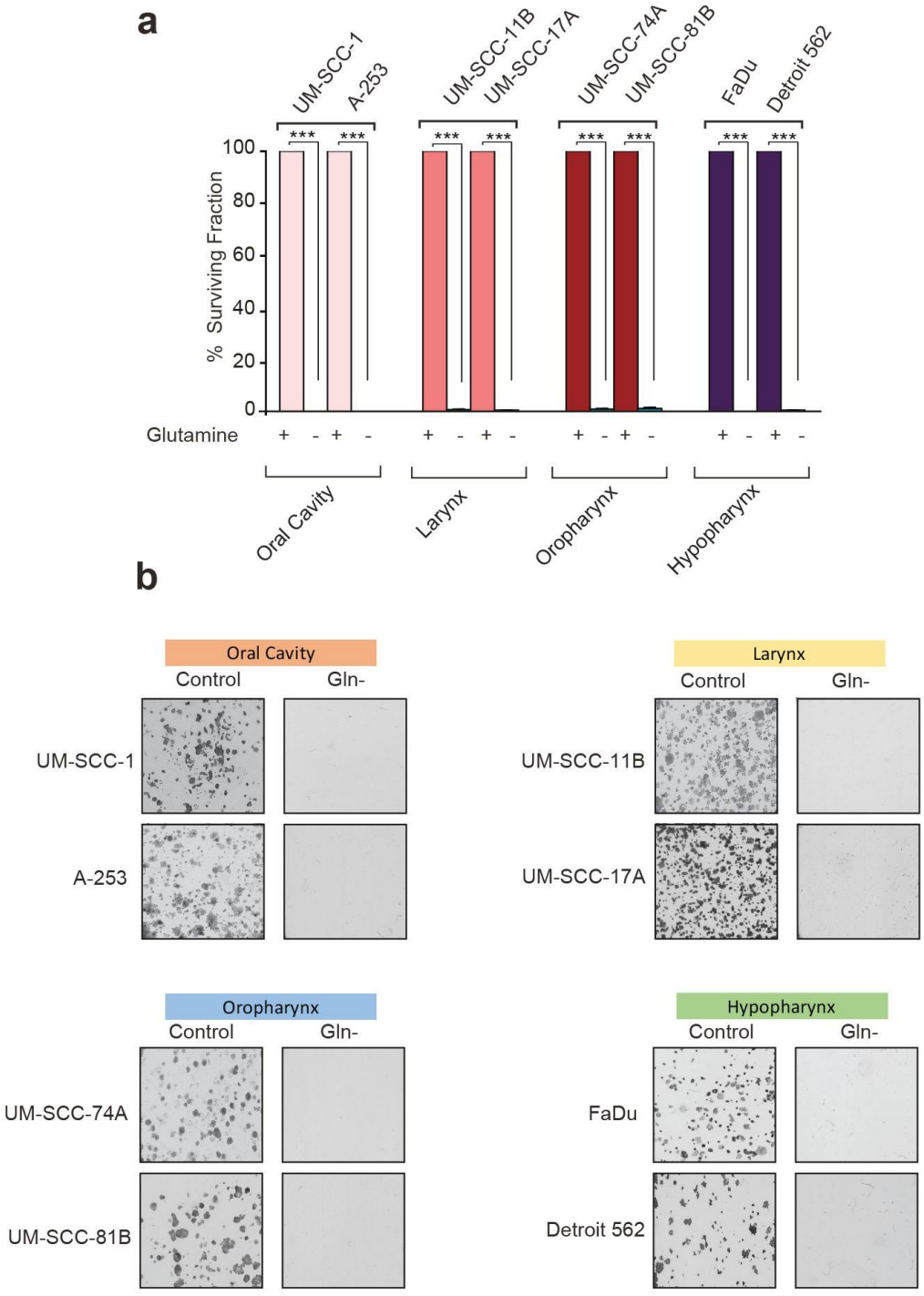

Fig 6.2.2. Glutamine deprivation inhibits the growth in HNSCC cell lines. (a-b) Eight HNSCC cell lines, described in the legend to Fig 5.2.1, were seeded and deprived of glutamine for a colony formation assay. Colonies formed after 7 days, were fixed, stained and counted by using a Gelcount tumour colony counter. ***P ⩽0.001; Error bars = Mean ± SEM (n=3).

6.2.2 Downregulation of GLS genetically and pharmacologically inhibits cell colony formation in HNSCC cell lines

To assess whether inhibition of GLS could mimic the inhibition of clonogenicity due to glutamine deprivation, GLS was inhibited genetically using two different siRNA or pharmacologically using CB-839. Knockdown of GLS showed a significant loss in the clonogenic potential in all the cell lines (Fig 6.2.3). CB-839 inhibited the clonogenic formation significantly in cell lines from the oral cavity, larynx and oropharynx with a much smaller effect on the hypopharynx (Fig 6.2.4). The response to CB-839 varied even within one region, as particularly illustrated by the larynx (Fig 6.2.4 b). The lack of effect of CB-839 on the hypopharynx was not in agreement with the previous results utilising glutamine deprivation (Fig 6.2.2) or silencing GLS (Fig 6.2.3).

Next, to assess whether CB-839 would inhibit the growth of UM-SCC-17A and FaDu, cell lines were cultured as spheroids in order to more closely mimic 3D-growth *in vivo*. CB-839 inhibited cell growth significantly with UM-SCC-17A cells (Fig 6.2.5), whereas it did not inhibit FaDu cells (Fig 6.2.6). These results were in agreement with the previous results using 2D-culture (Fig 6.2.4 b and d). Taken together, these results suggested targeting GLS genetically or pharmacologically in all cell lines except those from the hypopharynx inhibited colony formation.

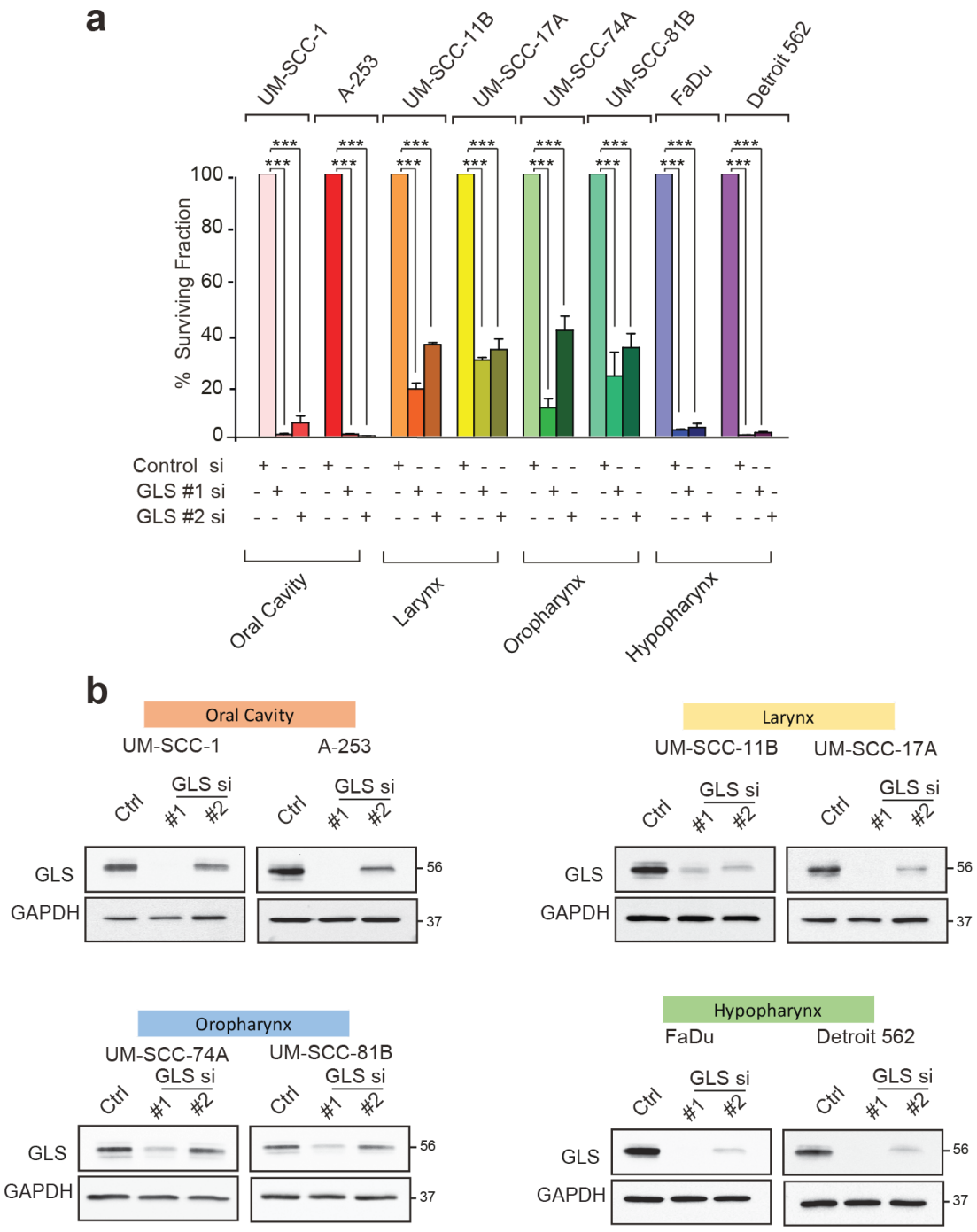

Fig 6.2.3. Genetic knockdown of GLS inhibits growth of HNSCC cell lines. (a) The indicated HNSCC cell lines were transfected with two different siRNAs against GLS (#1 and #2), incubated for 72 h and seeded for colony formation assay. Colonies, formed after 7 days, were fixed, stained and counted. (b) Western blots were performed to confirm the knockdown efficiency of GLS (#1 and #2). ***P ⩽0.001; Error bars = Mean ± SEM (n=3).

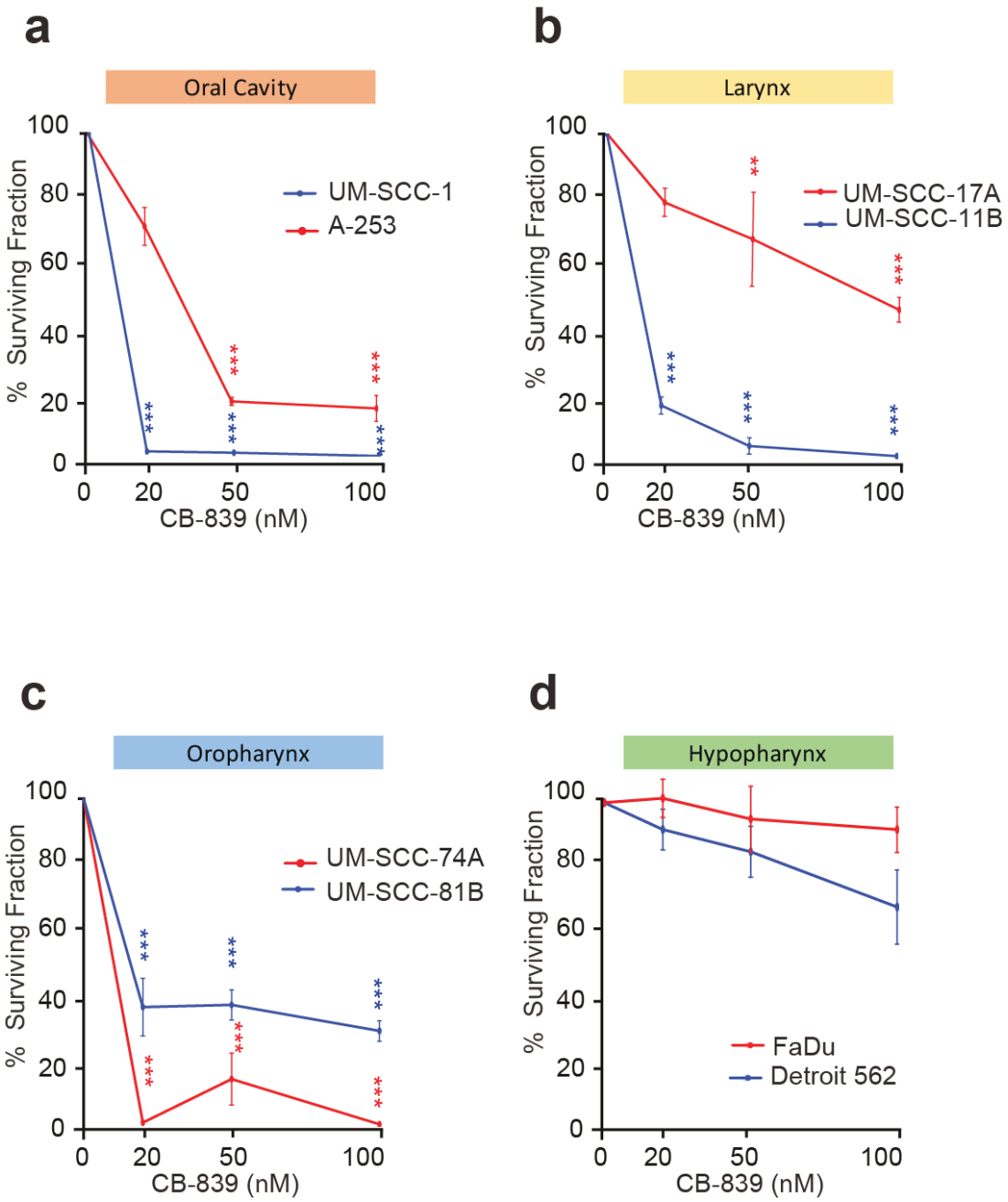

Fig 6.2.4. Targeting GLS decreases the clonogenicity of HNSCC cell lines. (a-d) The indicated HNSCC cell lines were seeded and incubated for 24 h then exposed to 3 concentrations of CB-839 (20, 50 and 100 nM). Colonies, formed after 7 days, were fixed, stained and counted. ***P ⩽0.001, **P ⩽0. 01 Error bars = Mean ± SEM (n=3).

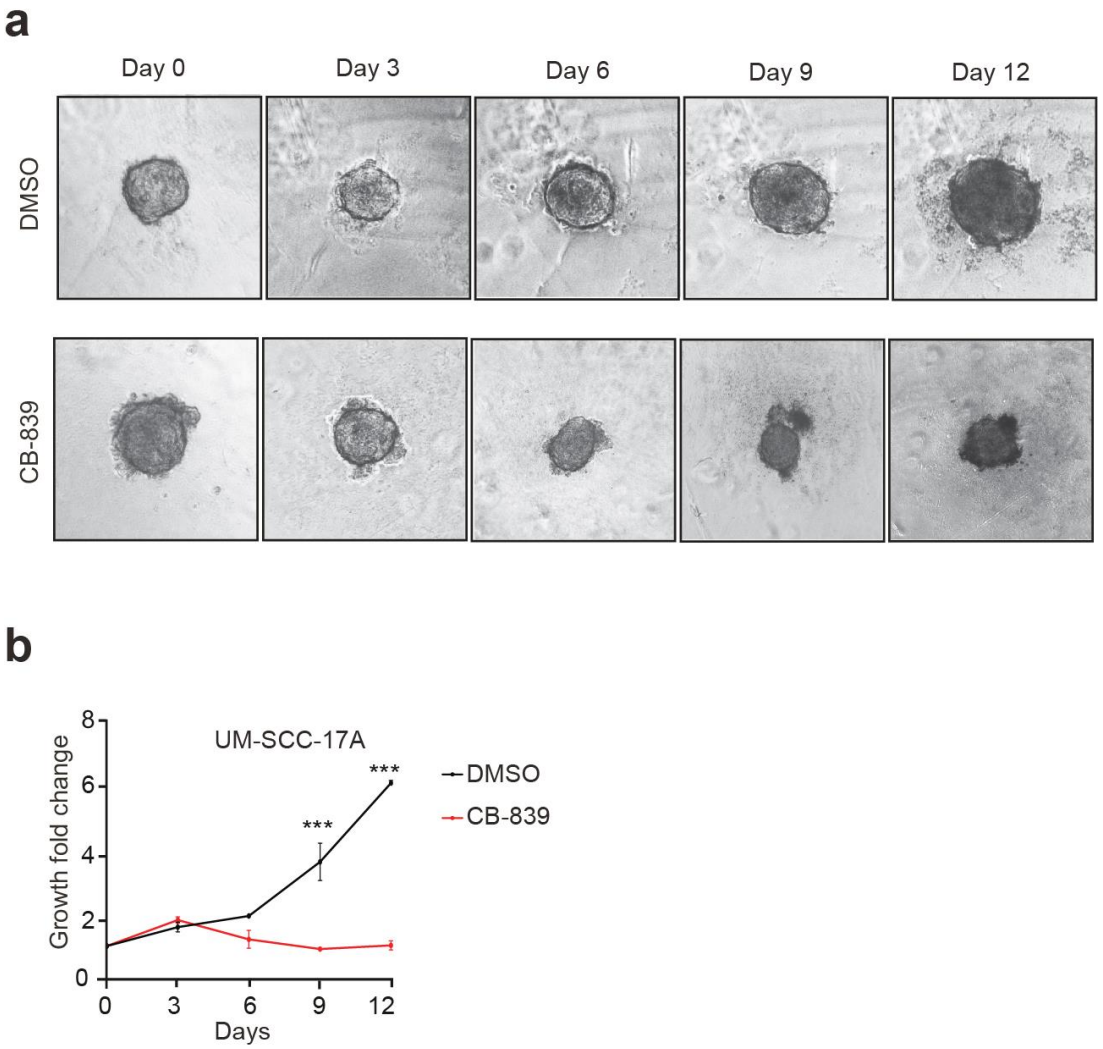

Fig 6.2.5. CB-839 inhibits the 3D-spheroid growth of the UMSCC-17A cell line. (a) UMSCC-17A cells, grown as 3D spheroid cultures, were exposed to CB-839 (20 nM) and incubated for a period of 12 days. Images were captured on days 0, 3, 6, 9 and 12, and changes in the spheroid volume measured using a plug-in for imageJ, as detailed in the methods section. (b) Graph depicting the reduction in the rate of spheroid growth following exposure to CB-839. ***P ⩽0.001; Error bars = Mean ± SEM (n=3).

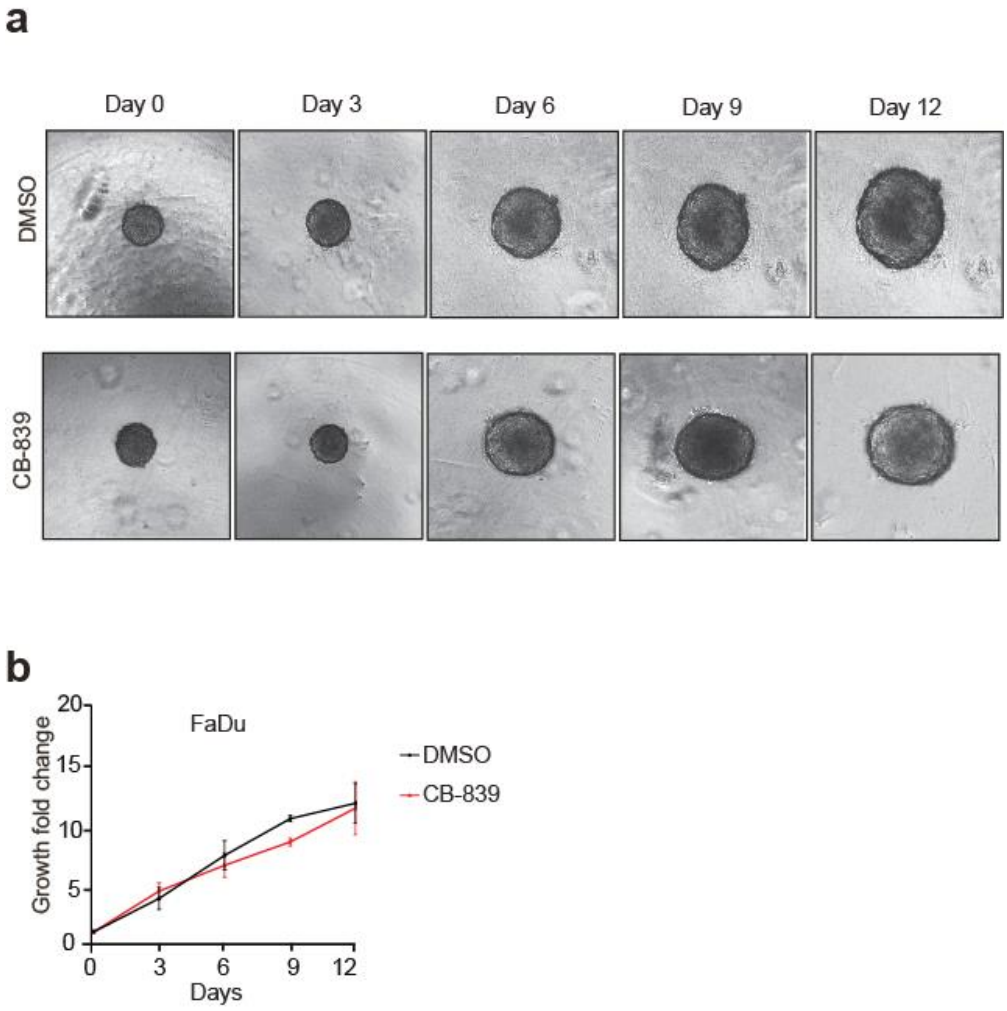

Fig 6.2.6. CB-839 failed to inhibit the 3D-spheroid growth of the FaDu cell line. (a) FaDu cells, grown as 3D spheroid cultures, were exposed to CB-839 (20 nM) and incubated for a period of 12 days. Images were captured on days 0, 3, 6, 9 and 12, and changes in spheroid volumes measured using a plug-in for imageJ, as detailed in the methods section. (b) Graph depicting the increase in the rate of spheroid growth following CB-839 exposure. (n=3)

6.2.3 High expression levels of GLS correlate with decrease survival rate in patients with oral cavity cancer.

It was important to assess whether the high expression of GLS in HNSCC cell lines was also evident in HNSCC patients. Tissue microarrays made up of triplicate oral cavity tumour cores and oral cavity/advancing front samples derived from patients were fixed and stained with GLS antibody (immunohistochemistry protocol). The H-score was then determined for each tissue sample following QuPath analysis and averaged to get the mean H-score per patient. According to the H-Score mean, the patients were divided into three groups – low, moderate and high expression (Figs 6.2.7 and 6.2.8).

Next, the expression levels of GLS were correlated with overall survival in HNSCC cancer patients. Kaplan-Meier survival graphs were generated using H-score values (re-classified as low, moderate or high) combined with the data of patients from the Liverpool/biobank. The statistical analysis using logrank (Mantel-Cox) test indicated that moderate and high expression levels of GLS correlated with poor survival rates in both oral cavity and advancing fronts (Figs 6.2.9 and 6.2.10). These results suggested that the expression levels of GLS may be a poor prognostic marker for HNSCC.

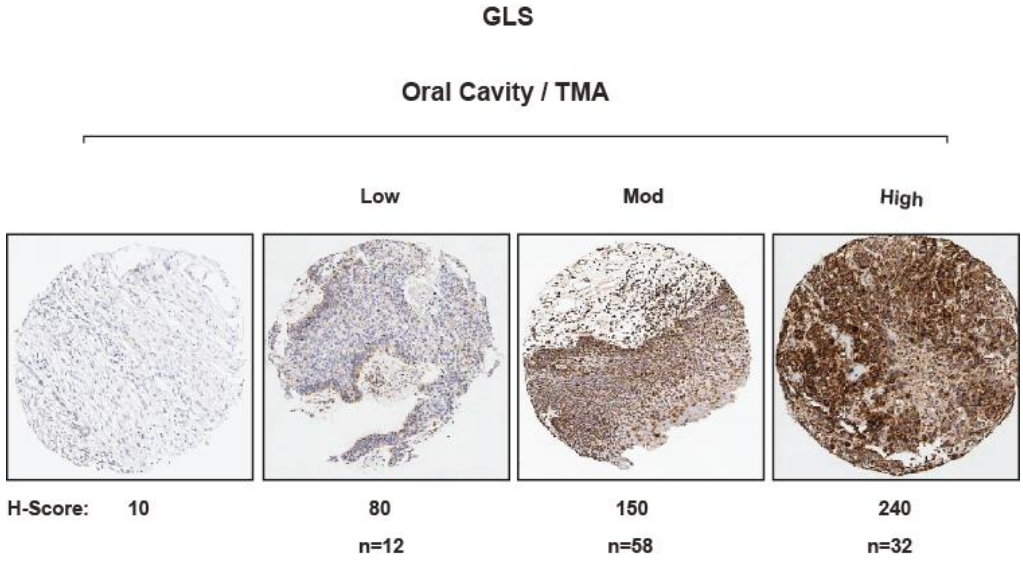

Fig 6.2.7. Defining the histo-score (H-Score) for oral cavity tumour cores using TMA analysis. Four examples of GLS expression are shown from a TMA (tissue microarray) containing oral cavity tumour cores and normal tissues from a cohort of about 100 HNSCC patients. The scoring method used QuPath (as detailed in the methods section) to define the range of H-scores to differentiate high, moderate and low expressing tumour cores. Experiment was done in collaboration with Dr. Rachel Carter.

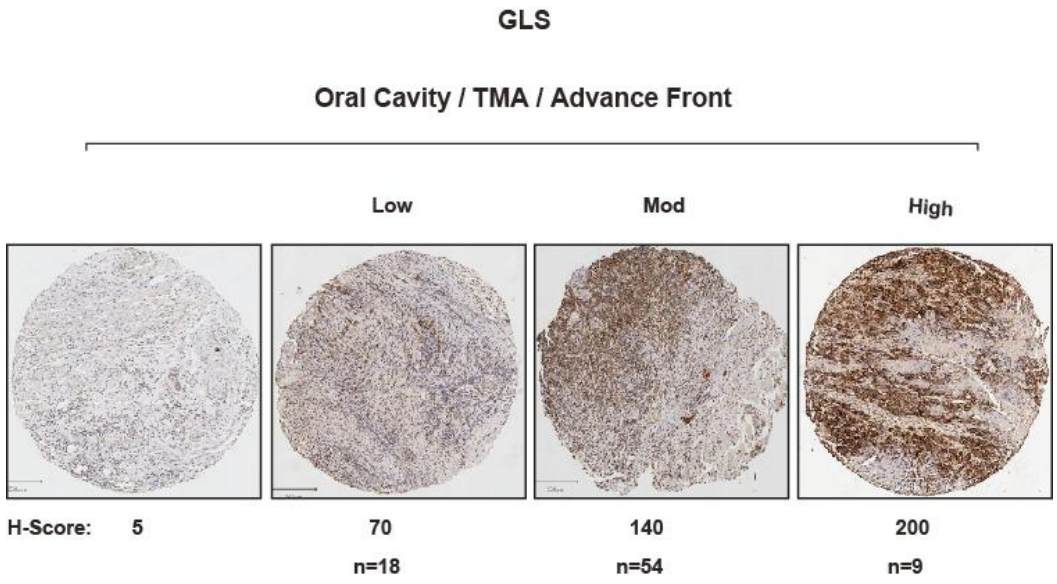

Fig 6.2.8. Defining the histo-score (H-Score) for oral cavity / Advancing fronts cores using TMA analysis. Four examples of GLS expression are shown from a TMA for oral cavity/advancing fronts containing tumour cores and normal tissues from a cohort of about 100 HNSCC patients. The scoring method used QuPath (as detailed in the methods section) to define the range of H-scores to differentiate high, moderate and low expressing tumour cores. Experiment was done in collaboration with Dr. Rachel Carter.

.

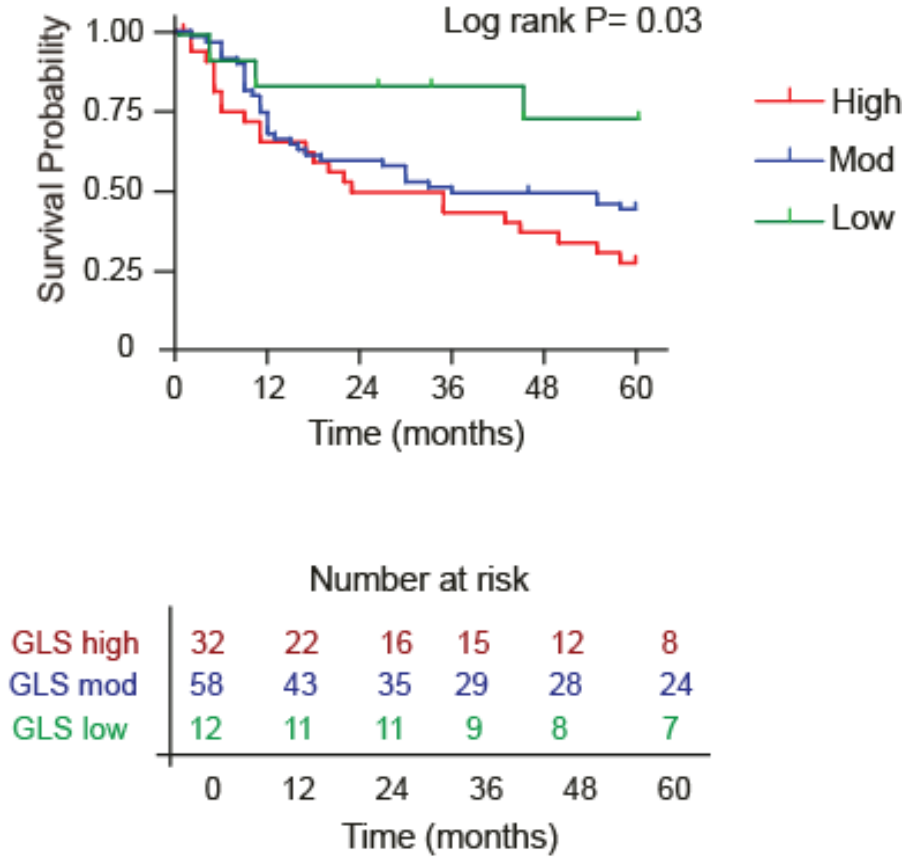

Fig 6.2.9. High expression level of GLS is associated with decreased survival in HNSCC oral cavity tumours. Kaplan-Meier survival graph, depicting the overall survival of patients relative to their expression levels of GLS, is shown. The lower part of the figure indicates the number of patients in each group at risk. P values were calculated by the log rank test P= 0.03. Experiment was done in collaboration with Dr. Rachel Carter.

.

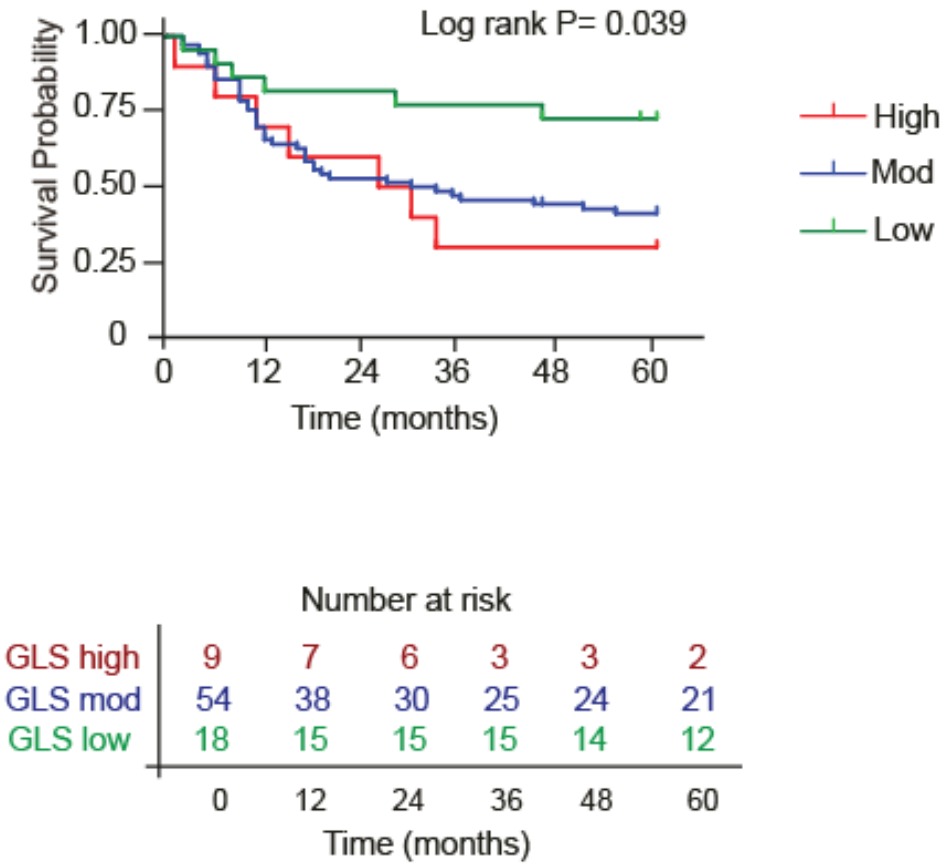

Fig 6.2.10. High expression level of GLS associated with decreased survival in HNSCC oral cavity /advancing fronts. Kaplan-Meier survival graph depicting the overall survival of patients relative to their expression levels of GLS is shown. The lower part of the figure indicates the number of patients in each group at risk. P values were calculated by the log rank test P= 0.039. Experiment was done in collaboration with Dr. Rachel Carter.

.

6.2.4 CB-839 is insufficient to induce significant apoptosis in patient samples

Since GLS was highly expressed in patient samples and correlated with poor overall survival, it may be a potential therapeutic target in HNSCC. To indicate potential toxicity of CB-839, an initial study was carried out with zebrafish from the Nacer *ubiq:sec* AnnexinV-mVenus strain (Morsch et al. 2015). Zebrafish were exposed to increasing concentrations of CB-839 for 48 h (between 72-120 hours post-fertilization**)** and the percentage of fish surviving was counted. CB-839 did not cause death in zebrafish embryos even at higher concentrations (Fig 6.2.11). However, one death was observed (0.5 μM), which may have been due to a technical issue. These results suggested that targeting GLS with CB-839 may be safe to use as an anticancer therapy as it did not exhibit gross toxicity to the zebrafish.

Increasing concentration of CB-839 for 72 h did not induce apoptosis in a patient tissue from the oropharynx (HPV-), as assessed by no increase in cleaved PARP (cPARP) (Fig 6.2.12). These results suggested that CB-839 alone as a single agent was insufficient to induce apoptosis in patient's tissue samples. However, this result is from a single patient and more samples will have to be analysed to assess the potential of CB-839 as a single agent in therapy against HNSCC. This study was completed in collaboration with Dr. Rachel Carter.

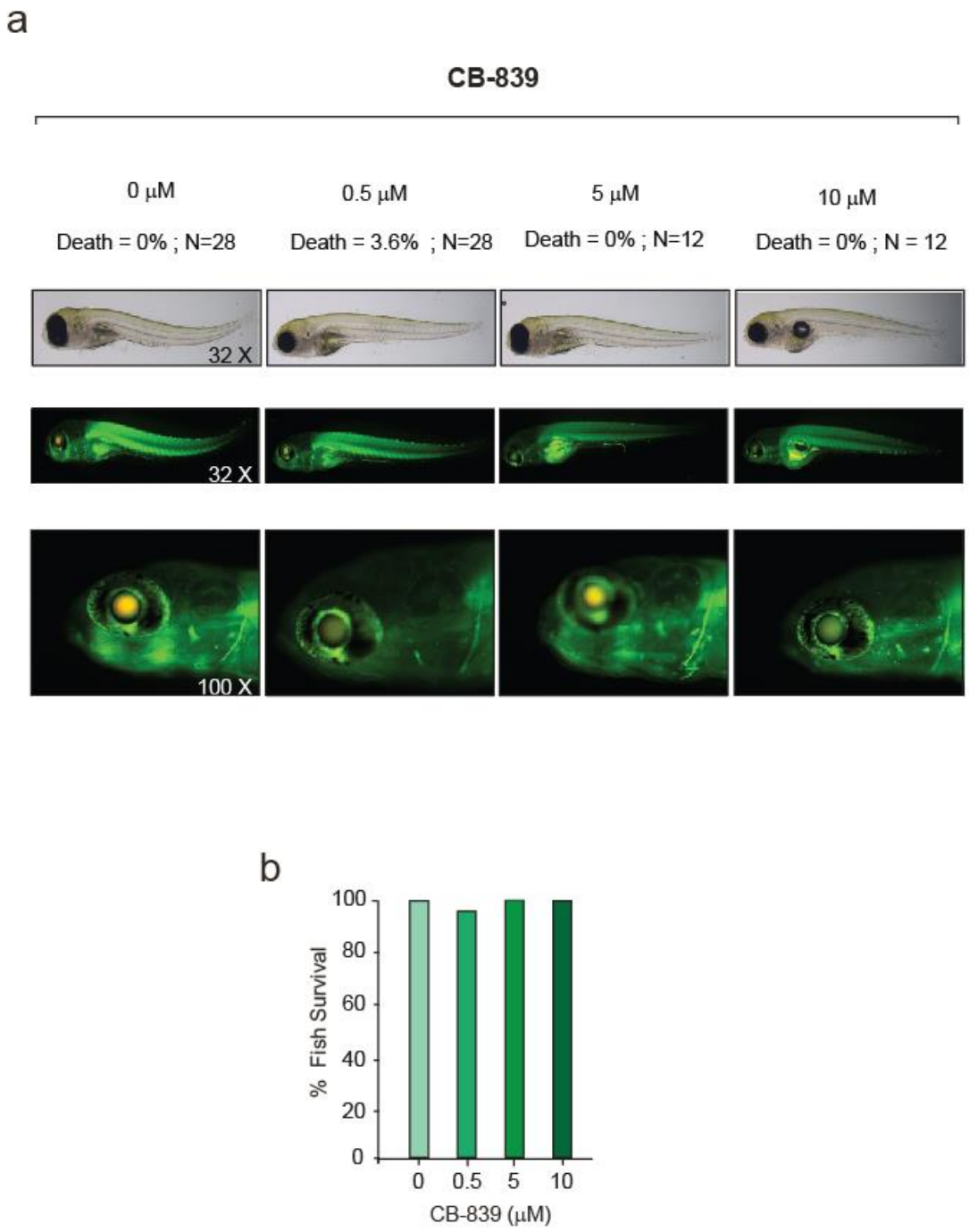

Fig 6.2.11. CB-839 did not exhibit gross toxicity in treated zebrafish. (a) Zebrafish were treated with increasing concentration of CB-839 (0, 0.5, 5 and 10 μM) for 48 h (between 72 and 120 hpf) (b) toxicity plot showed the fish survival rate. Images were taken at 32X and 100X magnifications. Experiment was done in collaboration with Dr. Rachel Carter.

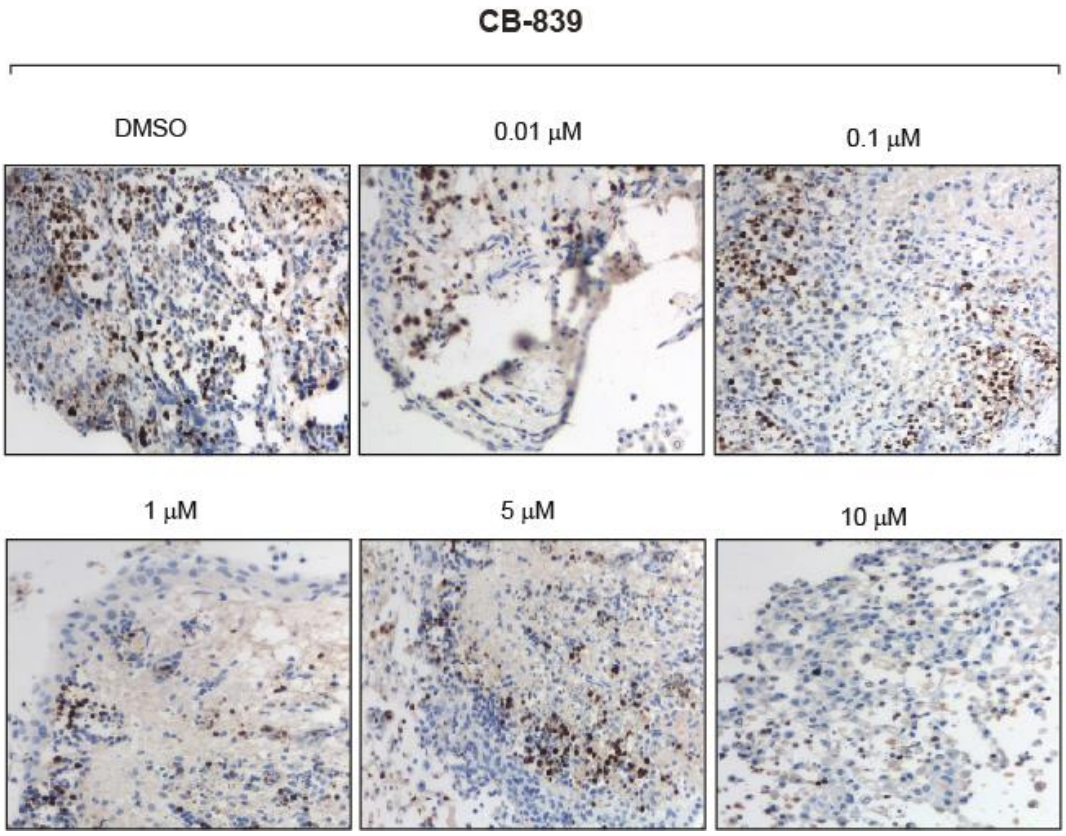

Fig 6.2.12. CB-839 as single agent is insufficient to induce apoptosis in oropharynx (HPV-) patients' tissue. Patients tissue samples were exposed to increasing concentration of CB-839 (0, 0.5, 5 and 10 μM) for 72 h fixed and stained against cPARP to detect apoptosis. Images were taken at 20X magnification. Experiment was done in collaboration with Dr. Rachel Carter.

6.2.5 Targeting GLS in combination with BH3 mimetics decreases the clonogenicity

CB-839 alone was insufficient to induce apoptosis in oropharynx (HPV-) tissue samples from a patient (Fig 6.2.12). Furthermore, the response to CB-839 varied in HNSCC cell lines (Fig 6.2.4). Therefore, the next experiment was aimed at identifying the potential of targeting GLS in combination with other therapies to improve treatment efficacy. Our recent findings from the laboratory confirm that two anti-apoptotic proteins, BCL-X_L and MCL-1 are highly expressed in HNSCC, in agreement with previous reports (Hotz et al. 1999; Trask et al. 2002; Bauer et al. 2007). Moreover, the previous findings (discussed in chapter 4) revealed that CB-839 enhanced BH3 mimetic-mediated apoptosis in haematological malignancies. Therefore, CB-839 was used in combination with BH3 mimetics to investigate whether this combination would decrease the clonogenicity of HNSCC cell lines. CB-839 combined with A-1331852 or S63845 decreased the clonogenicity of A-253, UM-SCC-17A and Detroit562 cells but not UM-SCC-81B cells (Figs. 6.2.13 and 6.2.14). These results suggested that CB-839 may be valuable in combination with BH3 mimetics.

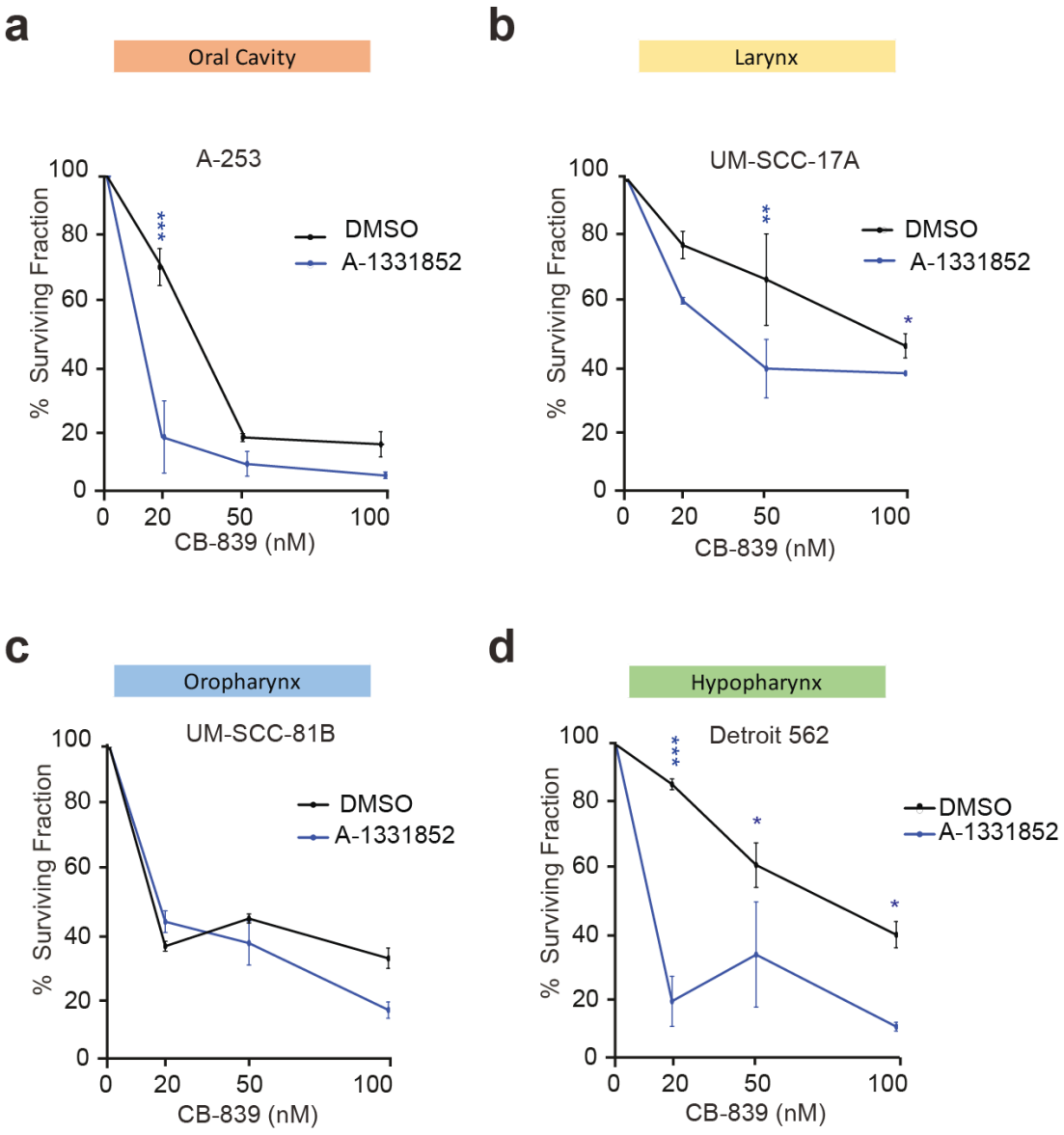

Fig 6.2.13. Targeting GLS in combination with A-1331852 decreases the clonogenicity of HNSCC cell lines. (a-d) The indicated HNSCC cell lines were seeded and incubated for 24 h then, exposed to increasing concentrations of CB-839 (20, 50 and 100 nM) alone or in combination with A-1331852 (100 nM). Colonies formed after 7 days, were fixed, stained and counted. ***P ⩽0.001, **P ⩽0.01, *P ⩽0.05 Error bars = Mean±SEM (n=3).

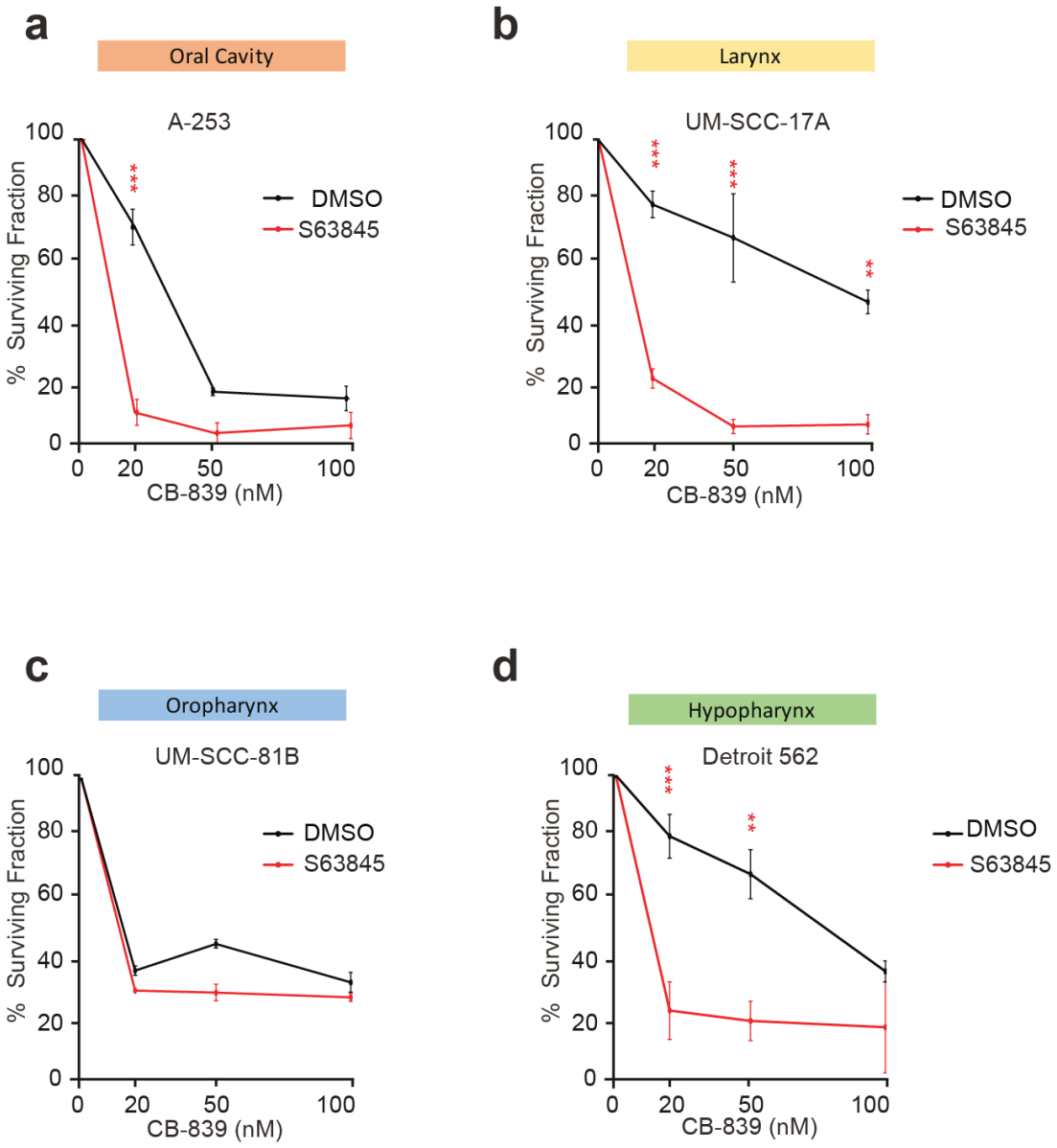

Fig 6.2.14. Targeting GLS in combination with S63845 decreases the clonogenicity of HNSCC cell lines. (a-d) The indicated HNSCC cell lines were seeded and incubated for 24 h then, exposed to increasing concentrations of CB-839 (20, 50 and 100 nM) alone or in combination with S63845 (100 nM). Colonies, formed after 7 days, were fixed, stained and counted. ***P ⩽0.001, **P ⩽0. 01, *P ⩽0. 05; Error bars = Mean±SEM (n=3).

6.3 Discussion

The poor survival rate of patients with HNSCC necessitates improved therapeutic possibilities. In the last few years much effort has been spent to further understand cancer metabolism and this has led to the identification of altering cancer metabolism as a possible therapeutic target. In previous chapters (four and five), it has been shown that targeting intermediary metabolism can overcome resistance to BH3 mimetic-mediated apoptosis (Al-Zebeeby et al. 2018). As a complement to glucose metabolism (Warburg effect), glutaminolysis provides another energy source as well as carbon to synthesize lipids (DeBerardinis et al. 2007; Warburg 1956). GLS is the first and rate limiting enzyme in the glutaminolysis pathway (Gao et al. 2009; Liu & Feng 2012). High levels of GLS expression were observed in a range of HNSCC cell lines and these cell lines were absolutely dependent on glutamine for cell proliferation (Figs 6.2.1 and 6.2.2), as observed in other systems (Wise & Thompson 2010; Medina et al. 1992)Taken together, these results demonstrate a critical role of glutamine in HNSCC cell lines. However, Sandulache et al. (2010) reported that HNSCC cell lines depended on glucose metabolism (as a dominant pathway) for energy production, while catabolism of glutamine did not appear to have a significant role for ATP production. Particularly important was the finding that GLS was also overexpressed in TMAs from both oral cavity tumours as well as the advancing front taken from patients with HNSCC (Fig 6.2.7 and Fig 6.2.8). This was in agreement with a recent study, which showed that GLS was overexpressed in oral squamous cell carcinoma compared to normal tissue (Cetindis et al. 2016). Using a multiomics approach, GLS was also shown to be highly expressed in a variety of tumours including breast, oesophagus as well as head and neck (Saha et al. 2019).

Most importantly the current study indicated that increased expression levels of GLS correlated with a decreased overall survival of patients (Fig 6.2.9 and Fig 6.2.10). In this regard, it was recently reported that glutamate levels, glutaminolysis activity and GLS expression levels were increased in primary and metastatic HNSCC tumours (Kamarajan et al. 2017). A more limited multiomics study also reported that GLS is a poor prognostic marker for HNSCC (Saha et al. 2019). In addition to being a possible prognostic marker, GLS may also be a therapeutic target. Some support for this suggestion was provided by targeting GLS genetically and pharmacologically, which inhibited cell growth in both 2- and 3-dimensional cell line models (Figs 6.2.2, 6.2.3, 6.2.4 and 6.2.5). In addition to being used as a single agent, CB-839 may also be used in combination with other agents and has been shown to be efficacious in renal cell carcinoma, non-small lung cell carcinoma, pancreatic ductal adenocarcinomas and triple-negative breast cancer (Gross et al. 2014; Chakrabarti et al. 2015; Garber 2016; Meric-Bernstam et al. 2016; Hoerner et al. 2019). A more limited multiomics study also reported that GLS is a poor prognostic marker for HNSCC (Saha et al. 2019). In addition to be a possible prognostic marker, GLS may also be a therapeutic target. Some support for this suggestion was provided by targeting GLS genetically and pharmacologically, which inhibited cell growth in both 2- and 3-dimensional cell line models (Figs 6.2.2, 6.2.3, 6.2.4 and 6.2.5). In addition to being used as a single agent, CB-839 may also be used in combination with other agents and has been shown to be efficacious in renal cell carcinoma, non-small lung cell carcinoma, pancreatic ductal adenocarcinomas and triple-negative breast cancer(Jacque et al. 2015). As some anti-apoptotic proteins are highly expressed in HNSCC (Hotz et al. 1999; Trask et al. 2002; Bauer et al. 2007), the combination of CB-839 together with some specific BH3 mimetics was examined. The combination of CB-839 with A-1331852 or S63845

showed a decrease in clonogenicity (Figs 6.2.13 and 6.2.14), suggesting a promising combination therapy for HNSCC. To my knowledge, this was the first study designed to use CB-839 in combination with BH3 mimetics for treating HNSCC. Interestingly, exposure of the hypopharynx cell lines (FaDu and Detroit) to CB-839 did not cause a decrease in clonogenicity in both 2D- or 3-D culture (Figs 6.2.3 d and 6.2.6). However, BPTES, another GLS inhibitor, has been reported to decrease cell growth in FaDu and Detroit 562 cells, whereas CB-839, which is structurally similar and more potent did not inhibit (Fig 6.2.4 d) (Gross et al. 2014; Yang et al. 2019). The reasons for this discrepancy are unclear but may be due to possible structural differences of the inhibitors or binding to the allosteric pocket of GLS (Thangavelu et al. 2012; Robinson et al. 2007; DeLaBarre et al. 2011).

Collectively, the results presented in this chapter indicate a critical role of glutamine in regulating cell proliferation and survival in HNSCC. Specifically, GLS could be a possible poor prognostic marker and also a potential target for improving chemotherapy in HNSCC. Support for this hypothesis was provided by the findings that CB-839 alone or in combination with BH3 mimetics highly efficacious in inhibiting the clonogenicity of HNSCC cell lines.

Chapter 7

General discussion

7.1 Different possible mechanisms that may drive resistance to BH3 mimetic-mediated apoptosis

BCL-2 family members are key regulators of apoptosis and hence are promising targets for cancer therapy. Inhibitors targeting these anti-apoptotic proteins at the transcriptional level (cyclin-dependent kinase inhibitor, Flavopiridol) (Zhai et al. 2002), as well as the post transcriptional level (deubiquitinase inhibitor, WP1130) (Peterson et al. 2015; Kapuria et al. 2011) have been developed in the last decade (Section 1.4). However, most of these inhibitors are not specific inhibitors of the BCL-2 family of proteins. The most specific and potent inhibitors of the BCL-2 family members are BH3 mimetics, which target protein-protein interactions among different BCL-2 family members (Tse et al. 2008; Souers et al. 2013; Leverson, Phillips, et al. 2015; van Delft et al. 2006; Leverson, Zhang, et al. 2015; Lucas et al. 2016; Qian et al. 2004; Oltersdorf et al. 2005; Caenepeel et al. 2017; Tron et al. 2018; Kotschy et al. 2016). BH3 mimetics have been shown to rapidly induce the intrinsic apoptotic pathway in a wide variety of cancers (Delbridge et al. 2016). Even with large amount of supportive *in vitro* data, the use of BH3 mimetics in treating cancer is still in its infancy, with ABT-199 (venetoclax), a BCL-2 specific inhibitor, only recently approved for treatment of refractory chronic lymphocytic leukaemia (Roberts et al. 2016). The recent development of specific BH3 mimetics that target other members of the BCL-2 family, such as BCL-X_L and MCL-1, may be enormously useful in treating patients suffering from different cancers. While BH3 mimetic therapy appears quite promising in several malignancies, undoubtedly challenges to this therapy will arise, particularly in the form of chemoresistance.

It is important to understand the mechanisms of resistance in order to identify strategies to overcome such resistance. Different mechanisms, including drug target

alteration, drug inactivation, drug efflux, cell death inhibition and DNA repair mechanisms, may trigger the development of chemoresistance in cancer (Housman et al. 2014). In the context of BH3 mimetics, drug efflux due to elevation of P-gp (P-glycoprotein) has been reported (Bao et al. 2011; Vogler, Dickens, et al. 2011; Yoshimori et al. 2015). Similarly, mutations in the drug target site, such as G101V detected in the BH3 domain of BCL-2 in CLL samples, which prevented the binding of ABT-199 have been observed (Blombery et al. 2019). Similarly, F101C and F101L have been detected in the BH3 domain of BCL2, which also resulted in resistance to ABT-199-mediated apoptosis (Fresquet et al. 2014). Moreover, a mutation (G179E) has been identified in BAX, which abrogated anchoring of this protein to the mitochondria, consequently inhibiting apoptosis (Fresquet et al. 2014).

Cancer cell plasticity also facilitates the adaptation of cancer cells to chemotherapy and targeted therapies. This is mostly driven *via* epigenetic and transcriptional reprogramming (Sharma et al. 2010; Ramirez et al. 2015; Hata et al. 2016; Koppikar et al. 2012; Knoechel et al. 2014). Very recently, it has been reported that resistance to ABT-199-mediated apoptosis in mantle cell lymphoma models and double hit lymphoma resulted from an outgrowth of clones that displayed a loss of BCL-2 amplicons (Zhao et al. 2019). A sharp decline in BCL-2 transcription coupled with the clonal expansion of persisting clones (*via* transcriptional reprogramming) resulted in ABT-199 resistance, which could then be overcome by transcriptional inhibition of CDK7 (cyclin dependent kinase 7) (Zhao et al. 2019).

Post-translational changes that alter the expression levels of the BCL-2 family members could also contribute to resistance. It has been reported that phosphorylation of BCL-2 induces resistance to ABT-737-mediated apoptosis (Konopleva et al. 2006). Studies have shown phosphorylation of MCL-1 at precise residues are important for

MCL-1 stability and the interaction with BH3-only proteins. For instance, phosphorylation in addition to overexpression of MCL-1 induces acquired resistance (Mazumder et al. 2012). In contrast, JNK-mediated MCL-1 phosphorylation decreases anti-apoptotic activity in response to oxidative stress (Inoshita et al. 2002).

There is also a possibility that the anti-apoptotic BCL-2 family members could bind novel BH3-only members to result in resistance. For instance, interaction of an unknown BH3-only protein called SUFU (suppressor of fused) with several anti-apoptotic BCL-2 family members has been recently reported (Wu et al. 2017). However, SUFU has been shown to not possess any role in apoptosis. Soon after this discovery, another protein called VLCAD (very long-chain acyl-CoA dehydrogenase) was shown to interact with MCL-1(Escudero et al. 2018). Similar to SUFU, VLCAD also did not play any major role in apoptosis (Wu et al. 2017; Escudero et al. 2018). It is well-known that BH3-only proteins directly activate BAX and/or BAK to exclusively regulate apoptosis by neutralization of pro-survival BCL-2 family members (Chipuk & Green 2008). However, it has been reported that BAX and/or BAK can be activated even in the absence of all known BH3-only proteins (O'Neill et al. 2016). The requirement of eight well characterized pro-apoptotic BH3-only proteins to induce BH3 mimetic-mediated apoptosis was further disproved in another study (Greaves et al. 2018). This study raised the possibility that an unknown protein that is responsible for the activation of BAX and/or BAK may exist and induce apoptosis. Likewise, a possible downregulation of this yet-to-be-characterised protein could result in decreased sensitivity of the cells to apoptosis, further resulting in the development of resistance. Furthermore, an interaction between DRP-1 (a mitochondrial fission protein) and pro-survival BCL-2 family members has been shown to control mitochondrial outer membrane permeabilisation and hence

apoptosis, following exposure to BH3 mimetics (Milani et al. 2016). This is particularly relevant to BH3 mimetic-mediated apoptosis, as cell death often occurs following extensive ultrastructural changes to the mitochondria (Fig.3.2.1, 3.2.2 and 3.2.3 b). It is therefore possible that mutations in or downregulation of DRP-1 could play a critical role in resistance to BH3 mimetics. While further understanding of such resistance mechanisms is important to improve BH3 mimetic therapy, ways to overcome resistance is more pressing in a therapeutic context, as resistance to BH3 mimetics is starting to emerge. Therefore, the next steps should focus on exploring different ways to overcome resistance to BH3 mimetic-mediated apoptosis.

7.2 Targeting glutamine metabolism pathways could be a promising way to overcome resistance to BH3 mimetics in different types of cancer

One of the unique features of cancer is its ability to escape from controlled regulatory events that dictate cell growth and fate. As a result, cancer cells undergo uncontrolled and rapid cell proliferation (Koppenol et al. 2011), which is achieved by their dependence on aerobic glycolysis, glutaminolysis and fatty acid synthesis (Vander Heiden et al. 2009). In addition to cell proliferation, cancer cells may depend on these pathways to also evade apoptosis, in response to chemotherapeutic agents. Resistance to chemotherapy is a recurring theme in cancer, and the recently developed BH3 mimetics are no exception to resistance. In the current study, resistance models (that mimic the rapid and modest resistance observed in the clinic) were generated in cell lines derived from distinct malignancies. There is an urgent need to develop successful ways to tackle cancer chemoresistance. Accumulating evidence suggests that cancer metabolism is an interesting area and promising therapeutic target (Levine & Puzio-Kuter 2010; Ward & Thompson 2012; Vander Heiden et al. 2010).

One of the oldest observations made by Otto Warburg was that cancer cells consumed more glucose than normal cells and produced more lactic acid due to an aerobic reaction (Warburg et al. 1927). Warburg hypothesized that cancer cells shared a metabolic system similar to that of a single cell eukaryote, due to the requirement for quick proliferation (Warburg 1956). However, not all cancers exhibit the Warburg effect. Some cancer cells depend on glutamine for their energy (Eagle 1955).

Glutamine is a versatile molecule, which contributes to many facets of intermediary metabolism. Glutamine metabolism is required to support cell proliferation by forming different metabolic blocks (Jiang et al. 2019). Glutamine consumption increases under stress conditions, such as sepsis (Noguchi et al. 1997). Glutamine deprivation induces rapid necrosis especially in cells that depend on glutamine (Lacey & Wilmore 1990). Moreover, rapidly dividing cells, such as cancer and oncogene-transformed cells, are glutamine-dependent and they undergo rapid apoptosis following glutamine deprivation (Still & Yuneva 2017; Petronini et al. 1996; Weinberg et al. 2010; Yuneva et al. 2007). The current study indicates that glutamine deprivation alone did not induce apoptosis in cell lines derived from haematological cancers (Figs 4.2.1, 4.2.2). Rather glutamine appeared to function as a co-factor to enhance the resistance of cells to BH3 mimetic-mediated apoptosis (Figs 4.2.1, 4.2.2). Similarly, glutamine deprivation enhanced the sensitivity of ibrutinib-resistant cells to ibrutinib-mediated apoptosis (Fig 4.2.9). In contrast, in HNSCC cell lines, glutamine deprivation inhibited cell survival (Fig 6.2.2), suggesting that HNSCC exhibits glutamine addiction, in agreement with most solid tumours.

Glutamine enters the cell *via* one of its transporters, several of which are upregulated in many types of cancer. It has been reported that tumour suppressors or certain oncogenes control the regulation of these transporters. For instance, SLC1A5

(ASCT2), a sodium coupled (Na^+-coupled) transporter for amino acids, such as glutamine, serine, alanine and cysteine, is upregulated by Myc (Gao et al. 2009) and downregulated by Rb (retinoblastoma protein) (Reynolds et al. 2014). Another glutamine transporter, SLC7A5 (LAT1) has a dual activity, controlling the simultaneous efflux of glutamine and the influx of leucine. It is regulated by Myc and HIF-2α and overexpressed in prostate cancer and renal cell carcinoma (Gao et al. 2009; Elorza et al. 2012). Many studies have suggested that SLC1A5 is required for cancer progression in AML (Willems et al. 2013), kidney cancer (Elorza et al. 2012; Willems et al. 2013), lung cancer (Hassanein et al. 2013; Hassanein et al. 2015), breast cancer (Geldermalsen et al. 2016) and melanoma (Wang et al. 2014). In addition, downregulation of SLC1A5 either by genetic knockdown (siRNA) or pharmacological inhibitors, including benzylserine and L-γ-glutamyl-p-nitroanilide (GPNA), decreased proliferation of cancer cells *in vitro* as well as the growth of tumours *in vivo* (Hassanein et al. 2013; Hassanein et al. 2015). Inhibition of glutamine uptake inhibits mTOR1 complex (mammalian target of rapamycin complex 1) causes cell cycle arrest (block the G1 stage) as well as increased ROS (reactive oxygen species) generation (Geldermalsen et al. 2016; Hassanein et al. 2013). Consistent with these findings, the current study indicated that resistant cells consumed more glutamine than sensitive cells (Fig 4.2.4 a). However, the expression levels of SLC1A5 did not change and targeting glutamine uptake increased the sensitivity of both sensitive and resistant cells to BH3 mimetic-mediated apoptosis (Figs 4.2.4 b and 4.2.6 b), suggesting that uptake of glutamine in resistant cells possibly increased due to an increase in the activity of SLC1A5. The resistant cells most likely needed more glutamine to support the anabolic process for different precursors, which was important for these cells to maintain resistance.

The first enzyme in the glutamine metabolic pathway is GLS that catalyses the glutaminolysis reaction. It has been reported the glutamine-mediated apoptosis is dependent on Myc (Yuneva et al. 2007) and that c-Myc is responsible for the overexpression of GLS (Liu et al. 2012; Wise et al. 2008). Moreover, GLS is believed to play a critical role in many cancers (Curthoys & Watford 1995; GTEX 2015). However, as previously mentioned, no increase in the expression levels of GLS was observed in haematological cancer cell lines, when sensitive and resistant cells were compared (Fig 4.2.7). In HNSCC cell lines, GLS was generally highly expressed (Fig 6.2.1). Since, many types of cancer exhibit a high expression levels of GLS and are addicted to glutamine, GLS is a very attractive target for cancer therapy. A number of inhibitors have been developed to target GLS (Hartman & McGrath 1973; Pinkus 1977; Katt & Cerione 2014; Vanhove et al. 2019). A novel, potent and selective inhibitor of GLS (targeting both isoforms KGA and GAC), CB-839, is currently in clinical trials (Phase I and II) (Calithera Biosciences NLM Identifier: NCT02071927; Calithera Biosciences NML Identifier: NCT02071888) (Gross et al. 2014; Katt & Cerione 2014; Thompson et al. 2017; Momcilovic et al. 2018). CB-839 demonstrated promising results as a monotherapy or in combination with other compounds to induce tumour regression (Katt & Cerione 2014; Thompson et al. 2017; Elgogary et al. 2016; Xiang et al. 2015). However, based on the IHC results from a single patient, CB-839 was insufficient to induce apoptosis in patient tissue (Fig 6.2.12). Although these findings are preliminary, it is possible that single agent therapy is insufficient to induce a strong anti-cancer effect, thus necessitating a more effective combination therapy (Kaushik & DeBerardinis 2018). It has been reported that targeting GLS using CB-839 synergises with ABT-199 to exhibit an anti-leukemic activity in AML (Jacque et al. 2015). In agreement with this study, the current findings demonstrated CB-839

synergised with A-1331852 or S63845 in reducing the clonogenicity of several HNSCC cell lines (Figs 6.2.13 and 6.2.14).

Inhibition of GLS did not exhibit any impact in terms of cell proliferation and/or survival in normal hematopoietic cells (Jacque et al. 2015). Furthermore, in a xenotransplanted breast cancer model, targeting GLS using CB-839 did not alter the body weight as well as blood cell count parameters of animals in all the experiment groups suggesting that CB-839 selectively targets the tumour (Gross et al. 2014). The potential toxicity of CB-839 was tested in a zebrafish embryo model, which revealed no death of fish even at high concentrations of CB-839 (Fig 6.2.11), in agreement with these studies (Gross et al. 2014; Jacque et al. 2015). However, targeting GLS genetically by deleting two identical alleles of *GLS gene* was lethal due to neurologic disorders (Masson et al. 2006).

The hexosamine pathway mimics the glutaminolysis pathway by also converting glutamine to glutamate through the rate-limiting enzyme GFAT (glutamine-fructose-6-phosphate transaminase). Overexpression of this enzyme has been correlated with a bad outcome in pancreatic cancer (Yang et al. 2016; Dong et al. 2016). In lung cancer, high expression levels of GFAT triggers epithelial-mesenchymal transition (Alisson-Silva et al. 2013). The current findings revealed no differences in the expression levels of GFAT between sensitive and resistant cells. Moreover, knockdown of this enzyme did not overcome resistance to A-1331852-mediated apoptosis (Fig 4.2.7). In accordance with earlier findings reporting that a glutamine analogue, azaserine (GFAT inhibitor), induced tumour regression in different cancer types (Tarnowski & Stock 1957; Moore & Lepage 1957; Foley & Eagle 1958; Prajda 1985; Viswanathan et al. 2008), the current study showed that azaserine overcame resistance to A-1331852-mediated apoptosis in K562 cells (Fig

4.2.6). Given that GFAT siRNA failed to enhance A-1331852-mediated apoptosis, the effects of azaserine could be due to its ability to inhibit synthesis of de novo purines and γ-glutamyl transpeptidase (Prajda 1985; King et al. 2009).

Another important enzyme in the glutaminolysis pathway is GLUD (glutamate dehydrogenase), which regulates the conversion of glutamate to α-KG, to enter the TCA cycle (Plaitakis et al. 2017; Craze et al. 2019; Kim et al. 2013). This enzyme is upregulated in different types of cancers, including breast, lung, leukaemia and colorectal cancers (Jin et al. 2015; Csibi et al. 2013; Friday et al. 2010; Liu et al. 2015; J. Zhang et al. 2016; Kim et al. 2013; Craze et al. 2019). Moreover, it has been reported that GLUD overexpression correlates with tumour size, metastasis and poor outcome (Liu et al. 2015; J. Zhang et al. 2016; Jin et al. 2015). Downregulation of GLUD arrests cell proliferation and reduces tumour size in breast and lung cancers (Jin et al. 2015). In contrast, the current study indicated that knocking down this enzyme did not overcome resistance to BH3 mimetic-mediated apoptosis (Fig 4.2.7). It has been found that EGCG (epigallocatechin gallate) inhibits GLUD (Li et al. 2006). Many studies have confirmed the potency of EGCG as a chemo-preventive agent against different types of cancer (Ju et al. 2007; Hao et al. 2007; Yang et al. 2009; Yang et al. 2011). In agreement with the results obtained following the genetic downregulation of GLUD (Fig 4.2.7), EGCG, either as a single agent or in combination with BH3 mimetics did not overcome the resistance to BH3 mimetic-mediated apoptosis (Fig 4.2.6). These results suggested that the activity of GLUD in the glutaminolysis pathway may be compensated by some other enzyme in these cell lines.

α-KG is also produced from glutamate through a group of aminotransferases enzymes. Of these enzymes, alanine aminotransferase (also known as glutamate-pyruvate transaminase) generates α-KG and alanine by transferring nitrogen from

glutamate to pyruvate (Washington & Hoosier 2012; Altman et al. 2016). Another transaminase, aspartate aminotransferase (also known as glutamate-oxaloacetate transaminase) produces α-KG and aspartate by transferring nitrogen from glutamate to oxaloacetate (Washington & Hoosier 2012; Altman et al. 2016). Similarly, phosphoserine aminotransferase 1 generates α-KG and phosphoserine by transferring nitrogen from glutamate to 3-phosphohydroxypyruvate (Altman et al. 2016; Sekula et al. 2018). These enzymes are elevated in some cancer types, including breast cancer, colon and cervical cancer (Vie et al. 2008; Thornburg et al. 2008; Veeramalla 2017). Overexpression of phosphoserine aminotransferase has been correlated with poor prognosis and chemoresistance in colon cancer (Vie et al. 2008), thus making aminotransferases potential targets for improving therapy. AOA (aminooxy acetate) is a broad-spectrum inhibitor, which inhibits aminotransferases (Altman et al. 2016) and induces apoptosis in breast cancer, osteosarcoma and neuroblastoma (Qing et al. 2012; Anso et al. 2013; Korangath et al. 2015). In agreement with the pervious findings, the current study showed that inhibiting aminotransferases using AOA in combination with BH3 mimetic overcame resistance to BH3 mimetic-mediated apoptosis (Fig 4.2.6), suggesting that these aminotransferases were controlling the production of α-KG from glutamate in these cell lines.

From the findings in the current study, it is clear that glutamine and glutaminolysis pathway key enzyme are playing an important role in driving cell survival. This led to the next step in this study, which was exploring the relationship between glutaminolysis and the intrinsic apoptotic pathway. Very interesting data in the current study was observation of the novel interaction between GLS and the specific survival member in the relevant cell lines (Fig 4.2.8 a and b). In an attempt to meet the requirements of proliferation and growth, it has been proposed that cancer

cells reprogram the apoptotic and metabolic roles of the BCL-2 family of proteins (Li et al. 2016). The earliest discovery of a metabolic function of BCL-2 family of proteins described their ability to regulate glycolysis through interaction with different components of the metabolic pathway (Danial et al. 2003). For instance, BAD interacts with and activates glucokinase (Danial et al. 2003). This is promoted through phosphorylation of BAD by upstream kinases, whereas dephosphorylation of BAD leads to dissociation with glucokinase (Danial et al. 2003) and increases apoptosis (Li et al. 2016; Winter et al. 2014; Sastry et al. 2014). As the current study suggested novel interactions between GLS and several pro-survival members, this interaction may have a function similar to that of BAD and glucokinase, thereby linking glutamine metabolism and cell survival. In agreement, targeting each step of the glutamine metabolic pathway increased sensitisation to BH3 mimetic-mediated apoptosis.

As mentioned previously, the final step of glutaminolysis is the conversion to α-KG, which enters the TCA cycle. α-KG is reduced by IDH1 and 2 to form citrate during a process known as reductive carboxylation (Ward et al. 2010; Altman et al. 2016). Therefore, the steps beyond α-KG needed to be explored to assess their role in resistance to BH3 mimetic-mediated apoptosis. Hypoxic cancer cells utilize glutamine-dependent reductive carboxylation to provide carbon and support the production of Acetyl-CoA (Mullen et al. 2012; Metallo et al. 2012; Filipp et al. 2012). Findings from the current study confirmed that citrate through reductive glutamine-dependent carboxylation played a crucial role in chemoresistance (Figs 5.2.2 and 5.2.3). Recently, mutations in IDH1/2 have been identified in many cancers, such as chondrosarcoma, acute myeloid leukaemia (AML), glioma, hepatic and colorectal cancer (Zou et al. 2015; Flavahan et al. 2016; Clark et al. 2016). However, this study indicates that resistance to A-1331852-mediated apoptosis is associated with wild type

IDH2, as confirmed by the knockdown study as well as citrate supplementation (Figs 5.2.2 and 5.2.3).

Acetyl-CoA thus formed, feeds into two pathways *via* ACLY: lipogenesis and cholestrogenesis. ACLY is overexpressed and activated in cancers of the lung, ovary, breast, pancreas and prostate, to support tumorigenesis and invasion of the tumour (Lucenay et al. 2016; Han et al. 2016; Chu et al. 2010; Lin et al. 2013; Migita et al. 2008; C. Zhang et al. 2016). Similarly, high expression levels of FASN also correlates with poor outcome in many cancers, such as prostate, lung, ovary, tongue, pancreas, head and neck, endometrium, colon, kidney, melanoma and nephroblastoma (Zhao et al. 2013; Flavin 2010; Swinnen et al. 2004; Shurbaji et al. 1996; Piyathilake et al. 2000; Silva et al. 2008; Silva et al. 2004; Sebastiani et al. 2004; Ogino et al. 2008; Horiguchi et al. 2008; Innocenzi et al. 2003; Camassei et al. 2003). It has been reported that resistance to DNA damaging agents, such as Adriamycin and mitoxantrone, correlates with FASN overexpression (Liu et al. 2008).

Inhibitors of the different metabolic enzymes detailed in the reactions above have been generated over the last few years. It has been reported that silencing IDH1 or IDH2 but not IDH3 reduces citrate production significantly as well as fatty acid synthesis and cell proliferation in an osteosarcoma cell line (Mullen et al. 2012). Moreover, AG-22 (Enasidenib), an inhibitor of mutant IDH1/2 has entered more than eleven clinical trials (Burris et al. 2015; Dinardo et al. 2015; Fujii et al. 2016; Mondesir et al. 2016). Similarly, targeting ACLY by genetic (RNAi) or pharmacological (SB204990) inhibition, has been revealed to inhibit the proliferation of cancer cells *in vitro* and *in vivo*, supporting a vital role of ACLY in carcinogenesis, thus offering a promising target for cancer therapy (Bauer et al. 2005; Hatzivassiliou et al. 2005; Zaidi et al. 2012). In agreement with these findings, targeting ACLY genetically or

pharmacologically in haematological cancer cell lines bypassed the resistance to BH3 mimetic-mediated apoptosis (Fig 5.2.4). Several drugs have been synthesised to inhibit FASN activity and these inhibitors, cerulenin, G28UCM, C75, orlistat, C93, GSK837149A and GSK2194069 (Zhao et al. 2013; Buckley et al. 2017; Alwarawrah et al. 2016; Hardwicke et al. 2014; Turrado et al. 2012; Puig et al. 2011; Ueda et al. 2009; Vázquez et al. 2008; Zhou et al. 2007; Tian 2006; McFadden et al. 2005; Thupari et al. 2002; Kuhajda et al. 2000) have demonstrated anti-cancer properties in several *in vitro* studies (Zhao et al. 2013; Y. Yang et al. 2011; Vazquez-Martin, Colomer, et al. 2007; Menendez et al. 2005; Menendez et al. 2004; Vazquez-Martin et al. 2007). However, most of these FASN inhibitors have not been successful in the clinic, most likely due to the lack of selectivity as well as unexpected toxicities. To date TVB-2640 is the only FASN inhibitor that has demonstrated promise to treat advanced solid tumours (Alwarawrah et al. 2016; Oslob et al. 2013). The current findings reveal that targeting FASN genetically or pharmacologically overcame resistance to BH3 mimetic-mediated apoptosis (Figs 5.2.5 and 5.2.6). The best characterised of these metabolic inhibitors are statins, such as simvastatin, pitavastatin and atorvastatin, which target HMGR to decrease serum cholesterol levels (Golomb & Evans 2008; You et al. 2016). It has been reported that statins have the ability to block tumour growth *in vitro* and *in vivo* (Soma et al. 1992; Newman et al. 1997; Denoyelle et al. 2001; Kim et al. 2001; Feleszko et al. 2002; Hindler et al. 2006). For instance, lovastatin has been demonstrated to stabilize the cell cycle kinase P21 and P27 which leads to cell cycle arrest G1 phase in breast cancer cell lines (Rao et al. 1998). Similarly, cerivastatin inhibits cell proliferation by inhibiting Ras and Rho GTPases (Denoyelle et al. 2001). Several clinical trials have investigated the anticancer effects of statins in different types of cancer, such as advanced liver

carcinoma, non-metastatic rectal cancer, colon cancer, paediatric tumours, head and neck cancer and AML (Lopez-Aguilar et al. 1999; Katz et al. 2005; Minden et al. 2001; Knox et al. 2005; Kawata et al. 2001; Cho et al. 2008). These studies concluded that administration of statins resulted in a significant reduction in tumour size as well as improved survival rate.

Taken together, this study demonstrates that the glutamine metabolic pathway is an important pathway for the regulation of cell survival and could be attributed to resistance to BH3 mimetics. The data highlights several possible targets, such as SLC1A5, GLS, IDH2, ACO2, ACLY, FASN and HMGR, to overcome resistance to BH3 mimetic-mediated apoptosis in haematological cancers (Figs 7.1 and 5.3.1). Furthermore, glutamine and the glutaminolysis key enzyme, GLS play redundant roles in energy production and regulating cell survival in HNSCC. This represents a promising therapeutic target for improving outcomes of HNSCC. Therefore, such a therapeutic strategy should be considered and developed further to help overcome the high prevalence of chemoresistance in cancers.

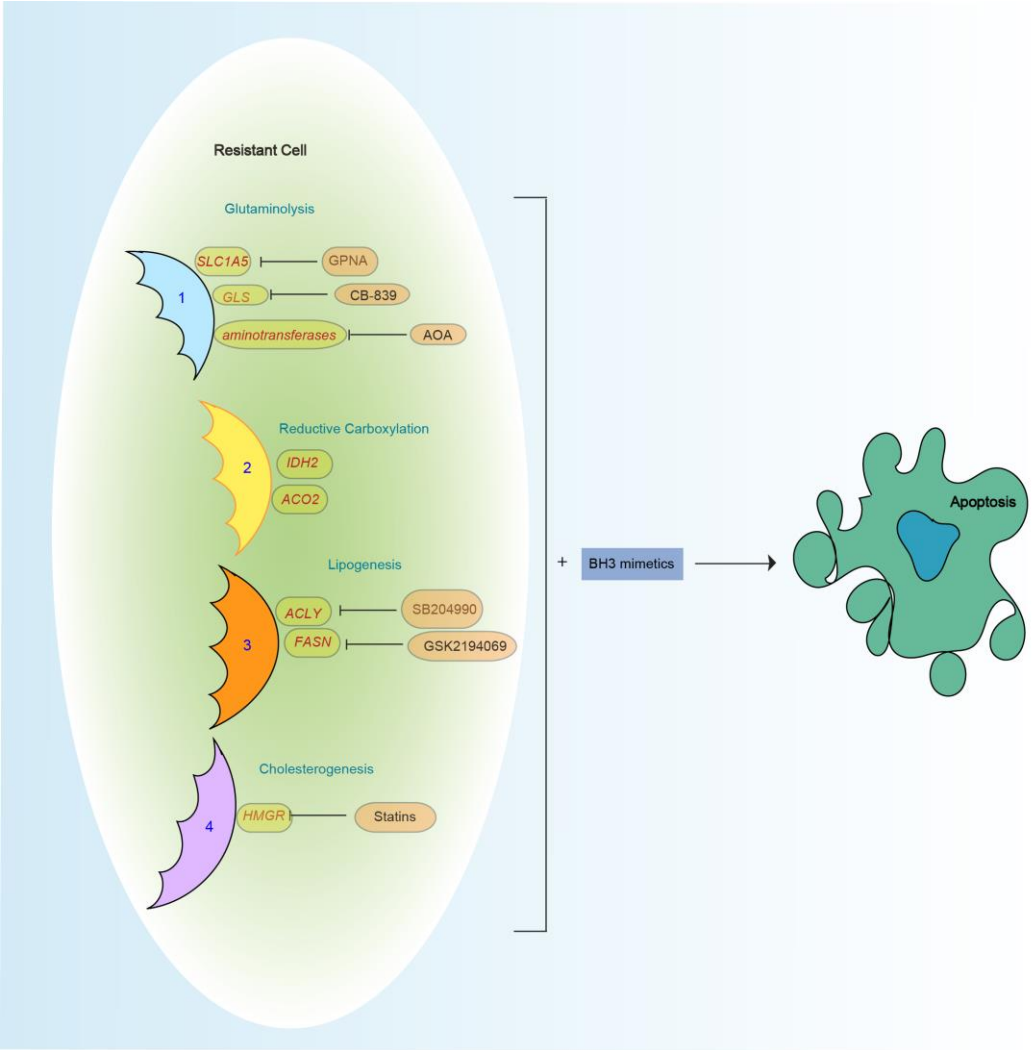

Fig 7.1. Targeting different defensive arms of the glutamine metabolic pathway enhances sensitivity to BH3 mimetic-mediated apoptosis. 1 glutaminolysis arm, 2 reductive carboxylation arm, 3 lipogenesis arm and 4 cholesterogenesis arm.

7.3 Conclusions

The main conclusions from this study are as follows:

- Rapid resistance that mimics the modest resistance observed in clinic can be observed in three distinct haematological cell lines, exposed to relevant BH3 mimetics, namely ABT-199, A-1331582 and A-1210477.
- Resistance to BH3 mimetics does not have to necessarily correlate with expression levels of BCL2 family of proteins or changes in protein-protein interaction.
- Resistance to BH3 mimetics can be overcome by simultaneous inhibition of multiple members of anti-apoptotic BCL-2 family of proteins.
- BCL-X_L and MCL-1 play a more important role than BCL-2 in resistance to BH3 mimetics in most cancers.
- Resistance to BH3 mimetics can be overcome by targeting glutamine dependent pathways, such as glutaminolysis, reductive carboxylation, lipogenesis and cholesterogenesis, in both cell line models and primary CLL patient samples.
- The primary enzyme driving glutaminolysis, GLS, could have important roles in apoptosis-regulated by the BCL-2 family, as evidenced by the novel interactions between GLS and a particular survival member in the relevant cell lines.
- These findings in haematological malignancies are also translatable in solid tumours, as GLS is highly overexpressed in the tumour cores and advancing front of the oral cavity of head and neck squamous cell carcinoma, with GLS expression levels correlating with low survival rates in patients.

- Targeting GLS using the pharmacological inhibitor, CB-839, offers promise in most regions of the head and neck squamous cell carcinoma, but not for the cancers of hypopharynx.
- A combination strategy involving CB-839 and BH3 mimetics could be therapeutically beneficial in head and neck cancers.
- Repurposing drugs that are already used by patients for other ailments to improve cancer therapy offers much promise, as evidenced by the findings with statins in enhancing BH3 mimetic-mediated apoptosis.

7.4 Future directions

In this study, rapid resistance to BH3 mimetics was developed in cell lines derived from haematological cancers. To extend this study and observations in solid tumours, it would be important to explore how soon resistance will develop in solid tumours and identify the main mechanism behind such resistance. In addition, it would be useful to distinguish if the type of resistance is innate or acquired. This study has explored the potential of several novel combinations with BH3 mimetics to improve therapy in haematological cancers and head and neck cancer cell lines. It would be beneficial to extend these findings to HNSCC patients. Also, it would be interesting to use these combinations in treating other type of cancers, in order to overcome resistance to BH3 mimetics, as well as other chemotherapeutic agents. Furthermore, it would be valuable to carry out appropriate experiments in both a xenograft model and also in tissue explants from patients. The data presented in this thesis demonstrated a novel interaction between GLS and the specific survival members of BCL-2 family of proteins. This interaction and the functional consequences need to be further explored to unravel potential cross-talk pathways between glutamine metabolism and the

intrinsic apoptotic pathway. Moreover, it would be interesting to explore other possible interactions between anti-apoptotic BCL-2 family of proteins and downstream enzymes, such as IDH2, ACLY, FASN or HMGR. Finally, it would be important to investigate whether targeting other amino acids pathways could overcome resistance to BH3 mimetic-mediated apoptosis.

Bibliography

Adams, C. et al., 2017. Non-Hodgkin and Hodgkin Lymphomas Select for Overexpression of BCLW. *Clinical Cancer Research*, 23, p. 7119–7129.

Alisson-Silva, F. et al., 2013. Increase of O-Glycosylated Oncofetal Fibronectin in High Glucose-Induced Epithelial-Mesenchymal Transition of Cultured Human Epithelial Cells. *PLOS ONE*, 8(4).

Altman, B., Stine, Z. & CV, D., 2016. From Krebs to clinic: glutamine metabolism to cancer therapy. *Nature*, 16(10), pp.619–634.

Alwarawrah, Y. et al., 2016. Fasnall, a Selective FASN Inhibitor, Shows Potent Anti-tumor Activity in the MMTV-Neu Model of HER2+ Breast cancer. *Cell Chemical Biology*, 23, pp.678–688.

Anso, E. et al., 2013. Metabolic changes in cancer cells upon suppression of MYC. *Cancer & metabolism*, 1(1), p.7.

Arnold, A. et al., 2008. Preclinical studies of Apogossypolone: a new nonpeptidic pansmall-molecule inhibitor of Bcl-2, Bcl-XL and Mcl-1 proteins in folicular small cleaved cell lymphoma model. *Molecular Cancer*, 7(20).

Ashkenazi, A. et al., 2017. From basic apoptosis discoveries to advanced selective BCL-2 family inhibitors. *Nature reviews. Drug discovery*, 16(4), pp.273–284.

Ashkenazi, A. & Dixit, V.M., 1998. Death receptors: signaling and modulation. *Science (New York, N.Y.)*, 281(5381), pp.1305–8.

Azmi, A.S. et al., 2011. Emerging Bcl-2 inhibitors for the treatment of cancer. *Expert opinion on emerging drugs*, 16(1), pp.59–70.

Bajpai, R., Matulis, S., Nooka, A., et al., 2016. Targeting glutamine metabolism in multiple myeloma. *Oncogene*, 35, pp.3955–3964.

Bajpai, R., Matulis, S. & et al., 2016. Targeting glutamine metabolism in multiple myeloma enhances BIM binding to BCL-2 eliciting synthetic lethality to venetoclax. *Oncogene*, 35(30), pp.3955–64.

Bankhead, P. et al., 2017. QuPath: Open source software for digital pathology image analysis. *Scientific Reports*, 7(16878).

Bao, L. et al., 2011. Increased expression of P-glycoprotein is associated with doxorubicin chemoresistance in the metastatic 4T1 breast cancer model. *The American journal of pathology*, 178(2), pp.838–52.

Bauer, D.E. et al., 2005. ATP citrate lyase is an important component of cell growth and transformation. *Oncogene*, 24(41), pp.6314–22.

Bauer, J.A. et al., 2007. Targeting apoptosis to overcome cisplatin resistance: a translational study in head and neck cancer. *International journal of radiation oncology, biology, physics*, 69(2 Suppl), pp.S106–8.

Bhang, H. et al., 2015. Studying clonal dynamics in response to cancer therapy using high-complexity barcoding. *Nature Medicine*, 21(5).

Billard, C., 2013. BH3 mimetics: status of the field and new developments. *Molecular cancer therapeutics*, 12(9), pp.1691–700.

Billard, C., 2012. Design of novel BH3 mimetics for the treatment of chronic lymphocytic leukemia. *Leukemia*, 26(9), pp.2032–8.

Blanchard, P. et al., 2011. Meta-analysis of chemotherapy in head and neck cancer (MACH-NC): a comprehensive analysis by tumour site. *Radiotherapy and oncology : journal of the European Society for Therapeutic Radiology and Oncology*, 100(1), pp.33–40.

Blombery, P. et al., 2019. Acquisition of the Recurrent Gly101Val Mutation in BCL2 Confers Resistance to Venetoclax in Patients with Progressive Chronic Lymphocytic Leukemia. *Cancer discovery*, 9(3), pp.342–353.

Bode, B.P. et al., 2002. Molecular and functional analysis of glutamine uptake in human hepatoma and liver-derived cells. *American journal of physiology. Gastrointestinal and liver physiology*, 283(5), pp.G1062–73.

Bodo, J. et al., 2016. Aquired resistance to venetoclax (ABT-199) in t(14;18) positive lymphoma cells. *Oncotarget*, 7(43).

Bonner, J. et al., 2010. Radiotherapy plus cetuximab for locoregionally advanced head and neck cancer: 5-year survival data from a phase 3 randomised trial, and relation between cetuximab-induced rash and survival. *The Lancet*, 11, pp.21–28.

Bonner, J.A. et al., 2006. Radiotherapy plus cetuximab for squamous-cell carcinoma of the head and neck. *The New England journal of medicine*, 354(6), pp.567–78.

Borst, P. et al., 2000. A Family of Drug Transporters: the Multidrug. *Journal of the national cancer institute*, 92, pp.1295–1302.

Bortner, C., Oldenburg, N. & Cidlowski, J., 1995. The role of DNA fragmentation in apoptosis. *Trends in Cell Biology*, 5.

Bratton, D.L. et al., 1997. Appearance of phosphatidylserine on apoptotic cells requires calcium-mediated nonspecific flip-flop and is enhanced by loss of the aminophospholipid translocase. *The Journal of biological chemistry*, 272(42), pp.26159–65.

Bratton, S.B. et al., 2001. Recruitment, activation and retention of caspases-9 and -3 by Apaf-1 apoptosome and associated XIAP complexes. *The EMBO journal*, 20(5), pp.998–1009.

Brien, G. et al., 2009. C-terminal Residues Regulate Localization and Function of the Antiapoptotic Protein Bfl-1. *Journal of Biological Chemistry*, 284(44), pp.30257–30257.

Brill, A. et al., 1999. The role of apoptosis in normal and abnormal embryonic development. *Journal of assisted reproduction and genetics*, 16(10), pp.512–9.

Buckley, D. et al., 2017. Fatty acid synthase - Modern tumor cell biology insights into a classical oncology target. *Pharmacology & therapeutics*, 177, pp.23–31.

Caenepeel, S. et al., 2018. AMG 176, a Selective MCL1 Inhibitor, Is Effective in Hematologic Cancer Models Alone and in Combination with Established Therapies. *Cancer Discovery*, 8, pp.1582–1597.

Caenepeel, S. et al., 2017. Preclinical evaluation of AMG 176, a novel, potent and selective Mcl-1 inhibitor with robust anti-tumor activity in Mcl-1 dependent cancer models. *Cancer Research*, 77(13).

Camassei, F. et al., 2003. Expression of the Lipogenic Enzyme Fatty Acid Synthase (FAS) as a Predictor of Poor Outcome in Nephroblastoma: An Interinstitutional Study. *Med Pediatr Oncol*, 40, pp.302–308.

Campos, L. et al., 1993. High expression of bcl-2 protein in acute myeloid leukemia cells is associated with poor response to chemotherapy. *Blood*, 81(11), pp.3091–6.

Carr, E. et al., 2010. Glutamine Uptake and Metabolism Are Coordinately. *The Journal of Immunology*, 185, pp.1037–1044.

Casara, P. et al., 2018. S55746 is a novel orally active BCL-2 selective and potent inhibitor that impairs hematological tumor growth. *Oncotarget*, 9(28), pp.20075–20088.

Cassago, A. et al., 2012. Mitochondrial localization and structure-based phosphate activation mechanism of Glutaminase C with implications for cancer metabolism. *PNAS*, 109, pp.1092–1097.

Castellsagué, X. et al., 2016. HPV Involvement in Head and Neck Cancers: Comprehensive Assessment of Biomarkers in 3680 Patients. *Journal of the National Cancer Institute*, 108(6), p.djv403.

Castilla, C. et al., 2006. Bcl-xL Is Overexpressed in Hormone-Resistant Prostate Cancer and Promotes Survival of LNCaP Cells via Interaction with Proapoptotic Bak. *Endocrinology*, 147(10), pp.4960–4967.

Certo, M. et al., 2006. Mitochondria primed by death signals determine cellular addiction to antiapoptotic BCL-2 family members. *Cancer cell*, 9(5), pp.351–65.

Cetindis, M.B.T. et al., 2016. Glutaminolysis and carcinogenesis of oral squamous cell carcinoma. *Eur Arch Otorhinolaryngol*, 273, pp.495–503.

Chakrabarti, G. et al., 2015. Targeting glutamine metabolism sensitizes pancreatic cancer to PARP-driven metabolic catastrophe induced by ß-lapachone. *Cancer and Metabolism* , 3(12).

Chaturvedi, A.K. et al., 2008. Incidence trends for human papillomavirus-related and -unrelated oral squamous cell carcinomas in the United States. *Journal of clinical oncology : official journal of the American Society of Clinical Oncology*, 26(4), pp.612–9.

Chen, L. et al., 2005. Differential targeting of prosurvival Bcl-2 proteins by their BH3-only ligands allows complementary apoptotic function. *Molecular cell*, 17(3), pp.393–403.

Chen, R. et al., 2014. The general amino acid control pathway regulates mTOR and autophagy during serum/glutamine starvation. *JBC*, 206(2), pp.173–182.

Chipuk, J.E. & Green, D.R., 2008. How do BCL-2 proteins induce mitochondrial outer membrane permeabilization? *Trends in cell biology*, 18(4), pp.157–64.

Chittenden, T. et al., 1995. A conserved domain in Bak, distinct from BH1 and BH2, mediates cell death and protein binding functions. *The EMBO journal*, 14(22), pp.5589–96.

Cho, S.-J. et al., 2008. Simvastatin induces apoptosis in human colon cancer cells and in tumor xenografts,and attenuates colitis-associated colon cancer in mice. *Int. J. Cancer*, 123, pp.951–957.

Chu, K. et al., 2010. ATP-Citrate Lyase reduction medited palmitate-induced apoptosis in pancreatic Beta cells. *Biological chemistry*, 285(42), pp.32606–32615.

Clark, O., Yen, K. & Mellinghoff, I., 2016. Molecular pathways: Isocitrate dehydrogenase mutations in cancer. *Clinical Cancer Research*, 22 , pp.1837–1842.

Cohen, J.J. et al., 1992. Apoptosis and programmed cell death in immunity. *Annual review of immunology*, 10(1), pp.267–293.

Cohen, M.A. et al., 2011. Transoral robotic surgery and human papillomavirus status: Oncologic results. *Head & neck*, 33(4), pp.573–80.

Core, C. & Reed, J., 2016. Finally, An Apoptosis-Targeting Therapeutic for cancer. *Cancer Research*, 76(20), pp.5914–5920.

Craze, M. et al., 2019. Glutamate dehydrogenase (GLUD1) expression in breast cancer. *Breast Cancer Research and Treatment*, 174, pp.79–91.

Crosby, H. & Miller, K., 2016. Evaluation the analgesic effect of the GLS inhibitor 6-diazo-5-oxo-I-norleucine in Vivo. *Pharmacy and Pharmacology international Journal*, 3(3).

Csibi, A. et al., 2013. The mTORC1 pathway stimulates glutamine metabolism and cell proliferation by repressing SIRT4. *Cell*, 153(4), pp.840–54.

Curthoys, N. & Watford, M., 1995. Regulation of Glutaminase Activity and Glutamine Metabolism. *Annu. Rev. Nutr*, 15, pp.133–59.

Dang, C., 2010. Glutaminolysis: Supplying carbon or nitrogen or or both for cancer cells? *Cell Cycle*, 9:19, pp.3884–3886.

Danial, N. et al., 2003. BAD and glucokinase reside in a mitochondrial complex that integrates glycolysis and apoptosis. *Nature*, 424(21).

Davids, M.S. & Letai, A., 2012. Targeting the B-cell lymphoma/leukemia 2 family in cancer. *Journal of clinical oncology : official journal of the American Society of Clinical Oncology*, 30(25), pp.3127–35.

DeBerardinis, R. et al., 2007. Beyond aerobic glycolysis: transformed cells can engage in glutamine metabolism that exceeds the requirement for protein and nucleotide synthesis. *PNAS*, 104(49), pp.19345–19350.

DeLaBarre, B. et al., 2011. Full-length human glutaminase in complex with an allosteric inhibitor. *Biochemistry*, 50(50), pp.10764–70.

Delbridge, A.R.D. et al., 2016. Thirty years of BCL-2: translating cell death discoveries into novel cancer therapies. *Nature reviews. Cancer*, 16(2), pp.99–109.

Van Delft, M.F. et al., 2006. The BH3 mimetic ABT-737 targets selective Bcl-2 proteins and efficiently induces apoptosis via Bak/Bax if Mcl-1 is neutralized. *Cancer cell*, 10(5), pp.389–99.

Deng, J. et al., 2007. BH3 profiling identified three distinct classes of apoptosis blocks to predict response to ABT-737 and conventional chemotherapeutic agents. *Cancer Cell*, 12, pp.171–185.

DeNicola, G.M. & Cantley, L.C., 2015. Cancer's Fuel Choice: New Flavors for a Picky Eater. *Molecular cell*, 60(4), pp.514–23.

Denoyelle, C. et al., 2001. Cerivastatin, an inhibitor of HMG-CoA reductase, inhibits the signaling pathways involved in the invasiveness and metastatic properties of highly invasive breast cancer cell lines: an in vitro study. *Carcinogenesis*, 22(8), pp.1139–48.

Dodia, R., 2014. *Structure and Function of Cytochrome c Oxidase*.

Dong, T. et al., 2016. Altered glycometabolism affects both clinical features and prognosis of triple-negative and neoadjuvant chemotherapy-treated breast cancer. *Tumor Biology*, 37, pp.8159–8168.

Duque-Parra, J.E., 2005. Note on the origin and history of the term "apoptosis". *Anatomical record. Part B, New anatomist*, 283(1), pp.2–4.

Eagle, H.M., 1955. The minimum vitamin requirements of the L and Hela cells in tissue culture the production of specific vitamin deficencies and their cure. *J Exp Med*, (102), pp.595–600.

Elgadi, K.M. et al., 1999. Cloning and analysis of unique human glutaminase isoforms generated by tissue-specific alternative splicing. *Physiological genomics*, 1(2), pp.51–62.

Elgogary, A. et al., 2016. Combination therapy with BPTES nanoparticles and metformin targets the metabolic heterogeneity of pancreatic cancer. *PNAS*, pp.E5328–E5336.

Elmore, S., 2007. Apoptosis: a review of programmed cell death. *Toxicologic pathology*, 35(4), pp.495–516.

Elorza, A. et al., 2012. HIF2α acts as an mTORC1 activator through the amino acid carrier SLC7A5. *Molecular cell*, 48(5), pp.681–91.

Escudero, S. et al., 2018. Dynamic Regulation of Long-Chain Fatty Acid Oxidation by a Noncanonical Interaction between the MCL-1 BH3 Helix and VLCAD. *Molecular cell*, 69(5), pp.729–743.e7.

Eskes, R. et al., 2000. Bid induces the oligomerization and insertion of Bax into the outer mitochondrial membrane. *Molecular and cellular biology*, 20(3), pp.929–35.

FDA, 2006. Cetuximab approved by FDA for treatment of Head and Neck Squamous Cell Cancer. *Cancer Biology &Therapy*, 5(4), pp.339–348.

Feleszko, W. et al., 2002. Synergistic interaction between highly specific cyclooxygenase-2 inhibitor, MF-tricyclic and lovastatin in murine colorectal cancer cell lines. *Oncoogy Reports*, 9, pp.879–885.

Feng, W. et al., 2007. Molecular Basis of Bcl-xL's Target Recognition Versatility Revealed by the Structure of Bcl-xL in Complex with the BH3 Domain of Beclin-1. *J. Mol. Biol*, 372, pp.223–235.

Ferlay, J. et al., 2015. Cancer incidence and mortality worldwide: sources, methods and major patterns in GLOBOCAN 2012. *International journal of cancer. Journal international du cancer*, 136(5), pp.E359–86.

Feun, L. et al., 2008. Arginine deprivation as a targets therapy for cancer. *Curr Phar Des*, 14(11), pp.1049–1057.

Filipp, F. et al., 2012. Reverse TCA cycle flux through isocitrate dehydrogenase 1 and 2 is required for lipogenesis in hypoxic melanoma cells. *Pigment Cell Melanoma*, 25(3), pp.375–383.

Flavahan, W. et al., 2016. Insulator dysfunction and oncogene activation in IDH mutant glioma. *Nature*, 529.

Flavin, R., 2010. Fatty acid synthase as apotential therapeutic target in cancer. *Cancer research*, 6(4), pp.551–562.

Foley, G. & Eagle, H., 1958. The cytotoxicity of anti-tumor agents for normal human and animal cells in first tissue culture passage. *Cancer research*, 18(9), pp.1011–6.

Fresquet, V. et al., 2014. Acquired mutations in BCL2 family proteins conferring resistance to the BH3 mimetic ABT-199 in lymphoma. *Blood*, 123(26), pp.4111–9.

Friday, E. et al., 2010. Glutaminolysis and glycolysis regulation by troglitazone in breast cancer cells: Relationship to mitochondrial membrane potential. *Cellular Physiology*, pp.511–519.

Gailiusis, J., Rinne, R. & Benedict, C., 1964. Pyruvate-Oxaloacetate exchange reaction in baker's yeast. *Biochimica Et Biophysica Acta*, 92, pp.595–601.

Del Gaizo Moore, V. et al., 2007. Chronic lymphocytic leukemia requires BCL2 to sequester prodeath BIM, explaining sensitivity to BCL2 antagonist ABT-737. *Journal of Clinical Inverstigation*, 17(1), pp.112–121.

Galluzzi, L. et al., 2012. Molecular mechanisms of cisplatin resistance. *Oncogene*, 31(15), pp.1869–83.

Galluzzi, L., Vitale, I. & et al, 2018. Molecular mechanisms of cell death: recommendations of the Nomenclature Committee on Cell Death. *Cell Death and Differentiation*, 25, pp.486–541.

Gandhi, L., Camidge, R. & et al, 2011. Phase I Study of Navitoclax (ABT-263), a Novel Bcl-2 Family Inhibitor, in Patients With Small-Cell Lung Cancer and Other Solid Tumors. *Journal of Clinical Oncology*, 29(7).

Gao, P. et al., 2009. c-Myc suppression of miR-23a/b enhances mitochondrial glutaminase expression and glutamine metabolism. *Nature*, 458(7239), pp.762–5.

Garber, K., 2016. Cancer anabolic metabolism inhibitors move into clinic. *Natural Biotechnology*, 8(34).

Garber, K., 2006. Energy deregulation: licensing tumors to grow. *Science (New York, N.Y.)*, 312(5777), pp.1158–9.

Geldermalsen, M. et al., 2016. ASCT2/SLC1A5 controls glutamine uptake and tumour growth in triple-negative basal-like breast cancer. *Oncogene*, 35, pp.3201–3208.

Germain, M. & Duronio, V., 2007. The N terminus of the anti-apoptotic BCL-2 homologue MCL-1 regulates its localization and function. *The Journal of biological chemistry*, 282(44), pp.32233–42.

Giralt, J. et al., 2015. Panitumumab plus radiotherapy versus chemoradiotherapy in patients with unresected, locally advanced squamous-cell carcinoma of the head and neck (CONCERT-2): a randomised, controlled, open-label phase 2 trial. *The Lancet. Oncology*, 16(2), pp.221–32.

Giuliano, A. et al., 2011. Incidence and clearance of genital human papillomavirus. *The Lancet*, 377, pp.932–940.

Goard, C. & Schimmer, A., 2013. An evidence-based review of obatoclax mesylate in the treatment of hematological malignancies. *Core Evidence*, 8.

Goldstein, J.L. & Brown, M.S., 1990. Regulation of the mevalonate pathway. *Nature*, 343(6257), pp.425–30.

Golomb, B.A. & Evans, M.A., 2008. Statin adverse effects : a review of the literature and evidence for a mitochondrial mechanism. *American journal of cardiovascular drugs : drugs, devices, and other interventions*, 8(6), pp.373–418.

Graham, N.A. et al., 2012. Glucose deprivation activates a metabolic and signaling amplification loop leading to cell death. *Molecular systems biology*, 8, p.589.

Gravel, S. et al., 2014. Serine Deprivation Enhances Antineoplastic Activity of Biguanides. *Cancer Research*, 74, pp.7521–7533.

Greaves, G. et al., 2018. BH3-only proteins are dispensable for apoptosis induced by pharmacological inhibition of both MCL-1 and BCL-XL. *Cell death and differentiation*, 26, pp.1037-1047

Green, D. & Reed, J., 1998. Mitochondria and Apoptosis. *Science*, 281, pp.1309–1312.

Griparic, L., Kanazwa, T. & Van der Bliek, A., 2007. Regulation of the mitochondrial dynamin-like protein Opa1 by proteolytic cleavage. *Journal of Cell Biology*, 178(5), pp.757–763.

Gross, M., Demo, S., Dennison, J., Chen, L., Chernov-Rogan, T., Goyal, B., et al., 2014. Antitumor Activity of the Glutaminase Inhibitor CB-839 in Triple-Negative Breast Cancer. *Molecular Cancer Therapeutics*, 13(4), pp.890–901.

Gross, M., Demo, S., Dennison, J., Chen, L., Chernov-Rogan, T. & Goyal, B. et al., 2014. Antitumor activity of the glutaminase inhibitor CB-839 in triple-negative breast cancer. *Mol Cancer Ther* , 13, pp.890–901.

Gross MI, D.S.D.J. et al, 2014. Antitumor Activity of the Glutaminase Inhibitor CB-839 in Triple-Negative breast cancer. *Molecular Cancer Therapeutics*, 13(4).

Grundy, M. et al., 2018. Genetic biomarkers predict response to dual BCL-2 and MCL-1 targeting in acute myeloid leukaemia cells. *Oncotarget*, 9(102), pp.37777–37789.

GTEX, C., 2015. The Genotype-Tissue Expression (GTEx) pilot analysis: Multitissue gene regulation in humans. *Science*, 348(6235), pp.648–660.

Guan, M. et al., 2017. Fatty acid synthase reprograms the epigenome in uterine leiomyosarcomas. *PloS one*, 12(6), p.e0179692.

Hacker, G., 2000. The morphology of apoptosis. *Cell Tissue Res*, 301, pp.5–17.

Han, C. et al., 2016. Amplification of USP13 drives ovarian cancer metabolism. *Nature Communications*,7(13525), pp.1-16

Hanahan, D. & Weinberg, R. a., 2011. Hallmarks of cancer: The next generation., 144(5), pp.646–674.

Hanahan & weinberg, R.A., 2000. The hallmarks of cancer. *Cell*, 100, pp. 57-70

Hao, X. et al., 2007. Inhibition of intestinal tumorigenesis in Apc(min/+) mice by green tea polyphenols (polyphenon E) and individual catechins. *Nutrition and cancer*, 59(1), pp.62–9.

Harb, J. et al., 2013. Bcl-xL anti-apoptotic network is dispensable for development and maintenance of CML but is required for disease progression where it represents a new therapeutic target. *Leukemia*, 27(10).

Hardwicke, M.A. et al., 2014. A human fatty acid synthase inhibitor binds β-ketoacyl reductase in the keto-substrate site. *Nature chemical biology*, 10(9), pp.774–9.

Hartman, S. & McGrath, T., 1973. Glutaminase A of Escherichia coli. *The Journal of Biological Chemistry*, 248(24), pp.8506–8510.

Hassanein, M. et al., 2013. SLC1A5 Mediates Glutamine Transport Required for Lung Cancer Cell Growth and Survival. *Clinical Cancer Research*, 19(3), pp.560–570.

Hassanein, M. et al., 2013. SLC1A5 mediates glutamine transport required for lung cancer cell growth and survival. *Clinical cancer research : an official journal of the American Association for Cancer Research*, 19(3), pp.560–70.

Hassanein, M. et al., 2015. Targeting SLC1A5-mediated glutamine dependence in non-small cell lung cancer. *Int J Cancer*, 137(7), pp.1587–1597.

Hata, A. et al., 2016. Tumor cells can follow distinct evolutionary paths to becom resistance to epidermal growth factor receptor inhibition. *Nature Medicine*, 22(3), pp.262–274.

Hatzivassiliou, G. et al., 2005. ATP citrate lyase inhibition can suppress tumor cell growth. *Cancer cell*, 8(4), pp.311–21.

Hellemans, P. et al., 1995. Prognostic value of bcl-2 expression in invasive breast cancer. *British journal of cancer*, 72(2), pp.354–60.

Hengartner, M., 2000. The biochemistry of apoptosis. *Nature* , 407, pp.770–776.

Hensley, C.T., Wasti, A.T. & DeBerardinis, R.J., 2013. Glutamine and cancer: cell biology, physiology, and clinical opportunities. *The Journal of clinical investigation*, 123(9), pp.3678–84.

Henson, P.M. & Hume, D.A., 2006. Apoptotic cell removal in development and tissue homeostasis. *Trends in immunology*, 27(5), pp.244–50.

Hermine, O. et al., 1996. Prognostic Significance of bcl-2 Protein Expression in Aggressive Non-Hodgkin's Lymphoma. *Blood*, 87(1), pp.265–272.

Hindler, K. et al., 2006. The role of statins in cancer therapy. *The Oncologist*, 11, pp. 306-315.

Hinson, D. et al., 1997. Post-translational regulation of mevalonate kinase by intermediates of the cholesterol and nonsterol isoprene biosynthetic pathways. *Journal of Lipid research*, 38, pp.2216–2223.

Hoerner, C., Chen, V. & Fan, A., 2019. The "Achilles Heel" of Metabolism in Renal Cell Carcinoma: Glutaminase Inhibition as a Rational Treatment Strategy. *Kidney cancer*, 3, pp.15–29.

Horiguchi, A. et al., 2008. Pharmacological inhibitor of fatty acid synthase suppresses growth and invasiveness of renal cancer cells. *The Journal of urology*, 180(2), pp.729–36.

Hotz, M. et al., 1999. Spontaneous apoptosis and the expression of p53 and bcl-2 family proteins in locally advanced head and neck cancer. *Arch Otolaryngol Head Neck Surg*, 125, pp.417-422.

Housman, G. et al., 2014. Drug resistance in cancer: an overview. *Cancers*, 6(3), pp.1769–92.

Huang, Q. et al., 2018. Characterization of the interactions of potent allosteric inhibitors with glutaminase C, a key enzyme in cancer cell glutamine

metabolisim. *Biol Chemistry*, 239(10), pp.3535-3545.

Innocenzi, D. et al., 2003. Fatty acid synthase expression in melanoma. *Journal of Cutaneous Pathology*, 30, pp. 23-28.

Inoshita, S. et al., 2002. Phosphorylation and inactivation of myeloid cell leukemia 1 by JNK in response to oxidative stress. *The Journal of biological chemistry*, 277(46), pp.43730–4.

Ishizwa, J. et al., 2015. Mitochondrial Profiling of Acute Myeloid Leukemia in the Assessment of Response to Apoptosis Modulating Drugs. *Plos One*, 10(9), pp.1-16.

Jacque, N. et al., 2015. Targeting glutaminolysis has antileukemic activity in acute myeloid leukemia and synergizes with BCL-2 inhibition. *Blood*, 126, pp. 1346–1356.

Jain, N. et al., 2016. Early T-cell precursor acute lymphoblastic leukemia/lymphoma (ETP-ALL/LBL) in adolescents and adults: a high-risk subtype. *Blood*, 127(15), pp.1863–1869.

Jiang, J., Srivastava, S. & Zhang, J., 2019. Starve Cancer Cells of Glutamine: Break the Spell or Make a Hungry Monster? *Cancers*, 11(804), pp.1-15.

Jiang, S.X. et al., 1995. Expression of bcl-2 oncogene protein is prevalent in small cell lung carcinomas. *The Journal of pathology*, 177(2), pp.135–8.

Jiang, X. & Wang, X., 2000. Cytochrome c promotes caspase-9 activation by inducing nucleotide binding to Apaf-1. *The Journal of biological chemistry*, 275(40), pp.31199–203.

Jin, L. et al., 2015. Glutamate dehydrogenase 1 signals through antioxidant glutathione peroxidase 1 to regulate redox homeostasis and tumor growth. *Cancer Cell*, 27(9), pp.257–270.

Ju, J. et al., 2007. Inhibition of carcinogenesis by tea constituents. *Seminars in cancer biology*, 17(5), pp.395–402.

Kagawa, S. et al., 2000. A binary adenoviral vector system for expressing high levels of the proapoptotic gene bax. *Gene therapy*, 7(1), pp.75–9.

Kale, J., Osterlund, E. & Andrews, D., 2018. BCL-2 family proteins: changing partners in the dance towards death. *Cell Death and Differentiation*, 25, pp.65–80.

Kalra & Brosnan, 1973. Subcellular localization of glutaminase isoenzymes in rat kidney cortex. *Bilogical Chemistry*, 240(10), pp.3255–3260.

Kamarajan, P. et al., 2017. Head and neck squamous cell carcinoma metabolism draws on glutaminolysis and stemness is specifically regulated by glutaminolysis

via aldehyde dehydrogenase. *Journal of Proteom Research*, 16, pp. 1315-1326.

Kang, M. & Reynolds, C., 2009. BCL-2 inhibitors: Targeting mitochondrial Apoptotic Pathways in cancer therapy. *Clinical Cancer Research*, 15(4), pp.1126–1132.

Kapuria, V. et al., 2011. A novel small molecule deubiquitinase inhibitor blocks Jak2 signaling through Jak2 ubiquitination. *Cellular signalling*, 23(12), pp.2076–85.

Katt, W. & Cerione, R., 2014. Glutaminase regulation in cancer cells: a druggable chain of events. *Drug Discovery Today*, 19(4), pp.450–457.

Katz, M. et al., 2005. Association of statin use with a pathologic complete response to neoadjuvant chemoradiation for rectal cancer. *Int. J. Radiation Oncology Biol.Phys.*, 62(5), pp.1363–1370.

Kaufmann, S. et al., 1998. Elevated Expression of the Apoptotic Regulator Mcl-1 at time of leukemic relapse. *Blood*, 91(3), pp.991–1000.

Kaushik, A. & DeBerardinis, R., 2018. Applications of metabolomics to study cancer metabolism. *BBA-Reviews on Cancer*, 1870, pp.2–14.

Kawata, S. et al., 2001. Effect of pravastatin on survival in patients with advanced hepatocellular carcinoma. A randomized controlled trial. *British journal of cancer*, 84(7), pp.886–91.

Kerr, J.F., Wyllie, A.H. & Currie, A.R., 1972. Apoptosis: a basic biological phenomenon with wide-ranging implications in tissue kinetics. *British journal of cancer*, 26(4), pp.239–57.

Kessler, D., Austin, R. & Levine, H., 2014. Resistance to Chemotherapy: Patient Variability and Cellular Heterogeneity. *Cancer Research*, 74(17), pp.4663–70.

Kian Ang, K. et al., 2014. Randomized Phase III Trial of Concurrent AcceleratedRadiation Plus Cisplatin With or Without Cetuximab forStage III to IV Head and Neck Carcinoma: RTOG 0522. *Journal of Clinical Oncology*, 32(27), pp.2940–2950.

Kim, H. et al., 2006. Hierarchical regulation of mitochondrion-dependent apoptosis by BCL-2 subfamilies. *Nature cell biology*, 8(12), pp.1348–58.

Kim, J.-H. et al., 2009. MCL-1ES, a novel variant of MCL-1, associates with MCL-1L and induces mitochondrial cell death. *FEBS letters*, 583(17), pp.2758–64.

Kim, J.-S., He, L. & Lemasters, J., 2003. Mitochondrial permeability transition: a common pathway to necrosis and apoptosis. *Biochemical and Biophysical Research Communications*, 304, pp.463–470.

Kim, S. et al., 2013. Expression of glutamine metabolism-related proteins according to molecular subtype of breast cancer. *Endocrine-related cancer*, 20(3), pp.339–

48.

Kim, W. et al., 2001. Phase II study of high-dose lovastatin in patients with advanced gastric adenocarcinoma. *Investigational New Drugs; Vol., Iss. 1, (Feb 2001): 81-3.*, 19(1), pp.81–83.

King, J.B. et al., 2009. A novel, species-specific class of uncompetitive inhibitors of gamma-glutamyl transpeptidase. *The Journal of biological chemistry*, 284(14), pp.9059–65.

Kirkin, V., Joos, S. & Zörnig, M., 2004. The role of Bcl-2 family members in tumorigenesis. *Biochimica et biophysica acta*, 1644(2-3), pp.229–49.

Knoechel, B. et al., 2014. An epigenetic mechanism of resistance to targeted therapy in T cell acute lymphoblastic leukemia. *Nature genetics*, 46(4), pp.364–70.

Knox, J. et al., 2005. A Phase I trial of prolonged administration of lovastatin in patients with recurrent or metastatic squamous cell carcinoma of the head and neck or of the cervix. *European Journal of Cancer*, 41, pp.523–530.

Koehler, M. et al., 2014. Structure-Guided Rescaffolding of selective antagonists of BCL-XL. *Medicinal Chemistry* , 5, pp.662–667.

Kofler, B., Laban, S. & Busch, C., 2014. New treatment strategies for HPV-positive head and neck cancer. *Eur Arch Otorhinolaryngol*, 271, pp.1861–1867.

Konopleva, M. et al., 2006. Mechanisms of apoptosis sensitivity and resistance to the BH3 mimetic ABT-737 in acute myeloid leukemia. *Cancer cell*, 10(5), pp.375–88.

Koppenol, W.H., Bounds, P.L. & Dang, C.V., 2011. Otto Warburg's contributions to current concepts of cancer metabolism. *Nature reviews. Cancer*, 11(5), pp.325–37.

Koppikar, P. et al., 2012. Heterodimeric JAK-STAT activation as a mechanism of persistence to JAK2 inhibitor therapy. *Nature*, 489(7414), pp.155–9.

Korangath, P. et al., 2015. Targeting Glutamine Metabolism in Breast Cancer with Aminooxyacetate. *Clinical Cancer Research*, 21(14), pp.3263–3273.

Kotschy, A. et al., 2016. The MCL1 inhibitor S63845 is tolerable and effective in diverse cancer models. *Nature*, 538(477).

Kovalchuk, O. et al., 2008. Involvement of microRNA-451 in resistance of the MCF-7 breast cancer cells to chemotherapeutic drug doxorubicin. *Molecular cancer therapeutics*, 7(7), pp.2152–9.

Kozopas, K.M. et al., 1993. MCL1, a gene expressed in programmed myeloid cell differentiation, has sequence similarity to BCL2. *Proceedings of the National*

Academy of Sciences of the United States of America, 90(8), pp.3516–20.

Krajewski, S. et al., 1995. Immunohistochemical analysis of MCL-1 protein in human tissues. *American Journal of Pathology*, 146(6), p.1309.

Kuhajda, F.P. et al., 2000. Synthesis and antitumor activity of an inhibitor of fatty acid synthase. *Proceedings of the National Academy of Sciences of the United States of America*, 97(7), pp.3450–4.

Kurosaka, K. et al., 2003. Silent Cleanup of Very Early Apoptotic Cells by Macrophages. *The Journal of Immunology*, 171, pp.4672–4679.

Kuwana, T. et al., 2005. BH3 Domains of BH3-Only Proteins Differentially Regulate Bax-Mediated Mitochondrial Membrane Permeabilization Both Directly and Indirectly. *Molecular Cell*, 17, pp.525–535.

Lacey, J. & Wilmore, D., 1990. Is Glutamine a Conditionally Essential Amino Acid? . *Nutrition Review*, 48(8), pp.297-309.

Lacey, J.M. & Wilmore, D.W., 1990. Is glutamine a conditionally essential amino acid? *Nutrition reviews*, 48(8), pp.297–309.

Lam, M. & Chan, G., 2017. Drug-induced amino acid deprivation as strategy for cancer therapy. *Hematology and Oncology*, 10(144), pp.1-18.

Lamers, F. et al., 2012. Targeted BCL2 inhibition effectively inhibits neuroblastoma tumour growth. *European journal of cancer (Oxford, England : 1990)*, 48(16), pp.3093–103.

Langendijk, J. et al., 2008. Impact of Late Treatment-Related Toxicity on Quality of Life Among Patients With Head and Neck Cancer Treated With Radiotherapy. *Journal of Clinical Oncology*, 26(22), pp.795–801.

Lawrence, M. & et al, 2015. Comprehensive genomic characterization of head and neck squamous cell carcinomas., 517(7536), pp.576–582.

Lazebnik, Y.A. et al., 1994. Cleavage of poly(ADP-ribose) polymerase by a proteinase with properties like ICE. *Nature*, 371(6495), pp.346–7.

Lazebnik, Y.A. et al., 1995. Studies of the lamin proteinase reveal multiple parallel biochemical pathways during apoptotic execution. *Proceedings of the National Academy of Sciences of the United States of America*, 92(20), pp.9042–6.

Le, A. et al., 2012. Glucose-independent glutamine metabolism via TCA cycling for proliferation and survival in B cells. *Cell metabolism*, 15(1), pp.110–21.

Leo, C. et al., 1999. Characterization of the Antiapoptotic Bcl-2 Family Member Myeloid Cell Leukemia-1 (Mcl-1) and the Stimulation of Its Message by Gonadotropins in the Rat Ovary. *Endocrinology*, 140(12), pp.5469–5477.

Lessene, G. et al., 2013. Structure-guided design of a selective BCL-X(L) inhibitor. *Nature chemical biology*, 9(6), pp.390–7.

Lessene, G., Czabotar, P. & Colman, P., 2008. BCL-2 family antagonists for cancer therapy. *Nature*, 7, pp.989–1000.

Letai, A. et al., 2002. Distinct BH3 domains either sensitize or activate mitochondrial apoptosis, serving as prototype cancer therapeutics. *Cancer Cell*, 2, pp.183–192.

Leverson, J., Phillips, D., et al., 2015. Exploiting selective BCL-2 family inhibitors to dissect cell survival dependencies and define improved strategies for cancer therapy. *Science translational medicine*, 7(279), p.279ra40.

Leverson, J., Zhang, H., et al., 2015. Potent and selective small-molecule MCL-1 inhibitors. *Cell Death and Disease*, 6(1590).

Levine, A. & Puzio-Kuter, A., 2010. The control of the metabolic switch in cancers by oncogenes and tumor suppressor genes. *Science*, 330(6009), pp.1340–1344.

Li, C. et al., 2011. Green tea polyphenols control dysregulated glutamate dehydrogenase in transgenic mice by hijacking the ADP activation site. *Biological Chemistry*, 286(39), pp.34164–34174.

Li, C. et al., 2006. Green Tea Polyphenols Modulate Insulin Secretion by Inhibiting Glutamate Dehydrogenase. *The Journal of Biological Chemistry*, 281(15), pp.10214–10221.

Li, C. et al., 2016. Metabolic reprogramming in cancer cells: glycolysis, glutaminolysis, and BCL-2 proteins as novel therapeutic targets for cancer. *World Journal of Surgical Oncology*, 14(15), pp.1-7.

Li, P. et al., 1997. Cytochrome c and dATP-dependent formation of Apaf-1/caspase-9 complex initiates an apoptotic protease cascade. *Cell*, 91(4), pp.479–89.

Li, X. et al., 2001. Overexpression of BCL-X(L) underlies the molecular basis for resistance to staurosporine-induced apoptosis in PC-3 cells. *Cancer research*, 61(4), pp.1699–706.

Li, Z., He, S. & Look, T., 2019. The MCL1-specific inhibitor S63845 acts synergistically with venetoclax/ABT-199 to induce apoptosis in T-cell acute lymphoblastic leukemia cells. *Leukemia*, 33, pp.262–266.

Lin, K. et al., 2016. Targeting MCL-1/BCL-XL Forestalls the Acquisition of Resistance to ABT-199 in Acute Myeloid Leukemia. *Scientific Reports*, 6(27696), pp.1-10.

Lin, R. et al., 2013. Acetylation stabilizes ATP-Citrate Lyase to promote Lipid biosyntheasis and Tumor growth. *Molecular Cell*, 51, pp.506–518.

Liu, G. et al., 2009. An Open-label, multicenter, phaseI/II study of single-agent AT-101 in men withcastrate-resistant prostate cancer. *Clinical Cancer Research*, 15(9), pp.3172–3176.

Liu, G. et al., 2015. Glutamate dehydrogenase is a novel prognostic marker and predicts metastases in colorectal cancer patients. *Journal of Translational Medicine*, 13(144).

Liu, H., Liu, Y. & Zhang, J.-T., 2008a. A new mechanism of drug resistance in breast cancer cells: fatty acid synthase overexpression-mediated palmitate overproduction. *Molecular cancer therapeutics*, 7(2), pp.263–70.

Liu, H., Liu, Y. & Zhang, J.-T., 2008b. A new mechanism of drug resistance in breast cancer cells: fatty acid synthase overexpression-mediated palmitate overproduction. *Molecular cancer therapeutics*, 7(2), pp.263–70.

Liu, J. & Feng, Z., 2012. PTEN, energy metabolism and tumor suppression. *Acta Biochim Biophys Sin*, 44(8), pp.629–631.

Liu, W.L.A. et al., 2012. Reprogramming of proline and glutamine metabolism contributes to the proliferative and metabolic responses regulated by oncogenic transcription factor c-MYC. *Proc Natl Acad Sci* , 109, p. 8983–8988.

Liu, X. et al., 1996. Induction of apoptotic program in cell-free extracts: requirement for dATP and cytochrome c. *Cell*, 86(1), pp.147–157.

Lømo, J. et al., 1996. Expression of the Bcl-2 homologue Mcl-1 correlates with survival of peripheral blood B lymphocytes. *Cancer research*, 56(1), pp.40–3.

Lomonosova, E. & Chinnadurai, G., 2008. BH3-only proteins in apoptosis and beyond: an overview. *Oncogen2*, 27(Suppl 1), pp.S2–19.

Lopez-Aguilar, E. et al., 1999. Security and Maximal Tolerated Doses of Fluvastatin In Pediatric Cancer Patients. *Archives of Medical Research*, 30, pp.128–131.

Lucas, C. et al., 2016. High CIP2A levels correlate with an antiapoptotic phenotype that can be overcome by targeting BCL-XL in chronic myeloid leukemia. *Leukemia*, 30(6), pp.1273–81.

Lucenay, K. et al., 2016. Cyclin E associated with the lipogenic enzyme ATP-Citrate Lyase to enable malignant growth of breast cancer cells. *Cancer Research*, 76(8).

Lyer, D., Vartak, M.A. & Goldsmith, G., 2016. Identification of a novel BCL2-specific inhibitor that binds predominantly to the BH1 domain. *FEBS Journal*, 283.

Mair, T., Leibundgut, M. & Ban, N., 2008. The crystal structure of a mammalin fatty acid synthase. *Science*, 321, pp.1315–1322.

Marquez, J., Mates, J. & Campos-Sandoval, J., 2016. The Glutaminase. In Schousboe, A and Sonnewald, U, ed. Advances in Neurobiology. Springer International PublishingSwitzerland: Springer, 13, pp. 133–180.

Marshall, S., Bacote, V. & Traxinger, R., 1991. Discovery of a Metabolic Pathway Mediating Glucose-induced Desensitization of the Glucose Transport System. *Biological Chemistry*, 266(8), pp.4706–4712.

Marur, S. & Forastiere, A., 2016. Head and Neck squamous cell carcinoma update on epidemiology, diagnosis and treatment. *Mayo Clin Proc*, 91(3), pp.386–396.

Marur, S. & Forastiere, A.A., 2008. Head and neck cancer: changing epidemiology, diagnosis, and treatment. *Mayo Clinic proceedings*, 83(4), pp.489–501.

Mashima, T. et al., 1995. Identification of Actin as a Substrate of ICE and an ICE-like Protease and Involvement of an ICE-like Protease but Not ICE in Vp-16-Induced U937 Apoptosis. *Biochemical and Biophysical Research Communication*, 217(3), pp.1185–1192.

Mashima, T., Seimiya, H. & Tsuruo, T., 2009. De novo fatty-acid synthesis and related pathways as molecular targets for cancer therapy. *British journal of cancer*, 100(9), pp.1369–72.

Mason, K.D. et al., 2007. Programmed anuclear cell death delimits platelet life span. *Cell*, 128(6), pp.1173–86.

Masson, J. et al., 2006. Mice Lacking Brain/Kidney Phosphate-Activated Glutaminase Have Impaired Glutamatergic Synaptic Transmission, Altered Breathing, Disorganized Goal-Directed Behavior and Die Shortly after Birth. *The Journal Neuroscience*, 26(17), pp.4660–4671.

Mates, J. et al., 2013. Glutaminase isoenzymes in the metabolic therapy of cancer. *BBA-Reviews on Cancer*.

Mattaini, K., Sullivan, M. & Vander Heiden, M., 2016. The importance of serine metabolism in cancer. *JCB*, 214(3), pp.249–257.

Mayers, J. & Vander Heiden, M., 2015. Famine versus feast: understanding the metabolism of tumors in vivo. *Trends in biochemical sciences*, 40(3), pp. 130-140

Mazumder, S. et al., 2012. Mcl-1 Phosphorylation defines ABT-737 resistance that can be overcome by increased NOXA expression in leukemic B cells. *Cancer research*, 72(12), pp.3069–79.

McFadden, J. et al., 2005. Application of a Flexible Synthesis of (5R)-Thiolactomycin To Develop New Inhibitors of Type I Fatty Acid Synthase. *Journal of Medicinal Chemistry*, 48(4), pp.946–961.

Medina, M.A. et al., 1992. Relevance of glutamine metabolism to tumor cell growth. *Molecular and cellular biochemistry*, 113(1), pp.1–15.

Menendez, J., Lupu, R. & Colomer, R., 2004. Inhibition of tumour-associated fatty acid synthase hyperactivity induces synergistic chemosensitization of HER-2/neu-overexpressing human breast cancer cells to docetaxel (taxotere). *Breast Cancer Research and treatment* , 84, pp.183–195.

Menendez, J.A., Vellon, L. & Lupu, R., 2005. Targeting fatty acid synthase-driven lipid rafts: a novel strategy to overcome trastuzumab resistance in breast cancer cells. *Medical hypotheses*, 64(5), pp.997–1001.

Meric-Bernstam, F. et al., 2016. Phase 1 study of CB-839, a small molecule inhibitor of glutaminase, in combination with everolimus in patients (pts) with clear cell and papillary renal cell cancer (RCC). *Eur J Cancer*, 69, pp.S12–S13.

Merino, D., Whittle, J., Vaillant, F., Serrano, A., Gong, J., et al., 2017. Synergistic action of the MCL-1 inhibitor S63845 with current therapies in preclinical models of triple-negative and HER2-amplified breast cancer. *Science Translational Medicine*, 9(eaam 7049).

Metallo, C. et al., 2012. Reductive glutamine metabolism by IDH1 mediates lipogenesis under hypoxia. *Nature*, 481, pp.380–384.

Migita, T. et al., 2008. ATP citrate Lyase: activation and therapeutic implications in Non-Small Cell Lung Cancer. *Cancer Research*, 68(20), pp.8547-8554.

Milani, M. et al., 2016. DRP-1 is required for BH3 mimetic-mediated mitochondrial fragmentation and apoptosis. *Cell Death and Disease*, 8(e2552).

Minden, M. et al., 2001. Lovastatin Induced Control of Blast Cell Growth in an Elderly Patient with Acute Myeloblastic Leukemia. *Leukemia and Lymphoma*, 40, pp.659–662.

Momcilovic, M. et al., 2018. The GSK3 Signaling Axis Regulates Adaptive Glutamine Metabolism in Lung Squamous Cell Carcinoma. *Cancer Cell*, 33, pp.905–921.

Moore, E. & Lepage, G., 1957. In vivo sensitivity of normal and neoplastic mouse tissues to azaserine. *Cancer research*, 17(8), pp.804–8.

Morsch, M. et al., 2015. In vivo characterization of microglial engulfment of dying neurons in the zebrafish spinal cord. *Frontiers in Cellular Neuroscience2015*, 9, pp.321–331.

Moujalled, D.M. et al., 2019. Combining BH3-mimetics to target both BCL-2 and MCL1 has potent activity in pre-clinical models of acute myeloid leukemia. *Leukemia*, 33(4), pp.905–917.

Mullen, A. et al., 2014. Oxidation of alpha-ketoglutarate is required for reductive carboxylation in cancer cells with mitochondrial defects. *Cell Report*, 12(7), pp.1679–1690.

Mullen, A.R. et al., 2012. Reductive carboxylation supports growth in tumour cells with defective mitochondria. *Nature*, 481(7381), pp.385–8.

Mullen, P. et al., 2016. The interplay between cell signalling and the mevalonate pathway in cancer. *Nature review*, 16, pp.718-731.

Nagy, B. et al., 2003. Abnormal expression of apoptosis-related genes in haematological malignancies: overexpression of MYC is poor prognostic sign in mantle cell lymphoma. *British Journal Haematology*, 120, pp.434–441.

Newman, A. et al., 1997. A Comparison of the Effect of the 3-Hydroxy-3-Methylglutaryl Coenzyme A (HMG-CoA) Reductase Inhibitors Simvastatin, Lovastatin and Pravastatin on Leukaemic and Normal Bone Marrow Progenitors. *Leukemia and Lymphoma*, 24, pp.533–537.

Nguyen, M. et al., 2007. Small molecule obatoclax (GX15-070) antagonizes MCL-1 and overcomes MCL-1-mediated resistance to apoptosis. *Proceedings of the National Academy of Sciences of the United States of America*, 104(49), pp.19512–7.

Ni Chonghaile, T. et al., 2014. Maturation Stage of T-cell Acute Lymphoblastic Leukemia Determines BCL-2 versus BCL-XL Dependence and Sensitivity to ABT-199. *Cancer discovery*, 4(9), pp.1074–1087.

Ni Chonghaile, T. et al., 2011. Pretreatment Mitochondrial Priming correlates with clinical response to cytotoxic chemotherapy. *Scirnce*, 334(25), pp.1129–1133.

Nielson, C.M. et al., 2007. Human papillomavirus prevalence and type distribution in male anogenital sites and semen. *Cancer epidemiology, biomarkers & prevention : a publication of the American Association for Cancer Research, cosponsored by the American Society of Preventive Oncology*, 16(6), pp.1107–14.

Noguchi, Y. et al., 1997. Increased glutamine consumption in small intestine epithelial cells during sepsis in rats. *Am J Surg*, 173(3), pp.199–205.

O'Brien, S. et al., 2007. Randomized Phase III Trial of Fludarabine Plus Cyclophosphamide With or Without Oblimersen Sodium (Bcl-2 antisense) in Patients With Relapsed or Refractory Chronic Lymphocytic Leukemia. *Journal of Clinical Oncology*, 25(9).

O'Neill, K.L. et al., 2016. Inactivation of prosurvival Bcl-2 proteins activates Bax/Bak through the outer mitochondrial membrane. *Genes & development*, 30(8), pp.973–88.

Ogino, S. et al., 2008. Cohort Study of Fatty Acid Synthase Expression and Patient Survival in Colon Cancer. *Journal of Clinical Oncology*, 26, pp.5713–5720.

Olalla, L. et al., 2002. Nuclear localization of L-type glutaminase in mammalian brain. *The Journal of biological chemistry*, 277(41), pp.38939–44.

Olichon, A. et al., 2003. Loss of OPA1 perturbates the mitochondrial inner membrane structure and integrity, leading to cytochrome c release and apoptosis. *The Journal of biological chemistry*, 278(10), pp.7743–6.

Olsson, A. et al., 2007. Upregulation of bfl-1 is a potential mechanism of chemoresistance in B-cell chronic lymphocytic leukaemia. *British journal of cancer*, 97(6), pp.769–77.

Oltersdorf, T. et al., 2005. An inhibitor of Bcl-2 family proteins induces regression of solid tumours. *Nature*, 435(7042), pp.677–81.

Ondera, J. & Ohsumi, Y., 2005. Autophagy is required for maintenance of amino acid levels and protein synthesis under nitrogen starvation. *The Journal of Biological Chmistry*, 280(36), pp.31582–31586.

Opferman, J. et al., 2003. Development and maintenance of B and T lymphocytes requires antiapoptotic MCL-1. *Nature*, 426, pp.671–676.

Oslob, J. et al., 2013. Imidazopyridine-Based Fatty Acid Synthase Inhibitors That Show Anti-HCV Activity and in Vivo Target Modulation. *Medinial Chemistry Letters*, 4, pp.113–117.

Palve, V. et al., 2014. Overexpression of Mcl-1L Splice Variant Is Associated with Poor Prognosis and Chemoresistance in Oral. *Plos One*, 9(11).

Palve, V.C. & Teni, T.R., 2012. Association of anti-apoptotic Mcl-1L isoform expression with radioresistance of oral squamous carcinoma cells. *Radiation oncology (London, England)*, 7, p.135.

Panosyan, E. et al., 2004. Deamination of Glutamine is a Prerequisite for Optimal Asparagine Deamination by Asparaginases In Vivo (CCG-1961). *Anticancer Research*, 24(March), pp.1121–1126.

Pavlova, N. & Thompson, C., 2016. The emerging hallmarks of cancer metabolism. *Cell metabolism*, 23(1), pp.27–47.

Peddi, P. et al., 2015. Cisplatin, Cetuximab, and Radiation in Locally Advanced Head and Neck Squamous Cell Cancer: A Retrospective Review. *Clinical Medicin Insights Oncology*, 9, pp. 1-7.

Perciavalle, R.M. et al., 2012. Anti-apoptotic MCL-1 localizes to the mitochondrial matrix and couples mitochondrial fusion to respiration. *Nature cell biology*, 14(6), pp.575–83.

Pérez-Gómez, C. et al., 2003. Genomic organization and transcriptional analysis of the human l-glutaminase gene. *The Biochemical journal*, 370(Pt 3), pp.771–84.

Peterson, L.F. et al., 2015. Targeting deubiquitanase activity with a novel small-molecule inhibitor as therapy for B-cell malignancies. *Blood*, 125(23).

Petronini, P. et al., 1996. Cell Susceptibility to Apoptosis by Glutamine Deprivation and Rescue: Survival and Apoptotic Death in Cultured Lymphoma-Leukemia Cell Lines. *Journal of Cellular Physiology*, 169, pp.175–185.

Petros, A.M. et al., 2000. Rationale for Bcl-xL/Bad peptide complex formation from structure, mutagenesis, and biophysical studies. *Protein science : a publication of the Protein Society*, 9(12), pp.2528–34.

Piche, A. et al., 1998. Modulation of Bcl-2 Protein Levels by an Intracellular Anti-Bcl-2 Single-Chain Antibody Increases Drug-induced Cytotoxicity in the Breast Cancer Cell Line MCF-71. *Cancer Research*, 58, pp.2134–2140.

Pignon, J. et al., 2000. Chemotherapy added to locoregional treatment for head andneck squamous-cell carcinoma: three meta-analyses of updated individual data. *The Lancet*, 355, pp.949–955.

Pinkus, L., 1977. Glutamine binding sites. *Methods in Enzymology*, pp. 414–427.

Piyathilake, C.J. et al., 2000. The expression of fatty acid synthase (FASE) is an early event in the development and progression of squamous cell carcinoma of the lung. *Human pathology*, 31(9), pp.1068–73.

Placzek, W. et al., 2010. A survey of the anti-apoptotic Bcl-2 subfamily expression in cancer types provides a platform to predict the efficacy of Bcl-2 antagonists in cancer therapy. *Cell Death and Disease*, 1(e40).

Plaitakis, A. et al., 2017. The Glutamate Dehydrogenase Pathway and Its Roles in Cell and Tissue Biology in Health and Disease. *Biology*, 6(11).

Porter, L.D. et al., 2002. Complexity and species variation of the kidney-type glutaminase gene. *Physiological genomics*, 9(3), pp.157–66.

Prajda, N., 1985. Advances in enzyme regulation. In Weber, G, ed. West Germany : Elsever, pp. 207–223.

Prukova, D. et al., 2019. Cotargeting of BCL2 with Venetoclax and MCL1 with S63845 Is Synthetically Lethal In Vivo in Relapsed Mantle Cell Lymphoma. *Clinical Cancer Research*, 25(14), pp.4455-4465.

Puig, T. et al., 2011. A novel inhibitor of fatty acid synthase shows activity against HER2+ breast cancer xenografts and is active in anti-HER2 drug-resistant cell lines. *Breast Cancer Research*, 13(R131).

Qian, J. et al., 2004. Discovery of novel inhibitors of Bcl-xL using multiple high-throughput screening platforms. *Analytical Biochemistry*, 328, pp.131–138.

Qing, G. et al., 2012. ATF4 regulates MYC-mediated neuroblastoma cell death upon glutamine deprivation. *Cancer cell*, 22(5), pp.631–44.

Quinn, B.A. et al., 2011. Targeting Mcl-1 for the therapy of cancer. *Expert opinion on investigational drugs*, 20(10), pp.1397–411.

Ramirez, M. et al., 2015. Diverse drug-resistance mechanisms can emerge from drug-tolerant cancer persister cells. *Nature Communications*, 7(10690).

Rao, S. et al., 1998. Lovastatin mediated G1 arrest in normal and tumor breast cells is through inhibition of CDK2 activity and redistribution of p21 and p27, independent of p53. *Oncogene*, 17, pp.2393–2402.

Reiner, T. et al., 2015. Mcl-1 protects prostate cancer cells from cell death mediated by chemotherapy-induced DNA damage. *Oncoscience*, 2(8), pp.703–715.

Reitzer, L.J., Wice, B.M. & Kennell, D., 1979. Evidence that glutamine, not sugar, is the major energy source for cultured HeLa cells. *The Journal of biological chemistry*, 254(8), pp.2669–76.

Reynolds, M.R. et al., 2014. Control of glutamine metabolism by the tumor suppressor Rb. *Oncogene*, 33(5), pp.556–66.

Roberts, A. et al., 2012. Substantial Susceptibility of Chronic Lymphocytic Leukemia to BCL2 Inhibition: Results of a Phase I Study of Navitoclax in Patients With Relapsed or Refractory Disease. *Journal of Clinical Oncology*, 30(5).

Roberts, A. et al., 2016. Targeting BCL2 with Venetoclax in Relapsed Chronic Lymphocytic Leukemia. *The New England Journal of Medicine*, 374(4).

Robinson, M.M. et al., 2007. Novel mechanism of inhibition of rat kidney-type glutaminase by bis-2-(5-phenylacetamido-1,2,4-thiadiazol-2-yl)ethyl sulfide (BPTES). *The Biochemical journal*, 406(3), pp.407–14.

Rogers, S., ́Wells, R. & Rechsteiner, M., 1986. Amino acid sequences common to rapidly degrade proteins: the PEST hypothesis. *Science*, 234, p.364 LP–368.

Rohrig, F. & Schilze, A., 2016. The Multifaceted Roles of fatty acid synthesis in cancer. *Nature*, 16, pp. 732-749.

Rudin, C. et al., 2008. Randomized Phase II Study of Carboplatin and Etoposide With or Without the bcl-2 Antisense Oligonucleotide Oblimersen for Extensive-Stage Small-Cell Lung Cancer: CALGB 30103. *Journal of Clinical Oncology*, 26(6).

Rudin, C.M. et al., 2012. Phase II study of single-agent navitoclax (ABT-263) and biomarker correlates in patients with relapsed small cell lung cancer. *Clinical cancer research : an official journal of the American Association for Cancer Research*, 18(11), pp.3163–9.

Rytelewski, M., 2015. *Overcoming Innate and Acquired Therapy Resistance by Targeting DNA Repair in Human Cancer Cells*. University of Western Ontario.

Saha, S. et al., 2019. Multiomics Analysis Reveals that GLS and GLS2 differentially modulate the clinical outcomes of cancer. *Journal of Clinical Medicine*, 8(355).

Sandulache, V. et al., 2010. Glucose, not glutamine, is the dominant energy source required for proliferation and survival of head and neck squamous carcinoma cells. *Cancer*, pp.2926–2938.

Sastry, K. et al., 2014. Targeting proapoptotic protein BAD inhibits survival and self-renewal of cancer stem cells. *Cell Death and Differentiation*, 21, pp.1936–1949.

Sato, T. et al., 1994. Cloning and sequencing of a cDNA encoding the rat Bcl-2 protein. *Gene*, 140, pp.291–292.

Savill, J. & Fadok, V., 2000. Corpse clearance defines the meaning of cell death. *Nature*, 407(6805), pp.784–8.

Schenk, R., Strasser, A. & Dewson, G., 2017. BCL-2: Long and winding path from discovery to therapeutic target. *Biochemical and Biophysical Research Communications*, 482, pp.459–469.

Scherr, A. et al., 2016. Bcl-xL is an oncogenic driver in colorectal cancer. Cell Death Dis. 7, e2342 (2016). *Cell Death and Disease*, 7(e2342).

Sebastiani, V. et al., 2004. Fatty acid synthase is a marker of increased risk of recurrence in endometrial carcinoma. *Gynecologic oncology*, 92(1), pp.101–5.

Seiwert, T. et al., 2015. Integrative and comparative genomic analysis of HPV-positive. *Clinical cancer research*, 21(1), pp.632–641.

Sekula, B., Ruszkowski, M. & Dauter, Z., 2018. Structural Analysis of Phosphoserine Aminotransferase (Isoform 1) From Arabidopsis thaliana. *Frontier inPlant Science*, 9, pp.876–888.

Sellers, K. et al., 2015. Pyruvate carboxylase is critical for non-small-cell lung cancer proliferation. *Clinical investigation*, 125(2), pp.687–698.

Sharma, S.V. et al., 2010. A chromatin-mediated reversible drug-tolerant state in cancer cell subpopulations. *Cell*, 141(1), pp.69–80.

Shen, L. et al., 2012. miR-497 induces apoptosis of breast cancer cells by targeting BCL-w. *Experimental and Therapeutic Medicine*, 3, pp.475–480.

Shurbaji, M.S., Kalbfleisch, J.H. & Thurmond, T.S., 1996. Immunohistochemical detection of a fatty acid synthase (OA-519) as a predictor of progression of prostate cancer. *Human pathology*, 27(9), pp.917–21.

Silva, S.D. et al., 2008. Differential expression of fatty acid synthase (FAS) and ErbB2 in nonmalignant and malignant oral keratinocytes. *Virchows Archiv : an international journal of pathology*, 453(1), pp.57–67.

Silva, S.D. et al., 2004. Expression of fatty acid synthase, ErbB2 and Ki-67 in head and neck squamous cell carcinoma. A clinicopathological study. *Oral oncology*, 40(7), pp.688–96.

Singh, R. & Saini, N., 2011. Downregulation of BCL2 by miRNAs augments druginduced apoptosis - A combined computational and experimental approach. *Journal of Cell Science*, 125(6), pp.1568–1578.

Soma, M., Corsini, A. & Paoletti, R., 1992. Cholesterol and mevalonic acid modulation in cell metabolism and multiplication. *ToxicologyLetters*, 64/65, pp.1–15.

Son, J. et al., 2013. Glutamine supports pancreatic cancer growth through a KRAS-regulated metabolic pathway. *Nature*, 496(7443), pp.101–5.

Souers, A.J. et al., 2013. ABT-199, a potent and selective BCL-2 inhibitor, achieves antitumor activity while sparing platelets. *Nature medicine*, 19(2), pp.202–8.

Stilgenbauer, S. et al., 2016. Venetoclax in relapsed or refractory chronic lymphocytic leukaemia with17p deletion amulticentre, open-label phase study. *Oncology*, 17, pp.768–78.

Still, E.R. & Yuneva, M.O., 2017. Correction: Hopefully devoted to Q: targeting glutamine addiction in cancer. *British journal of cancer*,116, pp.1375-1381.

Swellam, M. et al., 2004. Incidence of Bcl-2 expression in bladder cancer: relation to schistosomiasis. *Clinical biochemistry*, 37(9), pp.798–802.

Swinnen, J.V. et al., 2004. Androgens, lipogenesis and prostate cancer. *The Journal of steroid biochemistry and molecular biology*, 92(4), pp.273–9.

Szakács, G. et al., 2006. Targeting multidrug resistance in cancer. *Nature Reviews*, 5.

Tabe, Y., Lorenzi, P. & Konopleva, M., 2019. Amino acid metabolism in hematologic malignancies and the era of targeted therapy. *Blood*, 134(13), pp.1014–1023.

Tahir, S. et al., 2017. Potential mechanisms of resistance to venetoclax and strategies to circumvent it. *BMC cancer*, 17(1), p.399.

Tao, Z. et al., 2014. Discovery of a Potent and Selective BCL-XL Inhibitor with in Vivo Activity. *ACS Medicinal Chemistry Letters*, 5, pp.1088–1093.

Tarnowski, G. & Stock, C., 1957. Effects of Combinations of Azaserine and of 6-Diazo-5-oxo-L- norleucine with Furine Analogs and Other Antimetabolites on the Growth of Two Mouse Mammary Carcinomas. *Cancer Research*, 17, pp.1033–1039.

Thangavelu, K. et al., 2012a. Structural basis for the allosteric inhibitory mechanism of. *PNAS*, 109(20), pp.7705–7710.

Thomas, R.L. et al., 2013. Loss of MCL-1 leads to impaired autophagy and rapid development of heart failure. *Genes & development*, 27(12), pp.1365–77.

Thompson, R. et al., 2017. Glutaminase inhibitor CB-839 synergizes with carfilzomib in resistant multiple myeloma cells. *Oncotarget*, 8(22), pp.35863–35876.

Thornburg, J. et al., 2008. Targeting aspartate aminotransferase in breast cancer. *Breast Cancer Research* , 10(5).

Thupari, J.N. et al., 2002. C75 increases peripheral energy utilization and fatty acid oxidation in diet-induced obesity. *Proceedings of the National Academy of Sciences of the United States of America*, 99(14), pp.9498–502.

Tian, W.-X., 2006. Inhibition of fatty acid synthase by polyphenols. *Current Medicinal Chemistry*, 13(8), pp.967–977.

Touzeau, C. et al., 2016. BH3-profiling identifies heterogeneous dependency on Bcl-2 family members in Multiple Myeloma and predicts sensitivity to BH3 mimetics. *Leukemia*, 30(3), pp.761–764.

Trask, D.K. et al., 2002. Expression of Bcl-2 family proteins in advanced laryngeal squamous cell carcinoma: correlation with response to chemotherapy and organ preservation. *The Laryngoscope*, 112(4), pp.638–44.

Tricarico, P., Crovella, S. & Celsi, F., 2015. Mevalonate pathway blockade, mitochondrial dysfunction and autophagy: apossiple link. *Molecular Sciences*, 16, pp.16067–16084.

Tron, A. et al., 2018. Discovery of Mcl-1-specific inhibitor AZD5991 and preclinical activity in multiple myeloma and acute myeloid leukemia. *Nature Communications*, 9(5341).

Tse, C. et al., 2008. ABT-263: a potent and orally bioavailable Bcl-2 family inhibitor. *Cancer research*, 68(9), pp.3421–8.

Tsujimoto, Y. et al., 1984. Cloning of the chromosome breakpoint of neoplastic B cells with the t(14;18) chromosome translocation. *Science* , 80-(226), pp.1097–1099.

Turrado, C. et al., 2012. New synthetic inhibitors of fatty acid synthase with anticancer activity. *Journal of Medicinal Chemistry*, 55, pp.5013-5023.

Ueda, S.M. et al., 2009. Trophoblastic neoplasms express fatty acid synthase, which may be a therapeutic target via its inhibitor C93. *The American journal of pathology*, 175(6), pp.2618–24.

Vander Heiden, M. et al., 2010. Evidence for an alternative Glycolytic pathway in rapidly proliferating cells. *Science*, 329, pp.1492–1499.

Vander Heiden, M., Cantley, L. & Thompson, C., 2009. Understanding the Warburg Effect: The metabolic requirements of cell proliferation. *Science*, 324 , pp.1029–1033.

Vanhove, K. et al., 2019. Glutamine Addiction and Therapeutic Strategies in Lung Cancer. *International Journal of Molecular Sciences*, 20(252).

Varanita, T. et al., 2015. The Opa1-Dependent Mitochondrial Cristae Remodeling Pathway Controls Atrophic, Apoptotic, and Ischemic Tissue Damage. *Cell Metabolism*, 21, pp.834–844.

Vartak, S. et al., 2017. Novel BCL2 inhibitor, Disarib induces apoptosis by disruption of BCL2-BAK interaction. *Biochemical Pharmacology*, 131, pp.16–28.

Vázquez, M.J. et al., 2008. Discovery of GSK837149A, an inhibitor of human fatty acid synthase targeting the beta-ketoacyl reductase reaction. *The FEBS journal*, 275(7), pp.1556–67.

Vazquez-Martin, A., Ropero, S., et al., 2007. Inhibition of Fatty Acid Synthase (FASN) synergistically enhances the efficacy of 5-fluorouracil in breast carcinoma cells. *Oncology reports*, 18(4), pp.973–80.

Vazquez-Martin, A., Colomer, R., et al., 2007. Pharmacological blockade of fatty acid synthase (FASN) reverses aquired autoresistance to trastuzumab (Herceptin) by transcriptionally inhibiting HER2 super-expression' occuring in high-dose trastumab-conditioned SKBR3/Tzb100 breast cancer cells. *Internationa Journal of Oncology*, 31, pp.769–776.

Veeramalla, V., 2017. Pseudocholinesterase, aspartate transaminase, alanine transaminase as markers for cervical cancer: a study in a tertiary care hospital. *International Journal of Advances Medicine*, 4(6), pp.1557–1561.

Vermorken, J.B. et al., 2008. Platinum-based chemotherapy plus cetuximab in head and neck cancer. *The New England journal of medicine*, 359(11), pp.1116–27.

Vie, N. et al., 2008. ResearchOverexpression of phosphoserine aminotransferase PSAT1 stimulates cell growth and increases chemoresistance of colon cancer. *Molecular Cancer*, 7(14).

Viswanathan, C. et al., 2008. Synthesis-and-evaluation-of-lglutamic-acid-analogs-as-potential-anticancer-agents. *Indian Journal of Pharmaceutical Sciences*, 70(2), pp.245–250.

Vogelstein & Kinzler, 2004. Cancer genes and the pathways they control. *Nature medicine*, 10(8), pp. 789-799.

Vogler, M. et al., 2013. ABT-199 selectively inhibits BCL2 but not BCL2L1 and efficiently induces apoptosis of chronic lymphocytic leukaemic cells but not platelets. *British journal of haematology*, 163(1), pp.139–42.

Vogler, M., Hamali, H.A., et al., 2011. BCL2/BCL-XL inhibition induces apoptosis, disrupts cellular calcium homeostasis and prevents platelet activation. *Blood*, 117(26).

Vogler, M., Butterworth, M., et al., 2009. Concurrent up-regulation of BCL-XL and BCL2A1 induces approximately 1000-fold resistance to ABT-737 in chronic lymphocytic leukemia. *Blood*, 113(18), pp.4403–4413.

Vogler, M., Weber, K., et al., 2009. Different forms of cell death induced by putative BCL2 inhibitors. *Cell death and differentiation*, 16(7), pp.1030–9.

Vogler, M., Dickens, D., et al., 2011. The B-cell lymphoma 2 (BCL2)-inhibitors, ABT-737 and ABT-263, are substrate for P-glycoprotein. *Biochemical and Biophysical Research Communications*, 408, pp.344–349.

Vrablik, T. & Watts, J., 2012. Emerging roles for specific fatty acids in developmental processes. *Genes&Devvelopment*, 26, pp.631–637.

Wang, C. & Youle, R., 2009. The Role of Mitochondria in Apoptosis. *Annu Rev Genet*, 43(95-118).

Wang, J. et al., 2000. Structure-based discovery of an organic compound that binds Bcl-2 protein and induces apoptosis of tumor cells. *PNAS*, 97(13), pp.7124–7129.

Wang, Q. et al., 2014. Targeting glutamine transport to suppress melanoma cell growth. *International journal of cancer. Journal international du cancer*, 135(5), pp.1060–71.

Wang, X. et al., 2013. Deletion of MCL-1 causes lethal cardiac failure and mitochondrial dysfunction. *Genes & development*, 27(12), pp.1351–64.

Warburg, O., 1956. On the origin of cancer cells. *Science (New York, N.Y.)*, 123(3191), pp.309–14.

Warburg, O., Wind, F. & Negelein, E., 1927. The metabolism of tumors in the body. *The Journal of General Physiology*, 8, pp.519–530.

Ward, P. et al., 2010. The Common Feature of Leukemia-Associated IDH1 and IDH2 Mutations Is a Neomorphic Enzyme Activity Converting α-Ketoglutarate to 2-Hydroxyglutarate. *Cancer Cell*, 17, pp.225–234.

Ward, P. & Thompson, C., 2012. Metabolic reprogramming: a cancer hallmark even warburg did not anticipate. *Cancer cell*, 21(3), pp.297–308.

Washington, I. & Hoosier, G., 2012. Clinical Biochemistry and Haematology. In Elsevier Inc, pp. 57–116.

Wei, D. et al., 2015. Targeting Mcl-1 for Radiosensitization of Pancreatic Cancers. *Translational Oncology*, 8(1), pp.47–54.

Wei, J. et al., 2011. An optically pure apogossypolone derivative as potent pan-active inhibitor of anti-apoptotic bcl-2 family proteins. *Frontiers in oncology*, 1, p.28.

Weinberg, F. et al., 2010. Mitochondrial metabolism and ROS generation are essential for Kras-mediated tumorigenicity. *Proceedings of the National Academy of Sciences of the United States of America*, 107(19), pp.8788–93.

Westphal, D., Kluck, R.M. & Dewson, G., 2014. Building blocks of the apoptotic pore: how Bax and Bak are activated and oligomerize during apoptosis. *Cell death and differentiation*, 21(2), pp.196–205.

Willems, L. et al., 2013. Inhibiting glutamine uptake represents an attractive new strategy for treating acute myeloid leukemia. *Blood*, 122(20).

Willis, S.N. et al., 2005. Proapoptotic Bak is sequestered by Mcl-1 and Bcl-xL, but not Bcl-2, until displaced by BH3-only proteins. *Genes & development*, 19(11), pp.1294–305.

Wilson, J. et al., 2000. Bcl-w expression in colorectal adenocarcinoma. *British Journal of Cancer*, 82(1), pp.178–185.

Wilson, W. et al., 2010. Navitoclax, a targeted high-affi nity inhibitor of BCL-2, in lymphoid malignancies:phase1 dose-escalation study of safety pharmacokinetics, pharmacodynamics and antitumour activity. *Oncology*, 11(10), pp.1149–1159.

Winter, P. et al., 2014. RAS signaling promotes resistance to JAK inhibitors by suppressing BAD-mediated apoptosis. *Science Signaling*, 7(357), pp.ra122–133.

Wise, D. et al., 2011. Hypoxia promotes tsocitrate dehydrogenase dependent carboxylation of A-Ketoglutarate to citrate to support cell growth and viability. *PNAS*, 108(49), pp.19611–19616.

Wise, D. et al., 2008. Myc regulates a transcriptional program that stimulates mitochondrial glutaminolysis and leads to glutamine addiction. *PNAS*, 105(48), pp.18782–18787.

Wise, D.R. & Thompson, C.B., 2010. Glutamine addiction: a new therapeutic target in cancer. *Trends in biochemical sciences*, 35(8), pp.427–33.

Wu, X. et al., 2017. Extra-mitochondrial prosurvival BCL-2 proteins regulate gene transcription by inhibiting the SUFU tumour suppressor. *Nature cell biology*, 19(10), pp.1226–1236.

Wuillème-Toumi, S. et al., 2005. Mcl-1 is overexpressed in multiple myeloma and associated with relapse and shorter survival. *Leukemia*, 19(7), pp.1248–52.

Xiang, Y. et al., 2015. Targeted inhibition of tumour-specific glutaminase diminishes cell-autonomous tumorigenesis. *The Journal of Clinical Investigation*, 125(6), pp.2293–2306.

Yan, C. et al., 2000. Overexpression of the Cell Death Suppressor Bcl-w in Ischemic Brain: Implications for a Neuroprotective Role via the Mitochondrial Pathway. *Journal of cerebral Blood flow and metabolism*, 20, pp.620–630.

Yang, C. et al., 2016. High expression of GFAT1 predicts poor prognosis in patients with pancreatic cancer. *Nature/Scientific Reports*, 6(39044), pp. 1-9.

Yang, C.S. et al., 2009. Cancer prevention by tea: animal studies, molecular mechanisms and human relevance. *Nature reviews. Cancer*, 9(6), pp.429–39.

Yang, C.S. et al., 2011. Cancer prevention by tea: Evidence from laboratory studies. *Pharmacological research : the official journal of the Italian Pharmacological Society*, 64(2), pp.113–22.

Yang, J. et al., 2019. Targeting cellular metabolism to reduce head and neck cancer growth. *Scientific reports*, 9(1), p.4995.

Yang, T., Kozopas, K.M. & Craig, R.W., 1995. The intracellular distribution and pattern of expression of Mcl-1 overlap with, but are not identical to, those of Bcl-2. *The Journal of cell biology*, 128(6), pp.1173–84.

Yang, Y. et al., 2011. Role of fatty acid synthase in gemcitabine and radiation resistance of pancreatic cancers. *Int J Biochem Mol Biol*, 2(1), pp.89–98.

Yecies, D. et al., 2010. Acquired resistance to ABT-737 in lymphoma cells that up-regulate MCL-1and BFL-1. *Blood*, 115(16), pp.3304–3313.

Yin, J. et al., 2016. Copy-- number-variation-of-MCL1-predicts-overall-survival-of-non-- small-- cell-lung-cancer-in-a-Southern-Chinese-population. *Cancer Medicine*, 5(9), pp.2171–2179.

Yin, X., Oltval, Z. & Korsmeyer, S., 1994. BH1 and BH2 domains of Bcl-2 are required for inhibition of apoptosis and heterodimerzation withBAX. *Nature*, 369, pp.321–323.

Yoon, H. et al., 2003. Bfl-1 gene expression in breast cancer its relationship with other prognostic factors. *Journal Korean Medicin Science*, 18, pp.225–30.

Yoshimori, M. et al., 2015. P-glycoprotein is expressed and causes resistance to chemotherapy in EBV-positive T-cell lymphoproliferative diseases. *Cancer Medicine*, 4(10), pp.1494–1504.

You, H.-Y. et al., 2016. Pitavastatin suppressed liver cancer cells in vitro and in vivo. *Oncotargets and Therapy*, 152, pp.5383–5388.

Youle, R.J. & Strasser, A., 2008. The BCL-2 protein family: opposing activities that mediate cell death. *Nature reviews. Molecular cell biology*, 9(1), pp.47–59.

Young, A. et al., 2016. MCL-1 inhibition provides a new way to suppress breast cancer metastasis and increase sensitivity to dasatinib. *Breast Cancer Research*, 18(125).

Yuneva, M. et al., 2007. Deficiency in glutamine but not glucose induces MYC-dependent apoptosis in human cells. *J Cell Biol 2007*, 178, pp.93–105.

Zaidi, N., Swinnen, J.V. & Smans, K., 2012. ATP-citrate lyase: a key player in cancer metabolism. *Cancer research*, 72(15), pp.3709–14.

Al-Zebeeby, A. et al., 2018. Targeting intermediary metabolism enhances the efficacy of BH3 mimetic therapy in hematologic malignancies. *Haematologica*, 104(5), pp.1–9.

Zervantonakis, I. et al., 2017. Systems analysis of apoptotic priming in ovarian cancer identifies vulnerabilities and predictors of drug response. *Nature Communications* , 8.

Zhai, S. et al., 2002. Flavopiridol, a novel cyclin-dependent kinase inhibitor, in clinical development. *The Annals of pharmacotherapy*, 36(5), pp.905–11.

Zhang, C. et al., 2016. Cullin3–KLHL25 ubiquitin ligase targets ACLY for degradation to inhibit lipid synthesis and tumor progression. *Gene and Development*, 30, pp.1956-1970.

Zhang, H. et al., 2011. Mcl-1 is critical for survival in a subgroup of non-small-cell lung cancer cell lines. *Oncogene*, 30(16), pp.1963–8.

Zhang, J. et al., 2016. Glutamate dehydrogenase (GDH) regulates bioenergetics and redox homeostasis in human glioma. *Oncotarget*, 23(5), pp.1-12.

Zhang, K. et al., 2014. Original Article Bcl-xL overexpression and its association with the progress of tongue carcinoma. *Int J Clin Exp Pathol*, 7(11), pp.7360–

7377.

Zhao, D. et al., 2005. Prognostic significance of bcl-2 and p53 expression in colorectal carcinoma. *Journal of Zhejiang University. Science. B*, 6(12), pp.1163–9.

Zhao, X. et al., 2019. BCL2 Amplicon Loss and Transcriptional Remodeling Drives ABT-199 Resistance in B Cell Lymphoma Models. *Cancer Cell*, 35, pp.752–766.

Zhao, Y., Butler, E.B. & Tan, M., 2013. Targeting cellular metabolism to improve cancer therapeutics. *Cell death & disease*, 4, p.e532.

Zhou, P. et al., 1998. Mcl-1 in transgenic mice promotes survival in a spectrum of hematopoietic cell types and immortalization in the myeloid lineage. *Blood*, 92(9), pp.3226–39.

Zhou, W. et al., 2007. Fatty acid synthase inhibition activates AMP-activated protein Kinase in SKOV3 Human Ovarian Cancer Cells. *Cancer Res*, 67(7), pp.2964–2971.

Zou, Y. et al., 2015. Comparison of immunohistochemistry and DNA sequencing for the detection of IDH1 mutations in glioma. *Neuro-Oncology*, 17, pp.477–479.

Appendix

Short Communication

Kristina Henz[a], Aoula Al-Zebeeby[a], Marion Basoglu, Simone Fulda, Gerald M. Cohen, Shankar Varadarajan and Meike Vogler*

Selective BH3-mimetics targeting BCL-2, BCL-X_L or MCL-1 induce severe mitochondrial perturbations

https://doi.org/10.1515/hsz-2018-0233
Received April 25, 2018; accepted June 7, 2018

Abstract: Induction of apoptosis by selective BH3-mimetics is currently investigated as a novel strategy for cancer treatment. Here, we report that selective BH3-mimetics induce apoptosis in a variety of hematological malignancies. Apoptosis is accompanied by severe mitochondrial toxicities upstream of caspase activation. Specifically, the selective BH3-mimetics ABT-199, A-1331852 and S63845, which target BCL-2, BCL-X_L and MCL-1, respectively, induce comparable ultrastructural changes including mitochondrial swelling, a decrease of mitochondrial matrix density and severe loss of cristae structure. These shared effects on mitochondrial morphology indicate a similar function of these anti-apoptotic BCL-2 proteins in maintaining mitochondrial integrity and function.

Keywords: apoptosis; BCL-2 proteins; BH3-mimetics; mitochondria.

[a]**Kristina Henz and Aoula Al-Zebeeby:** These authors contributed equally to this work.
***Corresponding author: Meike Vogler,** Institute for Experimental Cancer Research in Pediatrics, Goethe-University Frankfurt, Komturstr. 3a, D-60528 Frankfurt/Main, Germany, e-mail: m.vogler@kinderkrebsstiftung-frankfurt.de
Kristina Henz: Institute for Experimental Cancer Research in Pediatrics, Goethe-University Frankfurt, Komturstr. 3a, D-60528 Frankfurt/Main, Germany
Aoula Al-Zebeeby, Gerald M. Cohen and Shankar Varadarajan: Department of Molecular and Clinical Cancer Medicine and Pharmacology, Institute of Translational Medicine, University of Liverpool, Liverpool, UK
Marion Basoglu: Department of Biology, Goethe-University Frankfurt, Frankfurt, Germany
Simone Fulda: Institute for Experimental Cancer Research in Pediatrics, Goethe-University Frankfurt, Komturstr. 3a, D-60528 Frankfurt/Main, Germany; German Cancer Consortium (DKTK), Heidelberg, Germany; and German Cancer Research Center (DKFZ), Heidelberg, Germany

Due to their central role in regulating apoptosis, the anti-apoptotic BCL-2 proteins are promising targets for the development of novel anticancer therapeutics (Adams and Cory, 2007). To this end, several so-called BH3-mimetics have been developed that bind with nanomolar affinities to the hydrophobic groove of anti-apoptotic BCL-2 proteins (Vogler et al., 2009). By binding and inhibiting anti-apoptotic BCL-2 proteins like BCL-2, BCL-X_L and MCL-1, BH3-mimetics can induce the activation and oligomerization of BAX and/or BAK, which form pores in the outer mitochondrial membrane. Although the precise molecular nature of these pores is still not fully characterized, it is well reported that activation of BAX and/or BAK is sufficient to facilitate the release of cytochrome *c* from the mitochondrial intermembrane space into the cytosol and hence induce the activation of caspases and apoptosis (Westphal et al., 2014). An alternative way for cytochrome *c* to escape from the mitochondrial intermembrane space involves the opening of the permeability transition pore (PTP) in the inner mitochondrial membrane, which results in mitochondrial swelling, loss of cristae structure, rupture of the outer mitochondrial membrane and subsequent release of pro-apoptotic factors like cytochrome *c* (Giorgio et al., 2018).

We previously reported that treatment of chronic lymphocytic leukemia cells with either ABT-199 or ABT-737, a BH3-mimetic inhibiting BCL-2 and BCL-X_L, causes apoptosis accompanied by mitochondrial swelling, loss of cristae structure and rupture of the outer mitochondrial membrane, features more commonly associated with the opening of the PTP in the inner mitochondrial membrane than with BAX/BAK pore formation in the outer mitochondrial membrane (Vogler et al., 2008, 2013). In this study, we utilized specific and selective inhibitors of either BCL-2 (ABT-199) (Souers et al., 2013), BCL-X_L (A-1331852) (Leverson et al., 2015) or MCL-1 (S63845) (Kotschy et al., 2016) to investigate the effects of BH3-mimetics on mitochondrial morphology during apoptosis in hematological malignancies. Treatment with low concentrations of ABT-199 induces rapid apoptosis in RIVA (diffuse large B-cell lymphoma, DLBCL) as well as MAVER-1 (mantle

cell lymphoma) cells as demonstrated by externalization of phosphatidylserine (PS) in the cell membrane of the apoptotic cells (Figure 1A). In line with an activation of the intrinsic apoptotic pathway, exposure to BH3-mimetics also induced simultaneous loss of mitochondrial membrane potential (Figure 1B). To investigate whether exposure to ABT-199 also resulted in ultrastructural changes, upstream and/or independent of caspase activation and subsequent cleavage of cellular targets, we treated RIVA and MAVER-1 with ABT-199 in the presence of the caspase inhibitor z-VAD.fmk before performing transmission electron microscopy. For these experiments, z-VAD.fmk was included as we had previously shown cell death induced by ABT-199 to be caspase-mediated (Vogler et al., 2008), and in these experiments were aiming to investigate only cellular effects that were induced upstream of caspase activation. As anticipated, in comparison to untreated control cells, cells treated with ABT-199 in the presence of z-VAD.fmk exhibit no overall change in nuclear or cellular morphology (data not shown). Mitochondria in the untreated control cells possess intact outer and inner membranes with well-defined cristae, characteristic of healthy mitochondria with structural and functional integrity (Figure 1C and D). In contrast, cells treated with ABT-199 exhibit strikingly swollen mitochondria, with a significant loss of mitochondrial matrix density and a ruptured outer mitochondrial membrane, suggesting that inhibition of BCL-2 resulted in marked mitochondrial ultrastructural changes, upstream and/or independent of the other hallmarks of apoptosis (Figure 1E and F).

To investigate the effect of BCL-X_L inhibition on mitochondrial structural changes, RCK8 (DLBCL) and K562 (chronic myeloid leukemia) cells that primarily rely on BCL-X_L for survival were chosen (Figure 2A and B). RCK8 cells exhibit a mixed mitochondrial morphology, with some cells displaying dark mitochondria indicative of

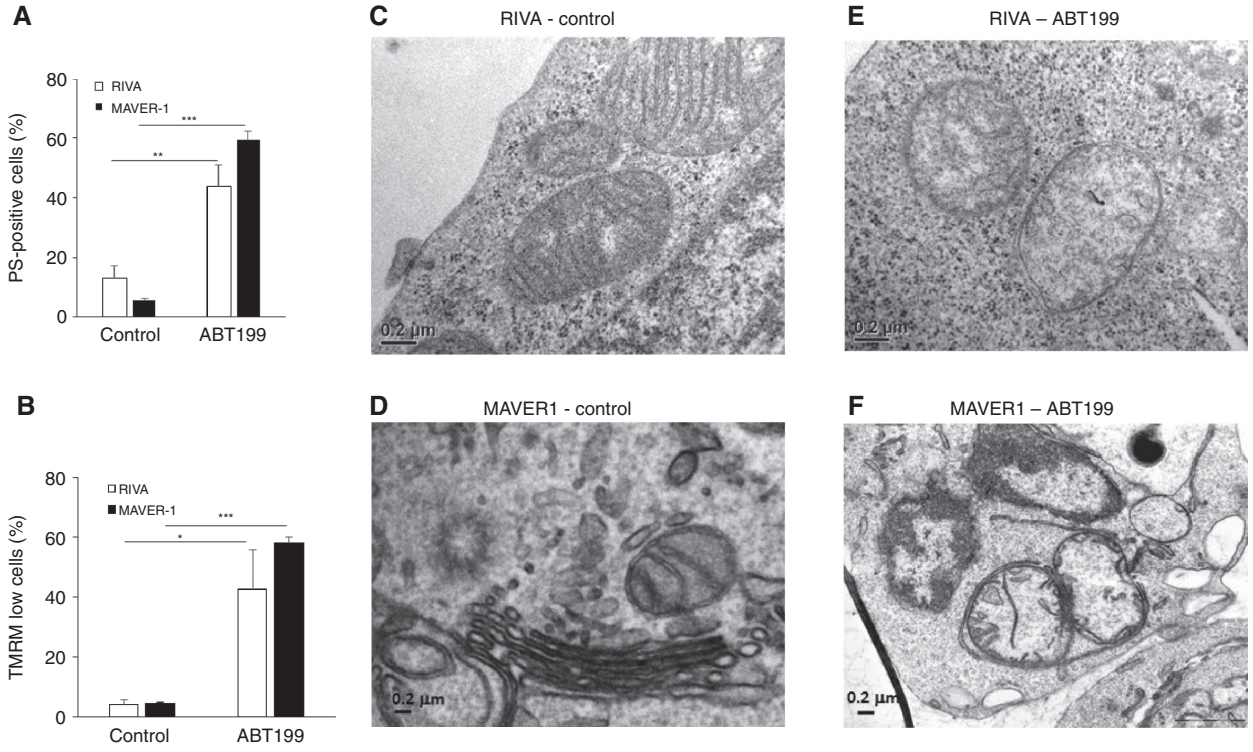

Figure 1: Mitochondrial perturbations induced by ABT-199 in BCL-2 dependent cells.
(A and B) RIVA and MAVER-1 cells were exposed to 10 nM ABT-199 (Selleck Chemicals, Houston, TX, USA) for 4 h before analysis of apoptosis by PS exposure and binding of AnnexinV-FITC followed by flow cytometry (A) or loss of mitochondrial membrane potential (B) as measured by staining with 50 nM tetramethylrhodamine methyl ester (TMRM, Sigma, Deisenhofen, Germany) and flow cytometry. Flow cytometry was performed using FACSCanto II (BD Biosciences, Heidelberg, Germany). Data presented are mean plus standard deviation (n = 3 for RIVA and n = 4 for MAVER-1). Asterisks indicate statistical significance as analyzed using Student's *t*-test with two-tailed distribution, two-sample, unequal variance (*$p < 0.05$; **$p < 0.01$; ***$p < 0.001$). (C and E) RIVA cells were either left untreated (C) or exposed to 10 nM ABT-199 for 4 h in the presence of 25 µM z-VAD.fmk (Bachem, Heidelberg, Germany) (E) before fixation in 2.5% glutaraldehyde and processing for electron microscopy. (D and F) MAVER-1 cells were either left untreated (D) or exposed to 10 nM ABT-199 for 2 h in the presence of z-VAD.fmk (25 µM) (F) before fixation in 2.5% glutaraldehyde and processing for electron microscopy.

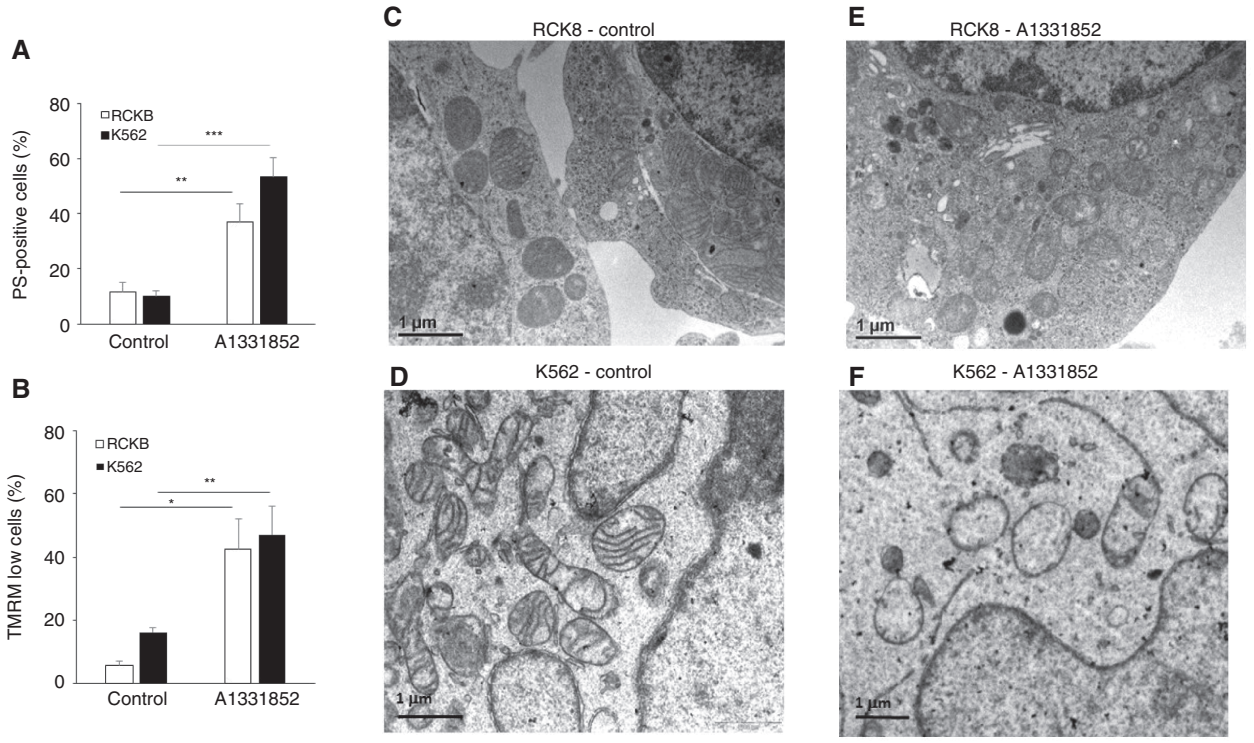

Figure 2: Mitochondrial perturbations induced by A-1331852 in BCL-X_L dependent cells.
(A and B) RCK8 and K562 cells were exposed to A-1331852 (Selleck Chemicals) (3 nM for RCK8 and 10 nM for K562 cells) for before analysis of apoptosis by PS exposure and binding of AnnexinV-FITC (A) or loss of mitochondrial membrane potential (B) as measured by staining with TMRM and flow cytometry. Data presented are mean plus standard deviation (n = 4). Asterisks indicate statistical significance as analyzed using Student's *t*-test (*$p < 0.05$; **$p < 0.01$; ***$p < 0.001$) (C and E) RCK8 cells were either left untreated (C) or exposed to 3 nM A-1331852 for 4 h in the presence of z-VAD.fmk (25 µM) (E). (D and F) K562 cells were either left untreated (D) or exposed to 10 nM A-1331852 for 2 h in the presence of z-VAD.fmk (25 µM) (F) before fixation in 2.5% glutaraldehyde and processing for electron microscopy.

higher matrix density, and other cells displaying larger and brighter mitochondria with less dense mitochondrial matrix and regular cristae structures (Figure 2C). In cells exposed to A-1331852, the mitochondrial cristae structure is largely lost and mitochondria appear smaller, indicative of mitochondrial fragmentation or fission. Rupture of the outer mitochondrial membrane is also evident in some swollen mitochondria (Figure 2E). Similarly, the well-defined mitochondrial cristae in the untreated K562 cells are completely lost following exposure to A-1331852, indicative of severe mitochondrial toxicity (Figure 2D and F). Interestingly, BCL-X_L has recently been described to maintain a functional mitochondrial network, and BCL-X_L knockout murine embryonic fibroblasts displayed fragmented mitochondria as assessed by fluorescence microscopy (Pfeiffer et al., 2017).

Next, we investigated the effects of a specific and potent inhibitor of MCL-1, S63845, whose derivative, MIK665 is currently being investigated in clinical trials for the treatment of multiple myeloma and acute myeloid leukemia (NCT02979366 and NCT02992483). Using SUDHL10 DLBCL cells that depend primarily on MCL-1 for survival, we observe a rapid induction of intrinsic apoptosis upon exposure to S63845 accompanied by a loss of mitochondrial membrane potential (Figure 3A and B). SUDHL10 cells contain large clearly defined bright mitochondria with regular cristae structures. Exposure to S63845 induces a prominent loss of cristae structures and rupture of the outer mitochondrial membranes in some affected mitochondria. Inhibition of MCL-1 by S63845 also induces more fragmented, smaller mitochondria with vesicular structures rather than the well-defined cristae structures, in line with our previous report on mitochondrial fragmentation induced by the related MCL-1 inhibitor, A-1210477 (Milani et al., 2017). Interestingly, a similar mitochondrial phenotype was previously reported in MCL-1 knockout murine embryonic fibroblasts (Perciavalle et al., 2012). In that study, MCL-1 deletion induced the appearance of punctate mitochondria, the loss of the tubular mitochondrial network as well as ultrastructural defects including defective cristae harboring balloon-like, vesicular structures.

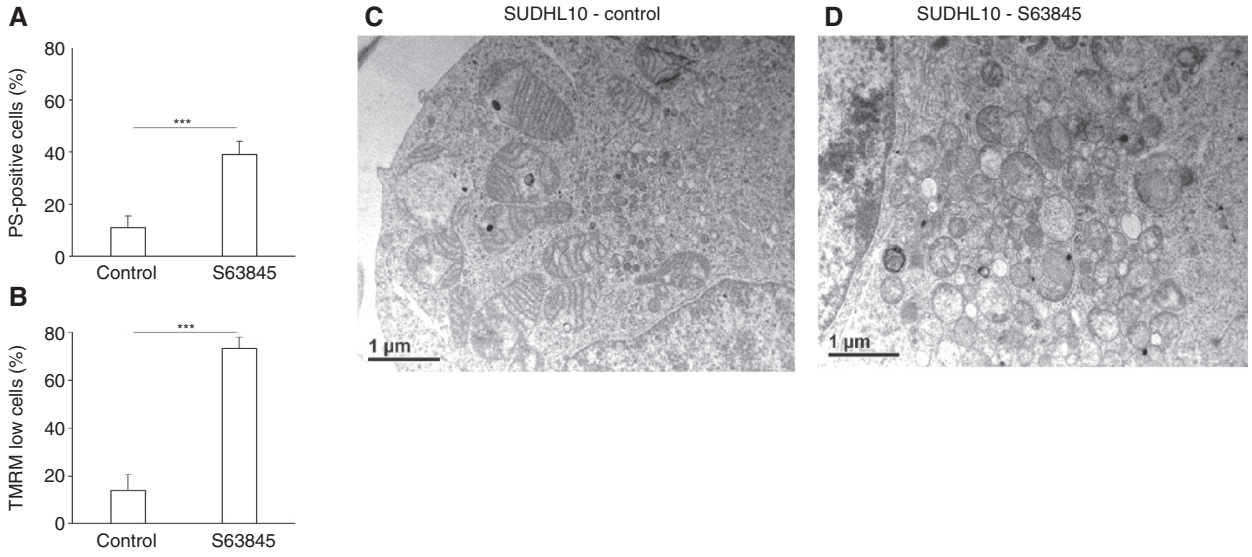

Figure 3: Mitochondrial perturbations induced by inhibition of MCL-1.
(A and B) SUDHL10 cells were exposed to 100 nM S63845 (Active Biochemicals, Bonn, Germany) for 4 h before analysis of apoptosis by PS exposure and binding of AnnexinV-FITC (A) or loss of mitochondrial membrane potential (B) as measured by staining with TMRM and flow cytometry. Data presented are mean plus standard deviation (n = 4). Asterisks indicate statistical significance as analyzed using Student's *t*-test (***$p < 0.001$). (C and D) SUDHL10 cells were either left untreated (C) or exposed to 100 nM S63845 for 4 h in the presence of z-VAD.fmk (25 µM) (D) before fixation in 2.5% glutaraldehyde and processing for electron microscopy.

Although mitochondria are involved in apoptotic and necrotic forms of cell death, the molecular characteristics of apoptosis and necrosis are very different. While classical apoptosis involves the formation of a BAX/BAK mediated pore in the outer mitochondrial membrane, necrotic cell death is facilitated by opening of the PTP, a calcium-dependent channel connecting inner and outer mitochondrial membranes (Kroemer et al., 2007). Upon PTP opening, small solutes and water move osmotically into the mitochondrial matrix, thus causing swelling and rupture of the outer mitochondrial membrane (Bernardi et al., 2006). Our data showing swelling of mitochondria upon exposure to selective BH3-mimetics indicate that BCL-2, BCL-X_L and MCL-1 all play a role in the regulation of PTP opening. This conclusion is supported by the finding that also BAX and BAK can be involved in the formation of the PTP (Karch et al., 2013), thus providing a molecular link between the anti-apoptotic BCL-2 proteins and PTP opening.

In addition to swelling we observe a prominent loss of cristae structures upon exposure to BH3-mimetics. A large fraction of mitochondrial cytochrome *c* is located and sequestered in the cristae, and hence efficient release of cytochrome *c* requires the opening of cristae structures (Scorrano et al., 2002). Opening of mitochondrial cristae junctions is regulated by the dynamin-related protein optic atrophy 1 (OPA1) (Frezza et al., 2006). Interestingly, several reports have linked the BCL-2 family to cristae opening, where BH3-only proteins and/or active BAX/BAK are required to facilitate OPA1 mediated cristae opening and subsequent cytochrome *c* release (Yamaguchi et al., 2008; Landes et al., 2010).

Taken together, we describe a common function of the anti-apoptotic BCL-2 proteins BCL-2, BCL-X_L and MCL-1 in maintaining mitochondrial integrity and cristae structures, which can be antagonized by using selective BH3-mimetics and occurs during BH3-mimetic induced apoptosis in malignant hematological cells.

Acknowledgments: This work was supported by a studentship by Ministry of Higher Education and Scientific Research and University of Al-Qadisiyah, Iraq (to A.A.).

Conflict of interest statement: The authors have no conflict of interest to declare.

References

Adams, J.M. and Cory, S. (2007). The Bcl-2 apoptotic switch in cancer development and therapy. Oncogene *26*, 1324–1337.

Bernardi, P., Krauskopf, A., Basso, E., Petronilli, V., Blachly-Dyson, E., Di Lisa, F., and Forte, M.A. (2006). The mitochondrial permeability transition from in vitro artifact to disease target. FEBS J. *273*, 2077–2099.

Frezza, C., Cipolat, S., Martins de Brito, O., Micaroni, M., Beznoussenko, G.V., Rudka, T., Bartoli, D., Polishuck, R.S., Danial, N.N., De Strooper, B., et al. (2006). OPA1 controls apoptotic cristae remodeling independently from mitochondrial fusion. Cell *126*, 177–189.

Giorgio, V., Guo, L., Bassot, C., Petronilli, V., and Bernardi, P. (2018). Calcium and regulation of the mitochondrial permeability transition. Cell Calcium *70*, 56–63.

Karch, J., Kwong, J.Q., Burr, A.R., Sargent, M.A., Elrod, J.W., Peixoto, P.M., Martinez-Caballero, S., Osinska, H., Cheng, E.H., Robbins, J., et al. (2013). Bax and Bak function as the outer membrane component of the mitochondrial permeability pore in regulating necrotic cell death in mice. eLife *2*, e00772.

Kotschy, A., Szlavik, Z., Murray, J., Davidson, J., Maragno, A.L., Le Toumelin-Braizat, G., Chanrion, M., Kelly, G.L., Gong, J.N., Moujalled, D.M., et al. (2016). The MCL1 inhibitor S63845 is tolerable and effective in diverse cancer models. Nature *538*, 477–482.

Kroemer, G., Galluzzi, L., and Brenner, C. (2007). Mitochondrial membrane permeabilization in cell death. Physiol. Rev. *87*, 99–163.

Landes, T., Emorine, L.J., Courilleau, D., Rojo, M., Belenguer, P., and Arnaune-Pelloquin, L. (2010). The BH3-only Bnip3 binds to the dynamin Opa1 to promote mitochondrial fragmentation and apoptosis by distinct mechanisms. EMBO Rep. *11*, 459–465.

Leverson, J.D., Phillips, D.C., Mitten, M.J., Boghaert, E.R., Diaz, D., Tahir, S.K., Belmont, L.D., Nimmer, P., Xiao, Y., Ma, X.M., et al. (2015). Exploiting selective BCL-2 family inhibitors to dissect cell survival dependencies and define improved strategies for cancer therapy. Sci. Transl. Med. *7*, 279ra240.

Milani, M., Byrne, D.P., Greaves, G., Butterworth, M., Cohen, G.M., Eyers, P.A., and Varadarajan, S. (2017). DRP-1 is required for BH3 mimetic-mediated mitochondrial fragmentation and apoptosis. Cell Death Dis. *8*, e2552.

Perciavalle, R.M., Stewart, D.P., Koss, B., Lynch, J., Milasta, S., Bathina, M., Temirov, J., Cleland, M.M., Pelletier, S., Schuetz, J.D., et al. (2012). Anti-apoptotic MCL-1 localizes to the mitochondrial matrix and couples mitochondrial fusion to respiration. Nat. Cell Biol. *14*, 575–583.

Pfeiffer, A., Schneider, J., Bueno, D., Dolga, A., Voss, T.D., Lewerenz, J., Wullner, V., and Methner, A. (2017). Bcl-x_L knockout attenuates mitochondrial respiration and causes oxidative stress that is compensated by pentose phosphate pathway activity. Free Radic. Biol. Med. *112*, 350–359.

Scorrano, L., Ashiya, M., Buttle, K., Weiler, S., Oakes, S.A., Mannella, C.A., and Korsmeyer, S.J. (2002). A distinct pathway remodels mitochondrial cristae and mobilizes cytochrome c during apoptosis. Dev. Cell *2*, 55–67.

Souers, A.J., Leverson, J.D., Boghaert, E.R., Ackler, S.L., Catron, N.D., Chen, J., Dayton, B.D., Ding, H., Enschede, S.H., Fairbrother, W.J., et al. (2013). ABT-199, a potent and selective BCL-2 inhibitor, achieves antitumor activity while sparing platelets. Nat. Med. *19*, 202–208.

Vogler, M., Dinsdale, D., Sun, X.M., Young, K.W., Butterworth, M., Nicotera, P., Dyer, M.J., and Cohen, G.M. (2008). A novel paradigm for rapid ABT-737-induced apoptosis involving outer mitochondrial membrane rupture in primary leukemia and lymphoma cells. Cell Death Differ. *15*, 820–830.

Vogler, M., Dinsdale, D., Dyer, M.J., and Cohen, G.M. (2009). Bcl-2 inhibitors: small molecules with a big impact on cancer therapy. Cell Death Differ. *16*, 360–367.

Vogler, M., Dinsdale, D., Dyer, M.J., and Cohen, G.M. (2013). ABT-199 selectively inhibits BCL2 but not BCL2L1 and efficiently induces apoptosis of chronic lymphocytic leukaemic cells but not platelets. Br. J. Haematol. *163*, 139–142.

Westphal, D., Kluck, R.M., and Dewson, G. (2014). Building blocks of the apoptotic pore: how Bax and Bak are activated and oligomerize during apoptosis. Cell Death Differ. *21*, 196–205.

Yamaguchi, R., Lartigue, L., Perkins, G., Scott, R.T., Dixit, A., Kushnareva, Y., Kuwana, T., Ellisman, M.H., and Newmeyer, D.D. (2008). Opa1-mediated cristae opening is Bax/Bak and BH3 dependent, required for apoptosis, and independent of Bak oligomerization. Mol. Cell *31*, 557–569.

Ferrata Storti Foundation

Haematologica 2019
Volume 104(5):1016-1025

Targeting intermediary metabolism enhances the efficacy of BH3 mimetic therapy in hematologic malignancies

Aoula Al-Zebeeby,[1] Meike Vogler,[2] Mateus Milani,[1] Caitlin Richards,[1] Ahoud Alotibi,[1] Georgia Greaves,[1] Martin J.S. Dyer,[3] Gerald M. Cohen[1,4] and Shankar Varadarajan[1,4]*

[1]Department of Molecular and Clinical Cancer Medicine, Institute of Translational Medicine, University of Liverpool, UK; [2]Institute for Experimental Cancer Research in Pediatrics, Goethe-University, Frankfurt, Germany; [3]Ernest and Helen Scott Haematological Research Institute, Leicester Cancer Research Centre, University of Leicester, Leicester Royal Infirmary, UK and [4]Department of Molecular and Clinical Cancer Pharmacology, Institute of Translational Medicine, University of Liverpool, UK

ABSTRACT

BH3 mimetics are novel targeted drugs with remarkable specificity, potency and enormous potential to improve cancer therapy. However, acquired resistance is an emerging problem. We report the rapid development of resistance in chronic lymphocytic leukemia cells isolated from patients exposed to increasing doses of navitoclax (ABT-263), a BH3 mimetic. To mimic such rapid development of chemoresistance, we developed simple resistance models to three different BH3 mimetics, targeting BCL-2 (ABT-199), BCL-X_L (A-1331852) or MCL-1 (A-1210477), in relevant hematologic cancer cell lines. In these models, resistance could not be attributed to either consistent changes in expression levels of the anti-apoptotic proteins or interactions among different pro- and anti-apoptotic BCL-2 family members. Using genetic silencing, pharmacological inhibition and metabolic supplementation, we found that targeting glutamine uptake and its downstream signaling pathways, namely glutaminolysis, reductive carboxylation, lipogenesis, cholesterogenesis and mammalian target of rapamycin signaling resulted in marked sensitization of the chemoresistant cells to BH3 mimetic-mediated apoptosis. Furthermore, our findings highlight the possibility of repurposing widely used drugs, such as statins, to target intermediary metabolism and improve the efficacy of BH3 mimetic therapy.

Correspondence:

SHANKAR VARADARAJAN
svar@liverpool.ac.uk

Received: August 16, 2018.

Accepted: November 20, 2018.

Pre-published: November 22, 2018.

doi:10.3324/haematol.2018.204701

Check the online version for the most updated information on this article, online supplements, and information on authorship & disclosures: www.haematologica.org/content/104/5/1016

Introduction

Failure to undergo apoptosis is a cardinal feature of cancer and several targeted therapies, such as the small molecule inhibitors targeting specific members of the anti-apoptotic BCL-2 family - navitoclax/ABT-263 (targeting BCL-2, BCL-X_L and BCL-w) and venetoclax/ABT-199 (BCL-2 specific) - are aimed at facilitating cancer cell clearance by enhanced apoptosis.[1-4] Recently, selective inhibitors of BCL-X_L (A-1331852) and MCL-1 (A-1210477 and S63845) have also been synthesized.[5-7] Despite their selectivity in targeting distinct anti-apoptotic BCL-2 family members, and remarkable potency in inducing rapid and extensive apoptosis in a wide variety of malignancies, resistance to BH3 mimetics, in particular venetoclax, is starting to be reported in the clinic. Elevated levels of multiple members of the anti-apoptotic BCL-2 family proteins, including BCL-X_L and MCL-1, are often implicated in such chemoresistance.[8-13] Although it may be possible to target these proteins with a combination of selective BH3 mimetics, the potential toxicities associated with such combination therapy may be problematic.

Altered metabolism is a promising approach to enhance the efficacy of chemotherapeutic agents, as a requirement for intermediary metabolites, such as glucose and glutamine, for the survival and proliferation of cancer cells is well doc-

umented.[1,14-19] This is a promising approach, as drugs targeting different stages of intermediary metabolism are already approved or in trials for treating different malignancies.[20,21] In this study, we found a low level of resistance that developed in cells from patients with chronic lymphocytic leukemia (CLL) exposed to navitoclax. To mimic this modest resistance, we developed simple models of resistance to different BH3 mimetics and demonstrated that downregulating glutamine uptake or metabolism as well as its downstream signaling cascades, such as reductive carboxylation, lipogenesis and cholesterogenesis, result in enhanced apoptosis of cancer cells resistant to different BH3 mimetics, thus highlighting the possibility that inhibition of key regulatory enzymes of these metabolic pathways may enhance sensitivity to BH3 mimetic therapy.

Methods

Reagents and antibodies

ABT-263, A-1331852 and A-1210477 were from AbbVie (North Chicago, IL, USA), ABT-199, epigallocatechin gallate (EGCG), CB-839, simvastatin, rapamycin and torin-1 from Selleck Chemicals (Houston, TX, USA), gamma-L-glutamyl-*p*-nitroanilide (GPNA) from Insight Biotechnology (Wembley, Middlesex, UK), azaserine from Cambridge Bioscience (Cambridge, UK), aminooxyacetate (AOA), sodium palmitate, dimethyl α-ketoglutarate, oxaloacetate and citrate from Sigma-Aldrich (Gillingham, UK), L-glutamine from Life Technologies (Paisley, UK) and GSK2194069, SB204990, atorvastatin, pitavastatin and bafilomycin A1 from Tocris (Abingdon, UK). Antibodies against PARP, BCL-2, MCL-1, BAX, BAK and GAPDH were from Santa Cruz Biotechnology (Santa Cruz, CA, USA), caspase-3, caspase-9, BCL-X_L, BCL-w, BIM, PUMA, BAD, IDH2, ACL, ACO2, ATG5 and ATG7 from Cell Signaling Technology (MA, USA), BID from Prof. J. Borst (The Netherlands Cancer Institute, Amsterdam, the Netherlands), NOXA from Millipore (Watford, UK) and SLC1A5, GLS, GFAT, GLUD1, IDH3, FASN and HMGR from Abcam (Cambridge, UK).

Primary chronic lymphocytic leukemia cells and cell lines

Peripheral blood samples from CLL patients were obtained with the patients' consent and ethics committee approval (06_Q2501_122) from Leicester Haematological Tissue Bank and cultured as described elsewhere.[38] CLL samples were obtained from patients enrolled in a phase I/IIa study of ABT-263 (navitoclax) in patients with relapsed or refractory CLL (NCT00481091). Lymphocytes were purified and cultured in RPMI 1640 medium supplemented with 10% fetal bovine serum (Life Technologies Inc.). Alternatively, blood from patients was incubated at 37°C in 48-well plates and apoptosis assessed as described previously.[39,40] Blood samples were collected prior to the first *in vivo* dose of navitoclax or 4 h after dosing during the lead-in period (day 1 of the lead-in period; L1D1), or day 1 of cycle 1 (C1D1), cycle 3 (C3D1) or cycle 5 (C5D1). Samples were collected 4 h after dosing as blood concentrations of ABT-263 were maximal at this time.[41] For culture of CLL cells, mouse fibroblast L cells were irradiated with 75 Gy and seeded in 24-well plates (3 x10^5 cells/well). CLL cells were cultured at 1.5 x 10^6 cells/well on the L cells and removed when required by gentle washing with RPMI before treatment. Mantle cell lymphoma (MAVER-1), chronic myeloid leukemia (K562) and multiple myeloma (NCI-H929) cell lines were cultured in RPMI 1640 medium but the medium was supplemented with 0.02% 2-mercaptoethanol for culturing H929 cells. Cell lines were from either the *Deutsche Sammlung von Mikroorganismen und Zellkulturen* (DMSZ; Braunshweig, Germany) or the American Type Culture Collection (ATCC; Middlesex, UK) and subjected to short tandem repeat profiling to confirm their identity.

Resistance models

The different resistance models to relevant BH3 mimetics were developed by treating control cells (represented as A in all schemes) of MAVER-1, K562 and H929 to the relevant BH3 mimetics, ABT-199 (10 nM), A-1331852 (10 nM) or A-1210477 (5 μM), respectively. In the first resistance model, cells were exposed to their appropriate BH3 mimetic for 24 h followed by 2 weeks without drug resulting in the cells depicted as B. These cells were then exposed to their appropriate BH3 mimetic for a further 24 h followed again by 2 weeks without drug resulting in C. This procedure was repeated twice more, resulting in E. In the second resistance model, cells were exposed to their appropriate BH3 mimetic for 24 h followed by 8 weeks without drug, resulting in the cells depicted as A4. The cells were collected every 2 weeks and labeled as A1, A2 and A3, respectively. In the third resistance model, cells were exposed to increasing concentrations of the appropriate BH3 mimetic every 5 days, resulting in cells depicted as A-a, A-b, A-c and A-d. The fourth model of resistance was made in a similar manner, but the 5-day treatment period was split into 2 days of treatment, followed by 3 days without drug, resulting in cells depicted as A-i, A-ii, A-iii and A-iv.

Metabolic deprivation, supplementation and apoptosis measurements

For glutamine deprivation experiments, cells were washed with phosphate-buffered saline and re-suspended in SILAC RPMI 1640 Flex Media (Life Technologies Inc.), supplemented with glucose (2 mg/mL) and 10% fetal bovine serum, for 16 h. For supplementation studies, the indicated concentrations of metabolites were added to the glutamine-free media, immediately before glutamine deprivation. For lipid supplementation studies, sodium palmitate [dissolved in water at 70°C to form a stock concentration of 100 mM and added dropwise into fatty acid-free bovine serum albumin (10%) to produce a final concentration of 10 mM] was supplemented in the culture media. The extent of apoptosis in cells following different treatments was quantified by fluorescence activated cell sorting (FACS) after having stained the cells with annexin V-fluorescein isothiocyanate and propidium iodide to measure phosphatidylserine externalization, as previously described.[42]

Short interfering RNA knockdown, immunoprecipitation and western blotting

Cells were transfected with 10 nM of short interfering RNA (siRNA) against SLC1A5 (SI00079730), GLS (SI03155019), GFAT (SI03246355), GLUD1 (SI02654743), IDH2 (SI02654820), IDH3 (SI00300524), ACO2 (SI03019037), ACLY (SI02663332), FASN (SI00059752), HMGR (SI00017136), ATG5 (SI02633946) and ATG7 (SI04344830) from Qiagen Ltd. (Manchester, UK) using interferin (Polyplus Transfection Inc, NY, USA), according to the manufacturer's protocol and processed 72 h after transfection. Immunoprecipitation and western blotting were carried out according to standard protocols.[43]

Statistical analysis

One-way analysis of variance (ANOVA) multiple comparisons and the Fisher least significant difference test ($P \leq 0.01$) were per-

formed to compare sensitive and resistant cells. For samples from CLL patients, one-way repeated measures ANOVA with the Fisher least significant difference test ($P \leq 0.01$) was used and statistics analyzed using GraphPad Prism 6 software (La Jolla, CA, USA).

Results

Hematologic malignancies rapidly acquire resistance to BH3 mimetics

The potential of BH3 mimetic therapy in cancer was first demonstrated in the treatment of BCL-2-dependent CLL using navitoclax/ABT-263. In a phase I/II clinical trial of navitoclax, CLL patients were treated for an initial lead-in period of 7 days with a low dose of navitoclax (100 mg daily) followed by five to seven cycles of treatment, with each cycle lasting 21 days during which the patients received 250 mg navitoclax daily. Analysis of blood samples collected from these patients, either prior to the first *in vivo* dose of navitoclax or 4 h after dosing, during the different cycles of therapy revealed marked changes in the ability of navitoclax to induce apoptosis in the CLL cells (Figure 1A). The first *in vivo* dose of navitoclax on day 1 of the lead-in period (L1D1) resulted in a time-dependent induction of apoptosis, as assessed by phosphatidylserine externalization and ultrastructural changes, in comparison to that of CLL cells from the same patients prior to treatment (Figure 1A and *Online Supplementary Figure S1*). A progressive increase in resistance to navitoclax was observed in CLL cells *in vivo* during the different cycles of treatment (Figure 1A). Since these studies were carried out in whole blood, we wanted to ascertain whether the decrease in ABT-263-induced apoptosis in CLL cells could be attributed to chemoresistance. To test this, CLL cells were isolated from these patients at the beginning of each treatment cycle and exposed to increasing concentrations of ABT-263. A significant decrease [3-fold difference in the half maximal inhibitory concentration (IC_{50}) values between the lead-in period and cycle 5] was observed in their ability to undergo ABT-263-induced apoptosis (Figure 1B), demonstrating that continued dosing of patients with ABT-263 resulted in a modest, yet significant increase in chemoresistance.

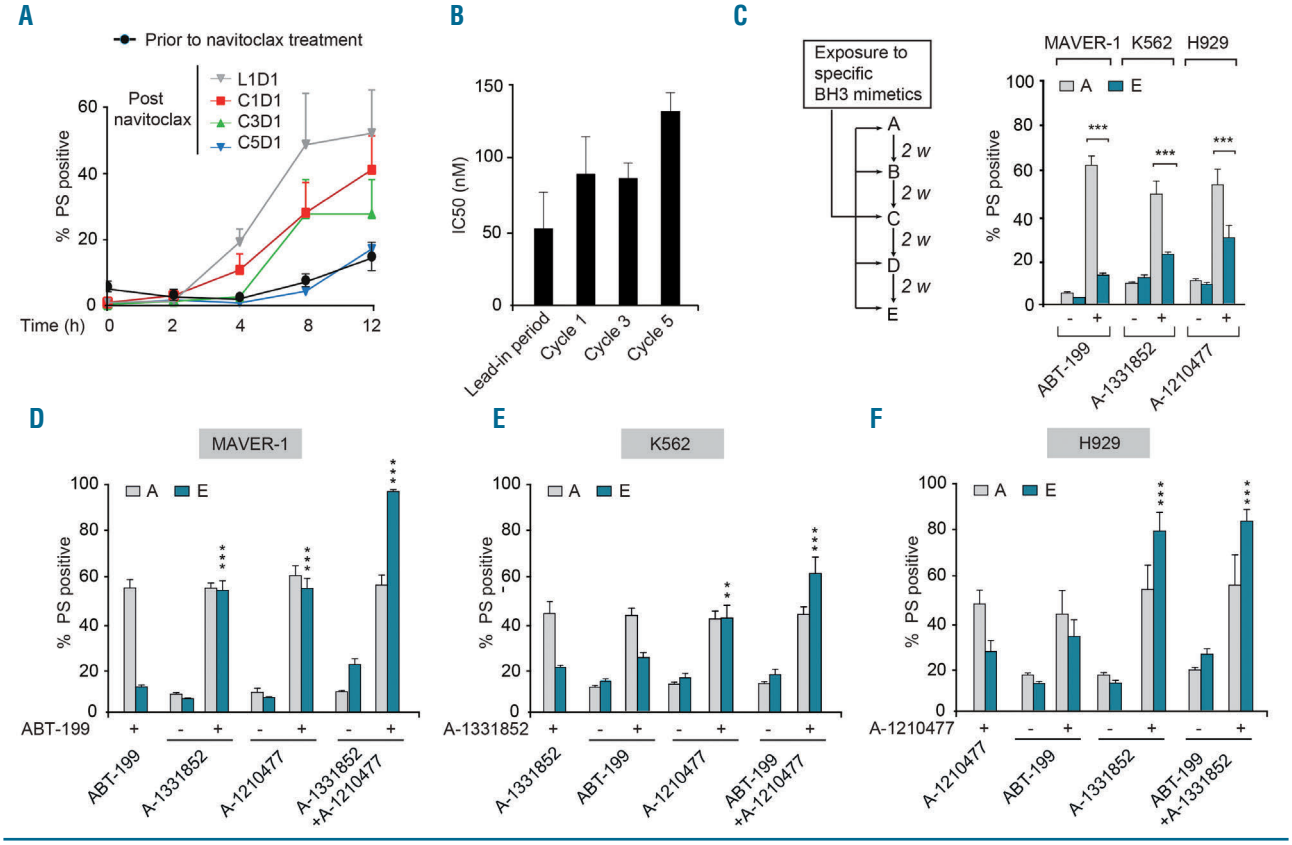

Figure 1. Hematologic malignancies rapidly acquire resistance to BH3 mimetics. (A) Blood samples collected from patients with chronic lymphocytic leukemia (CLL) (n=5), either prior to the first *in vivo* dose of navitoclax or 4 h after dosing during different stages of treatment - day 1 of the initial lead-in-period (L1D1), day 1 of cycle 1 (C1D1), day 1 of cycle 3 (C3D1) or day 1 of cycle 5 (C5D1) - were incubated *ex vivo* and the extent of apoptosis in the $CD19^+$ CLL cells was assessed at the indicated time points by measuring phosphatidylserine (PS) externalization. (B) CLL cells isolated from these patients at the beginning of each treatment cycle, as indicated in the figure, were exposed in vitro to increasing concentrations of ABT-263 and the extent of apoptosis was assessed: half maximal inhibitory concentration (IC_{50}) values are shown. (C) Scheme for establishing resistance to specific BH3 mimetics in relevant hematologic cell lines, as explained in the Methods section. Sensitive [A] and resistant [E] cells of MAVER-1, K562 and H929 cell lines were exposed for 4 h to ABT-199 (10 nM), A-1331852 (10 nM) and A-1210477 (5 μM), respectively, and apoptosis was assessed. (D-F) Combinations with some but not all BH3 mimetics restored apoptotic sensitivity of resistant [E] MAVER-1, K562 and H929 cells exposed for 4 h to ABT-199 (10 nM), A-1331852 (10 nM) or A-1210477 (5 μM), respectively. ***$P \leq 0.001$, **$P \leq 0.01$. Error bars = mean ± standard error of mean (n=3).

Since chemoresistance is an emerging problem in BH3 mimetic therapy, we extended these studies to more selective BH3 mimetics, such as ABT-199, which has replaced navitoclax owing to the dose-limiting thrombocytopenia associated with BCL-X_L inhibition.[3] Moreover, other selective BH3 mimetics that target BCL-X_L (A-1331852) and MCL-1 (A-1210477 and S63845) have been introduced for use in several other malignancies.[5-7] Using these BH3 mimetics and relevant cancer cell lines, we tried to mimic the rapid resistance observed in CLL patients following navitoclax treatment (Figure 1A,B), in order to identify ways to tackle chemoresistance, as it emerges. For this, we chose the BCL-2-dependent MAVER-1, BCL-X_L-dependent K562 and MCL-1-dependent H929 cell lines and exposed them to ABT-199, A-1331852 and A-1210477, respectively, to generate different models of resistance (Figure 1C and *Online Supplementary Figure S2*). Initial exposure of the relevant cell lines to the corresponding BH3 mimetic resulted in a rapid, time-dependent induction of apoptosis as assessed by the activation of caspase-9 and caspase-3 as well as cleavage of the canonical caspase substrate, PARP (*Online Supplementary Figure S2A*). Resistance to BH3 mimetics in these cells was generated by following the scheme presented in Figure 1C, when the initially sensitive cells [A] became relatively resistant [E], after four exposures (within 8 weeks) to their respective BH3 mimetic (Figure 1C). Similarly, a rapid resistance to the different BH3 mimetics was also observed using the other three resistance models (*Online Supplementary Figure S2B-D*). The rapid and modest resistance to the different BH3 mimetics in these cell lines was comparable to the extent of resistance observed in CLL cells during navitoclax therapy (Figure 1B).

Resistance to BH3 mimetics can be overcome by inhibiting multiple BCL-2 family members

Since resistance to BH3 mimetics has often been attributed to elevated expression levels of one or more anti-apoptotic BCL-2 family members, we wanted to identify whether such changes could be responsible for the observed resistance. Comparison of the sensitive [A], intermediate [C] and resistant [E] cells from the different cell lines did not reveal any consistent differences in BCL-2 family expression to explain the resistance (*Online Supplementary Figure S3*). We, therefore, sought to identify whether changes in protein-protein interactions among different pro-apoptotic BH3-only members and their anti-apoptotic counterparts could explain the resistance to BH3 mimetics. To do this, we performed immunoprecipitation studies to isolate the anti-apoptotic proteins bound to BIM and PUMA, which were abundantly expressed in the three different cell types. However, in the sensitive [A] and resistant [E] MAVER-1 cells, immunoprecipitation of BIM and PUMA revealed similar binding of BCL-2 and BCL-X_L and little or no binding to MCL-1 (*Online Supplementary Figure S4*). Likewise, no differences were observed in the binding of BIM and PUMA to BCL-X_L and MCL-1 in sensitive and resistant K562 or H929 cells (*Online Supplementary Figure S4*).

Although the protein expression levels and immunoprecipitation studies did not support an involvement of other BCL-2 family proteins in the observed resistance, the resistance to ABT-199 observed in MAVER-1 cells was completely overcome by a combination of ABT-199 with either A-1331852 or A-1210477, but not by either A-1331852 or A-1210477 alone, suggesting that the resistant cells depend not only on BCL-2 but also on BCL-X_L and/or MCL-1 for survival (Figure 1D). Furthermore, a combination of all three BH3 mimetics induced apoptosis in all the resistant cells, emphasizing the importance of all three anti-apoptotic BCL-2 family members in chemoresistance in these cells (Figure 1D). In K562 and H929 cells, the resistance was overcome by the combination of A-1331852 and A-1210477, but not ABT-199, thus implicating primary roles for BCL-X_L and MCL-1 in chemoresistance (Figure 1E,F). Similar to the MAVER-1 cells, the chemoresistant K562 cells also exhibited enhanced apoptosis following treatment with a combination of all three BH3 mimetics (Figure 1E), suggesting that some contribution of BCL-2 could not be totally excluded in these cells. These observations were almost entirely reproducible in the other three models of resistance (*Online Supplementary Figure S5*), supporting the notion that BCL-X_L and/or MCL-1 contributed significantly to the observed chemoresistance in the different models.

Modulation of glutamine uptake and/or metabolism enhances sensitivity to BH3 mimetics

Although the above results demonstrate that a combination of BH3 mimetics can overcome resistance, such an approach targeting multiple members of the BCL-2 family requires careful evaluation of the therapeutic index, as these proteins perform redundant functions in the maintenance of normal cellular homeostasis. An alternative strategy to overcome chemoresistance to BH3 mimetics could be achieved by altered metabolism, as depriving cells of glutamine has recently been shown to overcome MCL-1-mediated chemoresistance in multiple myeloma.[19] In our experiments, glutamine deprivation for 16 h alone did not exhibit any effect on overall cell survival and yet sensitized both the sensitive [A] and resistant [E] cells to BH3 mimetic-mediated apoptosis (Figure 2A). The increase in apoptosis observed in both sensitive and resistant cells indicates that glutamine deprivation most likely provides an additional cytotoxic cue that induces apoptosis in the sensitive and resistant cells, but could also bypass the resistance mechanism in the resistant cells. Nevertheless, our results suggest that targeting the glutamine metabolic pathway could enhance apoptosis and circumvent chemoresistance to BH3 mimetics in all our resistance models (Figure 2A and *Online Supplementary Figure S6*). To investigate the therapeutic potential of this approach, we wished to further understand how changes in glutamine metabolism might alter BH3 mimetic-mediated apoptosis.

Glutamine is transported into cells primarily via the SLC1A5 transporter and metabolized to glutamate, primarily via glutaminase (GLS)-mediated glutaminolysis.[22] Alternatively, glutamate can be generated from glutamine as a by-product of the hexosamine biosynthetic pathway, during the conversion of fructose-6-phosphate to glucosamine-6-phosphate, catalyzed by the enzyme, glutamine:fructose-6-phosphate-amidotransferase (GFAT) (Figure 2B).[22] Glutamate can then generate α-ketoglutarate (α-KG) either via glutamate dehydrogenase (GLUD)-mediated oxidative deamination or a series of aminotransferase reactions (Figure 2B).[14,22] Downregulation by RNA interference or pharmacological inhibition of key players involved in both glutamine uptake and its subsequent metabolism restored sensitivi-

ty of chemoresistant K562 cells to A-1331852-mediated apoptosis, albeit to varying degrees (Figure 2C,D). While downregulation of SLC1A5 and GLS resulted in enhanced sensitivity to A-1331852-mediated apoptosis in the different cell lines tested, inhibition of other enzymes in the glutamine metabolic pathway produced more modest effects (Figure 2C,D and *Online Supplementary Figure S7*).

Targeting reductive carboxylation enhances sensitivity to BH3 mimetics

Metabolic supplementation of the glutamine-deprived cells with either glutamine or α-KG restored the resistance of K562 cells to A1331852-induced apoptosis (Figure 3A). Since glutamine-derived α-KG feeds into the tricarboxylic acid cycle, we explored the functions of this cycle and its intermediates in chemoresistance to BH3 mimetics. For this, we supplemented glutamine-deprived cells with tricarboxylic acid intermediates, such as oxaloacetate and citrate. Strikingly, supplementation with citrate, but not oxaloacetate, restored the resistance of K562 cells to A-1331852-induced apoptosis (Figure 3A). These results suggest that conversion of α-KG to citrate via reductive carboxylation may play a role in regulating sensitivity to BH3 mimetics.

Reductive carboxylation involves the conversion of α-KG to isocitrate (catalyzed by isocitrate dehydrogenases 1 and 2; IDH1/2), which then generates citrate (catalyzed by aconitase) (Figure 3B).[23] While IDH1/2 catalyze reductive carboxylation of α-KG, another isoform of isocitrate dehydrogenase, IDH3, catalyzes the reverse conversion of isocitrate to α-KG.[23] Silencing the expression of IDH2 and aconitase, but not IDH3, restored the sensitivity of chemoresistant K562 cells to A-1331852-mediated apoptosis (Figure 3C,D), suggesting that the availability of citrate could be associated with the chemoresistance phenotype. To test this, IDH2-downregulated K562 cells were supplemented with citrate to identify whether addition of citrate could overcome the inhibition of reductive carboxylation and revert the associated increase in A-1331852-induced apoptosis. Supplementation with citrate, but not glutamine or α-KG, did indeed restore the chemoresistance of IDH2-downregulated cells (Figure 3E), thus confirming the involvement of reductive carboxylation and the availability of citrate as crucial players in the observed chemoresistance.

Downregulation of lipogenesis and cholesterogenesis enhances sensitivity to BH3 mimetics

Since citrate generated as a consequence of reductive carboxylation of α-KG is a major source of carbon for lipid synthesis, we investigated whether inhibition of lipogenesis could enhance sensitivity to BH3 mimetics

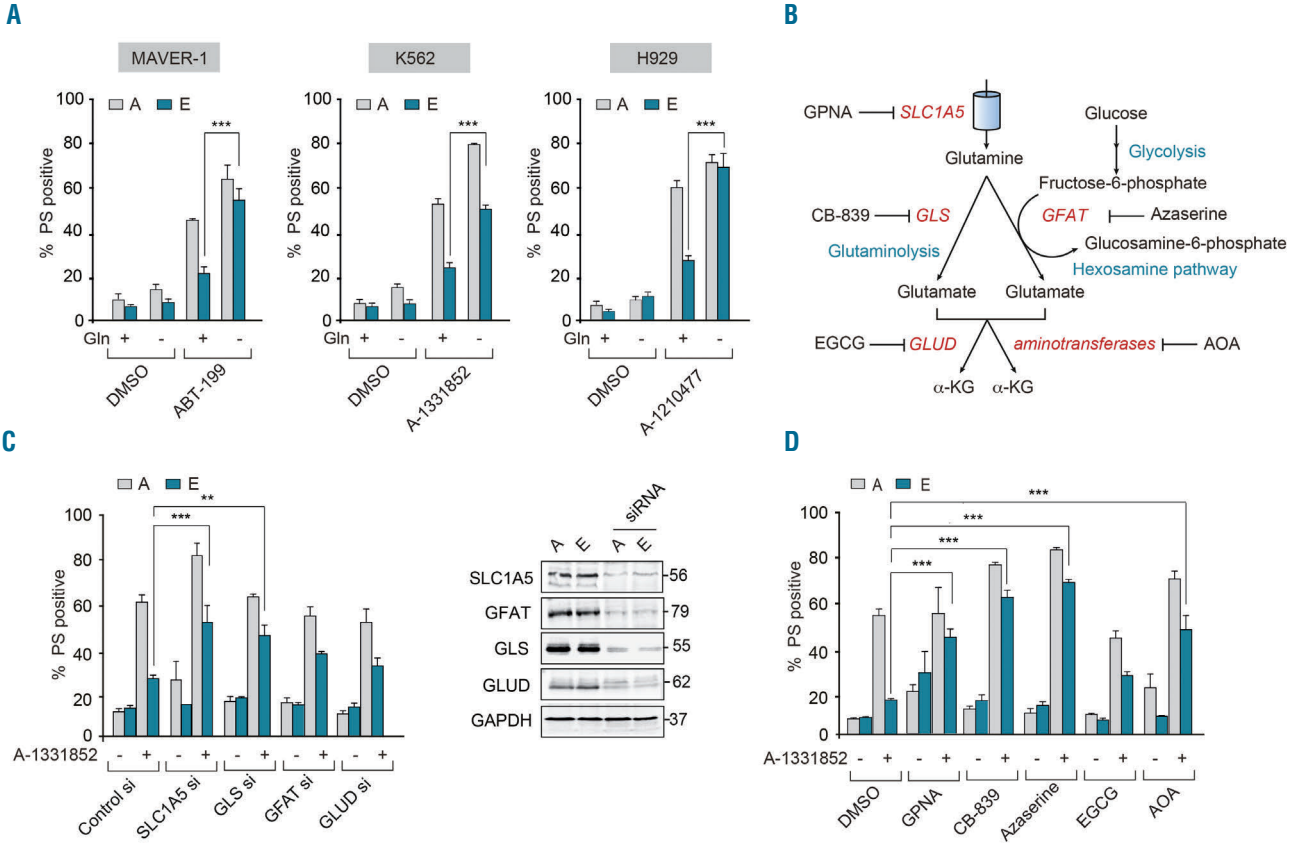

Figure 2. Inhibition of glutamine uptake and metabolism enhances sensitivity to BH3 mimetics. (A) Deprivation of glutamine (Gln) for 16 h restores the apoptotic sensitivity of resistant [E] MAVER-1, K562 and H929 cells to the indicated BH3 mimetic for 4 h. (B) Scheme representing the pathway of glutamine uptake and metabolism. (C) Apoptotic sensitivity of K562 resistant [E] cells exposed to A-1331852 (10 nM) for 4 h was restored following genetic knockdown for 72 h with the indicated short interfering (si) RNA. (D) Apoptotic sensitivity of K562 resistant [E] cells exposed to A-1331852 (10 nM) for 4 h was restored following pharmacological inhibition of glutamine uptake or metabolism with GPNA (5 mM) for 48 h, CB-839 (10 μM) for 72 h, azaserine (25 μM) for 16 h and AOA (500 μM) for 24 h but not with EGCG (50 μM) for 24 h. Western blots confirmed the knockdown efficiency of the different siRNA. ***$P \leq 0.001$, **$P \leq 0.01$. Error bars = mean ± standard error of mean (n=3). PS: phosphatidylserine; DMSO: dimethylsulfoxide.

(Figure 4A). Using a complementary approach of genetic and pharmacological inhibition of ATP-citrate lyase (ACLY), which catalyzes the conversion of citrate to acetyl-CoA,[24,25] as well as fatty acid synthase (FASN), which synthesizes long chain fatty acids following the condensation of acetyl-CoA and malonyl-CoA,[26,27] we identified that modulation of the lipogenesis pathway, using either genetic silencing or pharmacological inhibition of ACLY (with SB204990) or FASN (with GSK2194069) could enhance sensitivity of cells to BH3 mimetics (Figure 4B,C and *Online Supplementary Figure S7C,D*). Furthermore, metabolic supplementation with palmitate (the product of FASN (Figure 4A) in cells treated with GSK2194069 reverted the sensitized cells to their original chemoresistant phenotype (Figure 4D), thus obviating a requirement for FASN. These findings conclusively demonstrated that enhanced lipogenesis was associated with chemoresistance to BH3 mimetics and targeting lipogenesis could circumvent such resistance by enhancing BH3 mimetic-mediated apoptosis.

Acetyl-CoA generated from citrate can also feed into the cholesterol biosynthetic pathway, thus resulting in enhanced cholesterol production in cells. Targeting the rate-limiting step of cholesterol biosynthesis (catalyzed by HMG-CoA reductase; HMGR), either by genetic knockdown (Figure 4E) or pharmacological inhibition, using three widely used statins, simvastatin, atorvastatin and pitavastatin (Figure 4F), reversed resistance and restored the sensitivity of cells to BH3 mimetics (Figure 4E,F and *Online Supplementary Figure S7E*). Taken together, these data demonstrate that inhibition of several key players in lipid synthesis, including ACLY, FASN and HMGR, enhances the sensitivity to BH3 mimetics.

Targeting the mammalian target of rapamycin signaling cascade enhances sensitivity to BH3 mimetics

Since glutamine metabolism has been extensively implicated in mammalian target of rapamycin (mTOR) signaling,[22,28] we speculated whether targeting mTOR kinases could enhance sensitivity to BH3 mimetics. Inhibition of mTOR kinases with rapamycin and torin-1 resulted in significant sensitization of cells to BH3-mediated apoptosis (Figure 5A and *Online Supplementary Figure S7F*). To identify whether torin-1-mediated sensitization of cells to apoptosis was due to autophagy, we exposed the sensitive and resistant cells to bafilomycin A1 (Baf A1), which blocks autophagic flux by preventing lysosomal fusion of the autophagosomes. Exposure to

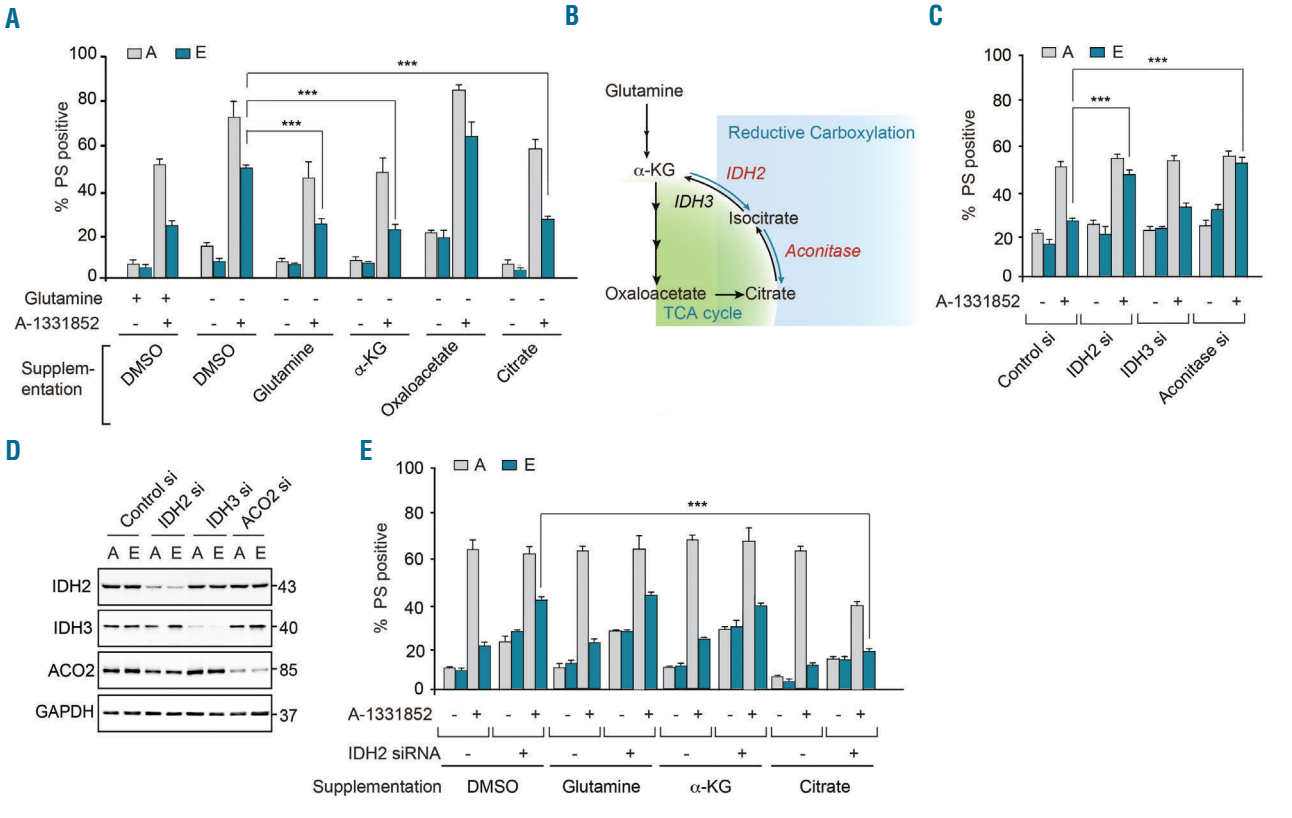

Figure 3. Modulation of reductive carboxylation enhances sensitivity to BH3 mimetics. (A) K562 sensitive [A] and resistant [E] cells were cultured in normal RPMI medium or glutamine-free medium with and without the supplementation of glutamine (2 mM), exposed to A-1331852 (10 nM) for 4 h and the extent of apoptosis assessed. Addition of citrate (4 mM) and α-ketoglutarate (α-KG) (4 mM) but not oxaloacetate (4 mM) for 16 h reversed the sensitivity of the resistant [E] cells in glutamine-deprived media. (B) Scheme representing the link between the tricarboxylic acid (TCA) cycle and reductive carboxylation. (C) K562 sensitive [A] and resistant [E] cells were transfected with short interfering (si) RNA against IDH2, IDH3 and aconitase for 72 h, followed by exposure for 4 h to A-1331852 and then apoptosis was assessed. (D) Western blots confirmed the knockdown efficiency of the different siRNA. (E) K562 [A] and [E] cells, transfected with a siRNA against IDH2 for 72 h, were glutamine-deprived and then given or not supplementation with glutamine (2 mM), α-ketoglutarate or citrate (both at 4 mM) for 16 h and the extent of apoptosis following exposure to A-1331852 (10 nM) for 4 h was assessed. ***$P \leq 0.001$. Error bars = mean ± standard error of mean (n=3). PS: phosphatidylserine; DMSO: dimethylsulfoxide.

bafilomycin A1 failed to revert torin-1-mediated chemosensitization, suggesting that this effect could be independent of autophagy (Figure 5B). Furthermore, genetic silencing of autophagy proteins, ATG5 and ATG7, which are critical for the induction of autophagy, also failed to revert torin-1-mediated sensitization (Figure 5C), confirming our finding that mTOR inhibition circumvented resistance and enhanced sensitivity to BH3 mimetics independently of autophagy. In summary, our findings demonstrate that modulation of glutamine metabolism and its downstream signaling pathways, namely reductive carboxylation, lipogenesis and cholesterogenesis, as well as inhibition of mTOR signaling could enhance the therapeutic efficacy of BH3 mimetic therapy thereby circumventing chemoresistance to BH3 mimetics (Figure 5D).

Targeting intermediary metabolism enhances sensitivity to navitoclax in primary samples from patients with chronic lymphocytic leukemia

Our results indicate that targeting various facets of intermediary metabolism enhanced sensitivity to different BH3 mimetics in cell lines derived from relevant hematologic malignancies. To further extend our observations in cell lines to primary samples from patients, we used CLL cells isolated from patients during the lead-in period (L1D1) as well as cells from the same patients after five cycles of navitoclax therapy (C5D1), as previously detailed in Figure 1. Using these samples, we wanted to determine whether modulating glutamine metabolism would enhance apoptosis mediated by navitoclax. For this, we exposed CLL cells to CB-839 and simvastatin for 24 h followed by navitoclax for 4 h and assessed the extent of apoptosis. In agreement with our cell line data, both CB-839 and statins overcame the resistance to navitoclax-mediated apoptosis in primary CLL cells (Figure 6), supporting the therapeutic translatability of our data from cell lines to patients.

Discussion

Anti-apoptotic BCL-2 family members are attractive drug targets both because of their high expression levels in several cancers and because of their well-characterized pro-survival roles. Even with extensive supportive *in vitro* data, the use of BH3 mimetics in treating cancer patients is still in its infancy, with venetoclax, a BCL-2-specific

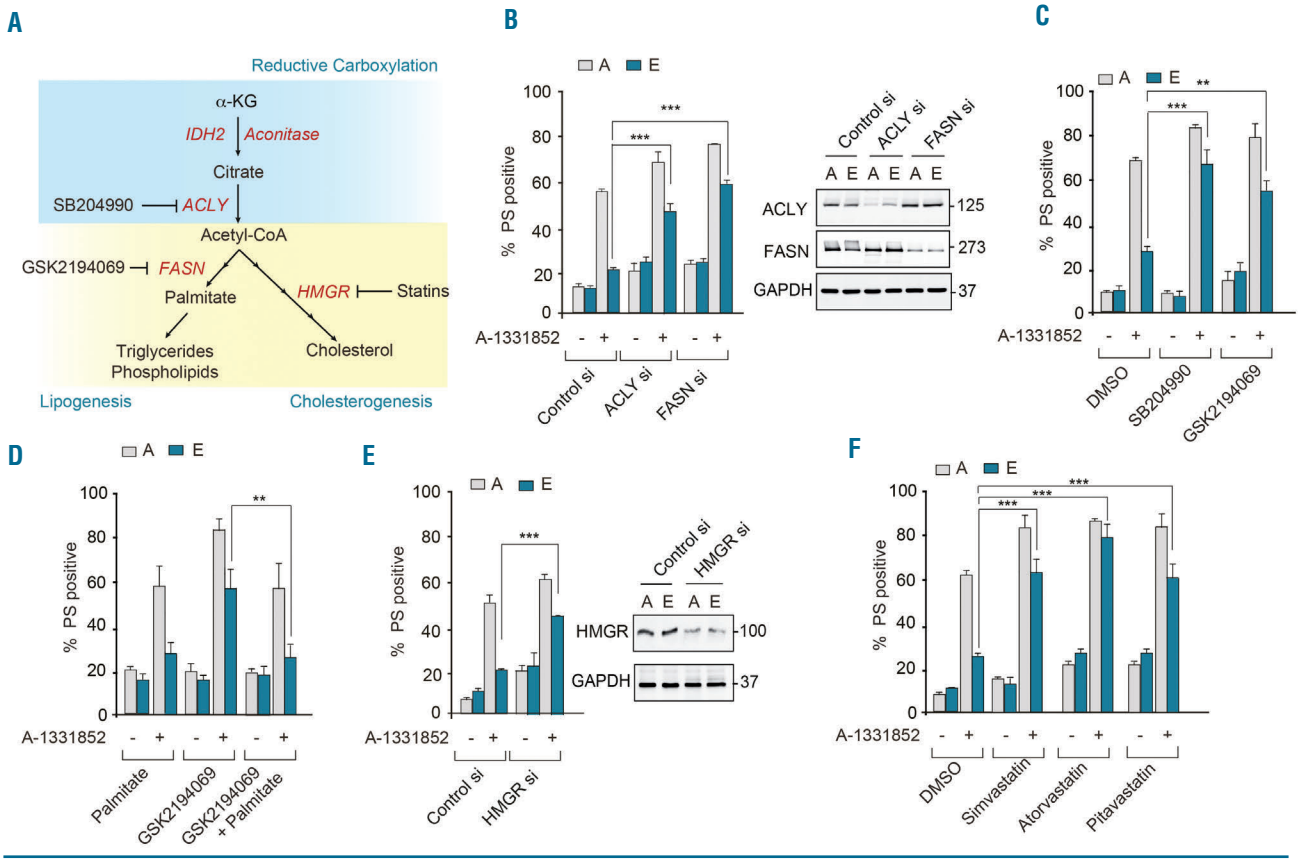

Figure 4. Inhibition of lipogenesis and cholesterogenesis enhances sensitivity to BH3 mimetics. (A) Scheme representing reductive carboxylation, lipogenesis and cholesterogenesis. (B) Apoptotic sensitivity of K562 resistant [E] cells exposed to A-1331852 (10 nM) for 4 h was restored following genetic knockdown for 72 h of key enzymes in fatty acid synthesis. Western blots confirmed the knockdown efficiency of the different short interfering (si) RNA. (C) Apoptotic sensitivity of K562 resistant [E] cells exposed to A-1331852 (10 nM) for 4 h was restored following pharmacological inhibition of key enzymes in fatty acid synthesis using SB204990 (1 μM) for 72 h or GSK2194069 (100 nM) for 48 h. (D) Metabolic supplementation of K562 sensitive [A] and resistant [E] cells with palmitate (50 μM) for 48 h prior to the exposure of cells to GSK2194069 (100 nM) overcame the sensitizing effect of GSK2194069 on A-1331852-mediated apoptosis. (E) Genetic knockdown for 72 h of HMGR or (F) pharmacological inhibition of HMGR by simvastatin (250 nM) for 72 h, atorvastatin (10 μM) for 48 h or pitavastatin (1 μM) for 72 h. ***$P \leqslant 0.001$; **$P \leqslant 0.01$. Error bars = mean ± standard error of mean (n=3). PS: phosphatidylserine; DMSO: dimethylsulfoxide.

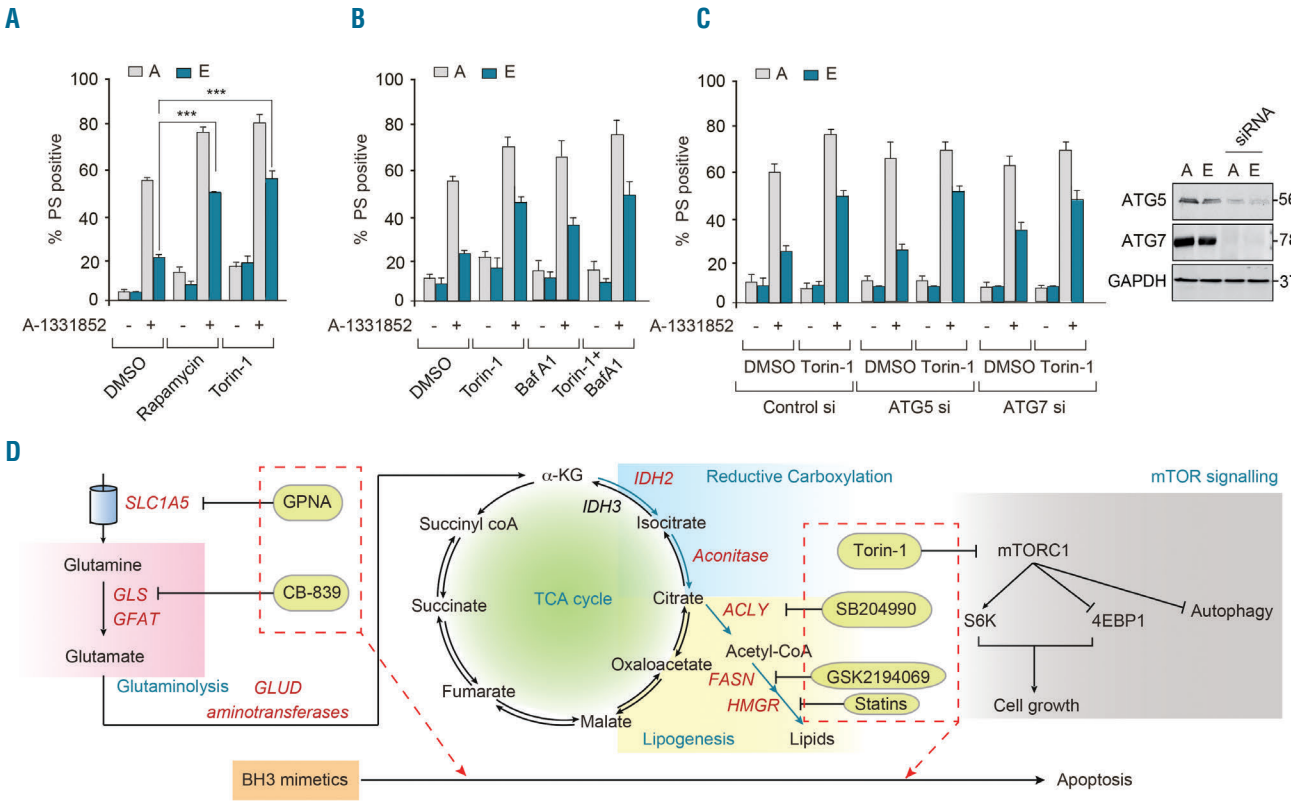

Figure 5. Modulation of mammalian target of rapamycin signaling enhances sensitivity to BH3 mimetics independently of autophagy. (A) Apoptotic sensitivity of K562 resistant [E] cells exposed to A-1331852 (10 nM) for 4 h was restored following pharmacological inhibition of mTOR signaling using rapamycin (100 nM) or torin-1 (10 nM) for 16 h. (B) Inhibition of mTOR-regulated autophagy using 3-MA (10 mM) or bafilomycin A1 (100 nM) for 1 h, followed by torin-1 (10 nM) for a further 16 h, resulted in varying effects on A-1331852-mediated apoptosis. (C) Genetic knockdown of ATG5 and ATG7 for 72 h failed to revert torin-1 (10 nM)-mediated sensitization of apoptosis in K562 resistant [E] cells, following A-1331852 (10 nM) for 4 h. Western blots confirmed the knockdown efficiency of ATG5 and ATG7 short interfering (si) RNA. ***$P \leq 0.001$. Error bars = mean ± standard error of mean (n=3). (D) Scheme representing glutamine uptake by SLC1A5 (inhibited by GPNA), glutaminolysis (inhibited by CB-839) to generate α-ketoglutarate, reductive carboxylation of α-ketoglutarate to generate citrate, which produces acetyl-CoA by a reaction catalyzed by ACLY (inhibited by SB204990), which eventually results in lipogenesis (inhibited by GSK2194069) and cholesterogenesis (inhibited by statins). Glutamine uptake, metabolism and its downstream signaling cascade can feed into mTOR signaling (inhibited by torin-1), all of which promote cell growth. In this study, we demonstrate that modulation of these distinct intermediary metabolic pathways could successfully sensitize cancer cells to BH3 mimetic-mediated apoptosis. PS: phosphatidylserine; DMSO: dimethylsulfoxide; TCA: tricarboxylic acid.

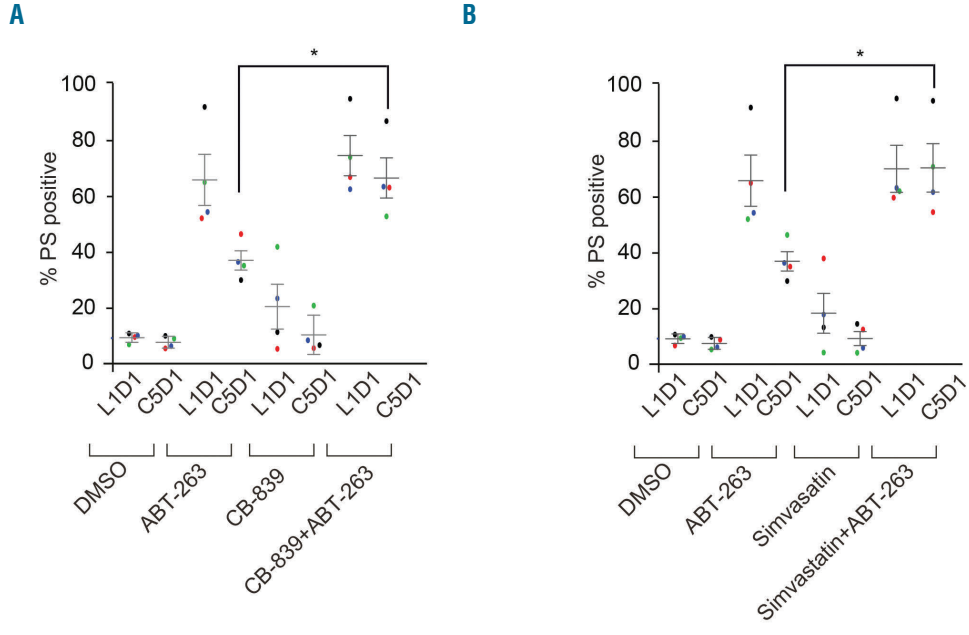

Figure 6. Inhibition of glutaminase and HMG-CoA reductase circumvents resistance to navitoclax-mediated apoptosis in primary chronic lymphocytic leukemia cells. Chronic lymphocytic leukemia cells isolated from five patients during the initial lead-in-period (L1D1) or day 1 of cycle 5 (C5D1) were cultured *ex vivo* on a feeder layer for 24 h and then exposed for a further 24 h to (A) CB-839 (50 nM) or (B) simvastatin (10 nM), and removed from the feeder layer for further exposure to navitoclax (50 nM) for 4 h. The extent of apoptosis was assessed as before. *$P \leq 0.05$. Error bars = mean ± standard error of mean (n=5). PS: phosphatidylserine; DMSO: dimethylsulfoxide.

inhibitor, only recently having received approval for treatment of refractory CLL.[4] The development of BH3 mimetics to target BCL-X_L and MCL-1 in patients will be extremely valuable in the treatment of several types of cancer. However potential mechanisms of resistance to BH3 mimetics need to be recognized as they emerge and ways to circumvent resistance identified. Several resistance mechanisms, including mutations of the target site,[29] post-translational modifications,[30,31] and elevated levels of anti-apoptotic BCL-2 family members,[8,11,32,33] have already been identified. While some of these resistance mechanisms could be overcome by co-administration of other specific BH3 mimetics that target BCL-X_L and/or MCL-1,[5-7] such inhibitors are not yet clinically available and the potential toxicities associated with the simultaneous inhibition of multiple BCL-2 family members are not known.

Attempts to identify measures that could overcome chemoresistance have led to exploration of the therapeutic potential of modulating intermediary metabolism in BH3 mimetic-mediated apoptosis.[19,20,34] Although the mechanisms by which glutamine could regulate cancer cell proliferation have been extensively studied, the interrelationship between glutamine metabolism and apoptosis requires further study. It has been previously reported that glutamine-mediated apoptosis is dependent on Myc[14] and that c-Myc activates glutaminolysis by upregulating both the glutamine transporter, SLC1A5, and glutaminase, GLS-1.[35,36] However, we were unable to detect an increase in expression levels of Myc, SLC1A5 or GLS-1 in our resistance models (Figure 3 and *data not shown*). The ability of glutamine to regulate apoptosis and/or chemoresistance could also be due to its regulatory effect on mitochondrial oxidative phosphorylation.[20] Although we do not entirely understand how glutamine metabolism impinges on apoptosis at this point, our data strongly support the notion that modulating glutamine metabolism and its related signaling pathways, such as reductive carboxylation, lipogenesis, cholesterogenesis and mTOR signaling, could enhance BH3 mimetic-mediated apoptosis in several hematologic malignancies (Figures 3-6). This is particularly promising, as glutaminase inhibitors, such as CB-839 and related drugs are already in clinical trials for the treatment of several malignancies[20,37] and other drugs targeting cholesterogenesis, such as statins are the most commonly prescribed drugs to millions of people worldwide. While this manuscript was in preparation, an independent study comparing a large cohort of CLL patients, many of whom were statin users, found that response to venetoclax/ABT-199 was enhanced among statin users in three different clinical trials.[44] These findings highlight the possibility of repurposing several drugs targeting the intermediary metabolic pathways in conjunction with BH3 mimetic therapy to enhance therapeutic effectiveness and overcome the emerging chemoresistance in several cancers.

Acknowledgments

We thank AbbVie for inhibitors and Prof. J. Borst for antibodies. This work was supported by a NorthWest Cancer Research grant CR1040 (to SV and GMC), a studentship from the Ministry of Higher Education and Scientific Research and the University of Al-Qadisiyah, Iraq (fpr AA-Z), a Science Without Borders studentship, CNPq 233624/2014-7, from the Ministry of Education, Brazil (for MM) and a studentship from the Prince Sattam Bin Abdulaziz University, Saudi Arabia (for AA).

References

1 Hanahan D, Weinberg RA. Hallmarks of cancer: the next generation. Cell. 2011;144(5):646–674.
2 Tse C, Shoemaker AR, Adickes J, et al. ABT-263: a potent and orally bioavailable Bcl-2 family inhibitor. Cancer Res. 2008;68(9):3421–3428.
3 Souers AJ, Leverson JD, Boghaert ER, et al. ABT-199, a potent and selective BCL-2 inhibitor, achieves antitumor activity while sparing platelets. Nat Med. 2013;19(2):202–208.
4 Roberts AW, Davids MS, Pagel JM, et al. Targeting BCL2 with venetoclax in relapsed chronic lymphocytic leukemia. N Engl J Med. 2016;374(4):311–322.
5 Leverson JD, Phillips DC, Mitten MJ, et al. Exploiting selective BCL-2 family inhibitors to dissect cell survival dependencies and define improved strategies for cancer therapy. Sci Transl Med. 2015;7(279):279ra40.
6 Leverson JD, Zhang H, Chen J, et al. Potent and selective small-molecule MCL-1 inhibitors demonstrate on-target cancer cell killing activity as single agents and in combination with ABT-263 (navitoclax). Cell Death Dis. 2015;6:e1590.
7 Kotschy A, Szlavik Z, Murray J, et al. The MCL1 inhibitor S63845 is tolerable and effective in diverse cancer models. Nature. 2016;538(7626):477–482.
8 van Delft MF, Wei AH, Mason KD, et al. The BH3 mimetic ABT-737 targets selective Bcl-2 proteins and efficiently induces apoptosis via Bak/Bax if Mcl-1 is neutralized. Cancer Cell. 2006;10(5):389–399.
9 Zhang H, Guttikonda S, Roberts L, et al. Mcl-1 is critical for survival in a subgroup of non-small-cell lung cancer cell lines. Oncogene. 2010;30(16):1963–1968.
10 Gores GJ, Kaufmann SH. Selectively targeting Mcl-1 for the treatment of acute myelogenous leukemia and solid tumors. Genes Dev. 2012;26(4):305–311.
11 Vogler M, Butterworth M, Majid A, et al. Concurrent up-regulation of BCL-XL and BCL2A1 induces approximately 1000-fold resistance to ABT-737 in chronic lymphocytic leukemia. Blood. 2009;113(18):4403–4413.
12 Tahir SK, Smith ML, Hessler P, et al. Potential mechanisms of resistance to venetoclax and strategies to circumvent it. BMC Cancer. 2017;17(1):399.
13 Bose P, Grant S. Mcl-1 as a therapeutic target in acute myelogenous leukemia (AML). Leuk Res Rep. 2013;2(1):12-14.
14 Yuneva M, Zamboni N, Oefner P, Sachidanandam R, Lazebnik Y. Deficiency in glutamine but not glucose induces MYC-dependent apoptosis in human cells. J Cell Biol. 2007;178(1):93–105.
15 Wise DR, Thompson CB. Glutamine addiction: a new therapeutic target in cancer. Trends Biochem Sci. 2010;35(8):427–433.
16 Graham NA, Tahmasian M, Kohli B, et al. Glucose deprivation activates a metabolic and signaling amplification loop leading to cell death. Mol Syst Biol. 2012;8:589.
17 Son J, Lyssiotis CA, Ying H, et al. Glutamine supports pancreatic cancer growth through a KRAS-regulated metabolic pathway. Nature. 2013;496(7443):101–105.
18 Still ER, Yuneva MO. Hopefully devoted to Q: targeting glutamine addiction in cancer. Br J Cancer. 2017;116(11):1375–1381.
19 Bajpai R, Matulis SM, Wei C, et al. Targeting glutamine metabolism in multiple myeloma enhances BIM binding to BCL-2 eliciting synthetic lethality to venetoclax. Oncogene. 2016;35(30):3955–3964.
20 Jacque N, Ronchetti AM, Larrue C, et al. Targeting glutaminolysis has antileukemic activity in acute myeloid leukemia and synergizes with BCL-2 inhibition. Blood. 2015;126(11):1346–1356.
21 Gross MI, Demo SD, Dennison JB, et al. Antitumor activity of the glutaminase inhibitor CB-839 in triple-negative breast cancer. Mol Cancer Ther. 2014;13(4):890–901.
22 Altman BJ, Stine ZE, Dang CV. From Krebs to clinic: glutamine metabolism to cancer therapy. Nat Rev Cancer. 2016;16(11):619–634.
23 Al-Khallaf H. Isocitrate dehydrogenases in physiology and cancer: biochemical and molecular insight. Cell Biosci. 2017;7:37.
24 Zaidi N, Swinnen JV, Smans K. ATP-citrate lyase: a key player in cancer metabolism. Cancer Res. 2012;72(15):3709–3714.

25 Khwairakpam AD, Shyamananda MS, Sailo BL, et al. ATP citrate lyase (ACLY): a promising target for cancer prevention and treatment. Curr Drug Targets. 2015;16(2):156–163.
26 Menendez JA, Lupu R. Fatty acid synthase and the lipogenic phenotype in cancer pathogenesis. Nat Rev Cancer. 2007;7(10): 763–777.
27 Mashima T, Seimiya H, Tsuruo T. De novo fatty-acid synthesis and related pathways as molecular targets for cancer therapy. Br J Cancer. 2009;100(9):1369–1372.
28 Saxton RA, Sabatini DM. mTOR signaling in growth, metabolism, and disease. Cell. 2017; 168(6):960–976.
29 Fresquet V, Rieger M, Carolis C, García-Barchino MJ, Martinez-Climent JA. Acquired mutations in BCL2 family proteins conferring resistance to the BH3 mimetic ABT-199 in lymphoma. Blood. 2014;123(26): 4111–4119.
30 Konopleva M, Contractor R, Tsao T, et al. Mechanisms of apoptosis sensitivity and resistance to the BH3 mimetic ABT-737 in acute myeloid leukemia. Cancer Cell. 2006;10(5):375–388.
31 Mazumder S, Choudhary GS, Al-Harbi S, Almasan A. Mcl-1 phosphorylation defines ABT-737 resistance that can be overcome by increased NOXA expression in leukemic B cells. Cancer Res. 2012;72(12):3069–3079.
32 Chen S, Dai Y, Harada H, Dent P, Grant S. Mcl-1 down-regulation potentiates ABT-737 lethality by cooperatively inducing Bak activation and Bax translocation. Cancer Res. 2007;67(2):782–791.
33 Lin KH, Winter PS, Xie A, et al. Targeting MCL-1/BCL-XL forestalls the acquisition of resistance to ABT-199 in acute myeloid leukemia. Sci Rep. 2016;6:27696.
34 Chan SM, Thomas D, Corces-Zimmerman MR, et al. Isocitrate dehydrogenase 1 and 2 mutations induce BCL-2 dependence in acute myeloid leukemia. Nat Med. 2015;21(2):178–184.
35 Wise DR, DeBerardinis RJ, Mancuso A, et al. Myc regulates a transcriptional program that stimulates mitochondrial glutaminolysis and leads to glutamine addiction. Proc Natl Acad Sci U S A. 2008;105(48):18782–18787.
36 Liu W, Le A, Hancock C, et al. Reprogramming of proline and glutamine metabolism contributes to the proliferative and metabolic responses regulated by oncogenic transcription factor c-MYC. Proc Natl Acad Sci U S A. 2012;109(23):8983–8988.
37 Vander Heiden MG, DeBerardinis RJ. Understanding the intersections between metabolism and cancer biology. Cell. 2017;168(4):657–669.
38 Vogler M, Weber K, Dinsdale D, et al. Different forms of cell death induced by putative BCL2 inhibitors. Cell Death Differ. 2009;16(7):1030–1039.
39 Vogler M, Dinsdale D, Dyer MJS, Cohen GM. ABT-199 selectively inhibits BCL2 but not BCL2L1 and efficiently induces apoptosis of chronic lymphocytic leukaemic cells but not platelets. Br J Haematol. 2013; 163(7):139–142.
40 Vogler M, Furdas SD, Jung M, Kuwana T, Dyer MJS, Cohen GM. Diminished sensitivity of chronic lymphocytic leukemia cells to ABT-737 and ABT-263 due to albumin binding in blood. Clin Cancer Res. 2010;16(16): 4217–4225.
41 Roberts AW, Seymour JF, Brown JR, et al. Substantial susceptibility of chronic lymphocytic leukemia to BCL2 inhibition: results of a phase I study of navitoclax in patients with relapsed or refractory disease. J Clin Oncol. 2012;30(5):488–496.
42 Varadarajan S, Poornima P, Milani M, et al. Maritoclax and dinaciclib inhibit MCL-1 activity and induce apoptosis in both a MCL-1-dependent and -independent manner. Oncotarget. 2015;6(14):12668–12681.
43 Lucas CM, Milani M, Butterworth M, et al. High CIP2A levels correlate with an anti-apoptotic phenotype that can be overcome by targeting BCL-XL in chronic myeloid leukemia. Leukemia. 2016;30(6):1273–1281.
44. Lee JS, Roberts A, Juarez D, et al. Statins enhance efficacy of venetoclax in blood cancers. Sci Transl Med. 2018;10(445).